

REPORT DOCUMENTATION PAGE

Form Approved
OMB NO. 0704-0188

Public Reporting burden for this collection of information is estimated to average 1 hour per response, including the time for reviewing instructions, searching existing data sources, gathering and maintaining the data needed, and completing and reviewing the collection of information. Send comment regarding this burden estimate or any other aspect of this collection of information, including suggestions for reducing this burden, to Washington Headquarters Services, Directorate for Information Operations and Reports, 1215 Jefferson Davis Highway, Suite 1204, Arlington, VA 22202-4302, and to the Office of Management and Budget, Paperwork Reduction Project (0704-0188), Washington, DC 20503.

1. AGENCY USE ONLY (Leave Blank)		2. REPORT DATE 10/10/01	3. REPORT TYPE AND DATES COVERED Final 14 Sep 98 - 13 Sep 01	
4. TITLE AND SUBTITLE Investigation of Preflame Reactions and Flame Propagation in Direct-injection Diesel Engines			5. FUNDING NUMBERS DAAG55-98-0494 1	
6. AUTHOR(S) K. T. Rhee			2001 OCT 24 AM 10:00	
7. PERFORMING ORGANIZATION NAME(S) AND ADDRESS(ES) Rutgers, the State University of New Jersey 98 Brett Road Piscataway, NJ 08855-0909				
9. SPONSORING / MONITORING AGENCY NAME(S) AND ADDRESS(ES) U. S. Army Research Office P.O. Box 12211 Research Triangle Park, NC 27709-2211			8. PERFORMING ORGANIZATION REPORT NUMBER	
11. SUPPLEMENTARY NOTES The views, opinions and/or findings contained in this report are those of the author(s) and should not be construed as an official Department of the Army position, policy or decision, unless so designated by other documentation.			10. SPONSORING / MONITORING AGENCY REPORT NUMBER 38364.3-EG	
			12 b. DISTRIBUTION CODE	
12 a. DISTRIBUTION / AVAILABILITY STATEMENT Approved for public release; distribution unlimited.				
13. ABSTRACT (Maximum 200 words) It was to investigate (invisible) preflame reactions taking place in a direct-injection compression ignition (DI-CI) engine during the ignition delay period and their effects on subsequent (visible) combustion reactions. The investigation was focused on the subject for an engine equipped with a high-pressure injection (HPI) unit in order to support the development of high-power-output Diesel engines. The use of HPI was found to facilitate more air utilization in a DI-CI engine even operated with intake air at unusually high temperatures (e.g. encountered in uncooled engines). In order to achieve these goals, several new research methods were developed-advanced for the study, including Rutgers or Super Imaging System (SIS), spectrometric methods, and Rutgers Animation Program. The tools were employed on an optical single-cylinder Cummins 903 engine. Among the significant results in system development is that the basic methods for high-speed imaging achievable at consecutive cycles, which shed some new insight into complex in-cylinder phenomena. The new research methods developed under the present ARO study permits observation of timed global pictures of preflame propagation under various engine-fuel conditions. New findings of the study include that the fuel injected into the cylinder immediately commences to chemically react, unlike the previous thought that there is a physical delay preceding actual chemical reactions. The reactions involved during the preflame reactions appear to be low-temperature kinetics controlled processes to affect the onset of visible-ray flame formation and combustion reactions. The preflame reaction species were found rapidly consumed as soon as the heat-releasing flame propagation took place.				
14. SUBJECT TERMS High-speed spectral infrared imaging System, Multiple movie display over a single PC screen, Spectral methods for quantitative imaging, Preflame reactions, Low-temperature kinetics reactions			15. NUMBER OF PAGES 118	
			16. PRICE CODE	
17. SECURITY CLASSIFICATION OR REPORT UNCLASSIFIED	18. SECURITY CLASSIFICATION ON THIS PAGE UNCLASSIFIED	19. SECURITY CLASSIFICATION OF ABSTRACT UNCLASSIFIED	20. LIMITATION OF ABSTRACT UL	

NSN 7540-01-280-5500

Standard Form 298 (Rev.2-89)
Prescribed by ANSI Std. Z39-18
298-102

Table of Contents

Cover Page with Abstract Table of Content	Page
1. Background	1
2. Objectives	3
3. Methodology of the Study	3
3-1. Spray Plume by HPI	4
3-2. Engine Apparatus	5
3-3. HIP Unit	5
3-4. Rutgers Super Imaging System (SIS)	7
4. Other Research Opportunities	8
5. Results and Discussion	8
5-1. High-speed Imaging from Consecutive Cycles (SAE paper 2001-01-3486)	8
5-2. Visualization of Pre flame and Combustion Reactions in Engine Cylinders (SAE Paper 2000-01-1800)	9
5-3. In-cylinder Liquid Layers, Cause of unburned hydrocarbon and Deposit Formation in SI Engines? (SAE paper 1999-01-3579)	10
5-4. Study of High-pressure Injection DI Diesel Engine (SAE Paper 1999-01-3494)	10
5-5. Direct Injection Diesel Engine Operated with Propane-DME Blend Fuel (SAE Paper 982536)	11
5-6. Diesel Engine Response to High Fuel-injection Pressures (SAE paper 982683)	12
5-7. Engine Performance and Exhaust Characteristics of Direct-injection Diesel Engine Operated with DME (SAE paper 972973)	12
5-8. Quantitative Imaging of In-cylinder Processes by Multispectral Methods (SAE Paper 970872)	13
6. Summary	14
7. References	16
Appendix	17

20011031 164

Final Report (DAAG55-98-0494)

Investigation of Preflame Reactions and Flame Propagation in Direct-injection Diesel Engines

K. T. Rhee

Department of Mechanical and Aerospace Engineering
Rutgers, The State University of New Jersey
Piscataway, New Jersey 08855-0909

1. Background

Development of high-efficiency and low-emission direct-injection (DI) Diesel or compression-ignition (CI) engine would be facilitated when reactions taking place in the cylinder is closely understood. More over those leading to the onset of self-ignition in the engine determine the period of ignition delay to affect the mixture preparation in the spray plume and to control subsequent in-cylinder heat-release processes as well as exhaust emissions.

In spite of such important need for understanding of these phenomena, their local as well as global reactions during the ignition delay period have not been well studied in the past, in either experimental or theoretical attempts. This seems mainly due to the absence of proper diagnostic tools and the complexity of fuel components as well as of the large number of elementary reactions.

In achieving a better understanding of those in-cylinder reactions, an improved high-speed spectral infrared imaging system and new spectrometric methods, all developed at Rutgers, were expected to help achieve the goals when applied to an optical DI-CI engine mated with a high-pressure injection (HPI) unit. Several main issues are briefly discussed prior to explaining objectives and results of the studying DI-CI with HPI as follows.

Why Direct-Injection Diesel Engine? DI-CI engines have advantages over an indirect injection engine, including higher efficiency and greater power density. The engine's simple induction system and open chamber permitting rapid heat release, however, produce low gas motions. This requires a greater role by the fuel injector for improved mixing, particularly if a high (smoke-limited) power output is to be obtained. A "better" injector is, therefore, desired for increasing the engine speed and induction pressure, and operating at over-all rich-fuel mixtures, which are present design practices employed for achieving a higher power density DI engine.

Any measure of improving the engine performance, however, is only useful when the new engine meets the regulatory emission standards and other desirable characteristics, e.g. low

noise and easy starting. In developing an improved DI-CI engine that delivers such desirable engine characteristics, some of which are mutually exclusive with each other, many unconventional changes in the engine-fuel system are implemented. They include very high pressure injection (HPI); multiple fuel injections per cycle [1,2]; pilot injection [3]; adiabatic engine [4]; new fuel additives [5]; fuel reformulation (e.g. oxygenated fuels having high cetane number) [6], and even oxygen-enrichment of the intake air [7].

High Pressure Injection System. The use of a precisely-controlled HPI with a tailored-shape rate may be the most aggressive method being taken toward achieving that goal. For example, a tailored-double fuel-injection achieved by an electronic-controlled (EC) injector was reported to produce low emissions of both NO_x and particulates [1,2].

Also, according to our earlier results obtained using both a conventional (cam-driven PT) injector and our new EC- HPI for a mutual comparison, a DI-CI delivered a superior performance when equipped with the latter. The EC-HPI is considered to complete the fuel injection within a short period of time by starting it relatively late but to deliver fuel at a high rate. The method would result in smaller droplets more uniformly spread over a large fuel spray plume, which gives rise to a short ignition delay. The uniform distribution is expected to reduce excessively fuel-rich (high-temperature) pockets. These all would help produce more rapid heat release occurring at a somewhat delayed time near the top-dead-center (TDC), which is expected to improve thermal efficiency and to produce low emissions of NO_x and also particulates.

Research and Development Issues. The development of a high-density power engine using the EC-HPI would be greatly facilitated (e.g. design of a new matching combustion chamber) if the in-cylinder reaction processes are better understood, especially when such radical changes are made in both the engine and fuel.

It seemed to be clear that some of the more important pieces of information missing at present are those concerning thermo-chemical behaviors as fuel and air are mixed during the period of early fuel injection or ignition delay, particularly when such injector parameters are greatly changed. (It is noted that the same is not well known for the existing engine either.) It is reasonable to predict that the preflame reactions altered by new advancement strategies (e.g. the EC-HPI highly) affects the subsequent in-cylinder processes. In backing up this statement, our study shows that the commencement of chemical reactions during the ignition delay period is greatly altered when an HPI is used in place of the conventional low-pressure injection unit, which is further discussed later.

As briefly mentioned earlier, the onset of the rapid heat-releasing reaction in a CI-DI engine is the culmination of many preflame reactions occurring during the ignition delay period. There are many basic questions associated with the phenomenon. For example, the onset may be either a result of reaction propagation around hot-spot kernel formations (as

local reaction centers) or of explosively generated radicals to create a global volume phenomenon, which no literature has clearly delineated by presenting solid evidence.

In addition, one may ask if the low-temperature kinetics involving the formation of radicals indeed dictates the onset of exothermic reactions. This consideration stems from some evidence reporting greater (preflame) reactions in an isooctane-air mixture than those in a comparable n-heptane mixture which has a greater tendency to knock than the former [8]. And more .

Need for new Engine Diagnostic Tools. It would be most desirable if one could determine the timed distribution of radical population representing the preflame reactions in the spray. Unfortunately many conventional diagnostic tools are unable to facilitate such a study of the phenomena. For example, in spite of their usefulness in various aspects, photos of very high-temperature reactions (during the post flame period), obtained by using conventional high-speed photography (or a visible-range light sensor), do not directly indicate what is happening during the preflame period.

In order to help study invisible (low-temperature) as well as visible in-cylinder processes, a new engine/flame diagnostic tool and spectrometric methods have been developed during last several years [9-12]. This Rutgers System simultaneously captures four geometrically identical infrared (IR) images in respective spectral bands at high rates for quantitative analysis, which is discussed more later.

This one-of-a-kind system, made operational in early 1994, was pronounced to be improper in achieving *rigorous quantitative imaging* by using our spectrometric methods due to various shortfalls, mainly erratic operations and noise modulated in electronic units.

2. Objectives

The present work was directed achieving a better understanding of the preflame reactions and their impact on the subsequent in-cylinder combustion processes in a high-pressure injection (HPI) direct-injection (DI) compression ignition (CI) engine.

This was performed using the Rutgers high-speed multi-spectral infrared (IR) system combined with data analysis spectrometric methods on a DI-CI engine apparatus equipped with a new electronic-controlled (EC) HPI system. The study was also conducted to help developing a high power density DI-CI engine by obtaining necessary engine information, which led us to the new study to be carried out next.

3. Methodology of the Study

The investigation of new EC HPI DI-CI engine combustion processes faces a new dimension of challenge: Difficulties at present appear to range over the physical processes as well as the chemical reactions in the engine cylinder, as briefly discussed next.

3-1. Spray Plume by HPI?

It is highly probable that Diesel fuel is under a super critical pressure in a HPI (of an operating engine) prior to exiting the injector tip. If it is the case, it is also probable that the fuel stream in the nozzle hole and-or off the tip before the break-up would have some form of cavitation. Also, it is a common observation in the use of an HPI that its fuel jet runs into a shock wave due to the high-speed flow leaving the injector-tip. This is not the same kind of operating environment as in the conventional low-pressure injection spray formation. The difference of which has little been documented or studied.

This consideration leads to an expectation that the existing droplet formation (model) formulae developed for a spray plume from the conventional low-pressure injector would no longer be useful for computational models simulating HPI Diesel combustion. There is no doubt that an HPI spray would generate a finer droplet distribution compared with its conventional counter part (if not a more of gaseous jet formation as it leaves the nozzle hole), which would then facilitate the preflame reactions in the spray.

In order to further support this argument, the following is discussed. According to our study, when the conventional (low pressure) cam-driven PT injector was used in the engine to be described below, no significant preflame reaction was observable. On the other hand, the in-cylinder reaction in the same engine equipped with an HPI exhibited quite obvious preflame reactions during almost the entire period of ignition delay. Does this finding mean that there are significant differences in chemical reactions in the spray plume by the respective injection units? Dramatically improved engine performance (as mentioned above) plus the immediate start of preflame reaction upon fuel injection were observed in our laboratory with the use of HPI. This raised the question of whether the fuel spray is altered not only in the physical nature (droplet distribution, etc.) but also in the chemical state of the fuel (e.g. promoting the break-up of molecules due to a rapid temperature rise in the post-shock-wave flow).

Again, the possible alteration of the chemical state of the fuel considered above is a condition after it has gone through the transition-expansion from a super critical state and the shock wave to a self-ignition environment, which is not expected in an engine with the conventional low-pressure injector.

Considering that the start of the progressive chemical reaction in the cylinder is not considered in the present DI-CI engine computational models, the inclusion of realistic preflame reactions over a HPI spray plume in a CI engine appears to be a remote possibility at present. Because of the limited amount of understanding at this time, some extensive experimental findings of the reaction are expected to help fill this void.

(For the sake of convenience, the preflame reactions observed in both a DI-CI engine with our HPI and an SI engine are explained after the apparatus is described.)

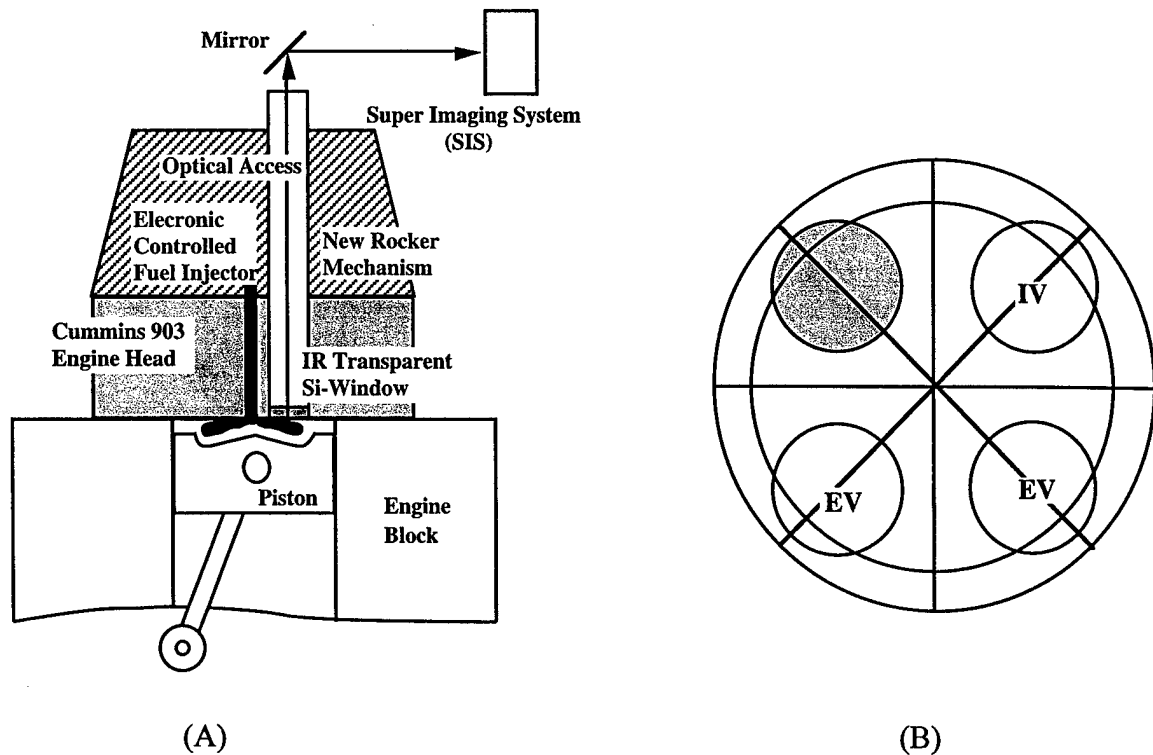


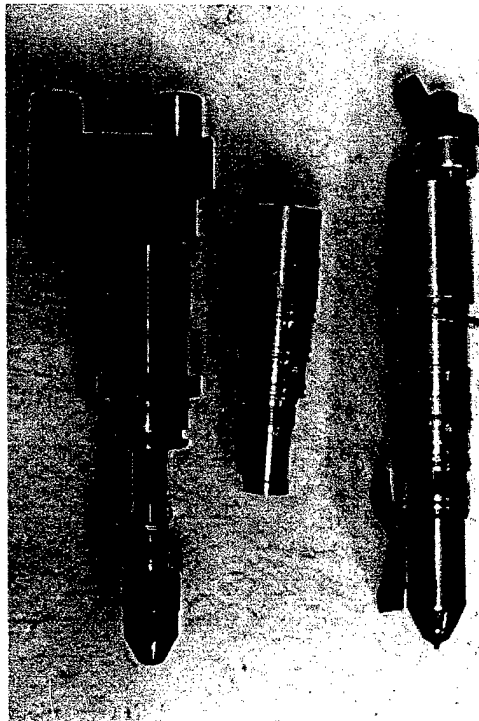
Fig. 1. (A) Single-cylinder Engine Mounted with Cummins 903 Cylinder Head with Optical Access and (B) Optical Access (shaded area).

3-2. Engine Apparatus.

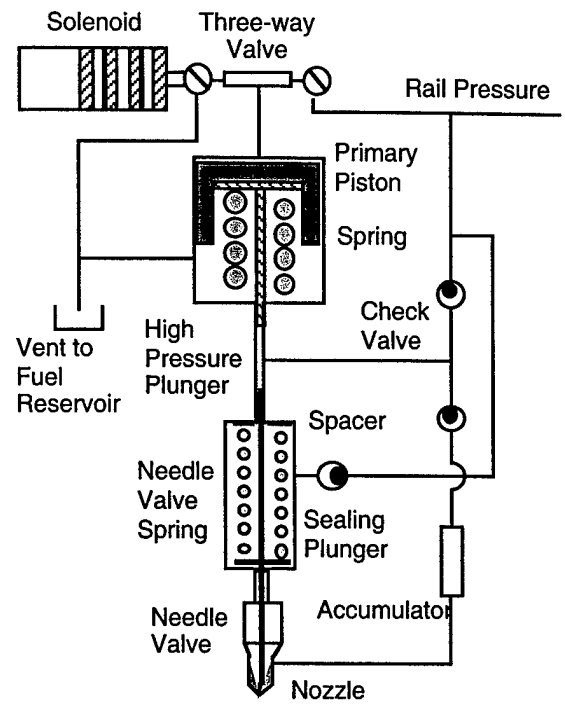
Our optical engine apparatus (Fig. 1) with a new HPI unit has the capability of investigating in-cylinder processes. This single cylinder engine was constructed based on Cummins 903 engine, where one of two intake valves was converted to an optical access (represented by a shaded circle), which is nearly big enough to investigate one spray plume as shown in Fig. 2. Since the Cummins 903 engine is widely known, no additional elaboration is made on the apparatus, although more details may be found in the Appendix.

3-3. HIP Unit.

Thanks to our earlier experience of fabricating an HPI as reported earlier [9, 12], a better high-pressure injection (HPI) unit has been designed, fabricated, tested and fully characterized in our ICE Laboratory. This system design was based on the BKM Servo-jet system [13] but the entire unit was redesigned in order to directly feed the low-pressure fuel through the cylinder head (in the same way as in a Cummins 903 engine), which ranges from 500 to 1800psi. To further elaborate this point, it is noted that the original BKM system required a separate fuel line connected to a gear pump providing the line pressure, which made it impossible to be in compatible with the cylinder head described above. Consequently, it was necessary to redesign the entire unit as shown in Fig. 3.



(A)



(B)

Fig. 3. (A) Photos of Our new High Pressure Injection Unit (Right, designed-fabricated-tested at Rutgers University, compared with BKM's Servo-jet (Left), (B) Schematics of Pressure-intensified System Concept.

The line pressure is intensified in the HPI by 17.5-fold to achieve an injection pressure as high as 31,500psi. This photo shows our new HPI unit after testing in the engine explained above and our earlier HPI in comparison with a PT unit. Note that our earlier HPI had injection pressure of about 26,000psi. (It is also mentioned here that the original goal of building our new HPI was to fabricate a unit capable of delivering over 40,000psi. It was found to be difficult to achieve, however, due to the uncertainty in selecting proper materials, which would dictate the durability of the unit. As a practical compromise and interim solution, the present unit for 31,500psi was built.)

Mentioning the characterization of this new unit, it seemed to be highly advantageous if the fuel flow rate is known for injection pressures independently varied (controlled by the line pressure) at different engine speeds. In exploring this possibility (instead of measuring the fuel flow rate in every engine operation), some extensive and repetitive measurement was conducted in order to ensure the reproducibility and predictability of the entire unit. The performance of this new hydraulic system was observed to be very precise: For example, the fuel delivery of this new injector system is found to be entirely independent of engine speed.

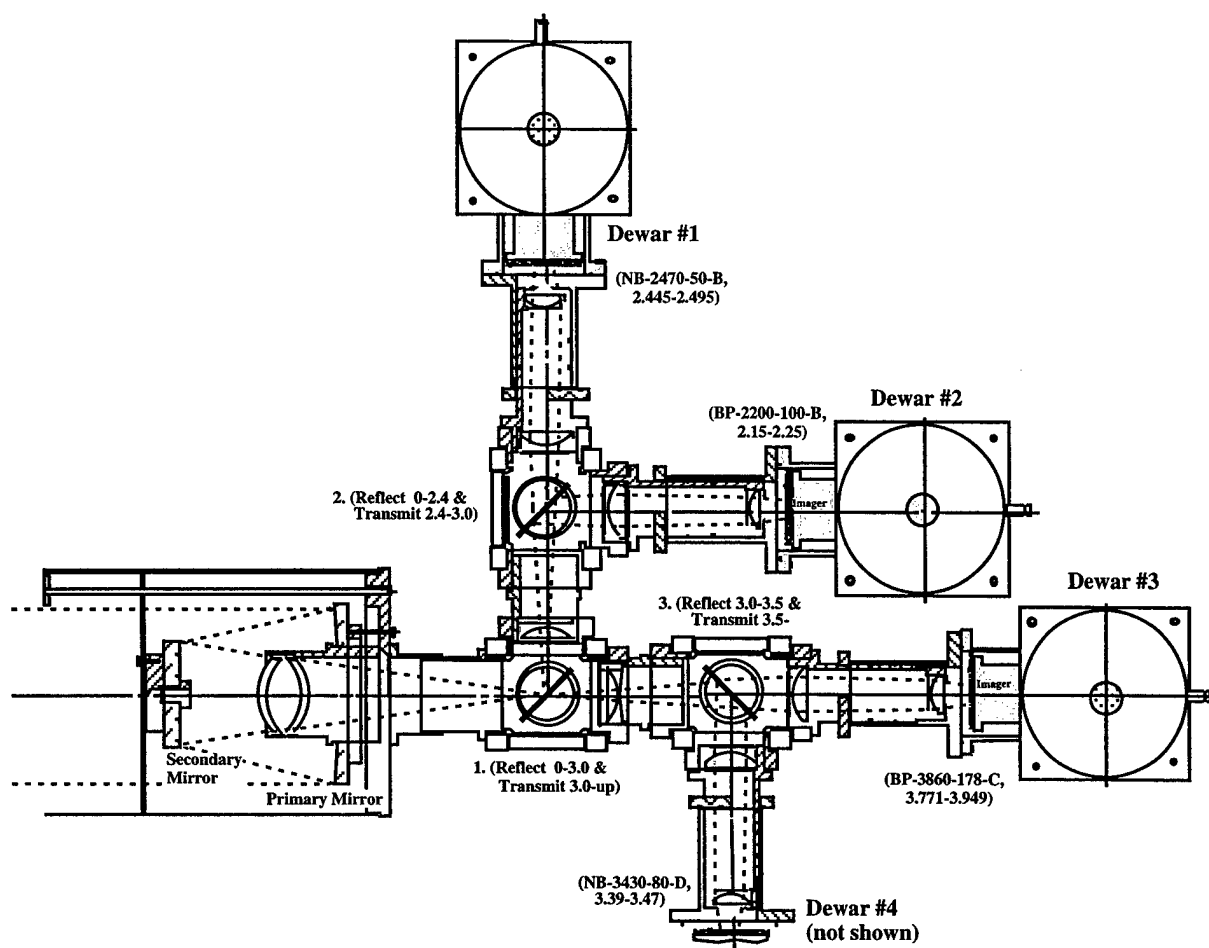


Fig. 4. Optical Portion of Rutgers High Speed Infrared Spectral Imaging System.

3-4. Rutgers Super Imaging System (SIS).

Technology advancements in the electro-optical area achieved in recent years offer new possibilities of *quantitative images* of the complex reactions, i.e., many data points simultaneously obtained over the reactor. The development of a high speed IR spectral imaging system, which is also referred to as the Rutgers System or Super Imaging System (SIS) by others, was an attempt to implement this possibility. Figure 4 shows the schematics of the optical portion of the SIS, which basically lines up four (4) units of the high speed digital IR imaging system (with 64x64 data point matrix) to a single optical assembly in order to simultaneously capture four images in separate spectral bands. Note that the new electronic units as mentioned earlier have made it possible to operate each imaging unit at a rate of over 2,000 frames/sec. The memory system, which was also designed and fabricated in our laboratory, is capable of handling over $4 \times 2,000 \times 64 \times 64$ - 12 bits per sec. Ideally, the system is to obtain four separate sets of time-resolved data distributions. Since this system has been explained in the past, and in recent publications [9-12], one of which is included in the Appendix, no further description is made here.

4. Other Research Opportunities

Recognizing usefulness of research diagnostic tools developed during the course of ARO-sponsored study, we have been able to attract some strong interest of employing the methods on study of spark-ignition (SI) engines. This led to close collaboration with research individuals from auto-manufacturers, fuel additive makers and refiners (e.g. Ford, Ethyl, and SUNOCO). (In a sense, the usefulness of the methods developed under ARO support has been truly recognized .) Some of results obtained in those collaborations are included in the following.

5. Results and Discussion

Probably the best way of presenting results obtained under the present sponsorship may be by listing the publications and summarizing what are reported in individual papers. The full text of these papers is included in Appendix.

1. High-speed Imaging from Consecutive Cycles
(SAE paper 2001-01-3486)
2. Visualization of Preflame and Combustion Reactions in Engine Cylinders
(SAE Paper 2000-01-1800)
3. In-cylinder Liquid Layers, Cause of unburned hydrocarbon and Deposit Formation in SI Engines? (SAE paper 1999-01-3579)
4. Study of High-pressure Injection DI Diesel Engine
(SAE Paper 1999-01-3494)
5. Direct Injection Diesel Engine Operated with Propane-DME Blend Fuel
(SAE Paper 982536)
6. Diesel Engine Response to High Fuel-injection Pressures
(SAE paper 982683)
7. Engine Performance and Exhaust Characteristics of Direct-injection Diesel Engine Operated with DME (SAE paper 972973)
8. Quantitative Imaging of In-cylinder Processes by Multispectral Methods
(SAE Paper 970872)
- 5-1. High-speed Imaging from Consecutive Cycles**
(SAE paper 2001-01-3486)

A new high-speed data handling method has been developed by advancing the Rutgers Super Imaging System (SIS) (having four units of infrared digital cameras) in order to capture successive in-cylinder spectral thermal images at high rates from consecutive cycles (HSI-CC).

The present HSI-CC method has been made possible by incorporating recent advancements in digital data handling peripheral devices and development of new dedicated computer programs including an MS Window-based operating system (WOS) for the SIS.

The SIS-HSI-CC permits simultaneous high-speed imaging of four (4) sets of 64 sequential images (or 128 images) at rates of over 2,000 frames/camera/sec in each cycle, which can be repeated for as many as 150 consecutive cycles. This amounts to a data volume of nearly 400 mega bytes (in 12-bit dynamic resolution) in an experiment. Key considerations for achieving the system performance include a new technique of storing the image data and relevant engine measurements (e.g. pressure-time and fuel injection histories) during the reaction period. The stored digital data is then transferred to two separate PC memory packs during the non-reacting period.

The image and corresponding engine data is reviewed in situ using the Rutgers Animation Program (RAP) (prior to conducting the next experiment). The RAP is a new computer program enabling simultaneous display on a PC screen of many (at present 50 pieces of animation) digital movies in a controlled manner, which is also used for analysis/presentation of raw and processed data. For example, the RAP can display results from 10 successive cycles of four geometrically identical spectral images and a matching pressure-time history per cycle.

This new SIS-HIS-CC-WOS-RAP is employed in investigation of flame development during the cold start on a spark-ignition engine. Some of the results discussed in this paper were obtained during the first 100 firing cycles from the engine at 13°C (55° F).

5-2. Visualization of Preflame and Combustion Reactions in Engine Cylinders (SAE Paper 2000-01-1800)

In-cylinder reactions of several internal combustion engine configurations were investigated using a high-speed four-spectral infrared (IR) digital imaging device. The study was conducted with a greater emphasis on the preflame processes by mutually comparing results from different engine-fuel systems.

The main features of the methods employed in the study include that the present multi-spectral IR imaging system permits us to capture progressively changing radiation emitted by new species produced in-cylinder fuel-air mixtures prior to being consumed by the heat-releasing reaction fronts.

The study of the Diesel or compression-ignition (CI) engine reactions was performed by varying several parameters, e.g. injection pressures, intake air temperature, fuel air ratio, and the start of injection. They were investigated also for the following mixture preparation-ignition methods: (1) direct-injection of Diesel fuel; (2) homogenous charge (fumigation) ignited by pilot injection and (3) homogeneous charge self-ignition.

For the spark-ignition (SI) engine processes, the reactions were investigated using different fuels including gasoline and propane, which were introduced by either the port-fuel-injection unit or carburetor.

The sequential images captured of in-cylinder preflame reactions were compared with those of the subsequent combustion reactions. In particular, they are expected to serve as an overall survey of visualizing the preflame processes in the cylinder.

5-3. In-cylinder Liquid Layers, Cause of Unburned hydrocarbon and Deposit Formation in SI Engines?
(SAE paper 1999-01-3579)

In-cylinder reaction processes in a production port-fuel-injection (PFI) spark-ignition engine having optical access were visualized using a high-speed four-spectra IR Imaging system. Over one thousand sets of digital movies were accumulated for this study. To conduct a close analysis of this vast amount of results, a new data analysis and presentation method was developed, which permits the simultaneous display of as many as twenty-eight (28) digital movies over a single PC screen in a controlled manner, which is called the Rutgers Animation Program (RAP for short).

The results of this parametric study of the in-cylinder processes (including the period before and after the presence of luminous flame fronts) suggest that, even after the engine was well warmed, liquid fuel layers (LFL) are formed over and in the vicinity of the intake valve to which the PFI was mated. The sluggish consumption of those LFL, which continued even until the exhaust valve opens, is expected to be one of the main emission sources of unburned hydrocarbon.

Inspection of deposit formation on over twenty-four (24) cylinders (of the engines provided by the manufacturer after some lengthy operation) revealed a predictable pattern. Deposits were found to occur only in areas where the reacting LFL were observed.

The mutually consistent findings from this parametric study are reported. Some of the results from the study will be presented by using the RAP at the meeting.

5-4. Study of High-pressure Injection DI Diesel Engine
(SAE Paper 1999-01-3494)

Visualization of in-cylinder reaction processes and performance analysis of a direct-injection Diesel engine equipped with a high injection pressure (HIP) unit were conducted. The study was directed towards evaluation of high-power-density (HPD) engine design strategies, which utilize more intake air operating at rich overall fuel-air ratios.

Two separate engine apparatus were used in this study: a Cummins 903 engine and a single-cylinder optical engine equipped with the same family engine components including the cylinder head. The engines were mated with an intensifier-type HIP fuel system fabricated at Rutgers which can deliver fuel injection pressure of over 200 MPa (30,000psi).

The one-of-a-kind high-speed four-band infrared (IR) imaging system was used to obtain over fifteen hundred sets of spectral digital movies under varied engine design and operating conditions for the present analysis. In order to analyze and present this large amount of results, a new data analysis and presentation method was developed (called Rutgers Animation Program, RAP for short). RAP is a computer program permitting simultaneous display of as many as twenty-eight (28) sets of digital movies over a single PC screen for mutual comparison in a controlled manner.

Among the findings from the study is that the in-cylinder imaging performed within the first several cycles may not represent what is happening in a typical warm engine. In addition, the spray development and subsequent reactions of the HIP unit may not be comparable to those of low-pressure conventional injector units. In-cylinder processes and engine performance of an HPD engine affected by various factors are also described in the paper which include: the injection pressure, intake air temperature, and overall air-fuel ratio.

5-5. Direct Injection Diesel Engine Operated with Propane-DME Blend Fuel (SAE Paper 982536)

A novel way of using low-cetane-number petroleum gases in a compression ignition (CI) engine is introduced, by directly injecting blends of such fuels with dimethyl ether (DME), a high-cetane-number alternative fuel for low soot emissions. This method both extends advantages of DME and complements its deficiency. Although DME mixes with most hydrocarbon fuels in any ratio, in order to demonstrate the feasibility of the new method and facilitate the analysis, DME-propane blends were investigated in a direct injection CI engine. Some findings of the study are listed.

In the engine operated by DME and propane blends, there was no need for significantly increasing the complexity of the fuel system than that employed in the use of neat DME. For the same reason, this method eliminates or minimizes cumbersome hardware necessary when the said gaseous fuels are separately introduced in CI engines.

When the content of propane was increased, which accordingly increased the heating value of the blend, the start of injection lagged, and self-ignition became sluggish itself, which resulted in a delayed start of heat release.

When the engine load was low, the more the propane content, the higher the specific fuel consumption and the greater the emissions of unburned hydrocarbon. This was interpreted in terms of an over-mixing due to rapid vaporization of propane out of the blend to diffuse and also low combustion chamber temperatures.

Mentioning other emissions with the DME-propane blends, soot emission was negligible, and the specific NO_x emission was in general lower than with neat DME, which decreased with an increase in both the propane content and engine load.

5-6. Diesel Engine Response to High Fuel-injection Pressures (SAE paper 982683)

A single-cylinder direct-injection (DI) Diesel engine (Cummins 903) equipped with a new laboratory-built electronically controlled high injection pressure fuel unit (HIP) was studied in order to evaluate design strategies for achieving a high power density (HPD) compression ignition (CI) engine.

In performing the present parametric study of engine response to design changes, the HIP was designed to deliver injection pressures variable to over 210 MPa (30,625psi).

Among other parameters investigated for the analysis of the HPD DI-CI engine with an HIP were the air/fuel ratio ranging from 18 to 36, and intake air temperature as high as 205°C (400°F). The high temperatures in the latter were considered in order to evaluate combustion reactions expected in an uncooled (or low-heat-rejection) engine for a HPD, which operates without cooling the cylinder.

Engine measurements from the study include: indicated mean effective pressure, fuel consumption, and smoke emissions.

It was found that a Diesel engine incorporated with an HIP under varied operational conditions, including those encountered in uncooled engine design needs variation of injection parameters, namely the start of injection and the rate shape.

When the engine operating condition shifts, the rapid variation of those parameters are needed in order to optimize the engine power delivery and fuel consumption as well as to minimize smoke emissions.

Other engine responses to the varied parameters in the high-pressure Diesel engine are also reported in the paper.

5-7. Engine Performance and Exhaust Characteristics of Direct-injection Diesel Engine Operated with DME (SAE paper 972973)

Neat dimethyl ether (DME), as an alternative fuel candidate for Diesel engines, was investigated by measuring primarily engine performance and exhaust gas characteristics. In addition, other responses of the engine to the new fuel were also determined at the same time, including the injector needle lift and heat release. The engine measurements with this fuel were compared with those obtained by using conventional Diesel fuel.

Findings from the present work include: (1) It was necessary to add a small amount of lubricating additives to DME, if a conventional fuel injection system is employed. This was to achieve satisfactory injector performance and to minimize some excessive wear. (2) Engine performance for both fuels was basically comparable to each other, except for a better energy conversion efficiency with DME. (3) In the DME-operated engine, emissions of soot and unburned hydrocarbon (THC) were almost negligible, but NO_x emission was about the same as in the Diesel oil operation. (4) The reduction of NO_x emission by delaying the injection time was highly significant with DME.

5-8. Quantitative Imaging of In-cylinder Processes by Multispectral Methods (SAE Paper 970872)

With the objective of achieving better investigation of engines-fuels by obtaining instantaneous quantitative imaging of in-cylinder processes, several steps have been taken for some years at Rutgers University. They are: (1) Construction of a new multispectral high-speed infrared (IR) digital imaging system; (2) Development of spectrometric analysis methods; (3) Application of the above to real-world in-cylinder engine environments and simple flames. This paper reports some of results from these studies.

The one-of-a-kind Rutgers IR imaging system was developed in order to simultaneously capture four geometrically (pixel-to-pixel) identical images in respective spectral bands of IR radiation issued from a combustion chamber at successive instants of time and high frame rates.

In order to process the raw data gathered by this Rutgers system, three new spectrometric methods have been developed to date: (1) dual-band mapping method; (2) new band-ratio method; and (3) three-band iteration method. The former two methods were developed to obtain instantaneous distributions of temperature and water vapor concentrations, and the latter method is to simultaneously find those of temperature, water vapor and soot in gaseous mixtures, i.e., to achieve quantitative imaging.

Applications of these techniques were made to both SI and CI engine combustion processes as well as bench-top burner flames. Discussion is made on the methods and new results.

6. Summary

During the course of the present study supported by ARO, some remarkable progresses were achieved as reflected by publications listed above. As mentioned briefly earlier, while the main research objectives were to investigate DI-CI combustion processes, the new research methods developed in the study were applied to investigation of SI engine in-cylinder reactions to obtain several significant findings.

It is noted that in spite of insufficient amount of resources in conducting this ambitious study (on support of one graduate student only), the financial support from industrial concerns (to study SI engine-fuels-additives) has greatly helped obtain the results. Some of achievements are summarized below.

- . The advance Rutgers Super Imaging System (SIS) having four units of high-speed infrared (IR) digital cameras have been achieved, which delivers unprecedented imaging capabilities compared to those employed by others in the past.

- . Since the SIS can capture not only images of visible high-temperature reactions but also those in the IR domain, some of invisible processes are obtained, e.g. thermal images of exhaust valve during non-combustion period and preflame reactions.

- . The SIS can simultaneously capture four (4) geometrically identical images in respective spectral bands at rates over 2,000 frames/sec/camera. Ideally, distributions of four separate sets of spatial distributions of information (as to in-cylinder reactions) are obtained at successive instants of time.

- . The raw data obtained by using the SIS is basically four sets of digital data matrices (64x64), which is equivalent to those obtainable when 16,384 ((64x64) x 4) units spectrometers. When they are processed by using our new spectrometric methods, "quantitative imaging" is achieved. (New advanced methods are being developed at present.)

- . The SIS has recently been further advanced. The system can be used now to capture high-speed spectral images from consecutive cycles, which has never been achieved by others in the past. Due to the special nature of handling vast amount of data from this work, it was essential to develop a package of efficient computer programs, which are all one-of-a-kind. Note that the present study was directed to "engine research," not toward development of "trouble-free commercial" system, there are many loose ends in the prototype methods requiring continuous maintenance and debugging.

- . When SIS is employed in a typical engine experiment, it was not unusual to accumulate more than thousand sets of movies. Letting aside analysis of those results, even a simple review is unattainable by the conventional methods, e.g. running them in video players. In order to most efficiently overcome such limitations, a new package of computer program has

been separately developed, which is called Rutgers Animation Program (RAP). Among the key features of the RAP that many movies can be simultaneously displayed over a single PC screen. Note that the matching pressure-time (p-t) history can be also displayed on the same screen. It is emphasized that the RAP developed during the course of this work is truly an essential tool facilitating the use of the SIS and the analysis of its results.

. When SIS was applied to our optical DI-CI engine, it was discovered that there is no distinction between physical and chemical delays, as reported by others in the past. In order words, the fuel spray introduced into the combustion chamber immediately commences chemical reaction. This therefore enabled us to determine spatial variations of preflame-reactions during the ignition delay period, which is also the first discovery of the kind.

. It was found that the regions having strongest preflame reaction matches with the having the first images of water vapor resulted from the flame kernel. It is noted however that they did not match with each other in some cases.

. The determination of progressively changing preflame reactions clearly confirmed that they are low-temperature chemical kinetic processes. That is, the images of preflame reactions ceased as soon as high-temperature reactions take over the processes.

. When four geometrically identical spectral images are simultaneously obtained from the same reaction chamber, it would be most reasonable to expect that they appear to be similar to each other. It was quite unusual to discover that it was not the case in some cases of spray combustion (and also in SI engine when liquid fuel was consumed). In some extreme cases, while global motions of flows (reaction fronts) were in opposite directions. Without further elaboration, this observation will be more closely studied in the nest study.

. Thanks to unique diagnostic features of the SIS, the presence of liquid fuel being consumed at the later stage of combustion (typically after the visible radiation from high-temperature reaction fronts disappeared) in relatively warm SI engines was first discovered.

. The slowly consumed liquid fuel layers, particularly around the intake valves as mentioned above, was suggested to be a main source of unburned hydrocarbon emissions from (even warm) SI engine. Again, this was first reported in the engine research community.

It is mentioned here that the use of the SIS and other new diagnostic methods offered exciting opportunities of *exploratory* investigation of in-cylinder processes. That is, whenever the results obtained by the SIS, it was not unusual to find something unexpected. In addition to the limitations in manpower (one graduate student) and resources, the excitement from those experience are believed to have drove us away from development of quantitative imaging methods, which may carry more academic values.

Looking back the first time when the first step taken for development of the SIS system (i.e., design and fabrication of single-unit IR camera) about 13 years ago, the system construction know-how accumulated to date are considered to be remarkable: we are greatly grateful for the opportunity of working under the ARO program.

7. References

1. Tow, T.C., Pierpont, D.A. and Reitz, R.D., "Reducing Particulate and NOx Emissions by using Multiple Injections in a Heavy Duty D.I. Diesel Engine," SAE Paper-940897.
2. Han, Z., Hampson, G., Reiz, R., and Uludongan, A., "Mechanism of Soot and NOx Emission Reduction using Multiple-injection in a Diesel Engine," SAE Paper-960633, 1996.
3. Shundoh, S., Komori, M., Tsujimur, K., Kobayashi, S., "NOx Reduction from Diesel Combustion using Pilot Injection with HPI," SAE Paper-920461, 1992.
4. Kamo, L., Kleyman, and Bryzik, W. and Reid, M., "Coatings for Improved Engine Performance," SAE Paper-970207, 1997.
5. Clasen, E., Song, K., Campbell, S., and Rhee, K.T., "Fuel Effects on Diesel Combustion Processes," SAE Paper-962066, 1996.
6. Kajitani, S., Chen, Z., Konno, M., Rhee, K.T., "Engine Performance and Exhaust Characteristics of Direct-injection Diesel Engine Operated with DME." SAE Paper-972973, 1997.
7. Desai, R.R., Gaynor, E., Watson, H.C., "Giving Standard Diesel Fuels Premium Perfmc. using Oxygen-Enriched Air in Diesel Engines, " SAE Paper-932806, 1993.
8. Cernansky, N. "High-pressure Preignition Chemistry of Hydrocarbons and Hydrocarbon Mixtures," ARO/AFOSR Contractors Meeting, June 17-19, 1997.
9. Clasen, E., Campbell, S., and Rhee, K.T., "Spectral IR Images of Direct-Injection Diesel Combustion by High-Pressure Fuel Injection," SAE Paper-950605, 1995
10. Song, K., Clasen, E., Chang, C., Campbell, S., Rhee, K.T., "Post-flame Oxidation and Unburned Hydrocarbon in a Spark-ignition Engine," SAE Paper-952543, 1995.
11. Capmbell, S., Clasen, E., Chang, C., ad Rhee, K.T., "Flames and Liquid Fuel in an SI Engine during Cold Start," SAE Paper-961153, 1996.
12. Chang, C., Clasen, E., Song, K., Campbell, S., Jiang, H., Rhee, K.T., "Quantitative Imaging of In-cylinder Processes by Multispectral Methods," SAE Paper-970872, 1997.
13. Abata, D., Stroia, B.J., Beck, N.J., and Roach, A.R., "Diesel Engine Flame Photographs with High Pressure Injection," SAE Paper-880298, 1988.
14. Ludwig, C.B., Malkmus, W., Reardon, J.E., and Thomson, J.A.L., Handbook of Infrared Radiation from Combustion Gases, NASA SP-3080, 1973.
15. Gaydon, A.G. and Wolfhard, H.D., *Flames, Their structure, radiation and temperature*, Chapman and Hall, Ltd., London, 1970.

High-speed Imaging from Consecutive Cycles

M. Jansons, S. Lin, and KT Rhee

Rutgers, The State University of New Jersey

Piscataway, NJ 08854-0909

Copyright © 1998 Society of Automotive Engineers, Inc.

ABSTRACT

A new high-speed data handling method has been developed by advancing the Rutgers Super Imaging System (SIS) (having four units of infrared digital cameras) in order to capture successive in-cylinder spectral thermal images at high rates from consecutive cycles (HSI-CC).

The present HSI-CC method has been made possible by incorporating recent advancements in digital data handling peripheral devices and development of new dedicated computer programs including an MS Window-based operating system (WOS) for the SIS.

The SIS-HSI-CC permits simultaneous high-speed imaging of four (4) sets of 64 sequential images (or 128 images) at rates of over 2,000 frames/camera/sec in each cycle, which can be repeated for as many as 150 consecutive cycles. This amounts to a data volume of nearly 400 mega bytes (in 12-bit dynamic resolution) in an experiment. Key considerations for achieving the system performance include a new technique of storing the image data and relevant engine measurements (e.g. pressure-time and fuel injection histories) during the reaction period. The stored digital data is then transferred to two separate PC memory packs during the non-reacting period.

The image and corresponding engine data is reviewed in situ using the Rutgers Animation Program (RAP) (prior to conducting the next experiment). The RAP is a new computer program enabling simultaneous display on a PC screen of many (at present 50 pieces of animation) digital movies in a controlled manner, which is also used for analysis/presentation of raw and processed data. For example, the RAP can display results from 10 successive cycles of four geometrically identical spectral images and a matching pressure-time history per cycle.

This new SIS-HIS-CC-WOS-RAP is employed in investigation of flame development during the cold start on a spark-ignition engine. Some of the results discussed in this paper were obtained during the first 100 firing cycles from the engine at 13°C (55° F).

INTRODUCTION

High-speed imaging (HSI) methods have been employed in engine-fuel studies in various aspects, e.g. in-cylinder spray

development in a Diesel or compression ignition (CI) engine [1]*; flame kernel growth in an SI engine [2]; jet impingement in a bench-top device [3]; and many more. In addition to such imaging in the visible range, HSI was also made in the infrared (IR) range simultaneously in several spectral bands [4,5].

Although some of the HSI were performed at very high framing rates, the number of sequential images was often relatively small and they were mostly gathered within a single cycle. (In some cases, only one picture was taken at a crank angle (CA) per cycle, which was repeated at other CAs then to compose a series of "consecutive" images.) While those HSI techniques have undoubtedly helped improve our understanding of many complex rapid processes, they may be useful to a limited extent, however, in studying many problems, particularly those involving cyclic variations and transient changes (such as those during the cold start period).

For example, there is some evidence that CI in-cylinder processes observed during the first several cycles even in a "preconditioned" engine for HSI may be still different from those in a fully warmed engine [6]. (The preconditioning means that the engine is circulated with a heated coolant at over 90°C and imaging is done within the first several cycles thereafter.) A possible interpretation of this observation was that in such an engine with heated coolant the combustion chamber surface did not reach a temperature high enough to exhibit representative compression-ignition and flame propagation as found at a well-warmed condition achieved after many cycles of continuous firing.

In order to achieve a better understanding of such problems, it would be desirable to achieve HSI from many consecutive cycles (HSI-CC). Such a goal has been unthinkable in the past, however, due to many reasons. Chief among them are the facts that the existing HSI systems mostly permits within a single cycles due to the data handling limit and that the optical window is rapidly covered with soot layers degrading the quality of images when the conventional (visible-range) cinematography is employed.

This paper reports the new HIS-CC technique and some results obtained by the methods, which had to overcome those difficulties.

*Numbers in parentheses designate references at end of paper.

APPARATUS

Since the new system developed for the HSI-CC has been achieved by advancing our earlier system, a brief discussion is in order on this high-speed four-color digital IR imaging system, called Rutgers or Super Imaging System (SIS) [4-7]. The SIS has four units of high-speed digital IR camera (with imaging rates over 2,000 frames/sec/camera) connected to a single optical package containing three custom-made spectral beam splitters. This divides the spectral range into four separate sub-ranges relayed to individual cameras. With a narrow-band filter assigned to each camera, the SIS was operated to obtain four sets of geometrically identical digital data matrices (i.e., images) in respective spectral bands by using the same electronic control unit and an operating system (OS). Images taken by the SIS were typically 64 sequential images simultaneously obtained from a cycle in spectral bands with center-wavelengths (bandwidth in nm) of 3.80 (185), 3.42 (250), 2.47 (70), and 2.20 (100) μm .

Reasons for choosing these filter bands in the SIS described earlier [5,7] are briefly explained here. According to spectral data included in NASA IR Handbook SP-3080 [8], the "3.80-band" and 2.2-band include almost no radiatively participating species (out of hydrocarbon-air combustion products), which therefore in principle enables capturing thermal images behind the flame fronts. On the other hand, the 2.47- and 3.42-bands are expected to exhibit radiation emitted by water vapor. The digital data matrices in those spectral bands were processed in order to achieve quantitative imaging by using our spectrometric methods, that is distributions of water vapor, soot and temperature [9].

In the past the digital data read from a Pt-Si focal-plane-array in 64x64 form in each cryogenically cooled camera of the SIS were temporarily stored in four laboratory-built memory packages prior to being transferred to the PC hard drive using a special imaging system. Note that when development of the earlier SIS was initiated in late 1980, there was no reasonable high-speed memory package in the market applicable for the purpose, and therefore they were all newly designed and fabricated in our laboratory. (The special image processing system was also necessary in the data handling, which is now readily attainable by using commercially available frame-grabbers.) The data transfer from those memory packages to the PC took approximately 30 seconds, which was a minimum amount of time required prior to undertaking the next HSI by the old SIS.

Before discussing the methodology of HSI-CC, the new OS for SIS is briefly explained, which was concurrently developed together with the new data handling techniques. The earlier OS for the four-camera SIS was a collection of many mutually incorporating computer programs prepared during the course of our system development since our first single-camera imaging system design was initiated, which were all written in DOS.

Recognizing needs for a Windows-based OS (WOS) several years ago, let alone obvious reasons for convenience, its development was initiated as a part of activities towards the SIS HSI-CC, which incorporates various I/O devices and software controlled by similar Windows-base programs. The

new WOS was constructed (using MS C++) to offer a greater flexibility in data handling in Rutgers Animation Program (RAP), which has been developed also in a Windows environment.

Mentioning the advantages of using RAP, when high-speed imaging is performed in an engine study it is not unusual to accumulate many hundreds of movies, in separate spectral bands under different conditions, for example. Even a simple review of those results using the conventional methods (e.g. multiple units of video player) would take an enormous amount of time. When RAP was developed, therefore, in order to achieve goal of simultaneously displaying many movies over a single PC screen in controlled manner, such as the display can be stopped, or reversed, and others. The matching pressure-time (p-t) history is also displayed along with spectral movies (as presented in the meeting). The WOS combined with RAP became an essential requirement in achieving efficient data handling for HSI-CC as discussed next.

In particular, the new WOS came to greatly facilitate the new data handling-controlling capacity of the SIS-HSI-CC, which employs two separate packages of I/O data board housed in two units of PC, respectively. It permits to review results in situ prior to recording them in the hard drive. For example, when an experiment is performed by using this diagnostic system, four hundred sets of movies (in four spectral bands from 100 consecutive cycles) are accumulated plus corresponding p-t histories, which requires some preview before deciding if the result is recorded in the hard drive for subsequent analysis. RAP, an integrated part of the new WOS, is employed to meet this need.

Imaging from Consecutive Cycles. In achieving the HSI-CC capability, two separate PCs were employed. One is loaded with two I/O data boards (Matrox Metro II Digital) having respective factory installed memory packages. The data flow from two cameras is interfaced with each board. The other PC is equipped with a separate I/O data board dedicated to handle various engine data output including p-t and fuel injection histories. (These arrangements of course eliminate the earlier special image-processing device.) The new WOS controls the data acquisition in both computers by using the same timing signals generated from a single central clock and corresponding engine CA markers, which ensures the individual sets of data to be captured concurrently.

The basic idea for achieving the new features of handling data in the HSI-CC is to temporarily store data generated from cameras in the memory package of each I/O board, then to intermittently transfer the data to a high-capacity PC RAM. That is, digital data obtained during the reaction period is rapidly sent to the PC RAM during the remaining (non-reaction) period. The matching data routed via the separate I/O unit in the other computer is transferred to the same RAM at this time. With this data management package, we are able to obtain either 64 or 128 successive images in each cycle per camera from over 150 consecutive cycles, which amounts to a data volume of approximately 400 mega bytes per each experiment. Since this attempt was never made in engine studies earlier, entirely new sub-circuit-boards, cables and software were constructed.

Optical Window and Soot Deposit. One of the most vexing problems encountered in imaging in-cylinder activities is rapid formation of soot layers over the optical window so that the study has been performed only during the first several cycles. Unless this problem is eliminated, the HSI-CC would be useful to only a limited extent.

While the imaging in the visible range is hampered by the soot deposits, it was found that the same in the IR range is relatively less affected by the deposit layer formation [5,6]. For example, thanks to the transparency of soot layers to IR radiation, the quality of IR images obtained from a CI engine after over 200 continuous firing cycles (having the optical window covered with thick opaque soot deposit formation) was still comparable to those captured within a few cycles after the start. The effect of soot deposits was far smaller when imaging was conducted from an SI engine, which was difficult to quantify compared with those in imaging from a CI engine.

Engines with Optical Window. The new HIS-CC has been applied to the investigation of transient processes in an SI engine having optical access. This engine is basically the same engine employed in earlier studies [5,7]. The apparatus was built using a V-8 engine (Ford-4.6) to make only a single cylinder operational. The radiation ray is relayed via an optical path through an extended piston as shown in Fig. 1. Note that the surface-mirror is mounted at 45 degrees with respect to the axis of the hollow extended-piston to, which directs the ray perpendicular to the page. Briefly, Ford-4.6 engine has bore of 90.2mm (3.552in), stroke of 90mm (3.543in) compression ratio of 9.9 to 1. It has four-valve head so that when the engine is warm some distinctive thermal images of two exhaust valves and the spark plug (located at the center) can be obtained even in the absence of flame fronts (or lighting), such as during the intake stroke.

Among the uniqueness of this apparatus include that an entire cylinder block is mated with the actual cylinder head loaded with the factory intake unit and other accessories. This measure of minimizing engine modifications was to preserve the integrity of the real world engine as close as possible. For example, if the coolant flow and intake airflow patterns are altered, the in-cylinder activities would be different from those in the actual engine, particularly when investigating transient (cold-start) phenomena. Note that the crankshaft was newly balanced by taking into consideration of the exact amount of mass added due to the introduction of the extended piston.

Engine Condition. This engine apparatus was circulated through its water jacket with a refrigerated coolant in order to achieve controlled engine temperatures facilitating the investigation of flame propagation such as during the cold start. Some of the results discussed in this paper were obtained during the first 100 cycles from the start after the engine is circulated with a coolant at 13°C (55°F) for a long time (typically an hour).

RESULTS AND DISCUSSION

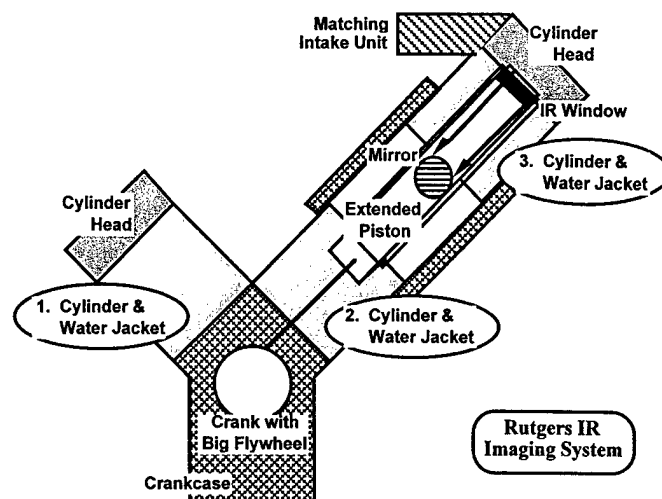


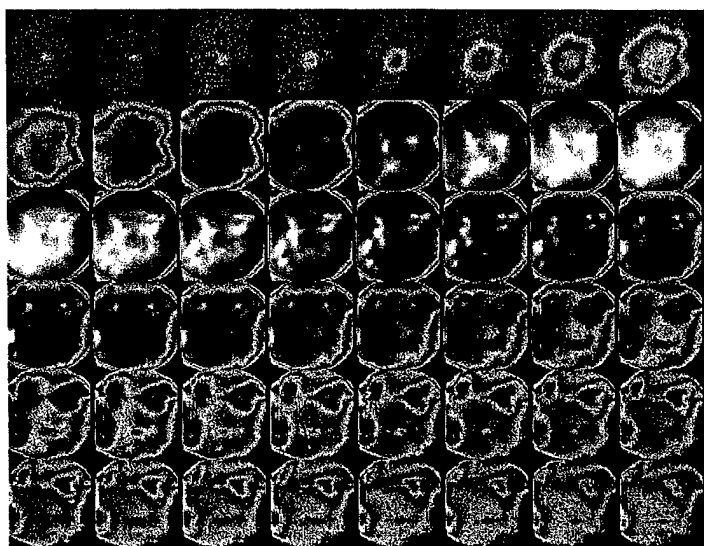
Fig. 1. SI Engine Apparatus for Duplicating Representative In-cylinder Reaction Conditions.

Since one of main purposes of this paper is to explain how the HSI-CC techniques would help understand transient processes in engines, sample results are presented in a way to achieve the goal. It is noted that many sets of movies will be introduced in the actual presentation by using RAP, which is not feasible unfortunately in a printed paper.

Results to be explained in this paper were all obtained at engine speed of 600 rpm for the intake vacuum level of 27.58 kPa (4 psi). The spark time was at 6 CA before top-dead-center (bTDC). The gasoline used in the experiment was regular unleaded acquired from the pump.

Since it was not possible to start the cold engine (e.g. with coolant temperature at 4°C) when the fuel was introduced at a rate for producing a stoichiometric air-fuel ratio, a simple over-rich method was employed. That is, after circulating the cold coolant through the engine for a long time, the fuel was introduced at a rate approximately 4 times ("400-rate") the rate for the stoichiometric ("100-rate") for several consecutive cycles expecting to produce sufficient amount of fuel vapor for the onset of ignition followed by successful flame propagation. After this initial over-rich fueling was repeated for a while, the fuel injector was swiftly adjusted to fuel at a rate to produce the stoichiometric fuel-air ratio as detailed in the later discussion.

Determination of the fuel injection rate for the stoichiometric combustion is explained. In order to minimize soot deposit formation (over the window if gasoline is used particularly when the engine is cold), first the engine was operated with a propane-air mixture for a while in order to attain a warmed engine condition. Then, the fuel was switched to gasoline to monitor the output from the universal exhaust gas oxygen sensor (UEGO), which led to determination of a desired adjustment of fuel injection for the stoichiometric rate. The UEGO was calibrated in actual engine operations.



-7	-5	-3	-1	1	3	5	7
9	11	13	15	17	19	21	23
25	27	29	31	33	35	37	39
41	43	45	47	49	51	53	55
57	59	61	63	65	67	69	71
73	75	77	79	81	83	85	87

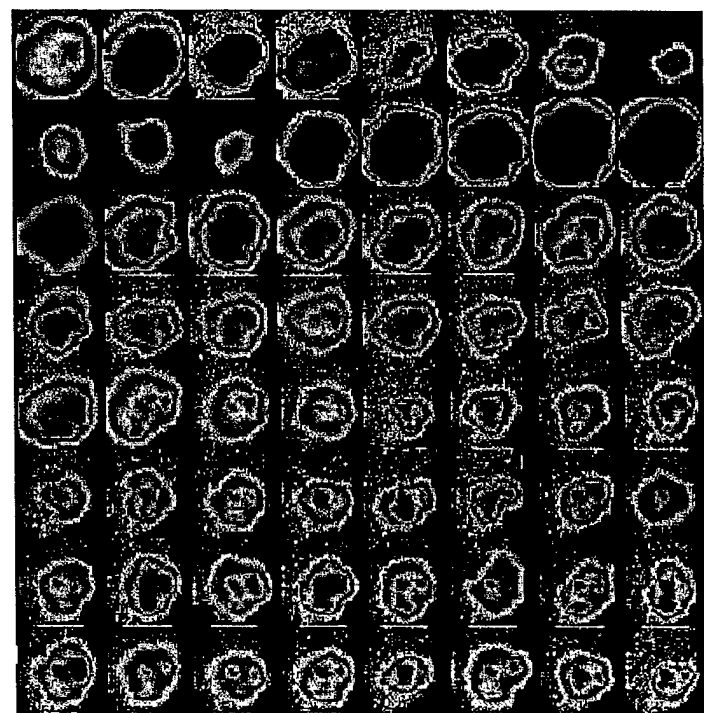


Fig. 2 (top). High-speed IR Images in 18th Cycle from Start.

Table-I (middle). Look-up-table Indicating CA for Fig. 2.

Fig. 3 (bottom). Images at 9 aTDC from Consecutive Cycles.

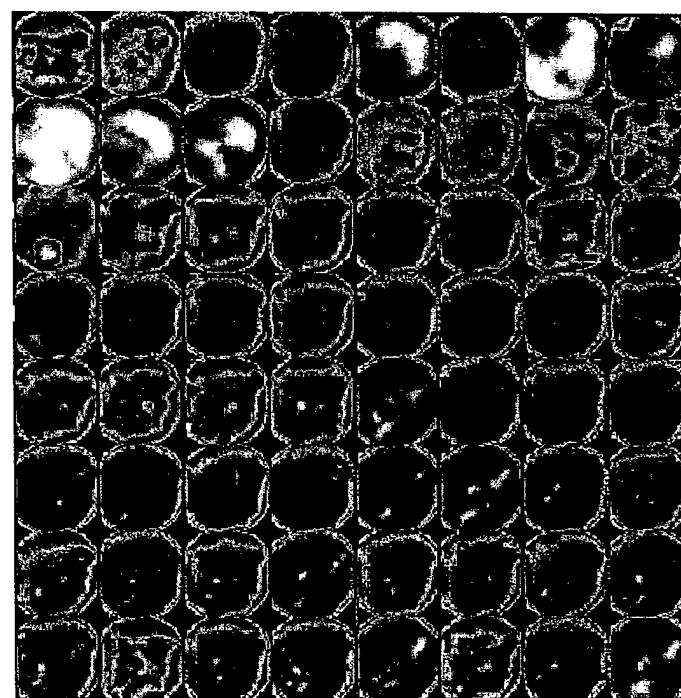
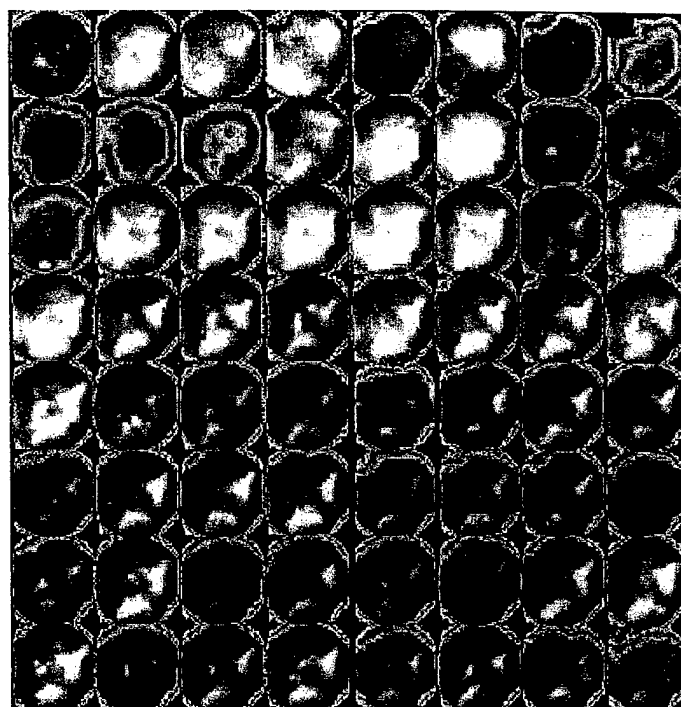


Fig. 4. (top). Images at 25 aTDC from Consecutive Cycles.

Fig. 5 (bottom). Images at 53 aTDC from Consecutive Cycles.

Engine Operating and Imaging Condition: 600 rpm; 13°C Coolant Temperature; 6 bTDC Spark Ignition; 27.58 kPa (4 psi) Intake Manifold Vacuum; First 11 Cycles at 400-rate, followed by 100-rate (stoichiometric) Fuel Injection; Imaging by PtSi Area-arrays; via 3.8μm band.

When the intake vacuum was 41.37 (6 psi) kPa with coolant at 4°C, even after over ten consecutive cycles at 400-rate (followed by fuel injection at 100-rate), flame propagation was very weak to exhibit IR images seemingly indicating misfire cycles. Weak "flame propagation" is referred to some considerably weak radiation images appearing upon ignition, but extinguished in most of cases (without fully covering the imaging area). The consideration of misfire in spite of some presence of IR image was supported by insignificant difference in pressure-time (p-t) history compared with those under motoring condition. Weak IR images of flame propagation at this time, which were most discernable in 3.43 μ m band of all, reminded the preflame images observed in an earlier study [5].

When comparing this observation with those obtained in earlier studies, the reaction images under this condition appeared to take place through gaseous mixtures. There were only a few cycles indicating "pool" burning expected to occur due to liquid fuel layers out of all captured from consecutive cycles. This was quite unexpected in view that such pool burning was observable even when the engine was relatively warmed [7], which is further discussed later.

The absence of "liquid fuel burning" under this condition (in spite of sufficient amounts of fuel provided at 400-rate), which was inferred from diffusion-flame like flame fronts [7], was considered to be due to a too low engine temperature. That is, in this cold engine the liquid fuel was not vaporized to be consumed by reaction fronts prior to being either wasted through the exhaust valve or washed down to the crankcase. Note that the washing-down was observable by finding wet layers of liquid fuel formed over the 45-degree surface mirror (Fig. 1) in this engine operation.

Expecting that an increase in the cylinder temperature would accelerate fuel vaporization off the liquid layers, the intake pressure, therefore, was increased (i.e., by an increased amount of heat-release per cycle) in the next experiment to have a vacuum of 27.58 kPa (4 psi). The same 400-rate was employed, which required an increased amount of fuel compared to the rate in the former experiment in order to match the increase in the airflow, which was identified earlier by using the UEGO sensor.

Since images obtained under this condition still were not considered to be effective particularly in demonstrating advantages of HIS-CC, results obtained with the coolant temperature of 13°C are included here. (Note that those in 3.8 μ m band is only discussed although results in other bands are explained in the paper presentation.) In order to help explain the results, steps taken in the imaging are briefly explained first.

As soon as the engine speed attained 600rpm, imaging by the SIS was initiated according to a preprogrammed schedule (e.g. starting after 323 CA from the first TDC marker signal after clicking the PC mouse). This was basically imaging from the motoring condition. In obtaining the present results, after this "empty" imaging was repeated for eight (8) consecutive cycles, the fuel injection at 400-rate was started, which led to successful firing in the immediate cycle. This 400-rate continued for 11 successive cycles, and thereafter the fuel

injection was swiftly changed to 100-rate (stoichiometric), which was starting from 12th firing cycle. It is pointed out that this sequence of fueling is by no means the most common schedule employed in typical SI engines.

Shown in Fig. 2 were sequential images obtained in 26th imaging cycle, that is Cycle #18 from the first ignition and 7th cycle after the fuel injection started in the 100-rate. The sequence of these images goes like that in a calendar as shown in a look-up-table (LUT) included in Table-I. The minus numbers represents CA bTDC. Note again that the ignition was given at -6CA. Images are shown in false-color in order to reveal more local variations of reaction activities.

Since they were taken in a cycle after 17 consecutive firings, the thermal radiation from the (heated) spark plug (located at the center of images) can be seen in even at -7CA, which is right before spark ignition. The propagation of flame fronts appears to be predictable as it gradually grew over the imaging area.

At this time, it is pointed out that high-speed images obtained in visible-range are meaningful mostly in those taken typically before approximately 30CA because thereafter reaction fronts cease to emit sufficiently strong radiation for imaging. During this period with propagating flame fronts, strong radiation from combustion products (also by doping chemicals, often metallic oxides included in fuel, in order to increase visible radiation for imaging) masks thermo-chemical signatures issued near the cylinder head. Such masking effects also seem to be the case in the present IR imaging due to strong radiation from combustion products making it hard to extract useful pieces of information as to reaction activities until 35CA. It is noted that when propane-air mixtures are used in place of gasoline the masking is much less.

Spectral IR images obtained after reaction fronts disappeared, e.g. those after 39CA (Fig. 2 and Table-I), however, exhibit continuing post-flame reactions, which is difficult to observe by visible-range imaging obtained even if using lighting. Images of reaction pockets over two intake valves (located at upper center and right-hand side) appear to be something expected from diffusion flames, which was explained to be due to liquid fuel layers as briefly mentioned earlier. Note that such images from seemingly reactions over liquid fuel layers were observed even in relatively warm engines. The consideration of liquid fuel layers is also backed up by the absence of such pool-burning images near (high-temperature) exhaust valves and spark plug. According to earlier study [5,7], such images of reaction over liquid fuel layers were seen only after almost the completion of flame propagation. This was explained by heat transfer to occur from combustion product to fuel layers.

It is pointed out that images captured in other spectral bands did not exhibit such liquid-layer activities near the wall, again due to radiation from combustion product in front. This may also explain reasons why the presence of liquid fuel layers in warm engine is reported little in literature.

Next three sets of images are included here in order to help demonstrate potential usefulness of HIS-CC (Figs. 3-5). In Fig. 3, those obtained at 9CA from the very first firing cycle

through 64 consecutive cycles are shown again in a calendar-like sequence. For example, 18th image at 2nd column – 3rd row is the same as identifiable at 9CA in Fig. 2 and Table-I, which was taken in 18th firing cycle as mentioned earlier.

Looking at Fig. 3, although it was necessary to provide extra amounts of fuel injected in order to start the engine, flame propagation became quite sluggish after 6th firing cycle from the start. This slowness is considered to occur due to excessive amounts of fuel vapor for the amount of intake air (instead of facilitating flame propagation). This consideration is backed up by lasting reactions at later stages of the stroke as explained later. Flame propagation became obviously faster as soon as the injection was changed to 100-rate (at 12th cycle from the start, image at 4th column – 2nd row in Fig. 2). This enhanced flame propagation brought up by the stoichiometric rate, however, became significantly slower after around 20th cycle from the start (8th cycle after switched to the stoichiometric rate) to achieve a steady manner having smaller cyclic variations.

The relatively strong flame propagation during the period from 12th to 20th cycles may be explained by the residual fuel, which had been accumulated over the chamber surfaces during the earlier cycles with 400-rate fuel injection. That is, fuel vapor formed from liquid fuel introduced at the 100-rate was augmented by additional amounts of fuel vapor out of those residual liquid layers. In view of liquid fuel layers being sluggishly consumed at the later stage of reaction (refer to images after 41CA in Fig. 2), it may be reasonable to expect that (in spite of the fuel input at 100-rate) reacting fuel-vapor mixtures (even in relatively warm engines) may be more or less leaner than stoichiometric.

Images captured upon further flame propagation are considered, which are displayed in Fig. 4. They are similar to those in Fig. 3 except that they were from 25CA aTDC. Again, image at 2nd column – 3rd row is the same as identifiable at 25CA in Fig. 2. After approximately six cycles from the start (with fuel injection at 400-rate), "poor" flame propagation in subsequent cycles, until the fuel injection was shifted to the 100-rate, was observed in Fig. 2. Flame propagation at the corresponding cycles seen at 25CA aTDC is also slow compared with that in other cycles. The expectation of over-rich fuel-vapor causing the slow reaction is supported by the most strongly continuing reactions observed from those at 53CA aTDC (Fig. 5). The consideration of excessively rich fuel-air ratio is also consistent with flame images in the first two firing cycles where flame propagation was strongest in the early stage (Fig. 3) and completed most at the later stages (Figs. 4 and 5). It is expected that in these first two cycles excessive fuel accumulation would be smaller compared with those in the later cycles (from Cycle #3 through #11).

The signature of post flame reaction over liquid fuel layers, which became more discernable starting around 39CA aTDC (Fig. 2), is still quite obvious in images at 53CA aTDC (Fig. 5). It is noted that the post flame reactions, thereafter, continued in a manner (in most of cycles with 100-rate) similar to that seen in Fig. 2. That is, the reaction pockets are seen mostly around the intake valves (and never around the

exhaust valve and spark plug in a warm engine) as explained earlier.

While little thermal radiation from two exhaust valves is recognizable in the early stage, some obvious valve images are seen after 30 cycles from the engine start (Fig. 4). The strong radiation from post flame reaction products, however, somewhat masks radiation from the high-temperature exhaust valves (Fig. 5). (Note that the bright spot seen in image of 17th cycle is considered from fuel deposit being oxidized over the optical window (Fig. 1), and therefore it does not represent any activity expected in a typical SI engine.)

It is clear that extra amounts of fuel introduced during the cold start of an SI engine, for example, at 400-rate instead of 100-rate, which help lead to successful ignition and flame propagation, can also cause sluggish over-all in-cylinder reactions. Timely adjustment of the fuel injection schedule (programmed) according to varied engine conditions (such as affected by cylinder temperature during the start) appears to be an important requirement in minimizing amounts of fuel wasted to exhaust.

SUMMARY

A new high-speed spectral infrared imaging method has been developed to capture images of in-cylinder reaction processes from consecutive cycles (HSI-CC). The technique development involves incorporation of new massive data handling hardware and new computer programs with the earlier system, called Rutgers or Super Imaging System (SIS). In achieving the present SIS-HSI-CC, development of a new Window-based operating system (WOS) was also a requirement.

This system has the capability of simultaneously capturing a set of four spectral IR digital images at successive instants of time at rates over 2,000frames/sec/camera from as many as 150 sequential cycles. The data accumulated in a single experiment amounts to as much as 400 mega bytes. Review and analysis of massive amounts of results obtained by SIS-HSI-CC was achieved by using a new computer program, called Rutgers Animation Program (RAP), which permits display of a large number of spectral digital movies over a single PC screen in a controlled manner.

The SIS-HSI-CC-RAP is applied to investigation of in-cylinder reactions in a spark-ignition (SI) engine, particularly for transient processes such as during the warm-up period. The present tool offers a new research capability of improving our understanding of some of in-cylinder processes, otherwise difficult to achieve.

ACKNOWLEDGEMENT

Authors would like to express their appreciation for support from the US Army Research Office (Contract No. DAAG55-98-0494. Program Manager, Dr. David Mann) and Ford Motor Company.

REFERENCES

1. Chaves, H., Hentschel, W., Obermeier, F., and Staslcki, B., "In Cylinder High Speed and Stroboscopic Video Observation of Spray Development in a DI Diesel Engine," SAE Paper-961206, 1996.
2. Tossefi, D., Belmont, M.R., Thurley, R., Thomas, J.C., Hacohen, J., "A Coupled Experimental-Theoretical Model of Flame Kernel Development in a Spark Ignition Engine," SAE Paper-932716, 1993,
3. Fujimoto, H., Hyun, G.S., Nogami, M., Hirakawa, K.H., Asai, T., and Senda, J., "Characteristics of Free and Imaging Gas Jets by Means of Image Processing," SAE Paper-970045, 1997.
4. Chang, C., Clasen, E., Song, K., Campbell, S., Jiang, H., Rhee, K.T., "Quantitative Imaging of In-cylinder Processes by Multispectral Methods," SAE-970872, 1997.
5. Jansons, M., Lin, S., Fang, T., and Rhee, K.T., "Visualization of Pre flame and Combustion Reactions in Engine Cylinders," SAE Paper 2000-01-1800.
6. Jansons, M., Lin, S., Choi, D.S., Campbell, S. and Rhee, K.T., "Study of High-pressure Injection DI Diesel Engine," SAE Paper 1999-01-3494, 1999. SAE Paper-961206, 1996.
7. Campbell, S., Lin, S., Jansons, M., and Rhee, K.T., "In-cylinder Liquid Fuel Layers, Cause of Unburned Hydrocarbon and Deposit Formation in SI Engines?" SAE Paper 1999-01-3579, 1999.
8. Ludwig, C.B., Malkmus, W., Reardon, J.E., and Thomson, J.A.L., Handbook of Radiation from Combustion Gases, NASA SP-3080, 1973.
9. Chang, C., Clasen, E., Song, K., Campbell, S., Jiang, H., Rhee, K.T., "Quantitative Imaging of In-cylinder Processes by Multispectral Methods," SAE Paper-970872, 1997.

Visualization of Preflame and Combustion Reactions in Engine Cylinders

M. Jansons, S. Lin, T. Fang, and KT Rhee

Rutgers, The State University of New Jersey
Piscataway, New Jersey

Copyright © 2000 CEC and SAE International.

ABSTRACT

In-cylinder reactions of several internal combustion engine configurations were investigated using a high-speed four-spectral infrared (IR) digital imaging device. The study was conducted with a greater emphasis on the preflame processes by mutually comparing results from different engine-fuel systems.

The main features of the methods employed in the study include that the present multi-spectral IR imaging system permits us to capture progressively changing radiation emitted by new species produced in-cylinder fuel-air mixtures prior to being consumed by the heat-releasing reaction fronts. The study of the Diesel or compression-ignition (CI) engine reactions was performed by varying several parameters, e.g. injection pressures, intake air temperature, fuel air ratio, and the start of injection. They were investigated also for the following mixture preparation-ignition methods: (1) direct-injection of Diesel fuel; (2) homogenous charge (fumigation) ignited by pilot injection and (3) homogeneous charge self-ignition.

For the spark-ignition (SI) engine processes, the reactions were investigated using different fuels including gasoline and propane, which were introduced by either the port-fuel-injection unit or carburetor.

The sequential images captured of in-cylinder preflame reactions were compared with those of the subsequent combustion reactions. In particular, they are expected to serve as an overall survey of visualizing the preflame processes in the cylinder.

INTRODUCTION

Fuel-air mixtures under compression in the engine cylinder undergo chemical reactions prior to being consumed via the propagation of flame fronts. For example, those in Diesel or compression ignition (CI) engines during the ignition delay period and mixtures in the end gas of spark ignition (SI) engines produce new intermediate species widely suggested as being the precursors of self-ignition.

The processes of such preflame reactions in the cylinder (and their impacts) are not well understood probably because they are invisible. Where or when what is produced has hardly been depicted in the past particularly with respect

to the onset of (self-ignition) flame propagation exhibiting visible-ray radiation. Furthermore, new species produced in the invisible preflame reactions (PFR, for short) are diverse as well as numerous and complex especially when real-world fuels (opposed to a simple single-component fuel) are used in operating the engines.

A short description of the PFR as made above would help expecting that the reaction fronts in the engine cylinder would not be simple layers (sharply) dividing the reaction products and fresh mixtures. Rather, they would be zones diffusing radicals and transferring heat towards the "cooked" mixtures highly infested with active intermediate species including radicals and partially oxidized fuel fragments accumulated during the PFR processes. The consumption of such mixtures with rich intermediate species (after lengthy low-temperature induction periods) by the flame fronts would differ from those where fresh mixture is fed in other combustion devices, e.g. a simple laboratory gas-jet flames where high-temperature kinetics dictates the processes. This would further lead to an expectation that the seemingly fresh mixtures during the SI engine-compression-stroke (prior to the onset of spark ignition) would contain large amounts of oxides of fuel fragments and radicals (called as intermediate or PFR species). Also in a CI engine, the injected fuel would immediately start to produce the PFR species as soon as it is injected into the cylinder.

Among many reasons for investigating the PFR is that when the PFR are not properly controlled, engines undergo knock causing degraded behavior. In the past, various aspects of the PFR have been studied in both types of engines, including determination of intermediate species and visualization of their presence.

Determination of new species produced in the PFR was attempted by earlier and recent research individuals alike: For example, mentioning a few early studies, Clark and Thee (1926) found CH and CO in a CI engine by using ultra-violet spectrometry [1]* and Withrow and Rassweiler (1933) measured OH and formaldehyde in the SI end gas [2]. Since the species population in the engine are complex as stated above (and temperature information is required for quantitative determination when optical methods are employed), it has been difficult to achieve satisfactory results. As technology advances, nevertheless this attempt is expected to produce more prolific and in-depth results.

*Numbers in parentheses designate references at end of paper.

While the abovementioned speciation is explored, some recent studies came to report chemiluminescent images of PFR in CI engines [3-6] and SI engines [7,8]. It would be desirable to obtain such results (that is, overall pictures) at successive instants of time. When such temporal and spatial results are compared to subsequent events such as the onset of first (self-ignition) flame kernels (in CI combustion), despite the lack of speciation information, the impacts of PFR on the visible heat-releasing reaction processes may be understood better. It was also expected to improve our insight into the PFR in the cylinder when their global pictures from various engine-fuel configurations are mutually compared to each other.

It is reminded that observations in the engine cylinder are often difficult to explain in spite of the wealth of basic chemical kinetics information obtained under controlled laboratory reaction conditions due to various reasons. They include the fact that in-cylinder reaction variables rapidly change in time and space. Gas motions compounded with compression by the piston and reaction fronts, for example, cause the spatial variation of temperature exposing reacting mixtures to different chemical reaction regimes (either low-temperature or high-temperature domain) with time.

Such complexities are further increased by the stratification and alteration of fuel/air ratio as well as change of composition (mixing with residual gas and fresh combustion products) and also potentially by surface effects (e.g. high-temperature exhaust valve and spark plug). Therefore, what is observed in the cylinder represents largely the special nature of individual engine reaction conditions controlling the chemical reaction kinetics. Further when the observation is made through a small viewing window (in some extreme cases by measurements with a single stationary probe or via an optical path), the in-cylinder (bulk) gas motions will have to be carefully taken into consideration during data interpretation.

Motivation of the Present Study. The following is to discuss the uniqueness of our methods over others explaining what is reported to fill missing information in the literature, which is basically to discuss the importance of the global pictures of the PFR.

After developing a new high framing-rate infrared (IR) digital imaging camera [9], a new system having four (4) of the same units connected to a single optical train has been made operational and subsequently improved in our laboratory mainly for performing engine-fuel combustion studies [3,5,7-9]. The basic idea of this four-spectral imaging system, called as Rutgers or Super Imaging System (SIS), is to simultaneously capture four geometrically identical digital images (i.e., data matrices) in respective spectral bands at successive instants of time.

When in-cylinder images were obtained using the multispectral IR system in 1995, we came across to capture progressively changing radiation from the trapped mixture prior to being consumed by flames, which was revealed via only one of several bands we investigated [3,7]. The chemiluminescent images exhibited some distinctive and repeating spatially and temporally resolved patterns. They were in contrast to those simultaneously observed via other bands mostly exhibiting the formation of the (final) combustion product, e.g. water vapor resulting from the propagation of flame fronts. In spite of the fresh and new nature of the findings, since the objective of the earlier studies concerned other issues, the phenomena have not been extensively analyzed for documentation.

Upon accumulation of some considerable amounts of in-cylinder digital movies containing the signatures of PFR in the engine cylinder, additional engine measurements have been conducted as a broad survey over various engine-fuel systems. The presentation of results from the study was expected to serve as an opportunity for mutually comparing the nature of the PFR processes and offering visualization of the invisible reaction processes taking place in the internal combustion engine cylinder.

In particular, it is hoped that the present report of PFR images in the cylinders would encourage research individuals in the field of simulating engine combustion to include the processes of preflame reactions in the modeling. For example, it would be desirable that the new models include a more reasonable commencing time of reactions in implementing the chemical kinetics computations.

EXPERIMENT

Since the present visualization of PFR (made possible by the new development of the SIS) was a new attempt and produced often unexpected results, the present work became rather exploratory and experimental in nature.

Several engine configurations were employed in investigating the PFR: (1) Direct-injection (DI) CI engine; (2) DI-CI engine with fumigation ignited by pilot injection; (3) Homogenous-charge self-ignition DI-CI engine; and (4) SI engine operated by various fuels introduced by different delivery methods. The in-cylinder imaging was conducted using the SIS system and the results were analyzed by the Rutgers Animation Program (RAP, for short). They are briefly discussed next.

The engine apparatuses used for studying the above configurations were basically two separate units with infrared (IR) optical access, i.e., an SI engine and a CI engine. The optical access in the SI engine was achieved through an extended-hollow piston having a full-view IR window at the top of the piston [8]. The observation of the in-cylinder events of CI engine combustion was performed via an IR window mounted in place of one of the two intake-valves as the radiation is relayed upward through the cylinder head [5]. Although the engine apparatuses are described in the above references, a brief discussion is made on them next.

SI Engine with Optical Access. The new engine apparatus was designed-constructed to have a maximized optical view of the reaction chamber while maintaining several desirable engine characteristics (Fig. 1). Among the most important design requirements taken into consideration for this setup was that the entire portion of the cylinder bank (having the water-jacket around them) was mated with the original cylinder head and intake manifolds. Out of four cylinders in the bank, only one cylinder was utilized for combustion reaction that accommodates the extended piston. The crankshaft was balanced to achieve smooth operation even at relatively low speeds, which was also aided by incorporation of a new high-inertia flywheel.

Elaborating on this engine apparatus, the entire cylinder block was used in order to duplicate the coolant flow and induction-air-flow conditions of the stock engines as much as possible. A close duplication of the representative engine conditions, at least those associated with the cylinder head, was considered to be one of the critical requirements for the engine setup in which the progressing temperature-sensitive

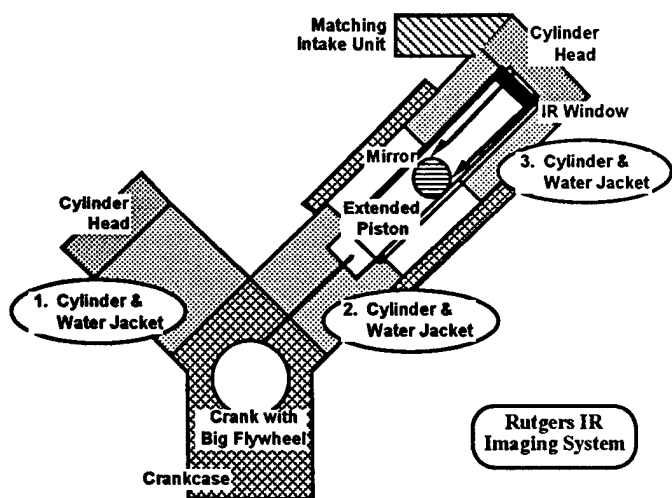


Fig. 1. A New Engine Apparatus for Duplicating Representative In-cylinder Reaction Conditions.

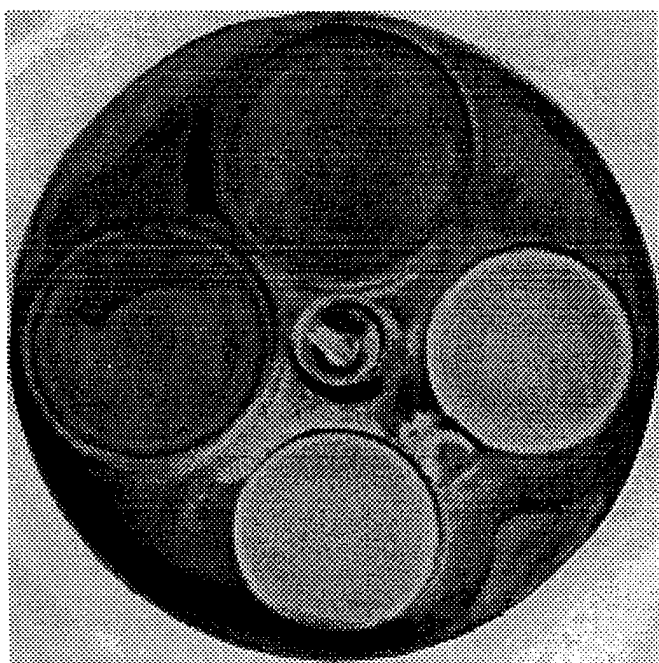


Fig. 2. Imaging View of the SI Combustion Chamber via the Optical Path.

PFR as observed would represent what is happening in the real-world engines. For example, misleading results would probably be obtained if the coolant flow-pattern were altered from the original. The duplication of the original layout angle of the cylinder bank was also considered to be important because the fuel-air mixture preparation may be significantly affected (particularly when the port-fuel-injection method is employed) if it were oriented vertically as in many similar apparatus with an extended piston.

Important engine specifications include: bore-stroke of 90-90 mm, connecting rod length of 151.5 mm, compression ratio of 9.9, clearance chamber volume of 50 cc. It had two intake valves and two exhaust valves having diameter with peak lift of, 44.5 mm with 6.59 mm and 34 mm with 6.59

mm, respectively. A more detailed description of the engine may be found in an earlier paper [8].

A photo of the cylinder head surfaces seen via a direction of 45-degree to the (oval) mirror (perpendicular to the page in Fig. 1) is shown in Fig. 2 (without the IR window, which is opaque to visible ray): Two intake valves on the upper left and two exhaust valves on the lower right of the figure with the spark plug in the middle can be seen, which will be referred to when the in-cylinder images are discussed later.

CI Engine with Optical Access. A single-cylinder engine with optical access employed in the present study was basically a Cummins-903 engine having a bore-stroke of 140-121 mm (displacement of 1.85 liters) and compression ratio of 13.5 to 1. In order to obtain images of in-cylinder reactions of the engine, one of two intake valves was converted to an optical access as briefly mentioned above, which is barely big enough to investigate one of eight (8) spray plumes [3,5]. A schematic presentation is shown of the optical engine, that is, a top-view of the combustion chamber having the spray plume axes with respect to the optical access as indicated by the shaded area (Fig. 3). Since the same family of 903 engines has been widely used in the past, no additional discussion on the engine dimensions is made here.

Several other features were incorporated in the apparatus including the following: This single-cylinder engine was installed with a new intake-air (electric) heating unit which can increase the air temperature over 205°C (400°F) at high speeds, because such a high intake air temperature was required to produce self-ignition in the PFR in the option of studying homogeneous charge CI engine combustion. (The air was supplied from the building via a pressure controller, for adjustment depending upon the intake air temperature, and a flow-metering unit.)

The engine was cooled using a closed-flow unit (with glycol as coolant) connected to a water-cooled heat exchanger for temperature control. The same also included a coolant heating unit in order to closely simulate a warmed engine where needed. The unit was designed to accommodate a coolant temperature as high as 149°C or 300°F.

High Injection Pressure Fuel System (HIP). The present CI engine was equipped with a laboratory-built electronically controlled high injection pressure fuel systems (HIP), which was basically the same design as BKM's Servo-jet type [10]. It is a pressure intensifier type whose functional details were described elsewhere [5,11].

The distinctive difference of this Rutgers-built HIP unit from the original Servo-jet is that the present system uses the existing Cummins nozzle tips (0.15 mm nozzle hole diameter) for technical and economical flexibility. Note that the fuel intake and return ports in the Cummins engine were directly interfaced with the new unit so that the new HIP assembly directly replaces the Cummins PT-type injector without any modification of the engine cylinder head. The low-pressure fuel supply was pressurized as high as over 12 MPa (1,750 psi) through the fuel gallery in the cylinder head, which was intensified to an injection pressure of 210 MPa (30,625 psi).

Among the important performance behaviors of the present HIP unit characterized was the start of injection, which was controlled by an electro-magnetic activating device. In order to evaluate the start of injection with the variations of the fuel injection pressure, injection rate and speed, a strain gage

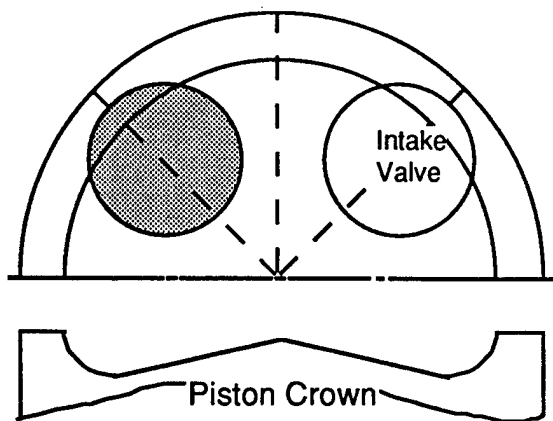


Fig. 3. Schematics of DI-CI Combustion Chamber and Optical Access (Shaded Area) with respect to Spray Axes.

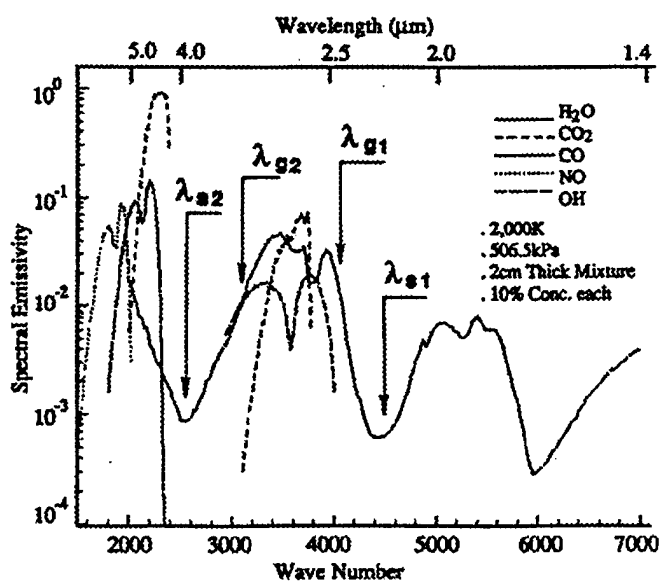


Fig. 4. Spectral Diagram of a Mixture and Bands Chosen in the Present Imaging by using the SIS.

was mounted over the surface of the injector-tip to monitor the fuel spilling with respect to the electronic actuation signals for the valve opening. The injector opening was found to be predictable and consistent as reported earlier [5, 11], which shows only small deviations of the start of injection with respect to the designated time of injection under varied injection rail pressures. It is noted that changes of the speed and rate of injection did not measurably affect these characteristics. The injection period of the present HIP was in the range of 3-5 msec, depending upon the amount of fuel injected per cycle.

IR System and Preflame Images. The radiation issued from a combustion chamber via the optical access explained above are selectively captured by using corresponding spectral band filters placed in respective cameras of the SIS. This system layout permits simultaneous acquisition of four geometrically identical images in respective spectral bands from the same radiation source at successive

instants of time at high rates. In order to explain the concept of multispectral imaging, the spectral emissivity of a mixture containing several designated species under a physical condition as indicated in Fig. 4 is included.

In discussing the advantages of using the SIS for studying the present problem and images of PFR, a set of results obtained from one of the SI engine experiments is included first. Figure 5 shows sequential spectral images simultaneously taken from the SI engine apparatus via three spectral bands (Refer to Fig. 4. Numbers in parentheses indicate individual band widths in nm): (A) 3.42μm (80), (B) 2.47μm (50) and (C) 3.8μm (170), when it was operated by propane-air mixture of a near stoichiometric ratio (also refer to Figs. 1 and 2). (Those in 2.20μm (100), λ_{g1} in Fig. 4, although available, are not shown here due to the space limitation. They will be shown in the paper presentation as a part of animation, however.) Results are displayed in false-color in order to illustrate the radiation intensity (in an increasing sequence of, black as background, white, orange, red and yellow for those in Figs. 5-B and -C) and in another color-map for exhibiting more obvious local variations (Fig. 5-A). A look-up-table (LUT) is also included in Table-I in order to indicate the matching crank angle positions for those obtained with spark ignition (SI) at 15 degrees of crank angle before the top dead center, 15 CA bTDC.

Before the images of PFR are explained, the visible flame propagation (exhibited by the radiation from mainly water vapor formed as a final combustion product) is explained by looking at those (Fig. 5-B) obtained in 2.47μm band (λ_{g1} in Fig. 4). The progressive growth of the reaction fronts initiated from the spark plug is relatively predictable as they propagate under some influence of gas motions, which seems to be in the one-o'clock-direction. On the other hand, the radiation mainly issued from the surfaces of the cylinder head (via 3.8μm, λ_{g2} in Fig. 4) has a time lag after being contacted by the flame fronts (Fig. 5-C). The relatively significant thermal signatures of exhaust valves and spark plug (prior to the spark ignition) indicate that the engine was warmed up: These surfaces start to exhibit much greater amounts of radiation upon the said lag suggesting the cooling depth (during the non-combustion period) to be rather shallow.

Discussing the images of PFR, those shown in Fig. 5-A captured via 3.42μm band (λ_{g2} in Fig. 4) are compared with the sequential images corresponding to the former in Figs. 5-B and 5-C. Obviously there are some detectable developments of new radiation as observable even from the start of imaging (37 CA bTDC) seemingly initiated near the high-temperature surfaces (e.g. spark plug and exhaust valves). This becomes more obvious as the piston nears TDC, e.g. as early as 21 CA bTDC. Such progressively developing radiation in the mixture prior to being swept by the flame fronts is considered to stem from new intermediate species formed in PFR. Further discussion will be made in Results and Discussion.

As an additional note related to the abovementioned imaging, the acquisition of other engine data (while the SIS is operated) was carried out by using the same timing-clock signals used for imaging. This was to simultaneously accumulate digital outputs from various sensors placed in the engine, including: the pressure transducer; thermocouples; and a calibrated universal exhaust gas oxygen sensor (to determine the overall engine-out fuel/air ratio). The measurements from those sensors are closely referred to when the progressing PFR is reviewed by using the data analysis method as discussed below.

-37	-35	-33	-31	-29	-27	-25	-23
-21	-19	-17	-15	-13	-11	-9	-7
-5	-3	-1	1	3	5	7	9
11	13	15	17	19	21	23	25
27	29	31	33	35	37	39	41
43	45	47	49	51	53	55	57
59	61	63	65	67	69	71	73

Table-I. Look-up-Table (LUT) for Sequential Images shown in this Paper (Some cases without the last row).

Among other advantages of the SIS is its versatility to permit in situ display of (either still or animated) images for immediate screening and analysis of results. Those regarded to be acceptable, which is the case in most measurements, were stored in the computer memory, and transferred to recordable CD disks for subsequent analysis.

Data Analysis and Presentation Method. In the investigation of even a single issue, a vast amount of results is accumulated by using the SIS, e.g. over one thousand sets of movies. This is too much to achieve a reasonable analysis by manual methods. Consequently it was decided to develop a new method, Rutgers Animation Program (RAP), which is basically a new computer program facilitating detailed analysis and presentation of sets of high-speed images.

Explaining the analysis of the results by the RAP, for example it permits a simultaneous display of as many as twenty-eight (28) separate animation over a single PC screen in respective (adjustable) color maps. (A greater number of movies may be displayed but at the expense of image quality over the screen.) In addition, corresponding pressure-time histories can be simultaneously displayed for mutual comparison. While such animation is made by the RAP, various adjustment features can be utilized, e.g. control of display speed during the animation, and freezing of the animation for reversing or forwarding (frame by frame) of the animation. At the same time, an entirely new set of similar animation can be performed, placing it over the existing one. This step is taken to review the entire volume of experimental results, in order to select a most representative set from multiple trials.

In addition, in order to facilitate the analysis of results, sets of sequential still pictures can be simultaneously displayed, which are either enlarged or reduced over the screen. Note that this option can be utilized while the abovementioned animation is conducted. When the multiple results are simultaneously reviewed, the RAP facilitates displaying corresponding pressure-time histories.

The RAP was also developed to make effective presentation of the selections made via the abovementioned screening and analysis steps. For example, modern projection devices can be directly connected to a PC in which such animation is being performed for the broad dissemination of

research results. The RAP is recognized as one of the most critical ingredients of the present research, leading to more meaningful findings, particularly when a large volume of imaging results are considered. (At present, RAP is compatible only with the image matrix from the SIS, which may be further developed for broader applications.)

RESULTS AND DISCUSSION

It is noted that the present report is focused on the global pictures of progressing invisible processes of preflame reactions in internal combustion engines, which is expected to serve as a road-map in conducting our next endeavor of speciation. The results of PFR imaging are discussed in comparison with those indicating the formation of the final combustion products, e.g. water vapor.

There are important questions in need of delineation prior to presenting the results. They are: (1) Does what is seen in the unflammed mixture (e.g. shown in Fig. 5-A) indeed indicate the presence of new (intermediate) species produced in PFR processes; and (2) If it is the case, what are the probable species to emit such chemiluminescent radiation?

Regarding the question if intermediate species are formed in the abovementioned unflammed mixture, it is reminded that the mixture is not only in contact with the high-temperature surfaces (e.g. spark plug and exhaust valves) but also under compression. Note that typical hydrocarbon-air mixtures start to react at under 300°C to produce free radical species (e.g. formation of hydroperoxide followed by aldehydes through its breakdown according to Walsh in 1947, and or peroxy radicals as proposed by Semenov in 1958). It is pointed out that an engine (with compression ratio of 8 to 1, for example) starting even at a room temperature would readily achieve over 400°C in the cylinder as the piston nears TDC. The presence of such new species in the engine environment under consideration is, therefore, most likely.

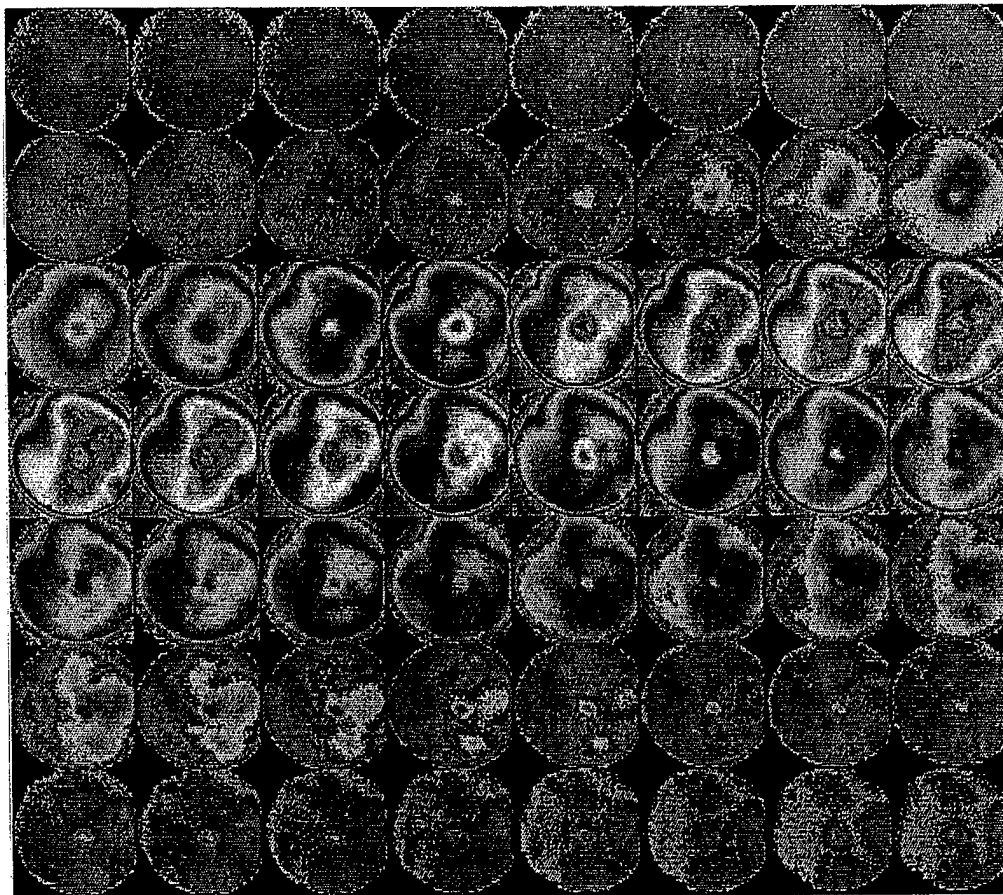
What is mentioned above is not new but known in the field for over a half century. For reference, the species formed during the two-stage combustion include, in addition to the partial oxides of hydrocarbon as mentioned above, various radicals including H, CH₃, OH, HO₂, and numerous fragmentary hydrocarbon species. Some of them are known to exhibit chemiluminescent radiation as formed under low-temperature reaction environments prior to running into rapid heat-releasing reactions. Since their formation and chemical kinetics are widely documented in the literature, further discussion is not attempted here.

What has not been well known as to their formation, however, is the spatial nature of their formation processes and transition to explosion (namely flame). It would be desirable to find, for example, if there are mutual relationships between the zones with PFR species populations to the first flame kernel formation and its subsequent propagation.

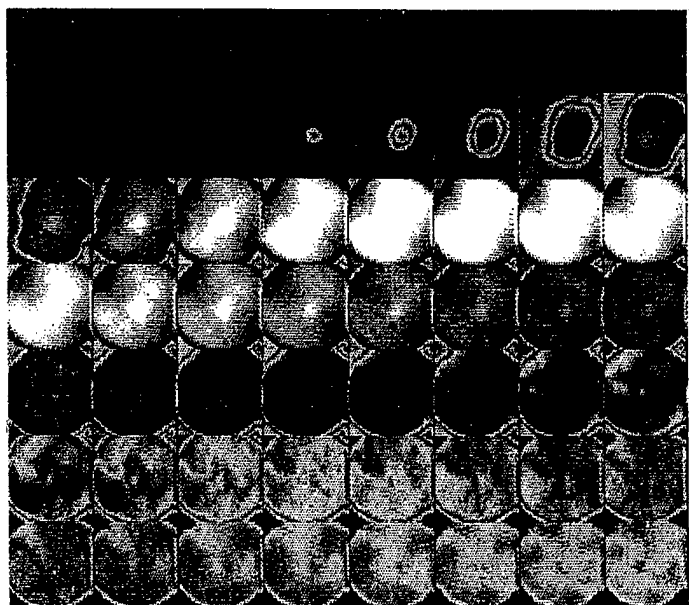
CI ENGINE COMBUSTION

Images of PFR were obtained for several fuel-ignition combinations including the conventional DI-CI engine and a homogeneous charge self-ignition system. After finding some unusual combustion behavior when in-cylinder imaging was performed during the first several cycles [8], which was suggested to occur due to incomplete engine warm-up, all of the CI engine results reported here were captured at least after the first twenty-five successive firings from the engine start.

(A)



(B)



(C)

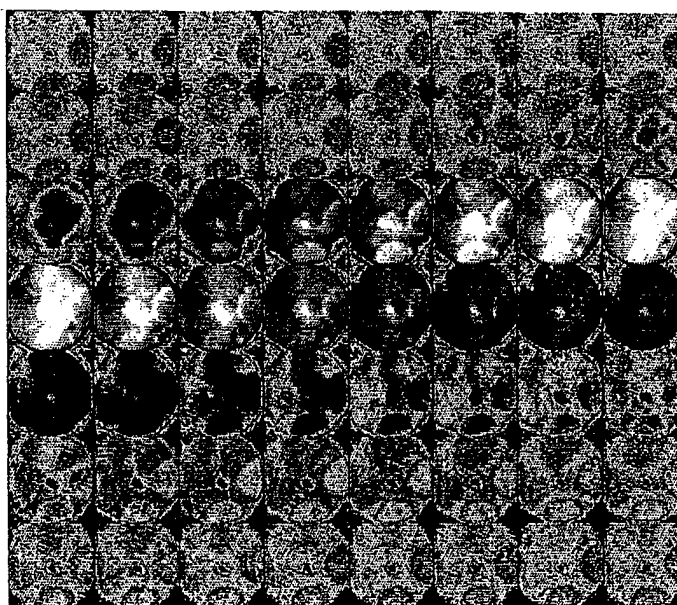


Fig. 5. High-speed Spectral Images obtained from SI Engine Operated by Propane-air Mixture via Bands of: (A) 3.42 μm ; (B) 2.47 μm ; and (C) 3.8 μm .

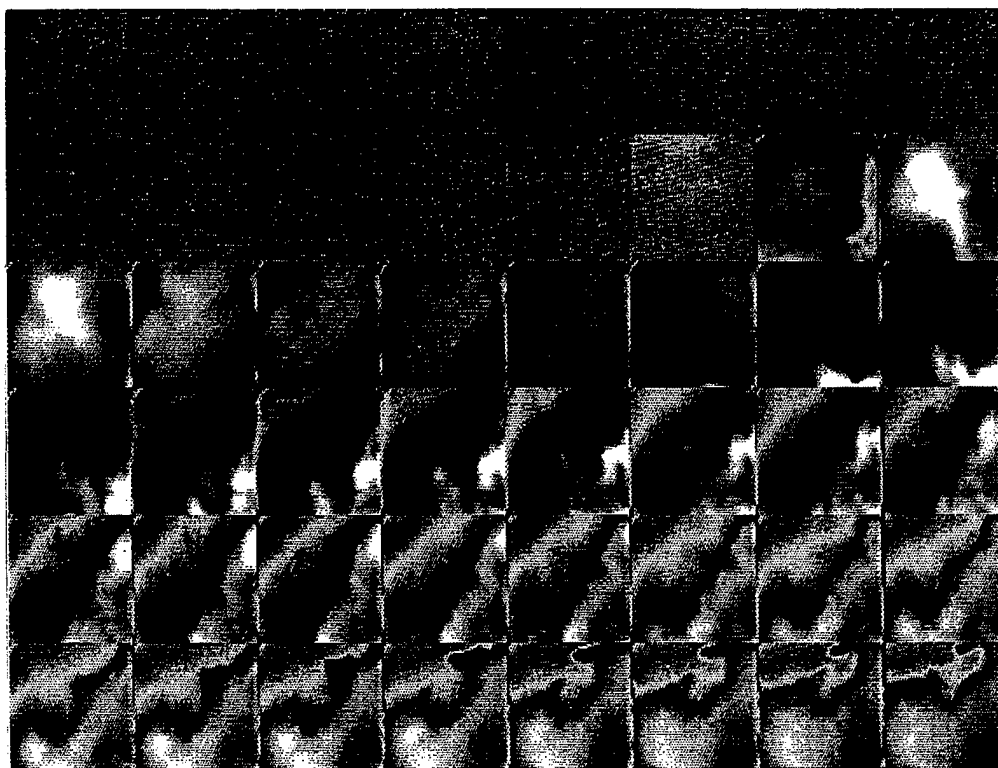
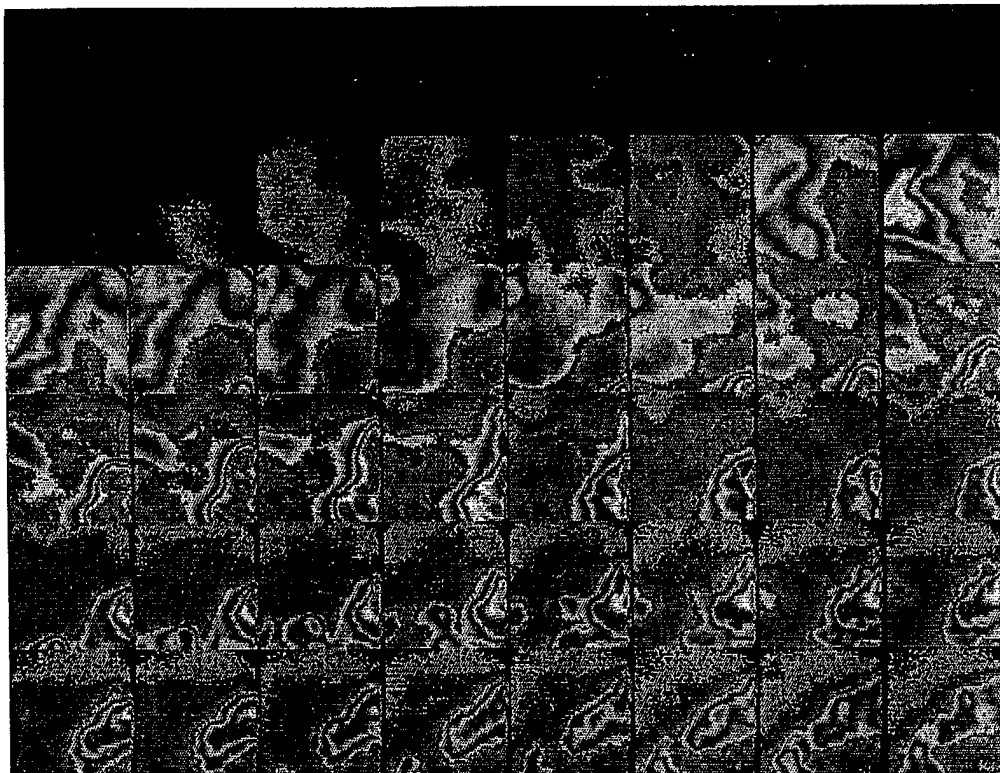


Fig. 6. High-speed Spectral Images obtained from DI-CI Engine via Bands of
(A) 3.42 μm (top) and (B) 2.47 μm (bottom).

Note that the coolant of the engine was preheated to 94°C before the experiment. Results obtained from a DI-CI engine are explained first.

DI-CI Engine. Sets of spectral images simultaneously captured, in 3.42 and 2.47 μm by the SIS via the optical view (Fig. 3) are shown in Figs. 6-A and -B, respectively. The same LUT (Table-I) may be referred to for identifying the matching CA. They were obtained under an engine operating condition of: 600 rpm; fuel injection pressure of 131 MPa (19,000 psi); injection starting at 20 CA (bTDC); intake air at room temperature; and overall air-fuel ratio of 23-1.

Recalling that the spray plume is directed from the lower right corner to the upper left end of the image and finding some signature of the first flame kernel at 11 CA bTDC (Fig. 6-B), the ignition delay is estimated to be approximately a period of 9 CA. The spray axis seems to match with the diagonal direction, which, however, may not be the case in view of images captured in other spectral bands as explained next. According to animation by RAP, the swirl direction is observed to be clockwise. (Since the subsequent flame propagation was extensively explained earlier [5], only a brief discussion is made here.)

During the ignition delay period, there are progressively developing radiation from the spray plume as seen in Fig. 6-A, which is considered to be from (chemiluminescent radiation) new species formed over the envelope of the plume. The sequential images exhibit a small zone of low radiation detected at 19 bTDC at first and it progressively grew with time portraying where the new radiating species located. This indicates that the fuel spray immediately started to produce such species when introduced into the cylinder.

According to these sets of images, the distribution of new species during the ignition delay period seem to be almost symmetric with respect to the diagonal axis of the image (e.g. those taken from -15 to -11 CA in Fig. 6-A).

On the other hand, the burning spray exhibited by the radiating combustion products (images at -9 and -7 CA) is somewhat off-symmetric and out of the axis, which probably resulted from the swirl motion. But such a mismatch may be explained better in terms of rapid consumption of PFR species once high-temperature reaction takes over the processes, as discussed later. The strongest radiation in both spectral images in the beginning is found near the perimeter of the piston bowl indicating that a great amount of fuel and active species are populated there per optical path.

Furthering the above discussion, the formation of intermediate species (as reflected in images at from -19 to -11 CA in Fig. 6-A) and their roles in progressing to the onset of heat-releasing flame kernels (radiation at -11 CA in Fig. 6-B) are known to be the essential processes for CI. When a fuel spray in a CI engine containing a cloud of fuel vapor is being introduced into the cylinder, the fuel-air mixture is directly under a self-ignition environment (typically at 800 K). It is not difficult to conceive that active radical species and partially oxidized fuel fragments start to appear over the envelope of the spray plume. This clearly suggests that there is no measurable time period of physical delay involved in the self-ignition processes in the CI engine, but that the fuel immediately commence chemical reactions in the cylinder.

In general, the zones having the strongest radiation representing PFR species formation do not always coincide with the places where the first self-ignition was observed [12],

in particular when the intake air temperature was high as discussed next.

Without showing the actual images (although they will be reported in animation at the paper presentation), some additional results obtained by varying several parameters are explained next.

When the intake air temperature was increased, the ignition delay was shortened as expected. The PFR, however, seem to be less significant with the increase of intake air temperature. The radiation supposedly exhibiting the formation of active species, in most cases, was very insignificant when the intake air temperature was over 94°C. Furthermore, the occurrence of (premixed flame) combustion reactions was observed even at the same time as the image of PFR in some cases. This observation may not be surprising in view that radical species would be rapidly depleted with the mixture temperature exceeding the low-temperature reaction regime.

The insignificant radiation in 3.42 μm band with intake air at such (unusually) high temperatures further supports the consideration of formaldehyde to be one of those greatly responsible for the PFR images during the ignition delay period under most normal engine operating conditions, as briefly mentioned earlier: Formaldehyde is known to exhibit chemiluminescent radiation (cool flame) and is abundantly formed when the mixture temperature is low, but at high temperatures it is attacked by O, H and OH, and found in only trace amounts [13].

When the injection pressure was varied, the initiation of the PFR did not seem to be affected although the ignition delay decreased with the pressure increase. This was not surprising because the spray plumes introduced via even a relatively low-injection pressure would also contain sufficient fuel vapor to produce radiating intermediate species. Since the volume of spray increases with the injection pressure, however, the radiating zone was more significant in size with increase of injection pressure. For example, it almost filled up the entire optical view at very high injection pressures (e.g. near 200 MPa) while the spray plume was narrow and small when the pressure was around 100 MPa.

For the wide range of overall air/fuel ratio investigated in the study, that is, from 50-1 to as low as 18-1, the PFR were all observed to be similar. When the air/fuel ratio decreased, i.e., becoming overall rich, the PFR was found to occur earlier, which may be partially due to some shift in the start of injection time to take place earlier.

Homogeneous Self-ignition CI Engine. The same spectral bands used for obtaining those in Figs. 5 and 6 were employed for imaging the in-cylinder events in a propane-homogenous-charge self-ignition CI engine. In order to induce the self-ignition, the engine intake air temperature was increased to approximately 210°C by using (an electric heating coil package). Propane was fed into the intake manifold after the heating coil. (It was not attempted to determine the lowest intake air temperature that produces self-ignition.)

The first image captured (-37 CA) already exhibits some significant PFR species (Fig. 7-A in 3.42 μm). Looking at the flame images taken at the same time (Fig. 7-B), the first self-ignition zone incidentally occurred at almost the same zone near the perimeter of the piston bowl as observed in the DI-CI combustion (refer to the image obtained at -9 CA in Fig. 6-B). This initial occurrence instantly spread over the entire optical view. The SIS did not achieve more enhanced temporal and spatial resolutions.

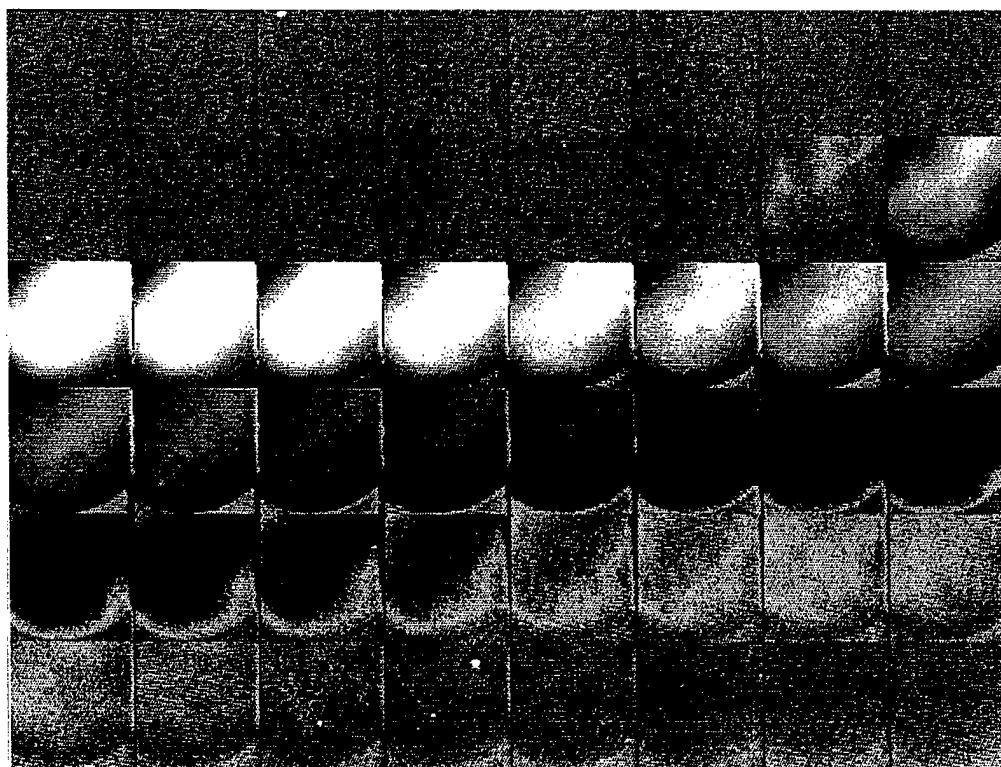
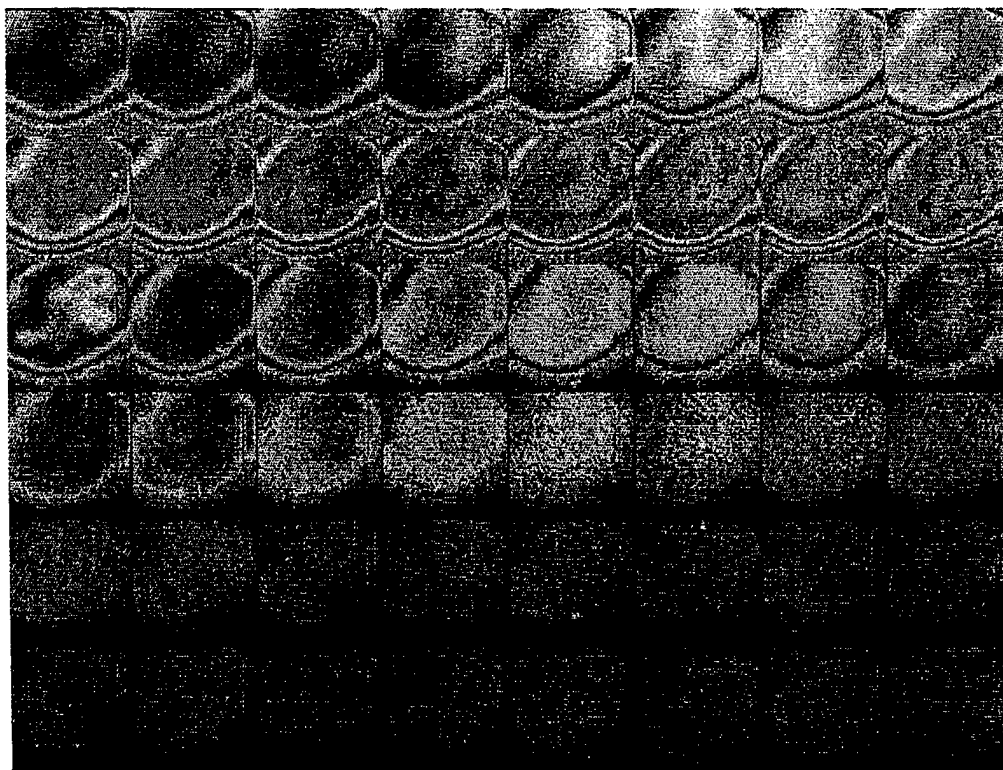


Fig. 7. High-speed Spectral Images obtained from Homogeneous-Charge (Propane) Self-ignition CI Engine via Bands of (A) 3.42 μm (top) and (B) 2.47 μm (bottom).

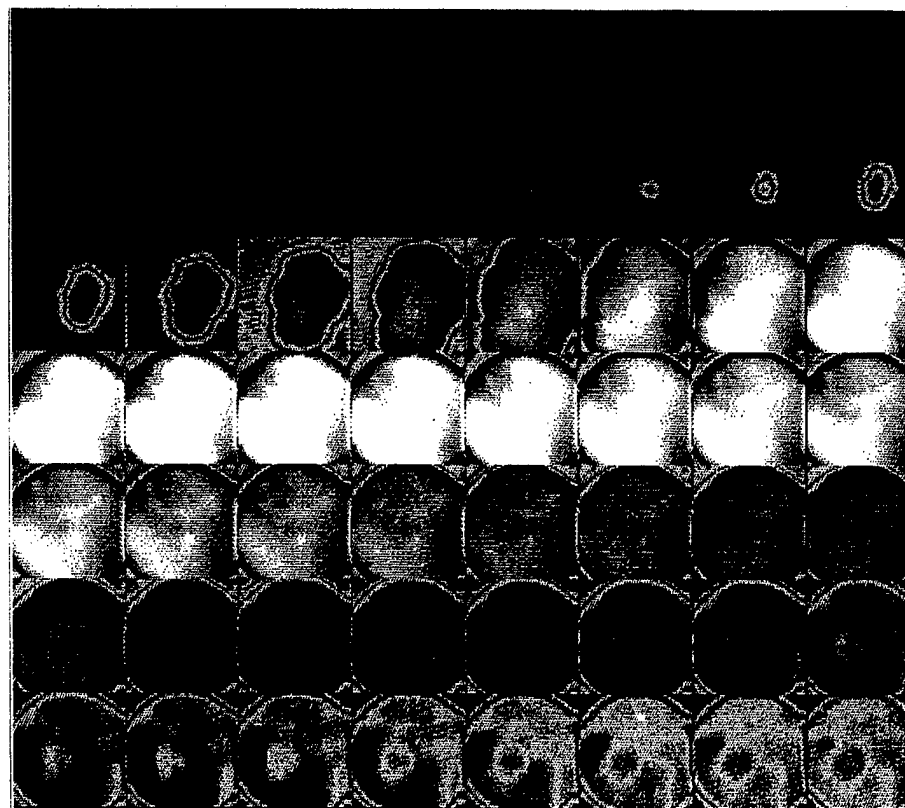
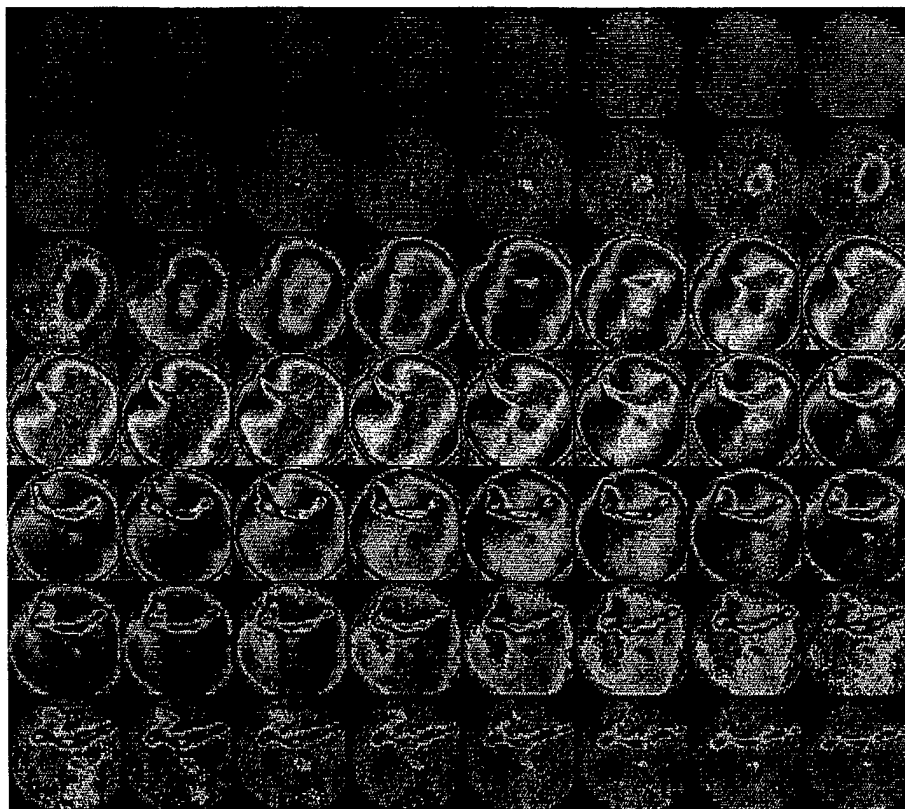


Fig. 9. High-speed Spectral Images obtained from SI Engine Operated by Gasoline introduced by Port-fuel-injection unit via Bands of (A) $3.42\ \mu\text{m}$ (top) and (B) $2.47\ \mu\text{m}$ (bottom).

When the PFR images and those of flames are compared to each other, it is difficult to find any mutual relationship between them in terms of the spatial variation. On the other hand, the gradually increasing intensity of radiation revealing PFR as piston moves up became insignificant as soon as the high-temperature flame reaction takes over the mixture. That is, the first heat-releasing reaction (as seen via $2.47\ \mu\text{m}$, Fig. 7-B) occurred when the highest intensity radiation from PFR was observed (Fig. 7-A). This observation is consistent with the observation of similarly insignificant PFR images captured when the intake air temperature was high in DI-CI engine combustion. That is, the decreased PFR radiation suggests a rapid consumption of formaldehyde and other active species as the reaction environment attains high temperatures.

As expected, the PFR activities were observed to be measurably dependent on the concentration of propane prior to the onset of self-ignition as found in the following experiment. The imaging was conducted, under the same engine condition, while the intake propane concentration was varied. Qualitatively, the PFR radiation was highest at a particular intake propane content and it became low when the content either decreased or increased therefrom.

DI-CI with Fumigation and Pilot Injection.

Unlike the increased intake temperature for the self-ignition in the above case, a small amount of Diesel fuel was injected when propane was fumigated in the intake air. Figures 8-A and -B show the sequential images taken via 3.42 and $2.47\ \mu\text{m}$ bands, respectively. They were obtained with the start of fuel injection at 17 bTDC and the inlet air at room temperature. The smallest amount of fuel injection that successfully landed self ignition when injected without fumigation was employed as the pilot injection: The relative portion out of the total energy (for the overall stoichiometric mixture) is not known, however.

The images of PFR in the propane-air mixture (Fig. 8-A) seem to be somewhat comparable to those in SI engine combustion (prior to spark ignition as shown in Fig. 5-A), which all had similarly progressing radiation over the imaging area. The entry of fuel plume does not seem to alter the progressing PFR in the propane-air mixture, except for the zone where the spray is expected to locate.

Recall the increasing radiation over the spray plume when injected alone into compressed air represents the formation of PFR species (refer to Fig. 6-A). In the present fumigation-pilot injection combustion, the presence of reacting gaseous fuel, however, seems not only to delay PFR in the spray but also to slow the species formation in the fumigated mixture itself (Fig. 8-A). The onset of the first flame kernel also appeared late resulting in a longer ignition delay compared to those in DI-CI combustion (where the same amount of fuel was injected as in the pilot injection.) Does this mean that (reactive) intermediate species formed earlier in the fumigated charge actually inhibit processes to the self-ignition in DI-CI combustion? Further study is warranted.

SI ENGINE COMBUSTION

Results obtained from an SI engine with two basic fuel-air preparation methods are discussed: port fuel injection (PFI) and carburetor. The engine was operated typically at 600rpm with room-temperature intake air having approximately 20 kPa (3 psi) vacuum. The fuel-air mixtures

were near stoichiometric for all fuels investigated. Results were obtained during the cold-start period as well as during fully warmed conditions.

Propane-Air Mixture. In spite of its relative simple molecular structure, propane is known to exhibit a cool flame when its mixture with air is exposed in the temperature range of $300\text{--}400^\circ\text{C}$ (More complex fuels have weaker CH bonds tending to produce radicals more readily). Revisiting Fig. 5, the new observation made in the SI engine fed with a premixed mixture is discussed.

According to the results shown in $3.42\ \mu\text{m}$ (it is reminded that those in the figure are in a false color-map designed to reveal local variations, but not in any way to indicate them in relative concentration), the first patch of newly radiating volume (compared to those in earlier CA) is found near the spark-plug which probably maintains the highest temperature in the cylinder. The patch of radiating zone grows rapidly, while the piston moved up, in a repeated pattern of all experiments. It appears that the radiating species are formed quite actively resulting from a surface phenomenon when the fuel molecules in the mixture receives heat transfer from high-temperature surfaces, i.e., from the spark plug (more obviously shown in images taken after -25 CA) and from two exhaust valves (refer to images taken after -19 CA).

The mass of thereof formed species seem to follow the same direction of in-cylinder gas motion. That is, the PFR images look as if they portray a cloud of revealing species as being spewed from the surfaces and blown away by the in-cylinder gas motions.

In particular, the enhanced local variation of radiation as manipulated by false-color exhibits repeatedly a consistent spatial pattern. For example, the radiation of sequential images in gray shade at -21 CA through -15 CA are well repeated by those in light green shade at -13 CA through -7 CA, which represents greater intensity of radiation than the former. Does it mean that they reveal the formation of separate species families, respectively? Or did the increased cylinder pressure enhance the radiation from the same cloud of species as the piston moved up? A great portion of such questions would be answered when time-resolved speciation is achieved as one our next research goals.

Upon the start of spark-ignition, the new radiation from the end gas starts to grow more rapidly than when the mixture was simply compressed by the ascending piston, because of the compounding compression by both the flame front and piston. For example, let us compare corresponding spectral images at -9 CA with each other. Identifying the zones of unignited mixture as seen via 2.47 or $3.8\ \mu\text{m}$ band, one can find some considerable development of radiation with great local variations in the same geometric portions in the $3.42\ \mu\text{m}$ band images (Fig. 5-A).

Again, the images of progressively changing radiation captured from unignited mixtures are considered to indicate the presence of new radiating species including formaldehyde which forms from the oxidation of fuel and radicals, which is consistent with PFR images obtained in other engine-fuel configurations.

Gasoline-Air Mixture. The same engine under a comparable operating condition as the above experiment was run using gasoline introduced via a port fuel injection (PFI) unit. The fuel injection was made starting about 90 CA aTDC during the power stroke of the previous cycle (closed-valve fuel injection at the port).

Unlike the experiment with propane-air mixture discussed above, the engine had some deposit formed over the cylinder head, particularly around one of the intake valves.

Figures 9-A and -B included the results acquired using 3.42 μ m and 2.47 μ m bands, respectively. The sequential images from the gasoline fueled experiment are quite comparable to those from the propane-air premixed case (Figs. 5-A and -B) throughout except for the seemingly pool-boiling flames appearing near the intake valve where the PFI is mated (becoming more obvious at 40-50 CA aTDC). Note that this late burning luminous mixture was suggested to stem from liquid fuel layers (LFL) formed over the surface [7,14], which became available for (late) consumption after the length periods of heat transfer. The LFL were considered to cause unburned hydrocarbon emissions and in-cylinder deposit formation [7,8].

When gasoline was introduced into the engine using a carburetor, the images were quite comparable to those obtained with propane-air mixtures. Again, the PFR in both cases of mixture preparation and also fuel (i.e., gaseous premixed mixture and PFI) seems to be greatly affected by the presence of the high-temperature spark plug (and exhaust valves) where the first radiating PFR zone was found.

The same imaging was conducted when the engine was started cold (room-temperature). During even the first few firing cycles, there was rather uniform change of chemiluminescent radiation over the entire cylinder as the piston moved up. That is, there was no discernible spatial variation of radiation around either the spark plug or exhaust valves, which seems to be reasonable because their surface temperatures were still too low to help expedite the formation of intermediate species.

After continuous operation of approximately 30 seconds, some local variations in PFR radiation were observed, more notably around the spark plug. About one minute later, the similar effects near the exhaust valves were observed. Those findings support the influence of high-temperature surfaces on the formation of intermediate species during the PFR period. (In view of some new findings in this particular experiment, a separate manuscript is being prepared in order to further the in-cylinder flame propagation processes during the cold-start period.)

SUMMARY

Images of radiation considered to originate from intermediate species formed in uninflamed mixtures in the engine cylinder are presented. Among the objectives of the present study was visualization of the spatial and temporal characteristics of such intermediate species formed as preflame reaction (PFR) products.

Invisible PFR in several engine-fuel systems were investigated using high-speed four-spectral infrared imaging system from engines with optical access. Note that the PFR images were captured via only one of several bands (i.e., 3.42 μ m band) of the system.

In the spark-ignition (SI) engine experiment, PFR of several fuels (including gasoline and propane) introduced by either a port fuel injection (PFI) or carburetor were investigated. For Diesel or compression-ignition (CI) engine reactions, the following fuel-preparation-ignition methods were investigated: direct-injection of Diesel fuel (DI-CI); homogenous charge (fumigation) followed by pilot injection; and homogeneous charge self-ignition.

Results obtained in all cases of the abovementioned engine-fuel configurations exhibit mutually consistent PFR images assuring that those captured via 3.42 μ m band represent emission from intermediate species formed under a low-temperature kinetics regime.

In general, the radiation from the PFR indicating the population of active species became remarkably weaker as soon as the high-temperature flame takes over the reactions, which suggest the rapid consumption of the intermediate species (e.g. formaldehyde and other radicals).

In the engine-fuel configurations with spark ignition, the PFR species formation appears to be strongly affected by the presence of high-temperature surfaces (e.g. spark plug and exhaust valves). That is, the PFR images seem to portray a cloud of revealing species as they are spewed from the surfaces to flow away with in-cylinder gas motions.

In the self-ignition configuration, in most cases where there were the high population of PFR species, there was found the first occurrence of flame kernel. This observation was frequently defeated, however, by their mutual inconsistency, in particular when the intake air temperature was very high.

The present survey of PFR in the engine cylinders was expected to serve as a road-map in pursuing the next goal of speciation, that is to determine species formed in the uninflamed mixtures as well as flames.

ACKNOWLEDGMENTS

Authors would like to express their appreciation for support from the US Army Research Office (Contract No. DAAG55-98-0494) and Ford Motor Company.

REFERENCES

1. Clark, G. L. and Thee, W., "Ultra-violet Spectroscopy of Flames of Motor Fuels," *Industrial Engineering Chemistry*, vol. 18, 5, 1926.
2. Withrow, L and Rassweiler, G.M., "Spectrometric Detection of Formaldehyde in an Engine Prior to Knock," *Industrial Engineering Chemistry*, vol. 25, 12, 1933.
3. Clasen, E., Campbell, S., and Rhee, K.T., "Spectral IR Images of Direct Injection Diesel Engine Combustion with High Pressure Fuel Injection," *SAE Paper-950605*, 1995.
4. Dec, J. and Espey, C., "Chemiluminescent Imaging of Autoignition in a DI Diesel Engine," *SAE Paper 982685*, 1998.
5. Jansons, M., Lin, S., Choi, D.S., Campbell, S. and Rhee, K.T., "Study of High-pressure Injection DI Diesel Engine," *SAE Paper 1999-01-3494*, 1999.
6. Hultqvist, A., Christensen, M., Johnson, B., Franke, A., Richter, M., and Alden, M., "A Study of the Homogeneous Charge Compression Ignition Combustion Process by Chemiluminescent Imaging," *SAE Paper 1999-01-3680*, 1999.
7. Song, K., Clasen, E., Chang, C., Campbell, S., Rhee, K.T., "Post-flame Oxidation and Unburned Hydrocarbon in a Spark-ignition Engine," *SAE Paper-952543*, 1995.
8. Campbell, S., Lin, S., Jansons, M., and Rhee, K.T., "In-cylinder Liquid Fuel Layers, Cause of Unburned

- Hydrocarbon and Deposit Formation in SI Engines?" SAE Paper 1999-01-3579, 1999.
9. Jiang, H. and Rhee, K.T., "High-Speed Imaging of Bunsen Burner Combustion Product," Paper No. 67, Proceedings of Canadian and Western States Section of the Combustion Institute, Spring Technical Meeting, Alberta, Canada, May 1990.
 10. Abata, D., Stroia, B.J., Beck, N.J., and Roach, A.R., "Diesel Engine Flame Photographs with High Pressure Injection," SAE Paper-880298, 1988.
 11. Themel, T., Jansons, M., Campbell, S. and Rhee, K.T., "Diesel Engine Response to High Fuel-Injection Pressures," SAE Paper 982683, 1998.
 12. Clasen, E., Song, K., Campbell, S., and Rhee, K.T., "Fuel Effects on Diesel Combustion Processes," SAE Paper-962066, 1996.
 13. Fristrom, R.M and Westenberg, A.A., *Flame Structure*, Chapter 9, McGrawhill, NY 1965.
 14. Rhee, K.T., "Engine/Fuel Studies using Rutgers IR System," Princeton University, US Department of Energy Working Group, March 31, 1995.

In-cylinder Liquid Fuel Layers, Cause of Unburned Hydrocarbon and Deposit Formation in SI Engines?

S. Campbell, S. Lin, M. Jansons, and KT Rhee
Department of Mechanical and Aerospace Engineering
Rutgers, The State University of New Jersey
Piscataway, New Jersey

ABSTRACT

In-cylinder reaction processes in a production port-fuel-injection (PFI) spark-ignition engine having optical access were visualized using a high speed four-spectra IR Imaging system. Over one thousand sets of digital movies were accumulated for this study. To conduct a close analysis of this vast amount of results, a new data analysis and presentation method was developed, which permits the simultaneous display of as many as twenty-eight (28) digital movies over a single PC screen in a controlled manner, which is called the Rutgers Animation Program (RAP for short).

The results of this parametric study of the in-cylinder processes (including the period before and after the presence of luminous flame fronts) suggest that, even after the engine was well warmed, liquid fuel layers (LFL) are formed over and in the vicinity of the intake valve to which the PFI was mated. The sluggish consumption of those LFL, which continued even until the exhaust valve opens, is expected to be one of the main emission sources of unburned hydrocarbon.

Inspection of deposit formation on over twenty-four (24) cylinders (of the engines provided by the manufacturer after some lengthy operation) revealed a predictable pattern. Deposits were found to occur only in areas where the reacting LFL were observed.

The mutually consistent findings from this parametric study are reported. Some of the results from the study will be presented by using the RAP at the meeting.

INTRODUCTION

Mixture preparation in a spark-ignition (SI) engine has been found to remarkably affect engine performance and combustion characteristics [1]*. As an aftereffect of the preparation processes, in-cylinder liquid fuel layers (ICLFL) were found to exist even in warmed SI engines equipped with a port fuel injection system (PFI). The ICLFL in *warm engines* were suggested to be main sources of unburned

hydrocarbon emissions (UHC) as reported in 1995 [2,3]. The same are now considered to cause deposit formation, one of the topics of the present paper.

UHC vs. In-cylinder Liquid Fuel Layers. Since the fuel is injected with the intake valve closed, it is likely that the liquid layers or fuel "puddles" are formed in the intake-port (IPLFL) prior to being "splashed up" or perforated by the back-flow of the combustion products when the intake valve opens. The IPLFL will be formed in greater amounts during the cold start when the fuel is provided at rates producing mixtures a few to several times richer than stoichiometric. Upon the onset of a successful start of combustion, even if the fueling rate is were lowered to provide a mixture preparation near stoichiometric, the IPLFL formation would continue.

Since the formation of IPLFL is obviously undesirable from the standpoint of achieving uniform mixing, one may explore the possibility of increasing the intake port temperature to help reduce or eliminate the IPLFL. Very high intake port temperatures are not presently utilized in SI engine design, however, because they will result in a low brake mean effective pressure (BMEP). Although for now the IPLFL appears to be unavoidable in naturally aspirated high BMEP SI-PFI, it causes various consequences on in-cylinder mixture preparation including the formation of ICLFL over the cylinder head, especially around the intake valve. The impacts of ICLFL may be observed in various forms.

When the flow visualization was made from an SI-PFI during the cold start period [4] and after the warm-up [2,3] using a high-speed spectral infrared (IR) imaging system whose advantages will be explained later, some highly strong locally burning luminous reaction centers (LRC) over the cylinder head were observed. They appeared as if they were diffusion flames similar to those expected

*Numbers in parentheses designate references at end of paper.

over a pool-boiling, in contrast to predictable reaction fronts whose imaging results were obtained from the same engine when operated by premixed propane-air mixtures. In view of liquid fuel ligaments streaming into the cylinder during the cold start as exhibited by others [5] such rich LRC seemingly over ICLFL even in the later stage of combustion period did not appear to be surprising when the engine was cold.

What was quite surprising, however, was that some similar LRC were observed in a relatively warm SI-PFI [2,3]. The LRC in the warm SI engine were only found around the intake valve, unlike during the cold start when the LRC were evident in other locations as well including those around the exhaust valves. It is emphasized that the present discussion, therefore, mainly concerns LRC in the warm engine and its impacts.

The formation and propagation of the LRC studied earlier in this engine are briefly explained. The radiation from these stationary centers, for example with the spark ignition given at 6 CA bTDC [2], typically become obvious only after approximately 15 crank angle degrees after top-dead-center (CA aTDC), a lagging response to the sweeping flame fronts over the surfaces. They thereafter grew stronger and larger in size. These glowing stationary LRC became a luminous reaction flow (LF) after around 60 CA aTDC.

The lagging response of the commencing LRC to the flame propagation suggested that the ICLFL was a likely cause for the LRC because the vaporization and oxidation of a layered liquid fuel would require time consuming heat transfer. (If it were by fuel in gaseous phase, the lagging would have been minimal even if it were discernible.) This is consistent with the consideration that the subsequent process to this initiating reaction therewith landed over the ICLFL would continue to increase the temperature of the fuel layers over the surfaces. Again, the time delay from the early formation of stationary diffusion reactions to those being recognized as LF suggested the role of liquid fuel over the surface.

Since the combustion reaction exhibiting visible radiation in a typical SI engine ends around 30 CA aTDC, the vaporization-oxidation of a great portion of fuel over the ICLFL observed as explained above was characterized as *post-flame* reactions [2].

According to the in-cylinder imaging results, the continuing post-flame oxidation of fuel, upon vaporization off the ICLFL taking place with the piston away from the TDC, appeared to be incomplete even by the time the exhaust valve opened. The incomplete combustion products would either stay over the surface or exist as a gaseous mixture throughout the cylinder volume. Some of the gaseous mixtures would be wasted as UHC, unless trapped in the cylinder as residual gas. The role of incomplete products remaining within the layer is considered later.

The consideration of relating the UHC to the ICLFL may be further backed up as explained next. The UHC measured from an SI engine operated by (1) a premixed mixture of gaseous fuel (e.g. propane) and air and (2) a comparable gasoline-air mixture provided by using a PFI, respectively, indicate that the measurement from the former is only a fraction of that from the latter. If an assumption that

the contribution to UHC by other possible sources (in physical aspects), e.g. crevice volumes, deposit layers, oil layers and quenching layers, stays comparable to each other in both cases is valid, the difference is expected to stem from the slowly reacting ICLFL. For reference, in spite of the system difference, the "wall wetting by liquid fuel" over the cylinder was suggested to be a source of UHC from a direct injection SI engine [6]. This discussion does not exclude probable effects in chemical aspects (e.g. fuel structure) on UHC emissions, which is briefly discussed later.

Note that the conventional consideration relating the deposit layers to UHC as reported in literature concerns gaseous hydrocarbon mixtures compressed into the voids in the layers which stay unreacted in the presence of flame fronts. They would then flow out of the porous shelter as the piston expands, in the absence of flame fronts becoming UHC. This effect is different from those by the ICLFL, which are found to form over the cylinder surfaces either with or without deposit layers as further explained by presenting results.

It is pointed out that the abovementioned fuel staying over the surface would be recycled in the following cycle and a part of it would cause the formation of in-cylinder deposit as discussed next.

Deposit Formation vs. In-cylinder Liquid Fuel Layers. Deposit formation is known to be affected by fuel composition and additives, lubricant, temperature of the surface, location, engine speed and others [7]. It does far more harm to the engine (hot spot, octane requirement increase, increased NOx emission and nuisance) than benefit (e.g. decreased specific consumption in some cases). Although they are all important aspects in need of further study, the present discussion is mainly directed to the formation considered to occur due to the ICLFL taking place in modern SI-PFI engines.

Suppose in-cylinder reactions occur throughout a near stoichiometric uniform gaseous mixture. Its combustion products or inert residue that may compose the formation of deposit in the reactor would be dry and in minute sizes, which would result in a rather uniform layer over the surface. The typical in-cylinder deposit layers in SI-PFI, however, are locally (very) thick, dark and glassy (DG) having the appearance of varnish layers around the intake valve(s), and white-gray in thin layers over (high-temperature) surfaces, notably the exhaust valve(s) and spark plug. DG thick layers around the intake valve in SI-PFI, which is a main subject in this paper, are not considered to be a result of accumulated layers of such floating dry minute particles in the combustion product. Rather, they seem to be a product of fuel layered over the surface *without* its having been involved in the combustion reaction (e.g. being atomized-mixed with air and distributed uniformly over the reaction volume). Note that the white-gray thin deposit layers, whose compositions are known to be different from those in the DG layers, will be considered in a separate study.

The deposit layers formed over the combustion chamber are basically the integrated balance of its new build-up subtracted by its removal. The removal processes include flake-off, burn-up, wash-way, and water absorption (during the cold engine shut-down period), which are

basically self-explanatory.

It has been suggested that when the liquid fuel from the IPLFL is thrown over an existing deposit layer, which is considered to cause ICLFL formation (resulting in slow burning LRC over the surface), the fresh liquid bombarding the in-cylinder deposit layer would help wash it away. While the washing action may play a role in partial removal of the deposit, at least a portion of the liquid fuel landed over the layer would be soaked into the existing formation.

In addition, the suggestion of sheltered fuel in the deposit layer is not new but a rather old concept employed to explain the sources of UHC emissions. Unlike gaseous mixtures pushed into the deposit causing UHC, the soaking of fuel at this time is suggested to occur in the liquid phase (i.e., ICLFL), which is considered to be a main source of not only the exhaust UHC as discussed earlier but also a cause of deposit layer formation.

Regarding the probable cause of deposit formation, when such fuel soaked in the layer is not all released during the remaining cycle, there would be a net gain in mass of the layer. The amount of gain will undoubtedly be affected by the temperature of the layer (and the surface underneath), which may be further seen from the fact that the exhaust valve does not accumulate such DG thick deposit layers, but thin whitish layers. This also means that where there is no ICLFL, there should be no significant amount of DG deposit formation in SI-PFI, which will be explained later.

High-speed Spectral Infrared Imaging System. As briefly explained earlier, a high-speed spectral IR imaging system was employed in the earlier engine studies which discovered rich-burning LRC over presumably liquid fuel layers or fuel-impregnated deposit layers in SI-PFI engines. They were suggested to be main sources of UHC emissions [2,3], and now of in-cylinder deposit formation. At the same time, it is pointed out that no similar finding has been reported by others (particularly prior to these studies) to corroborate the existence of ICLFL in *warm* SI engines and the suggested impacts.

Why then is the spectral IR imaging system mentioned here and why has no one reported the same in spite of the important nature of the phenomena in warm SI-PFI? While the concept of designing this new diagnostic IR system was to achieve in-cylinder quantitative imaging [7], it was simply by *accident* to find the LRC existing in the SI-PFI cylinder [2,3], which was only possible via certain spectral wave bands, as explained later. The absence of similar findings (e.g. LRC at the later stage of combustion in warm engines) by others may be due to a high probability of their employing conventional methods of in-cylinder imaging, e.g. via wide IR bands, or even narrow IR bands where radiation from main combustion products is dominant, or by visible-ray photography, which all do not facilitate imaging of reactions taking place *near* the surface.

Apparatus Closely Duplicating Real-World Engines. The present discussion on the formation of ICLFL in SI-PFI would immediately raise a suggestion for achieving real-world engine conditions in the experimental apparatus particularly as to the thermal and air-fuel flow characteristics in order to determine a generic nature of the phenomena. Since effects of such thermal and flow parameters are expected to decisively affect the formation of ICFL and LRC,

in order to minimize confusion and any potential misleading, it was attempted to avoid in the present paper the discussion of early reports prepared by employing other apparatus than production engine systems.

In spite of all measures taken in construction of the apparatus to meet such needs in the previous studies (e.g. using a real-world engine cylinder head), it was still considered to be insufficient in warranting its representation of the real-world engines. Consequently, it was decided to take some radically unusual steps in designing a new unit in order to minimize uncertain effects which may occur otherwise.

EXPERIMENT

As mentioned above, the present engine apparatus was prepared to represent the actual engine conditions as close as possible. Some unconventional methods were required in its design/construction. In order to capture the most reliable evidence of the new phenomena, a multispectral IR imaging system with an entirely new electronic package was employed, which will be separately discussed elsewhere.

In addition, a new data analysis and presentation method, which is referred to as Rutgers Animation Program or RAP for short, was developed for facilitating the implementation of the present objective. The importance of RAP may be seen from the fact that the present paper is prepared using results selected from over a thousand sets of high-speed (spectral) sequential images obtained under various experimental conditions. The analysis of this vast volume of images is beyond the limitation achievable while expanding a reasonable amount of time and resources by employing the conventional method, e.g. playing them via a video system individually for mutual comparison and analysis.

Engine Apparatus. One of the main requirements of the new engine apparatus was to have maximum optical access to the reaction chamber while maintaining the desirable engine characteristics as mentioned above. By taking advantage of the experience constructing a single-cylinder engine with optical access for earlier studies [2-4], the access was achieved via an extended piston with an IR window at the top as schematically shown in Fig. 1.

One of the most important features of this arrangement was that the entire portion of the cylinder bank (having the water-jacket around them) was mated with the original cylinder head and intake manifolds. Out of four cylinders in the bank, only one cylinder was utilized for combustion reaction that accommodates the extended piston. The crankshaft was balanced to achieve smooth operation even at relatively low speeds, which was also aided by incorporation of a new high-inertia flywheel.

The entire cylinder block was used to duplicate the coolant flow and induction air flow conditions of the stock engines as much as possible. A close duplication of the representative engine conditions, at least those associated with the cylinder head, was considered to be a critical requirement for the engine setup in which how the phase transition of fuel occurs during the combustion is questioned. For example, misleading results would probably be obtained if the coolant flow pattern is altered from the

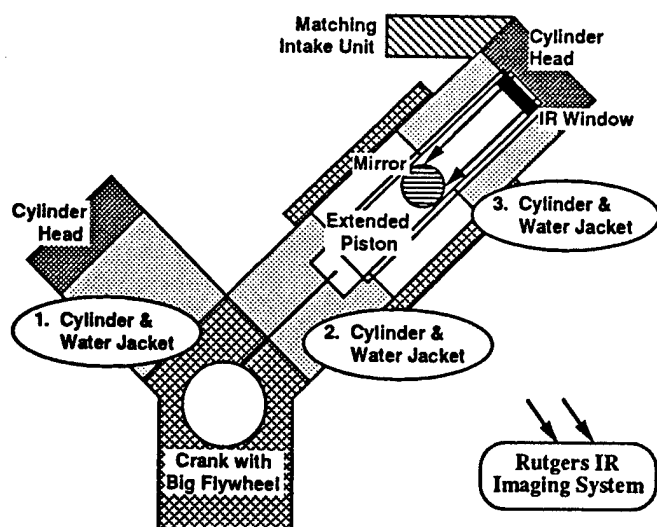


Fig. 1. A New Engine Apparatus for Duplicating Representative In-cylinder Reaction Conditions.

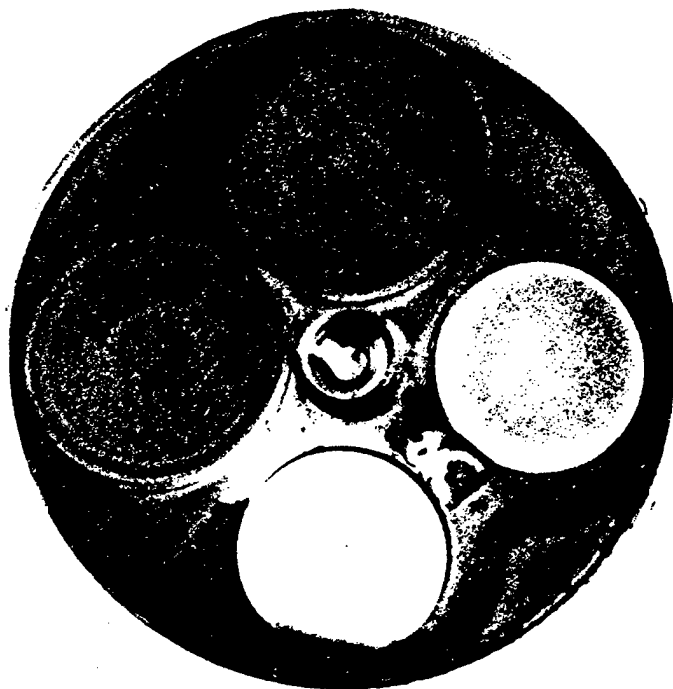


Fig. 2. Imaging View of the Combustion Chamber via the Optical Path.

original. The duplication of the original layout angle of the cylinder bank was also considered to be important because the induction of fuel out of IPLFL could be affected if it were oriented vertically as in many similar apparatus with an extended piston.

Among the important engine specifications are bore-stroke of 90-90 mm, connecting rod length of 151.5 mm, compression ratio of 9.9, clearance chamber volume of 50 cc. It had two intake valves and two exhaust valves having diameter with peak lift of, 44.5 mm with 6.59 mm

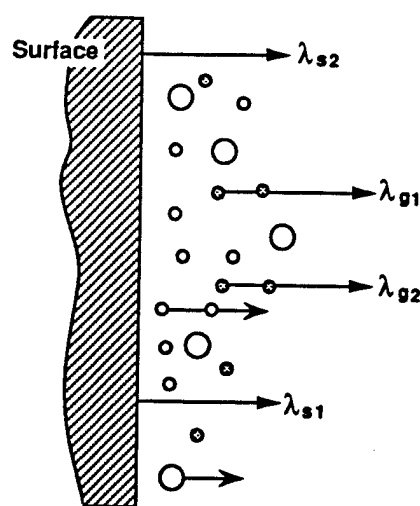


Fig. 3. Spectral Imaging Concept from a Combustion Chamber.

and 34 mm with 6.59 mm, respectively.

In order to eliminate fouling the optical windows by lubricating oil flowing over the piston-top, which commonly occurs during the intake stroke, five identical pieces of graphite rings (with exactly the same outer diameter of the steel ring of the original engine) were used. Two sets of compression rings (two rings in each groove) were used for sealing the mixture and one bearer ring was placed for aligning the piston with the center of the cylinder. In spite of some lengthy and elaborative work involved in the design-construction of this unique apparatus, since the scientific value about this set-up is considered to be limited, no further discussion is made here.

An image of the cylinder head surfaces seen via a direction of 45-degree to the (oval) mirror (i.e., perpendicular to the page in Fig. 1) is shown in Fig. 2 (without the IR window, which is opaque to visible ray), where two intake valves on the upper left and two exhaust valves on the lower right of the figure with the spark plug in the middle can be seen.

IR System. In order to explain the advantages of the multispectral imaging system in studying the impacts of ICLFL, a schematic presentation of the combustion chamber (Fig. 3) is included here.

Referring to Fig. 3, the spectral radiation issued from a combustion chamber (having combustion products in front of the reactor surface) may be selectively captured by using corresponding spectral band filters placed in respective cameras of the system. As explained later, it was possible to obtain relatively untainted images of the (high temperature) surface when a 3.8 μm band filter (as represented by λ_s in Fig. 3) was employed, and strong images of water vapor distribution were captured via other bands (e.g. in λ_g) [8-10].

Briefly, the basic idea of designing the present IR system was that four separate units of high-speed digital IR cameras (per each, 64x64 pixel matrix and over 2,000 frames/sec max.) were integrated to a single optical train containing three spectral beam splitters [2-4,8,9]. This system layout permits simultaneous acquisition of four geometrically

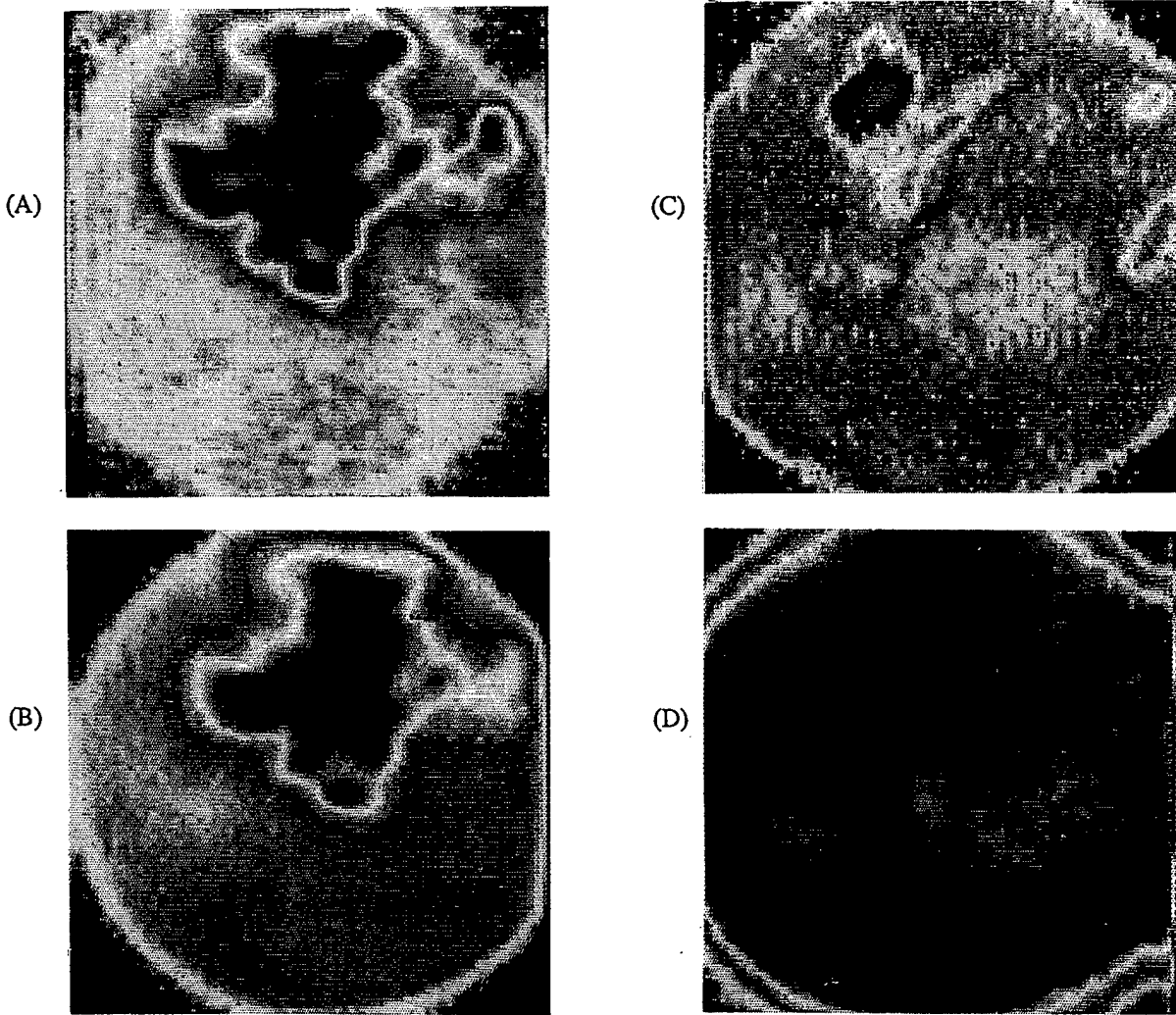


Fig. 4. Four Spectral Images Simultaneously Obtained at 55 CA aTDC in Spectral Bands of :
(A) 3.8 μm ; (B) 2.2 μm ; (C) 3.42 μm and (D) 2.47 μm .

identical images in respective spectral bands from the same radiation source (e.g. Fig. 3), which was named by others Super Imaging System (SIS) or Rutgers System. New spectrometric analysis methods were developed in order to process the digital data matrices from the SIS, which made it possible to achieve quantitative imaging [8].

Further discussing the advantages of using the SIS for studying the present problem, spectral IR images (Fig. 4) of the cylinder head with combustion products in front of it are shown here. These images were captured via the same optical view of the combustion chamber at 55 CA aTDC, and the sequential images in the 3.8 μm band are shown in Fig. 5. Prior to explaining Fig. 4, although they are discussed in Results and Discussion, those in Fig. 5 are briefly mentioned first. Note that a look-up-table (LUT) is included in Table-I in order to indicate the matching crank angle positions for those obtained with spark ignition (SI) at 15 CA bTDC.

-21	-19	-17	-15	-13	-11	-9	-7
-5	-3	-1	1	3	5	7	9
11	13	15	17	19	21	23	25
27	29	31	33	35	37	39	41
43	45	47	49	51	53	55	57
59	61	63	65	67	69	71	73

Table-I. Look-up Table (LUT) for Fig. 5

As seen from the matching LUT, the timing of images in Fig. 5 goes from left to right and from top to

- . injection pressure
- . coolant temperature
- . injection time
- (5) Deposit images when operated by propane
 - . cylinder head with some deposit
 - . clean cylinder head

Although it would be highly desirable to include many sets of results in the present paper, due to the logistic reasons, only a small amount is shown in a form of the hard copy. (It will be attempted that all the results to be discussed next, however, will be shown in animated form in the paper presentation.) While some findings are explained by giving selected representative images here, others are discussed without illustration.

Propane vs. Gasoline. At first, sets of sequential images obtained via 3.8 μm band by using near stoichiometric mixtures of (a) gasoline/air by PFI (b) propane/air (premixed) are presented, respectively (Fig. 5).

Note that four-color images in Fig. 4 include a 3.8 μm band image corresponding at 55 CA aTDC as shown in Fig. 5-(A). Reviewing the sequential images (Fig. 5) obtained from a warm engine condition (coolant temperature of 80°C), before the spark ignition (15 CA bTDC) thermal images of four valves and the spark plug are mutually similar to each other for operations by respective fuels. Upon ignition, the progressive propagation of flame fronts appears to be predictable and also comparable to each other until around 15 CA aTDC. Notice the rather immediate emission of strong thermal radiation from the exhaust valve and deposit around one of the intake valves in response to the flame fronts. This suggests that the cooling depth of their surfaces during the non-combustion period was shallow. Such a rather prompt thermal response of those high-temperature surfaces is in contrast to the lagging response of LRC to the sweeping flame propagation.

As the combustion reaction continues to spread over the entire reaction volume, looking at those obtained with gasoline (Fig. 5-(A)), local radiation centers (LRC), around 17 aTDC, are typically observed starting to grow some luminous centers near and over the intake valve (compared with those seen in Fig. 5-(B)), which is similar to the findings in the previous work [3,4]. These growing LRC became more luminous, and afterward detached themselves from the surface to become moving luminous volumes (i.e., luminous flow, LF), which appeared to be obvious around 51 aTDC. (Recall the lagging response of the growing LRC and LF was explained by the time required for heat transfer from combustion products to ICLFL.) Those from the propane/air mixture (Fig. 5-(B)) did not exhibit such radiating flows but stationary luminous surfaces (SLS, notably around one of the intake valves).

As discussed later in more detail, it is pointed out that images of the SLS captured during propane-air operation are expected to be from the glowing surfaces of deposit layers formed over the cylinder head. In contrast, images of LRC observed in gasoline-operated SI-PFI were considered to be from radiation emitted from locally reacting rich mixtures over the deposit layers (loaded with liquid fuel during the intake period). Therefore, the images of LRC would be the compounded results of reacting rich mixtures (over the wall) and radiating stationary deposit surfaces.

This consideration may be backed up by the observation that when the cylinder head surface was clean, the SLS was not observable in a propane-operated engine while the LRC was seen from the same engine when operated by gasoline.

Since the direct image of ICLFL formation has not been actually captured (e.g. a form of wet liquid film), only indirect evidence is presented in addition to the various reasons explained earlier in support of its existence in SI-PFI. First of all, it is pointed out that the LRC were not generally found over one of the intake valves through which only air is introduced, but near the other one where the PFI is mated. The LF after growing out of the LRC, however, moves over a great portion of the former, which will be further discussed later. It is reminded that an SI with no or minimum IPLFL was not expected to cause the formation of ICLFL.

Gasoline by a Carburetor. In order to help determine if such luminous LRC (as observed via the SIS) are unique combustion characteristics of gasoline-air mixtures even in the absence of ICLFL, the same engine was fueled by using a conventional carburetor which is not expected to produce IPLFL. Without presenting the high-speed images, it is noted that the results were quite similar to those observed with a comparable propane-air mixture, which did not exhibit any glowing LRC or an LF around either of the intake valves.

SI-carburetor operation (with the coolant temperature of 80°C) was expected to atomize the liquid fuel sufficiently to prepare a near premixed flow before the intake valve, resulting in a minimal IPLFL. The absence of LRC in these combustion processes therefore seems to indirectly indicate the absence of ICLFL over the cylinder head. This may suggest that where there is no ICLFL, there is no LRC.

Isooctane and Ethanol by PFI. Finding that a condition of having a minimum IPLFL (also ICLFL) resulted in no measurable LRC as explained above when using a carburetor, a similar measure was taken in the next experiment which was to feed the engine with high-volatility fuels by PFI.

Expecting the mixture preparation processes with PFI to be affected by the distillation characteristics, the engine was operated by near stoichiometric mixtures of isooctane (BP, 99.4°C) and ethanol (BP, 78°C), respectively, which would produce smaller amounts of IPLFL than with gasoline. For both fuels, there was no evidence of LRC in any way similar to those seen when the engine was operated with gasoline by using PFI.

Note that the absence of LRC as observed in this experiment, however, does not necessarily exclude the existence of ICLFL (IPLFL). For example, there is a possibility that combustion products of these fuels (with a lower molecular weight than those of the high-end portion of gasoline) may not produce high emissivity products even if they were layered over the surface.

If the high-volatility fuels do not produce the LRC as observed in the present experiment, would it be reasonable to expect that the LRC are most likely caused by the portion of low-volatility (high-end) fuel components (chemical aspects of fuel as briefly mentioned earlier) in gasoline?

Gasoline by PFI with Variation of Spark Timing. To further characterize the ICLFL and their impacts, the in-cylinder imaging was made under several varied conditions, including the spark ignition time as explained next. The results exhibited a definite trend with varied spark timing that the more the timing delay, the smaller the activities of LRC.

This observation seems to be consistent with the suggested role of IPLFL in affecting the ICLFL formation. When the spark timing is delayed, the combustion product temperature becomes higher due to its increase of internal energy, which would result in increases of both the engine (block) temperature and the back-flow of residual gas.

The temperature increases would not only accelerate the vaporization of fuel in the intake-port but also reduce the formation of ICLFL, which was considered to cause reduced amounts of LRC in the cylinder.

Lower UHC emissions [13] and smaller amounts of deposit formation [14] in SI-PFI with late spark ignition and high surface temperature as reported by others are consistent with the present observation as well as the consideration of relating the ICLFL with the emissions and deposit formation. (It is added that the UHC emission with retarded spark ignition is significantly reduced due to the increased oxidation of incomplete products after leaving the exhaust valve.)

Gasoline by PFI with Variation of Injection Pressure. Expecting effects of atomization-vaporization of the injected fuel at the intake port on the LRC, the fuel was delivered at several different pressures ranging from 110 to 206 kPa (16 to 30 psi). Observation made of the LRC, however, revealed only minor differences.

Some plausible reasons for the observation may be considered. Since the fuel is injected at the intake port with the valve closed, the extent of the atomization and vaporization of the fuel dictated by the injection pressure would be altered when the back-flow of high-temperature combustion products occurs. This may suggest that the condition of fuel delivered at the intake port was not greatly affected by the pressure change (due to the finite size of the port volume), or that the role of the back-flow was significant superseding the effects of injection pressure.

Gasoline by PFI with Variation of Coolant Temperature. The coolant temperature was varied from 33 to 82°C in the experiment in order to assess its effects on the LRC. The effect was remarkably obvious, which may not need an additional discussion. While some significant amounts of LRC were observed even with the coolant temperature at 82°C, there were cycles in a greater frequency exhibiting negligible LRC. It is noted that when the engine was operated with the coolant temperature of over 90°C at the measurement point (in a copper-tubing coolant-conduit, approximately 30 cm away from the cylinder head), which was considered to be improperly high for the engine, the LRC was negligible according to the present spectral IR imaging, which may be a gain but at the expense of engine BMEP.

Gasoline by PFI with Variation of Injection Time. The fuel injection was started at four different times to see the effects of its variation on the LRC (with the cooling temperature of 78°C): (a) before the start of the combustion period in the previous cycle; (b) near the end of

combustion period in the previous cycle; (c) at the beginning of intake period; and (d) in the middle of intake period.

As expected, the extent of LRC became more active in the sequence of the above list. Elaborating further on the observations, there was only a small difference between LRC in timings (a) and (b), while it became greater when the fuel was delivered with timings (c) and (d). The difference between (a) or (b) and (c) or (d), however, was not highly significant.

Deposit Images when Operated by Propane. When IR images captured in 3.8 μm (Fig. 5-(B)) were discussed, it was pointed out that there were stationary luminous surfaces around the intake valve where the injector is mated while the engine was operated by a propane/air mixture. Such luminous surfaces over a crescent geometry were not observed, however, in the early stage of experiment, which was right after the cleaned cylinder head was installed. After many hours of engine operations (using gasoline by PFI and also propane from time to time), the stationary luminous surfaces became noticeably obvious becoming a fixed part of imaging results, thereafter. It is not clear, however, if the size of the luminous surface (in the images) varied with time during the course of the present experiment.

An inspection of the cylinder head revealed that there was some amount of new deposit formation accumulated over an area, which was considered to match the stationary luminous surfaces identified in the imaging.

A new experiment was performed by running the engine with gasoline via PFI for a long period of time, which was expected to build up some additional deposit over the cylinder surface. The engine, then, was continuously operated upon switching to propane/air mixtures, and in-cylinder IR images were obtained at different times to see if the image of deposit is affected with time: (a) 0 minute with the new mixture; (b) 5 minutes; (c) 15 minutes; and (d) 25 minutes. Although it seems somewhat difficult to quantitatively characterize if the deposit was indeed burned away during the operation by propane/air mixtures, there was a trend of reducing image size of the stationary luminous surface with time during this engine operation.

In-cylinder Liquid Fuel Layers vs. Deposit Formation. Some of the results from a parametric study of LRC, which were observable using a high-speed spectral IR imaging system only when certain narrow spectral bands were employed, were discussed above. According to what has been found in the analysis, all evidence seems to suggest that ICLFL cause the LRC and that their sluggish post-flame oxidation reactions are expected to result in not only increased UHC but also formation of deposit layers over the cylinder head, which is further elaborated next.

During the course of the present study, three units of the original engine (4-valve, V-8) were overhauled, which were provided by the engine manufacturer after running them for extended periods of time. According to the evaluation of the deposit layers formed over the cylinder head surfaces of these engines (24 cylinders), some distinctive and mutually comparable patterns of the formation were realized as summarized next.

The deposit formation was found in most significant amounts around the intake valve where the PFI

was connected, in quite smaller amounts over the other intake valve, in very remarkable amounts and in greatest thickness over the triangular peninsular which divides two intake-valve areas (Fig. 2), and in insignificant amounts over the exhaust valves. While the formations over the intake valves and the triangular peninsular appeared dark and greasy, those over the exhaust valve surfaces and others which were expected to attain high temperatures looked gray-white and of thin and uniform thickness.

One important point to make, based on the above summary and imaging results analyzed by using the RAP for the entire engine operating conditions, is that the LRC (and luminous volumes, LF, grown out of the stationary locations, i.e., flows off the centers) were most active where the dark and greasy (DG) deposit formations were found in significant amounts. The animation by the RAP revealed that the (deposit-loaded) peninsular seemed to serve as a deflecting wall which often altered the direction of LF. It is reemphasized that no warm engine condition exhibited any noticeable LRC over the exhaust valves. It may be reasonable, thus, to expect that where there was no LRC and luminous flow, there was no DG deposit formation in remarkable amounts.

As briefly noted earlier, when the cylinder head surfaces were clean, no noticeable stationary luminous surfaces (SLS) were observed in the propane-operated engine, while the same clean engine exhibited LRC when operated by gasoline. The SI-PFI after running by gasoline for an extended period of time, however, started to reveal images of SLS when operated even by propane (without any sign of LRC). It is reminded that those SLS were only found where the LRC were repeatedly located while operated by gasoline. The radiation from LRC under the gasoline operation, which were much stronger than those by SLS, were considered to represent those from fuel-rich oxidation reactions over SLS as well as those from SLS themselves.

Removing the IR optical window from the engine, it was observed that the geometric location of SLS (seen when operated by propane) and the new deposit formations seemed to match each other. This further suggested that the SLS became glowing centers as heated by propane-air combustion products. Summarizing the above findings, it is expected that the ICLFL in the SI-PFI cause the LRC, which produced deposit formation over the cylinder surface whose image was partially reflected as SLS (even when operated by propane).

Deposit Formation via ICLFL? If the ICLFL are indeed a main cause of the DG deposit formation, what processes would be involved? Two possible routes of formation may be considered after the liquid fuel is layered over the combustion chamber surfaces. It is most probable that the ICLFL would land in greatest amounts around the intake valve having the PFI, and in smaller amounts over the other intake valve and other surfaces.

It is expected that fuel landing on high-temperature surfaces including the exhaust valves would be instantly vaporized and dispersed over the chamber before the spark ignition, which means the fuel would not be accumulated over those areas to become DG deposit formations. It is physically quite possible that some portion of ICLFL landing on low-temperature surfaces (e.g. intake valves, and the

surrounding area being cooled by the intake air and also fuel) would stay as residue to be reexposed to flames in the following cycles. When the fuel added over the previous residue becomes exposed to high-temperature combustion product (with insufficient oxygen), the fuel would be decomposed, e.g. dehydrogenation. (Although the accumulation would not continue without any removal, the processes are not considered here.) It is pointed out that some of the ICLFL may not even exhibit any detectable radiation (as a result of either combustion or post-flame oxidation), such as when landing over remote corners of the combustion chamber where the wall quenching is more significant.

Unlike the above suggested formation of DG deposit via the liquid phase of fuel loaded in ICLFL, the gaseous fuel leaving the ICLFL (recall the observation of such luminous flows starting around 50-60 CA aTDC, *which is after the luminous flame fronts are gone*) undergoing post-flame oxidation may also cause the formation of DG deposit. According to highly luminous radiation issued by those flows, the reaction products are expected to contain soot in significant amounts, which probably become part of the DG deposit formation. When such fuel-rich oxidation products (formed in absence of flame) bombard a cold surface or existing DG deposit whose surface temperature is expected to be low (otherwise, it would have not been formed or eliminated such as over an exhaust valve), it would become an additional accumulation. This consideration is particularly intriguing because there were some remote corners of the chamber having some considerable amounts of DG formation without corresponding appearance of LRC (as mentioned above) but having LF sweeping. It is added here that the patterns of LF growing out of the LRC, i.e., radiating flows over the chamber, were generally similar to each other among all data observed-analyzed by using the RAP.

Finally, according to the same imaging during the cold start, LRC were found, however, over many different areas including the exhaust valves. The absence of DG deposit formation over those high-temperature surfaces may be an indication that any DG deposit formed during this period was flaked out or burned up as their surface temperature increased. The gray-white deposit formation over such high temperature surfaces, therefore, may be composed of mostly inert materials which are no longer oxidized.

SUMMARY

High-speed spectral infrared imaging was employed to capture images of rich-burning (stationary) locally reacting centers (LRC) as well as moving luminous volumes (i.e., flows) over the cylinder head surface of a gasoline-operated spark-ignition equipped with port fuel injection system (SI-PFI). The images of LRC and luminous flows (LF) were only observable when some selected spectral bands (3.8 μm and 3.43 μm bands, as identified to date) were employed.

The design-construction of engine apparatus was made in a way to closely simulate the fuel-air preparation and reaction conditions representing those in real-world SI-

PFI engine populations. The high speed IR system is one-of-a-kind prototype (continuously developed-improved during the last twelve years) to permit imaging of four sets of geometrically identical digital matrices of 64x64 in respective spectral bands at rates over 2,000/sec/camera. The vast amount of imaging data obtained by the system was analyzed using a new data analysis and presentation method (RAP), which is basically a computer program to achieve animation of in-cylinder information. For example, the RAP can be used to simultaneously display many separate animation (28 movies at present) over a single PC screen to expedite screening and analysis of the raw image data.

Some of the results, obtained by using the above techniques from the SI-PFI (with coolant temperature, 78-80°C) operated by fuel/air mixtures of near stoichiometric, reveal the following:

(1) Some stationary luminous surfaces (SLS) were identified around the intake valve mated with the PFI (IV-PFI) when propane-air mixtures were used in the SI-PFI, which was operated by gasoline for an extended period, presumably accumulating deposit formation. (The SLS were not observed when the cylinder head surface was clean.)

(2) When the same engine was operated by gasoline, (stationary) LRC became obvious over the SLS area starting approximately 17 CA aTDC. Around 50-60 CA aTDC, some luminous volumes (flows, LF) growing over the LRC were detached from them basically spreading over areas in the vicinity of the IV-PFI.

(3) The luminous flows had quite similar patterns under all operating conditions, such as bouncing off the triangular land which divides two intake valve areas.

(4) The imaging results of LRC and LF (revealing post-flame oxidation) suggest that some liquid fuel layers formed in the cylinder (ICLFL), stemming from intake-port liquid fuel layers, caused such fuel-rich reaction volumes with remarkable time lags to the presence of flame fronts. The time lagging suggests that the ICLFL requires some amounts of time period for heat transfer before being vaporized to react or to produce in amounts sufficient to be seen as flows. (These considerations are consistent with some results from a parametric study as summarized in the following.)

(5) When the mixture preparation of the same engine was made by using a carburetor, the imaging results were quite comparable to those with propane-air mixtures. That is, there was no LRC or LF, but some SLS.

(6) When the same engine was operated either by isooctane (BP 99.4°C) or ethanol (BP, 78°C), there was no remarkable LRC or LF.

(7) When the engine fueled by gasoline was operated at varied spark times, the later the spark ignition, the less the amount of LRC and LF, which seems to be consistent with the expectation of ICLFL formation in smaller amounts at reported spark times due to increased cylinder temperature and back-flow at the IV-PFI opening.

(8) When the fuel injection pressure was varied, there were insignificant changes in the occurrence of LRC and LF.

(9) When the coolant temperature was varied, there was some remarkable changes in the amounts of LRC and

LF. That is, the higher the coolant temperature, the smaller the amounts.

(10) When the start of fuel injection was varied, i.e., in the beginning and later part of the combustion period (in the previous cycle), and in the beginning and middle of intake period, respectively, the amounts of LRC and LF increased in the sequence list here.

The ICLFL-caused sluggishly reacting combustion and post-flame oxidation reactions over the cylinder head surfaces and chamber volume were observed to continue even by the exhaust valve opening time. It seems to be reasonable to suggest that the ICLFL, thus, is a main source of UHC and the formation of dark and greasy deposit (DG) layers in the cylinder. Several indirect evidences are extensively discussed (in the text) in support of the relationship of ICLFL to UHC.

The consideration of relating ICLFL to DG deposit formation is backed up by the observation of LRC and LF from the present study using the new RAP. That is, the DG deposit layers were only found to form over regions where the LRC and LF were observed to occur.

ACKNOWLEDGMENT

Authors wish to express their appreciation for support from the US Army Research Office (Contract No. DAAG55-98-0494) and Ford Motor Company.

REFERENCES

1. Kajitani, S., Sawa, N., Rhee, K.T., "Mixture Preparation in Spark-ignition Engine and its Effect on Engine Performance and Combustion Characteristics," SAE Paper-900711, 1990.
2. Song, K., Clasen, E., Chang, C., Campbell, S., Rhee, K.T., "Post-flame Oxidation and Unburned Hydrocarbon in a Spark-ignition Engine," SAE Paper-952543, 1995.
3. Rhee, K.T., "Engine/Fuel Studies using Rutgers IR System," Princeton University, US Department of Energy Working Group, March 31, 1995.
4. Campbell, S., Clasen, E., Chang, C., and Rhee, K.T., "Flames and Liquid Fuel in an SI Engine during Cold Start," SAE Paper-961153, 1996.
5. Shin, Y., Cheng, W., Heywood, J., "Liquid Gasoline Behavior in the Engine Cylinder of a SI Engine," SAE Paper-94187, 1994.
6. Stanglmaier, R., Li, J., and Matthews, R., "The Effect of In-cylinder Wall Wetting Location on the HC Emissions from SI engines," SAE Paper 1990-01-0502.
7. Obert, E.F., *Internal Combustion Engines and Air Pollution*, 1973 Harper & Row, Publishing.
8. Chang, C., Clasen, E., Song, K., Campbell, S., Jiang, H., Rhee, K.T., "Quantitative Imaging of In-cylinder Processes by Multispectral Methods," SAE Paper-970872, 1997.

9. Clasen, E., Campbell, S., and Rhee, K.T., "Spectral IR Images of Direct Injection Diesel Engine Combustion with High Pressure Fuel Injection," SAE Paper-950605, 1995.

10. Jansons, M., Lin, S., Choi, D.S., Campbell, S. and Rhee, K.T., "Study of High-pressure Injection DI Diesel Engine," SAE Fuels and Lube Meeting, October 1999.

11. Jiang, H. and Rhee, K.T., "High-Speed Imaging of Bunsen Burner Combustion Product," Paper No. 67, Proceedings of Canadian and Western States Section of the Combustion Institute, Spring Technical Meeting, Alberta, Canada, May 1990.

12. Jiang, H., Qian, Y. and Rhee, K.T., "High-Speed Dual-Spectra Infrared Imaging," Optical Engineering, 32 (6), pp. 1281-1289, 1993.

13. Sodre, J. R. and Yates, D. A., "An Improved Model for Spark Ignition Engine Exhaust Hydrocarbons," SAE Paper-971011, 1997

14. Cheng, S-W and Kim, C., "Effect of Engine Operating Parameters on Engine Combustion Chamber Deposits," SAE Paper 902108, 1990.

Study of High-pressure Injection DI Diesel Engine

M. Jansons, S. Lin, D.S. Choi, S. Campbell, and KT Rhee
Rutgers, The State University of New Jersey
Piscataway, New Jersey

ABSTRACT

Visualization of in-cylinder reaction processes and performance analysis of a direct-injection Diesel engine equipped with a high injection pressure (HIP) unit were conducted. The study was directed towards evaluation of high-power-density (HPD) engine design strategies, which utilize more intake air operating at rich overall fuel-air ratios.

Two separate engine apparatus were used in this study: a Cummins 903 engine and a single-cylinder optical engine equipped with the same family engine components including the cylinder head. The engines were mated with an intensifier-type HIP fuel system fabricated at Rutgers which can deliver fuel injection pressure of over 200 MPa (30,000psi).

The one-of-a-kind high-speed four-band infrared (IR) imaging system was used to obtain over fifteen hundred sets of spectral digital movies under varied engine design and operating conditions for the present analysis. In order to analyze and present this large amount of results, a new data analysis and presentation method was developed (called Rutgers Animation Program, RAP for short). RAP is a computer program permitting simultaneous display of as many as twenty-eight (28) sets of digital movies over a single PC screen for mutual comparison in a controlled manner.

Among the findings from the study is that the in-cylinder imaging performed within the first several cycles may not represent what is happening in a typical warm engine. In addition, the spray development and subsequent reactions of the HIP unit may not be comparable to those of low-pressure conventional injector units. In-cylinder processes and engine performance of an HPD engine affected by various factors are also described in the paper which include: the injection pressure, intake air temperature, and overall air-fuel ratio.

INTRODUCTION

Among development strategies recently being taken for achieving a high-power-density (HPD, high horsepower

per displacement or weight) low-emission direct-injection (DI) Diesel or compression-ignition (CI) engine is the use of an electronically controlled high-injection-pressure (HIP) fuel system. This is basically because an HIP system permits better utilization of the intake air by using overall rich smoke-limited fuel/air mixtures at high engine speeds [1]*, and because it may facilitate reduced emissions by the rate shaping [2].

HIP in HPD. The injection pressure of some recent HIP systems ranges near 200 MPa (over 30,000psi), and the in-cylinder fuel-air mixture preparation by an HIP is considered to be different from that in the conventional low-injection-pressure (LIP) DI-CI engines. For example, the processes of an HIP are expected to result in more cavitation in the flow stream within the nozzle and sac volume [3], and the high-speed fuel stream leaving the nozzle hole may reach a near sonic speed, which is not expected to occur in the conventional LIP systems. (Note that although some shock wave may be observed in an HIP spray under laboratory condition, the same is not likely to occur within the high-temperature cylinder.) Under such conditions of HIP involving greater possibility of unstable fuel flows, the cyclic variation and altered spray development may be significantly different from those in the conventional LIP systems.

The use of ceramic components is considered to be a viable approach for achieving an HPD CI engine, which brings on additional technical challenge. Their use would help eliminate or reduce parasitic components found in the conventional cooling system, producing a compact and tidy engine design. In such a low-heat-rejection (LHR) engine, the compressed air charge (also very probably the fuel temperature at the injector tip) will attain higher temperatures than in the existing (water-cooled) LIP CI engines, which is expected to lead the spray formation and preflame reactions during the ignition delay period to fall in new regimes of physical as well as thermochemical processes.

*Numbers in parentheses designate references at end of paper.

When the thermal changes by the LHR design strategy are compounded with new physical effects stemming from the HIP, the spray formation and subsequent reactions would be further altered from those in the conventional LIP CI systems.

The present analysis of HPD engine development strategies, therefore, considers in-cylinder reactions in the environment of an LHR DI-CI engine equipped with an HIP system. Since the study was planned also to assess the cases with relatively low intake air temperatures for a wide range of injection pressures, as base-line information, a better insight into the engine responses to the HPD engine design strategies was expected to be achieved.

In analyzing the engine response to those new changes, the engine performance was evaluated earlier [1] to find that a DI-CI engine with an HIP permits operation at an air-fuel ratio as rich as 18-1 with exhaust smoke emissions not worse than in the same with a mechanical PT-type injector operated lean, i.e., over 30 to 1. In this performance evaluation, it was also discovered that since the ignition delay shifts (with injection pressure and intake air temperature) there was some need for adjusting the injection time for obtaining the best torque for individual speeds. The present study of a HPD with HIP LHR DI-CI engine was directed towards both visualization of in-cylinder reactions and additional performance analysis under mutually comparable engine reaction conditions. Discussion of imaging results done by others under "cold conditions" was avoided because of reasons as explained later.

Preflame Reactions. The changes in injection pressure and temperature are expected to affect the (invisible) preflame (chemical) processes during the ignition delay period, which would dictate the subsequent heat release reactions: In a conventional understanding, the longer the ignition delay period the more the mixing of fuel with air, producing soot emission in smaller amounts. When the intake charge temperature is high, the ignition delay will be shortened by reducing the preflame reactions, which would then lessen the amount of heat released during the premixed combustion stage leaving the balance to take place during the slowly-reacting-diffusion combustion stage. Such undesirable impacts of high intake-air temperature were expected to be offset by the use of an HIP since it would produce a spray having better air utilization, increasing the amount of heat release during the premixed combustion period.

The abovementioned invisible preflame processes, including the disintegration of fuel and spray formation with concurrent chemical reactions seem to require an additional explanation: When the fuel is delivered into the cylinder, unlike a conventional expectation that physical delay, involving the droplet formation and vaporization combined with mixing, precedes the chemical delay commencing endo- and exothermic reactions, it was found that the injected fuel immediately starts some significant chemical reactions [4,5]. The finding seems to be reasonable in view that the fuel exposed to the compressed charge whose temperature is well over the self-ignition point would start to decompose, for example, producing radicals as soon as the injection starts. In other words, there is no clear division in time between the physical and chemical delay periods in sequence but both processes appear to be concurrent.

Advancements of Methods. Encouraged by the images of preflame as well as heat-releasing flame propagation captured by using the high-speed four-color IR digital imaging system (referred to by others as Rutgers or Super imaging System, or SIS for short), it was decided to employ the same in investigating the in-cylinder processes of the HIP LHR DI-CI engine. The study involved both the use of SIS for visualization of in-cylinder processes from an optical engine and extensive engine measurements using a separate but same-family engine apparatus.

The SIS is a one-of-a-kind system designed and fabricated at Rutgers specifically for performing investigation of flames such as in-cylinder reactions. It has four units of high-speed IR digital cameras lined up to an optical package that includes an object lens assembly with 155 mm diameter, three customized spectral beam splitters, and several relay lenses per camera. Since it was made operational in 1994, many deficiencies have been identified in this four-color prototype system, mostly in electronic units, that is, having found what is not working right in the existing system. (The development of the SIS is preceded by the system design of a single-head digital IR camera unit started on an external support in 1988.)

An additional learning process, therefore, was initiated in order to newly design and fabricate the electronic parts of the SIS: At this time, advantage was taken of recent advancements in peripheral areas (such as faster speed of A/D converter and memory components at lower costs) by abandoning some of the design packages based on pre-1990 technology. More details about this new system will be described in a separate report.

Mentioning a new data analysis and presentation method, whenever a photographic study is conducted (of in-cylinder reactions), generally the results, which are accumulated under often duplicated conditions to ascertain their repeatability, in most cases amount to enormous volumes. Analysis of such a vast volume of results is extremely time consuming and inefficient. For example, a typical parametric study of the in-cylinder processes using the present four-head digital imaging system compiles over a thousand sets of images in need of viewing for screening and mutual comparison. It became absolutely necessary to develop a new tool or method of efficiently performing the analysis of large volumes of raw data as well as presentation of the final results. In order to meet this end, a new package of PC-based software (in combination with commercially available computer peripheral equipment) was developed during the last several years at Rutgers, which is a work in progress but whose main features became available for the present study.

EXPERIMENTAL

The present study was experimental in order to evaluate engine behavior when equipped with an HIP operated under the reaction environment of an LHR DI-CI engine. The apparatus and methods employed in the study include: an engine with optical access for in-cylinder imaging and a separate but same family engine for performance analysis; an intake air preparation unit; the SIS; and a data analysis and presentation method.

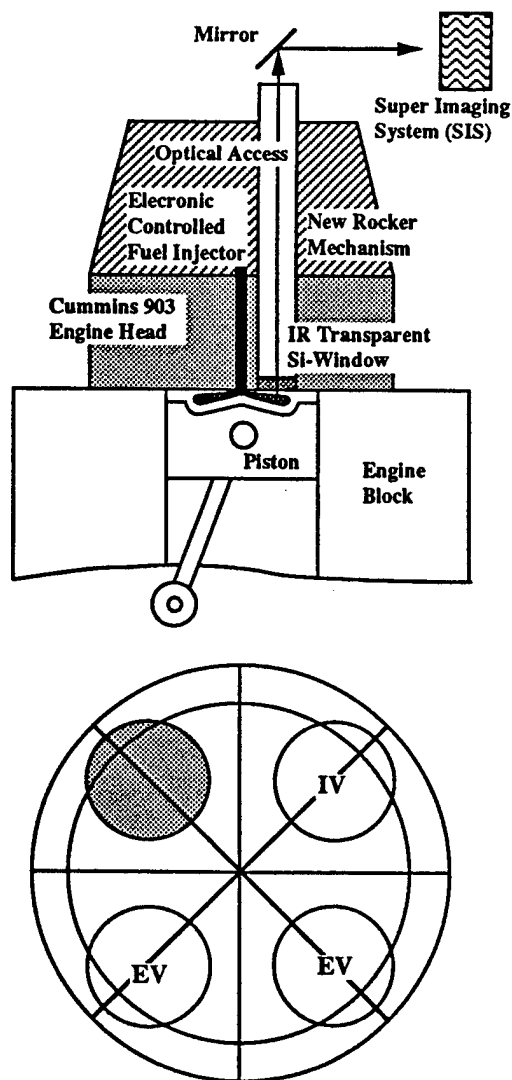


Fig. 1. Schematics of Combustion Chamber and Optical Access (Shaded Area) with respect to Spray Axes.

Engine. The single-cylinder engine with optical access is basically a Cummins-903 engine having a bore-stroke of 140-121 mm (displacement of 1.85 liters) and compression ratio of 13.5 to 1. In order to obtain images of in-cylinder reactions of the engine, one of two intake valves was converted to an optical access, which is barely big enough to investigate one of eight (8) spray plumes [4,5]. A schematic presentation of the optical engine is included in Fig. 1 with a top-view of the combustion chamber having the spray plume axes with respect to the optical access as indicated by the shaded area. Another engine unit employed for the performance measurement in the study was basically a saw-off of the original V-8 Cummins 903 engine operating as a V-2, which had only one active cylinder, the other for dynamic balancing. Since the same family of 903 engines have been widely used in the past, no additional discussion on the engine dimensions is made here.

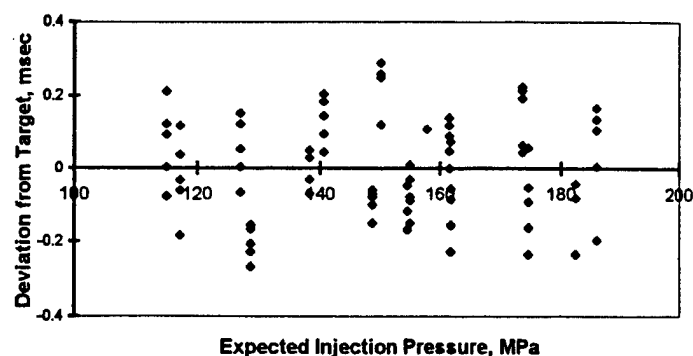


Fig. 2. Reproducibility of Start of Fuel Injection as Characterized by the Present HIP System.

These single-cylinder engines were installed with a new intake-air (electric) heating unit which can increase the air temperature as high as 205°C (400°F) at high speeds, because such a high intake air temperature was expected in an LHR engine whose combustion reactions were to be investigated in the present work. The air was supplied from the building via a pressure controller (for adjustment depending upon the intake air temperature) and a flow metering unit. The engine cooling was done by using a closed-flow unit (with glycol as coolant) connected to a water-cooled heat exchanger for temperature control. The unit was designed to accommodate a coolant temperature as high as 149°C or 300°F. The engine was sufficiently instrumented as needed for conducting the present study including a pressure transducer in the cylinder head, many thermocouples at critical places of the engine, an universal exhaust gas oxygen (UEGO) sensor and a smoke meter.

It is pointed out that the determination of air-fuel ratio of the engine was difficult to achieve, particularly when the engine operation was brief for the in-cylinder imaging. To overcome this, a calibrated UEGO unit was installed in the exhaust surge tank for prompt and more consistent measurement of the overall air-fuel ratio, which is further explained later.

High Injection Pressure (HIP) Fuel System. The electronically controlled HIP used in the present study was basically the same design as BKM's Servo-jet type [6]. It is a pressure intensifier type whose functional details were described elsewhere [1,4]. Since the factory delivered unit was not compatible to the engine explained above, an entirely new unit was fabricated to deliver injection pressure of somewhat over 165 MPa (24,000 psi) for earlier studies [4,5]. The experience with this early unit construction offered the basic expertise toward the new design-construction of an improved HIP employed in a recent study [1], which was also used in the present investigation upon making additional improvement particularly in the in-situ determination of injector performance.

The distinctive difference of the Rutgers-built unit from the original Servo-jet is that the present unit uses the existing Cummins nozzle tips (0.15mm nozzle hole diameter) for technical and economical flexibility and that the fuel intake and return ports in the Cummins engine were

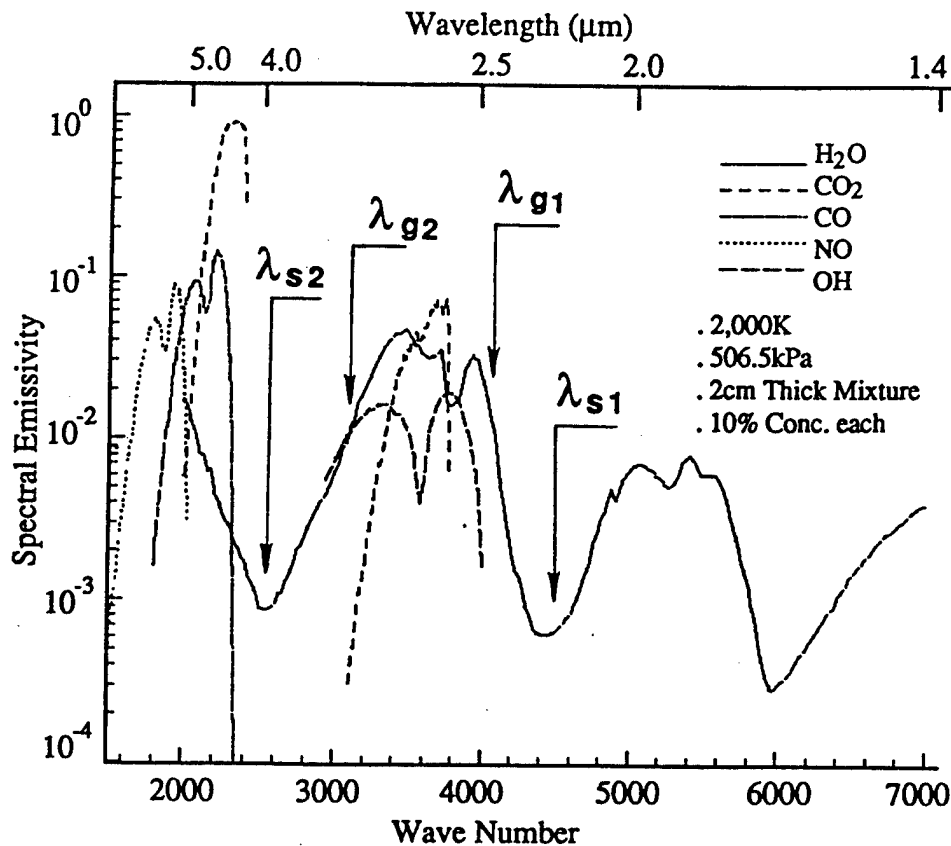


Fig. 3. Spectral Diagram of a Mixture and Bands Chosen in the Present Imaging by using the SIS.

directly interfaced with the new unit. That is, the new HIP assembly directly replaces the Cummins PT-type injector without any modification of the engine cylinder head. The low-pressure fuel supply was made as high as 12 MPa (1,750 psi) through the fuel gallery in the cylinder head, which was intensified to an injection pressure of 210 MPa (30,625 psi).

Among the important performance behaviors of the present HIP unit characterized was the start of injection, which was controlled by an electro-magnetic activating device. In order to evaluate the start of injection with the variations of the fuel injection pressure, injection rate and speed, a strain gage was mounted over the surface of the injector-tip to monitor the fuel spilling with respect to the electronic actuation signals for the valve opening. The injector opening was found to be predictable and consistent as shown in Fig. 2, which shows the deviation of the start of injection with respect to the designated time of injection under varied injection rail pressures. It is noted that these characteristics were not measurably affected by changes of the speed and rate of injection. The injection period of the present HIP was in the range of 3-5 msec, depending upon the amount of fuel injected per cycle.

High-speed Four-band IR Digital Imaging System. As briefly mentioned earlier, the new SIS was to simultaneously capture four geometrically identical (pixel-to-pixel) images (of radiation issued through the optical access in the cylinder head) in respective spectral bands.

Ideally, the four sets of matrices (64x64) of digital information captured at a time would indicate distinctive and unique quantities representing respective thermochemical states of the reaction volume (object).

The system, therefore, may be viewed as 64x64 units of a four-band spectrometer, that is, distributions of four pieces of unknown information may be determined from the set of matching spectral data points. It is reminded that a newly developed three-band iterative method was applied to perform quantitative imaging of spray combustion by processing spectral data obtained using the SIS, which determined simultaneous distributions of temperature, water vapor and soot in the combustion products [5]. (The in-cylinder quantitative imaging results will be reported in a separate publication.)

The present SIS utilizing the new electronic packages delivers more enhanced and predictable performance (most notably with minimized amount of noise modulated over the measurements). The top imaging rate was increased in the present system to a rate over 2,000 frames/sec per camera. Additional features were added to the new system to increase the versatility of the former system namely, control-presetting of (1) the start of imaging; (2) the interval of imaging; (3) the number of images to be captured per channel-cycle; and others.

In order to dispose of large amounts of digital data (in 12-bit dynamic resolution) from the SIS, that is, as many as 32 million measurements per second $\{(64 \times 64) \times 4 \text{ cameras}\}$

x 2,000 images/sec), a memory package was newly designed and fabricated. Note that the memory unit in the earlier SIS was also built at Rutgers due to unavailability of a reasonable and compatible unit in the market. Unlike the former memory pack utilizing dynamic RAM, the present memory unit employs static RAM. Note also that software packages for operating the SIS were newly developed-modified from those in the earlier SIS as new electronic units replaced the old.

At present, the SIS is being further extended to compile as many as 126 images/cycle-camera over 120 successive cycles, such as from the start of the first firing of the engine. In addition, in order to take advantage of advancements in commercially available software packages, the existing DOS-based SIS operating system is being converted to a new Window-based in situ review software system.

It is also added here that thanks to high transmission of IR radiation through the soot layers coating the optical window, the in-cylinder images captured even after many cycles of continuous firing reveal no detrimental effect on the quality of the images.

Although the spectral bands employed in the present imaging were identified with respect to the spectral diagrams in earlier reports [4,5], the same is included here in order to help explain the nature of the combustion processes in the engine (Fig. 3).

Data Analysis and Presentation Method. The amount of data accumulated by the SIS is far more than one can possibly handle manually, such as by printing the sets of images (in colors) and placing them side by side, which was highly inefficient even for performing the initial screening work. It came to realize an absolute need for developing something efficient to replace the manual data analysis method. For this, development of a new PC-based computer software was initiated several years ago, and improvement has become reality and proven useful, which is referred to as Rutgers Animation Program (RAP) for convenience of discussion.

Briefly, using the RAP, the raw data transferred into a PC from the SIS can be individually displayed over the PC screen and at the same time the sets of images can be animated side by side, which helps to understand the dynamics of in-cylinder reactions. (Recall that the new SIS operating system permits in situ review of images captured from the immediate experiment, which may be regarded as on-site screening of the results.) Versatile choices of animation are also partial functions of the program, namely simultaneous display of any number of movies up to twenty-eight (28). Mentioning a special advantage of the features, when the six-movie animation is employed, three sets of spectral (raw) data can be simultaneously animated along with three sets of quantitative results obtained by using the corresponding raw data and spectral methods (i.e., three band iterative method) on the same screen. (Other features will be demonstrated when the paper presentation is made.) For more utility and versatility, the RAP is being further developed, including individualized formulation of animation as well as still-picture results, which will facilitate the search for a desired piece of information from the growing volume of the data-base.

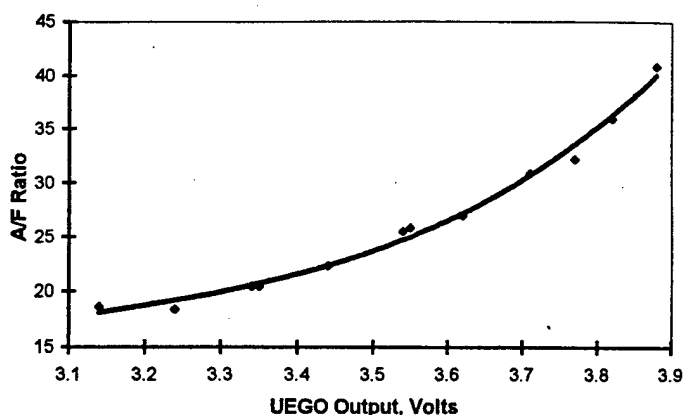


Fig. 4. Calibration of UEGO Sensor for Determining the Overall Air/Fuel Ratio of a DI-CI Engine Operated by Diesel Fuel (D-2).

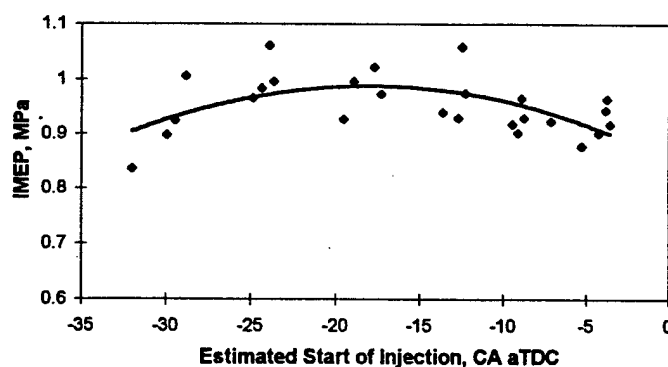


Fig. 5. Indicated Mean Effective Pressure of an HDP DI-CI Engine (A/F Ratio, 19.6) with Fuel Injection at 181 MPa (26,300psi) and Intake Air Temperature of 94°C.

Determination of Air/Fuel Ratio. In order to expedite the measurement of the overall air/fuel ratio (without running the engine for a long periods of time) in particular when the in-cylinder imaging was performed, a UEGO sensor was employed. The unit was calibrated using a bench-top apparatus, as shown in the calibration curve (Fig. 4). Since the response of the UEGO sensor was found to be relatively prompt and consistent in this bench-top test, the tedious and often erroneous flow measurement of fuel and air was replaced by this method.

RESULTS AND DISCUSSION

Engine Performance. Over one thousand sets of separate measurements from various engine operations were evaluated by averaging digitized pressure-time data accumulated over eight (8) successive cycles to determine the indicated mean effective pressure (IMEP), as shown in a typical set of results (Fig. 5), which was obtained from the engine operation (A/F ratio, 19.6) with fuel injection of 181 MPa (26,300psi) and intake air at 94°C. Note that the range of air/fuel ratio studied was from 18-1 to over 35-1, the injection pressure investigated was as high as 30,625 psi (210 MPa) under varied intake air temperature over 150°C.

The following summary of the results from the survey of the HPD DI-CI engine performance is listed without including matching figures:

(1) The effects of intake-air temperature under a fixed volumetric efficiency (achieved by varying the intake-air pressure) may not deteriorate the engine's thermal efficiency, as long as the start of injection is adjusted to obtain the best torque for each condition.

(2) When the intake air temperature was relatively low (under 40°C), the effect of injection pressure on IMEP was insignificant. On the other hand, when it was around 94°C, the effect was rather remarkable, but this trend became less noticeable when the intake air was fed at 149°C.

(3) As expected, the soot emission decreased with increase of the injection pressure.

(4) The soot emission was greatly dictated by the intake air temperature, that is, the higher the intake air temperature, the more the soot emission. The "property" of soot appeared to vary with both the injection pressure and intake temperature. For example, while the soot deposit formed over the optical window was much less with a high injection pressure although the soot layer was difficult to remove (i.e., cleaning the window), the soot layer with a low injection pressure was thicker and "fluffier," which was easy to remove. When the intake air temperature was high, the soot deposit was in greater amounts and was also fluffier.

(5) The engine noise (evaluated by human ear) was higher with both the injection pressure and fuel/air ratio, and became considerably lower when the intake air temperature increased.

(6) The injection time for best torque (or IMEP) was identifiable but relatively insensitive to the variables investigated as mentioned above (Fig. 5).

(7) The variation of ignition delay and alteration of preflame reactions, that is, invisible chemical reactions occurring prior to the onset of the visible premixed flame kernel(s), are considered to be the main phenomena to explain the above findings. (This will be further discussed when the visualization of in-cylinder reactions is discussed.) For example, the higher the intake air temperature, the shorter the ignition delay period resulting in a smaller amount of well mixed and reactive fuel-vapor causing a greater amount of soot formation. This, on the other hand, produced a relatively smooth engine pressure rise causing a low engine noise.

Visualization of In-cylinder Reactions. Whenever in-cylinder reactions are investigated by photographic means, the optical window is rapidly covered with combustion products notably by soot layers, especially if it is done from a Diesel engine. Formation of such opaque layers permits imaging only within the first few cycles of firing particularly when a visible-ray imaging-system is employed.

Representative Results? In order to achieve a condition of "warmed" engine operation in such photographic studies, a high temperature coolant is often circulated in the engine block or a flow of preheated air is used by motoring for a while prior to starting an experiment. (In order to minimize the soot deposit formation over the optical window, instead of using the actual Diesel fuel, a fuel producing low soot is also used, often by firing only every other cycle.)

A question arises, then, whether the results obtained under such engine conditions would represent what is happening in a typical warm engine. This leads to an issue of delineating a compromise between the length of preparatory engine operation time and the amount of window fouling affecting the image quality.

Consequently, it was decided to determine the least number of sequential firing-cycles from the start with the heated coolant before the engine reveals "representative and unabridged" in-cylinder reactions. It is reminded here that thanks to the high transmissivity of soot layers to IR radiation, as mentioned above, the IR imaging suffers a far smaller deterioration of image-quality by the soot-deposit on the window compared with the visible-ray imaging. For example, some reasonable IR images of the in-cylinder flame propagation can still be captured after over 200 successive firing cycles having a heavy deposit formation over the window.

It would be desirable, however, to determine the least number of sequential firings from the start before the engine condition becomes representative of the warm real-world in-cylinder engine condition, which will be the time when the imaging is performed so that the effect of the window fouling on the image quality is minimized.

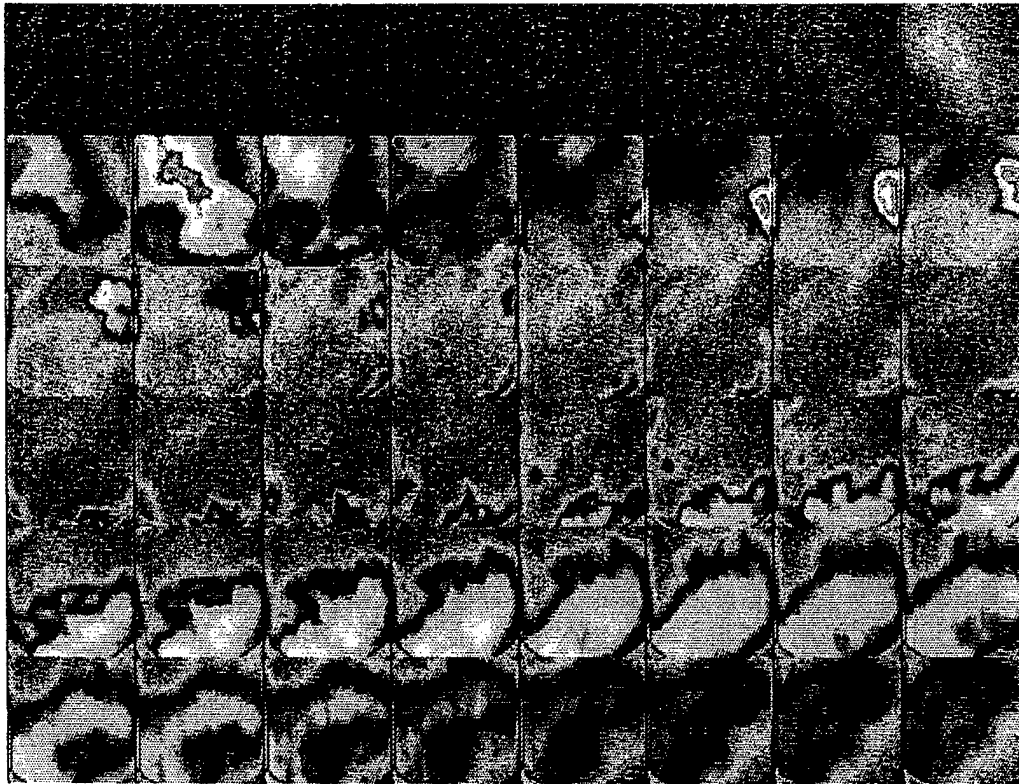
In order to achieve this evaluation goal, using actual Diesel fuel (D-2), the engine was first prepared to operate at an air-fuel ratio of around 25-1 with the fuel injection pressure of approximately 178 MPa (26,000 psi). Under this condition, a set of images (in four separate spectral bands) was simultaneously obtained within the same cycle at a rate over 2,000 frames/sec-camera after the following scheduled numbers of continuous firing-cycles of the engine (from the start with a warmed coolant of 91°C): The imaging was respectively made: Case-(1) after five successive-firing cycles; Case-(2) after fifteen firing cycles; and Case-(3) after twenty-five firing-cycles. The imaging was repeated at least six times per schedule, which amounted to a total of far more than seventy-two (72) sets of high-speed spectral movies for this analysis.

According to close review of these results using the RAP, as explained earlier, which permits a simultaneous display of as many as 28 sets of animation over a PC screen (e.g. the six sets for an identical case plus one representative set from another case for mutual comparison purposes), the following was found:

Imaging of in-cylinder reactions done after the first five successive firing-cycles, that is, Case-(1) as listed above, revealed some obvious abnormal combustion behaviors including strong after-burning in the late stage of combustion. Elaborating the active late combustion behaviors with regards to Case-(1) and -(3), Figs. 6 and 7 are presented. The image of spray is directed diagonally from the lower right-hand side to the upper left end, which matches with the axis shown in the optical access (Fig. 1).

The figure compares two sets of sequential spectral images in bands of (A) 3.8 μ m and (B) 3.42 μ m obtained during the 6th (Fig. 6) and 26th (Fig. 7) successive firing-cycles, respectively. Note that Fig. 7 also show those from other spectral bands ((A) 3.8 μ m; (B) 3.42 μ m; (C) 2.2 μ m ; and (D) 2.47 μ m) for the subsequent discussion. A look-up-

(A)



(B)

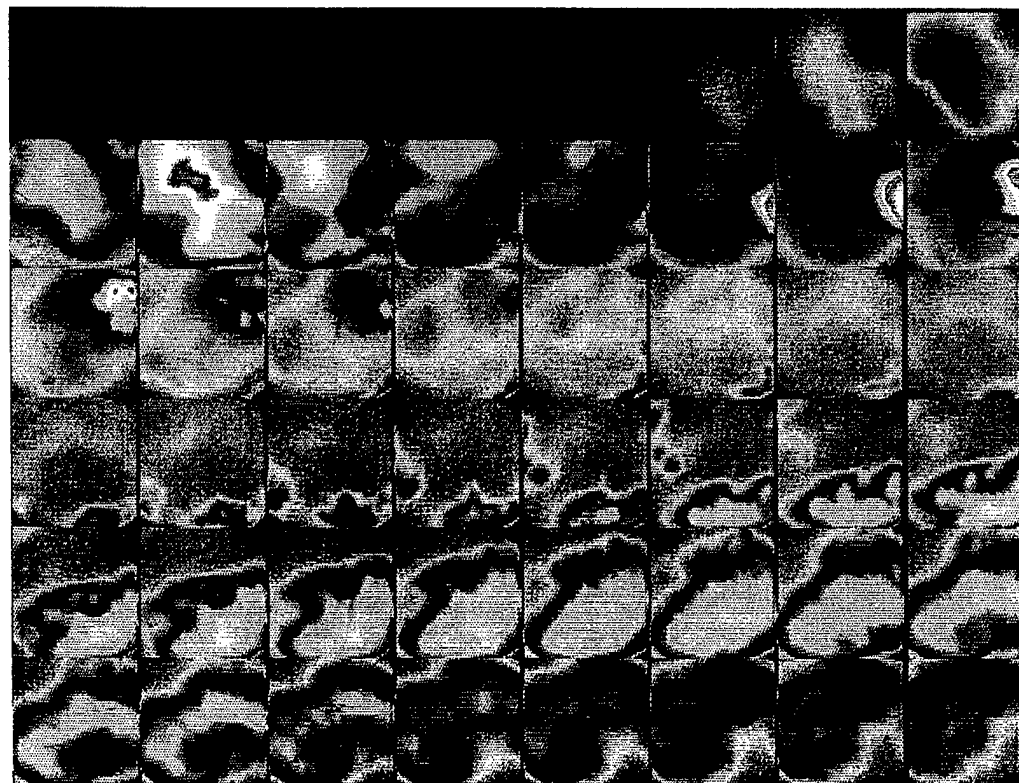
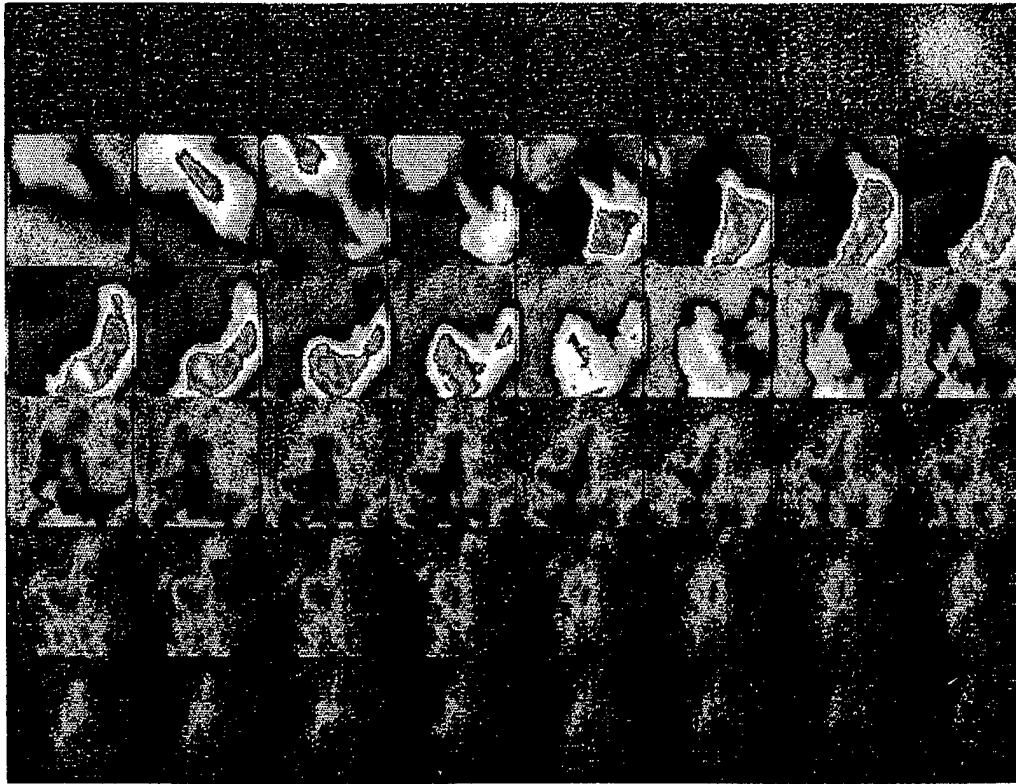


Fig. 6. High-speed Spectral IR Images in Bands of (A) $3.8\mu\text{m}$ and (B) $3.42\mu\text{m}$ from an HPD DI-CI Engine with HIP Obtained after First Five Successive Firing Cycles. Under Identical Engine Conditions as for Fig. 7 (obtained after Twenty-five Successive Firing Cycles).

(A)



(B)

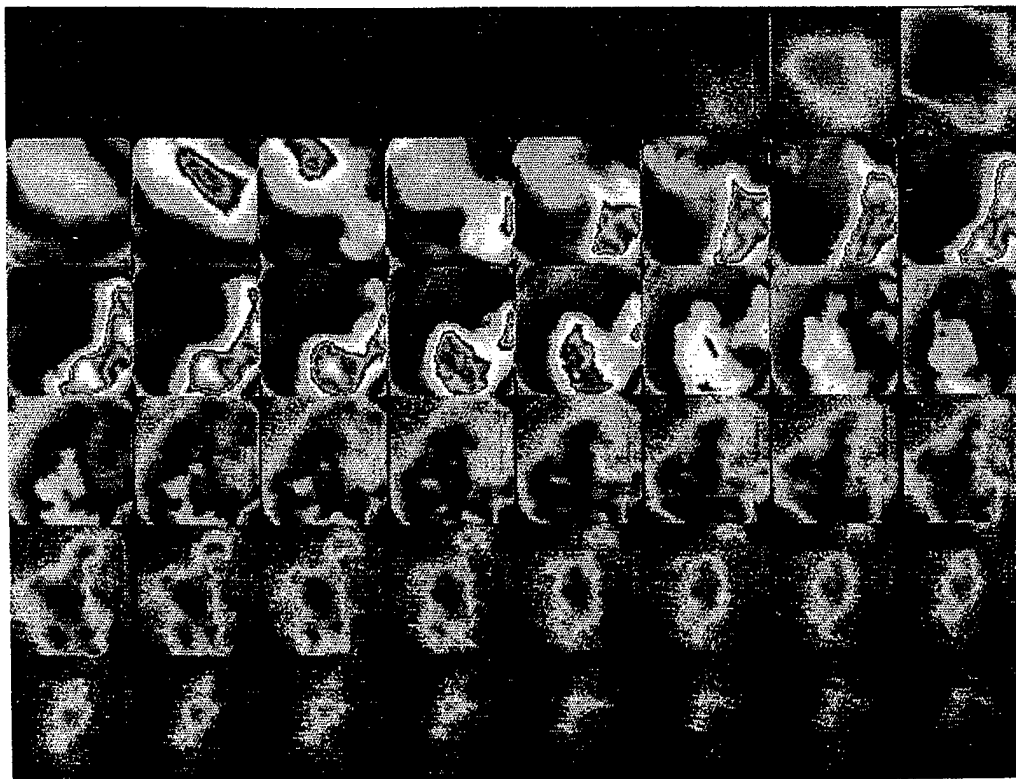
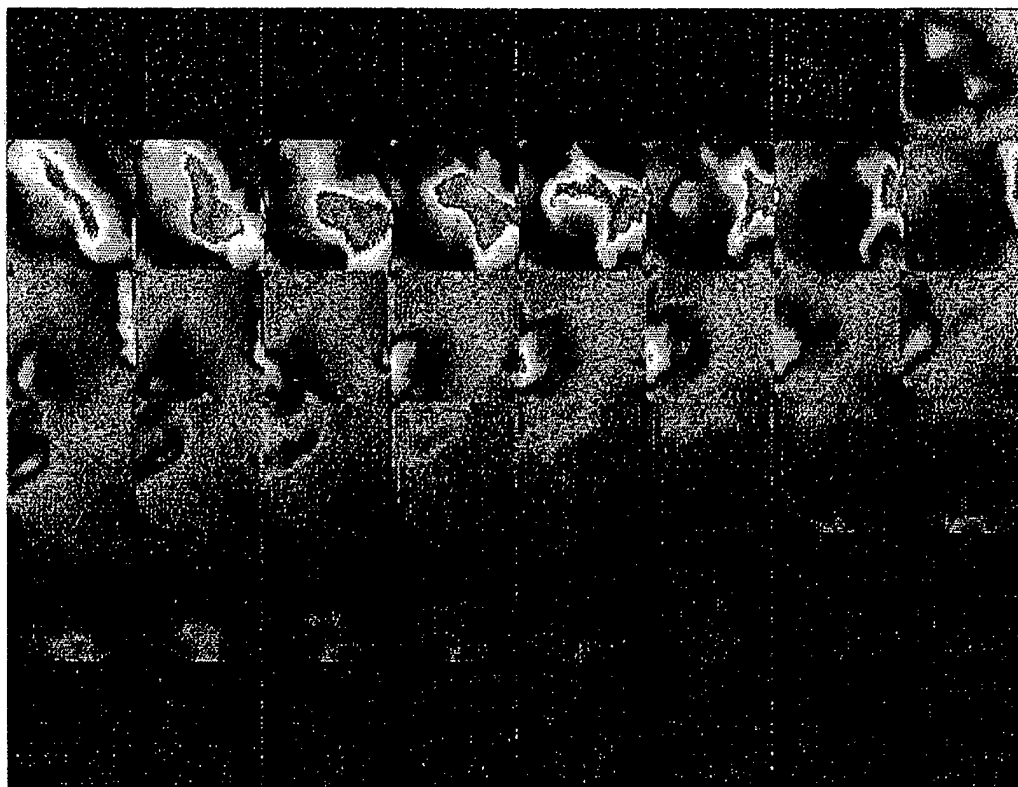


Fig. 7. Spectral IR Images in Bands of (A) $3.8\mu\text{m}$; (B) $3.42\mu\text{m}$; Obtained after First Twenty-five Successive Cycles under Operating Condition of: Injection Pressure at 178 MPa (26,000psi); Air-fuel Ratio of 25-1; Coolant Temperature at 91°C ; and Intake Air at 38°C .

(A)



(B)

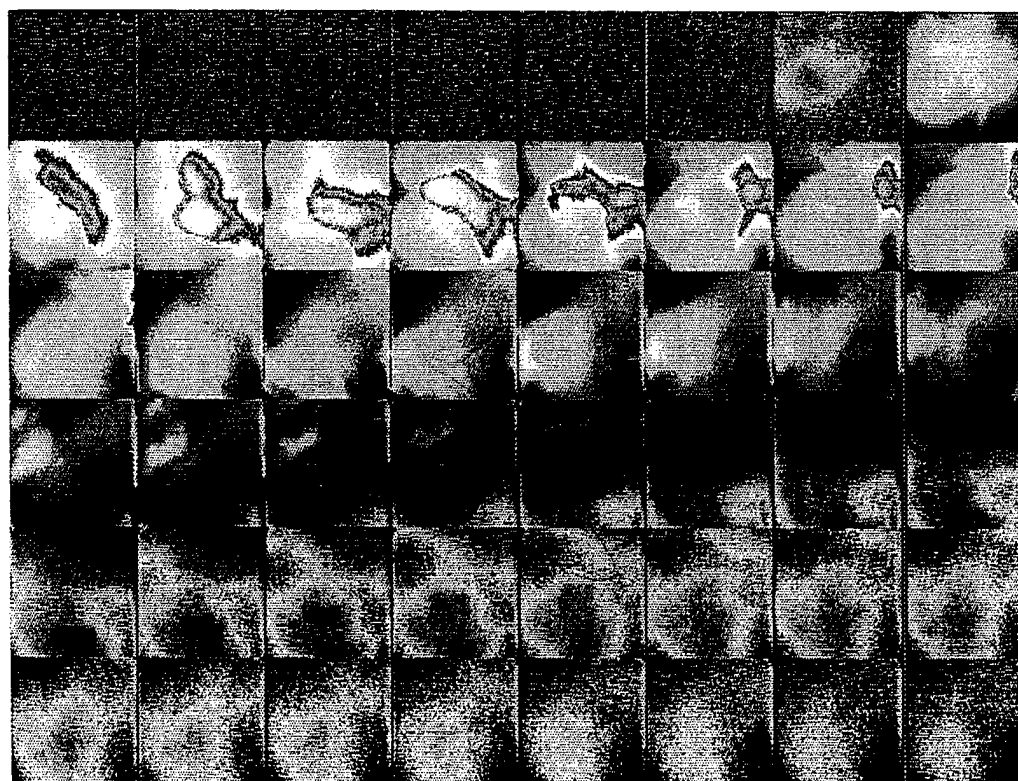


Fig. 7. Spectral IR Images in Bands of (C) $2.2\mu\text{m}$; (D) $2.47\mu\text{m}$; Obtained after First Twenty-five Successive Cycles under Operating Condition of: Injection Pressure at 178 MPa (26,000psi); Air-fuel Ratio of 25-1; Coolant Temperature at 91°C ; and Intake Air at 38°C .

table (LUT) is also presented in Fig. 8 in order to help identify the crank position with respect to the start of injection at 14 crank angles before top-dead-center (CA bTDC).

Such a strong late radiation phenomenon was also found in Case-(2), but not in a high frequency as in Case-(1). The results obtained in Case-(3), however, were mostly free from such combustion behaviors under the present controlled operating condition. At the same time, any impact of soot layers over the IR window on the image quality of Case-(3) was not discernible.

Although the reasons for such "late-burning" phenomena are not clearly known at present, a probable explanation is that the fuel injected (and likely impinged over the piston bowl to form a liquid layer) during these early cycles may not all be timely consumed but result in sluggish reaction volumes appearing in the late stage of combustion in an unpredictable manner. Possibly, the fuel spray may not all properly bounce off the piston bowl surface when its skin temperature is not high enough. It might be added, however, that the occurrence of preflame reactions and the onset of premixed combustion reactions observed in Case-(1) and -(2) were seemingly comparable to each other and with those in Case-(3).

In some results of Case-(1) under other operating conditions, the late-burning appeared as localized intense "fire-balls" instead of cloud-like reaction volumes shown in Fig. 6. The same evaluation was made for an engine operation condition with a fuel injection pressure of 130 MPa (19,000 psi) to conclude that the imaging done after the first five sequential cycles was generally different from those obtained after 25 cycles. Most notably the former revealed more late burning and exhibited stronger radiation.

In spite of a seemingly understandable transient nature of in-cylinder conditions in a DI-CI engine as observed in the present investigation, this issue will have to be further studied in view of an important question if the engine results obtained in a way similar to Case-(1) may not properly help us understand the in-cylinder process of a warm engine.

It is also added that the engine (speed) and the injection system performance were observed to require many more cycles than several firings prior to attaining an acceptably steady state condition for yielding representative pieces of results, such as reliable determination of the overall air-fuel ratio. Therefore, it was decided that the entire four-color simultaneous imaging of the in-cylinder processes and the engine measurement were performed according to the schedule of Case-(3) throughout the present experiment.

High-speed Multispectral IR Images of HIP DI-CI Combustion. Nearly fifteen hundred separate sets of spectral digital movies have been accumulated to date for the study. Accumulation of such a vast amount of visualization of in-cylinder reactions became possible thanks to the versatility of the present SIS and RAP as explained earlier. Importantly, it was necessary to obtain a large amount of results simply in order to determine the most representative trend under each condition.

For example, under each experimental condition, the same imaging was repeated at least six (6) times, which results in twenty-four (24) sets of spectral animation for

-21	-19	-17	-15	-13	-11	-9	-7
-5	-3	-1	1	3	5	7	9
11	13	15	17	19	21	23	25
27	29	31	33	35	37	39	41
43	45	47	49	51	53	55	57
59	61	63	65	67	69	71	73

Fig. 8. Look-up Table (LUT) for Identifying Crank Angles for Figs. 6, 7, 9 and 10.

close review side by side with each other. In some cases, they were repeated again days or weeks later. The repetition was necessary in the present study because of the exploratory nature of using this new tool to discover something new. When a new phenomenon was observed by this tool, it was necessary to confirm "if-it-really-happens," which involved a parametric analysis in order to uncover the generic nature of the finding.

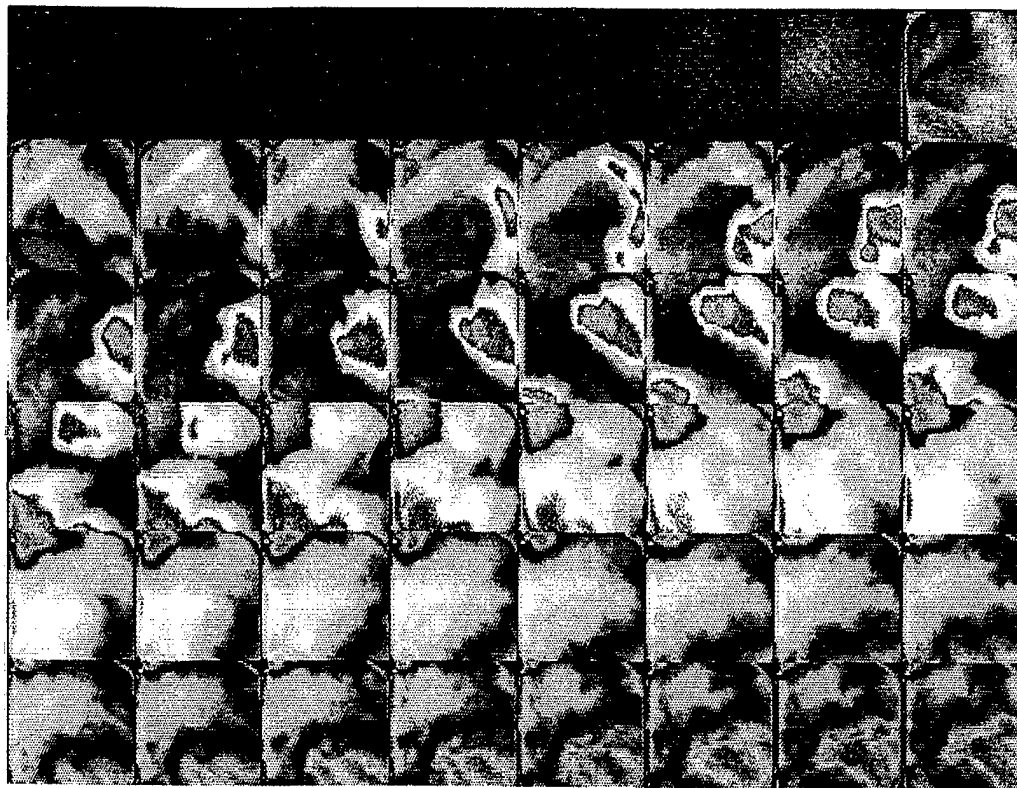
The main observations obtained from these results are summarized below: (Note that, in the oral presentation at the meeting, these discussions will be made by presenting respective sets of animation pertinent to the results.)

At first, typical spectral IR images are explained. A set of IR images obtained in respective spectral bands is presented in Fig. 7 as indicated earlier: (A) 3.8 μ m; (B) 3.42 μ m; (C) 2.2 μ m; and (D) 2.47 μ m. Refer to Fig. 3 in order to help identify the spectral nature from various combustion product expected in CI combustion with respect to the imaging bands listed above. Briefly, in the absence of radiation by main combustion products, radiation images captured via 3.8 μ m are most likely expected to represent the presence of soot, and those via 2.47 μ m would exhibit the formation of water vapor (such as the result of premixed flame reactions).

It is emphasized that while we continue to accumulate additional in-cylinder imaging results and conduct their analysis, it was considered to be important to share what has been obtained with professionals in the field by presenting them as much as possible. They are included in a pseudo-color in order to exhibit enhanced local variations and a sense of dynamics of the reaction processes. (It is not attempted to offer any quantitative value over the present imaging results.) Three additional sets of typical results obtained at varied injection pressures are also included: 178MPa (Fig. 7); 130MPa (Fig. 9); and 70MPa (Fig. 10).

When their spectral images are compared to each other, digital matrices obtained with HIP seem to indicate radiation issued from a relatively optically thin reaction volumes while those with low injection pressure (LIP) fuel delivery represent a result of optically thick reaction mixtures. In particular when the HIP was employed, it seems like almost the entire viewing area is filled with reaction volumes while the LIP exhibited otherwise.

(A)



(B)

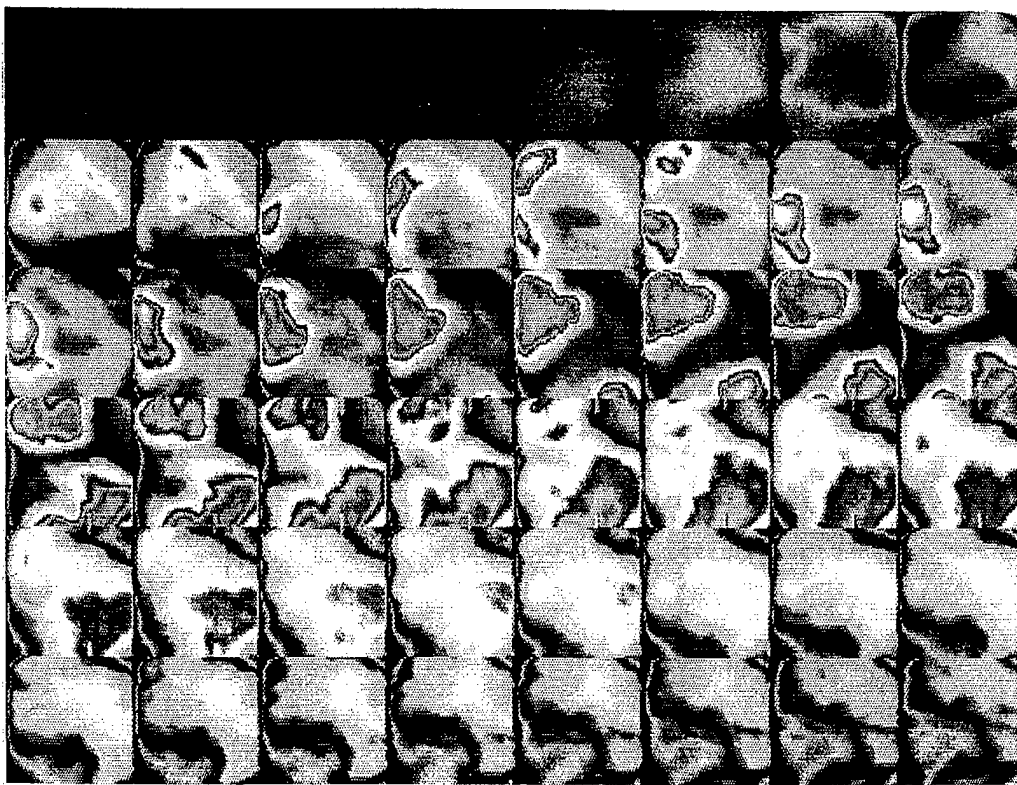
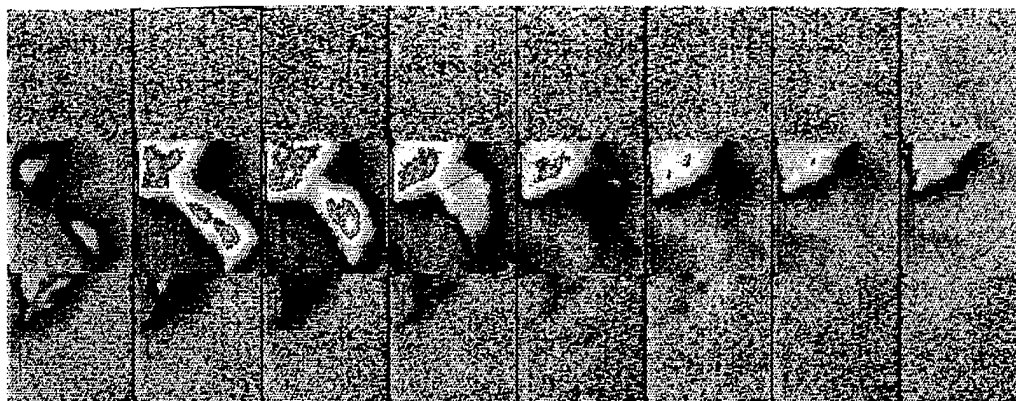
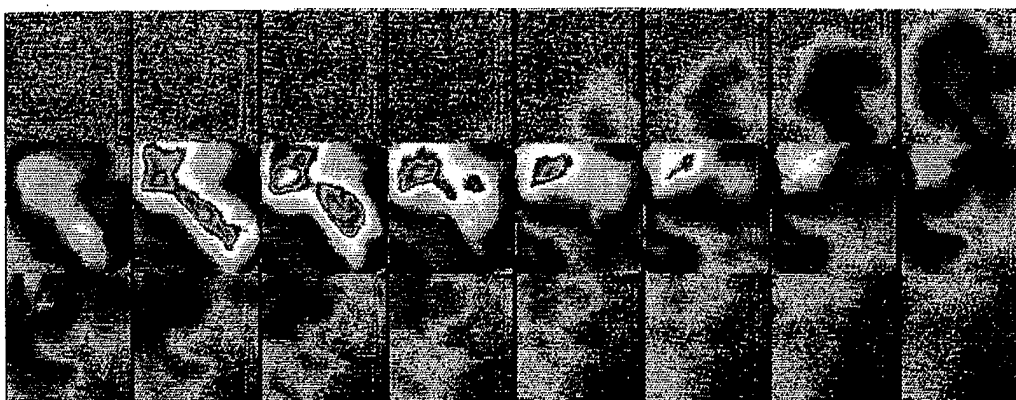


Fig. 9. Spectral IR Images in Bands of (A) 3.8mm; (B) 3.42mm; Obtained after First Twenty-five Successive Cycles under Operating Condition of: Injection Pressure at 130 MPa (19,000psi); Air-fuel Ratio of 23-1; Coolant Temperature at 91°C; and Intake Air at 38°C.

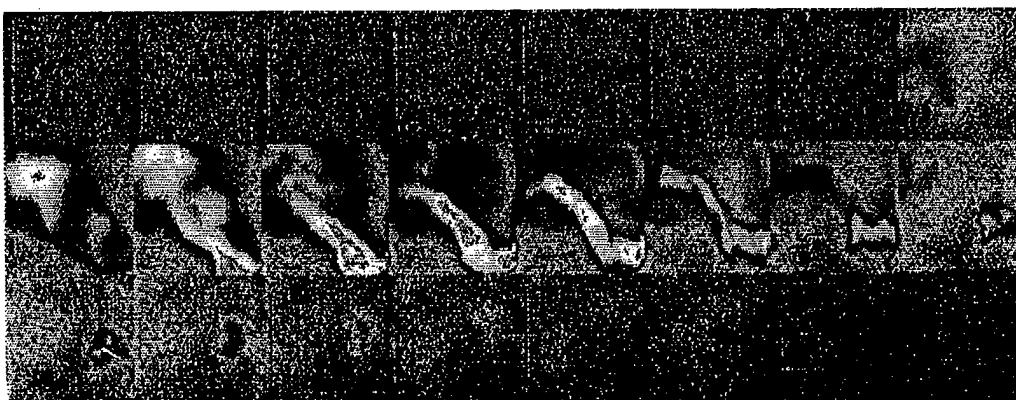
(A)



(B)



(C)



(D)

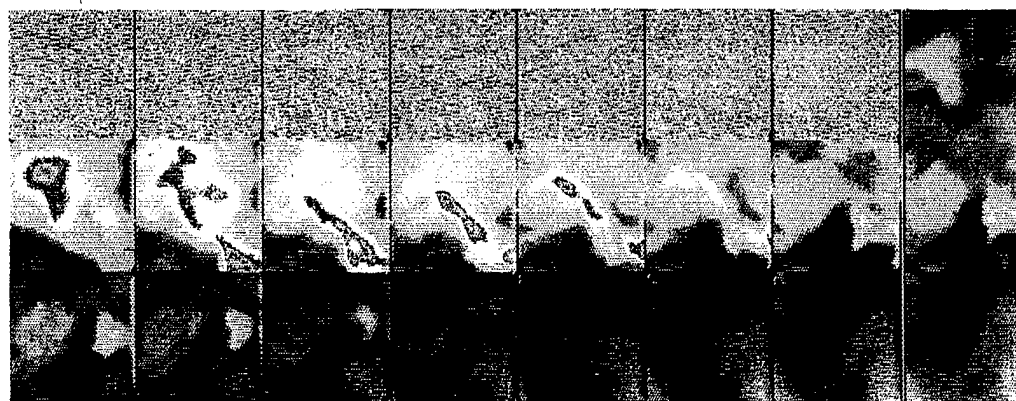


Fig. 10. Spectral IR Images in Bands of (A) 3.8mm; (B) 3.42mm; (C) 2.2 μ m; (D) 2.47 μ m: Obtained after First Twenty-five Successive Cycles under Operating Condition of: Injection Pressure at 70 MPa (10,000psi); Air-fuel Ratio of 50-1; Coolant Temperature at 91°C; and Intake Air at 38°C.

(1) **Preflame Reactions.** Referring to the LUT in Fig. 8 to discuss the images in Fig. 7, with the start of fuel injection at 14 CA bTDC under the same engine operation as that for Fig. 6 (speed of 620 rpm with the overall air fuel ratio of 25-1 at the fuel injection pressure of 178 MPa (26,000 psi), and intake air temperature of 38°C), the spray development appears to be revealed by images via 3.8 and 3.42 μm . At the same time, the reaction-like early images captured in 3.42 μm indicates that the injected fuel immediately starts to produce radical species emitting some measurable chemiluminescent radiation, which compares to the earlier finding as reported in 1995 [4]. That is, there was no remarkable time period, after the fuel is injected, involving only the physical processes preceding the chemical reactions. It is yet to determine what preflame species cause the radiation images via this band.

In general, the regions revealing the strongest chemiluminescent radiation matched with those of the first kernel producing the main combustion products (e.g. water vapor) as seen via 2.47 or 2.2 μm . It is pointed out, however, that in many cases they did not match with each other as observed under various engine conditions, which is further discussed later.

(2) **Progress of Chemical Reactions.** After the ignition delay period emitting the chemiluminescent radiation as mentioned above, some strong radiation via 2.47 μm band is recognized most probably indicating water vapor formation from the onset of the premixed combustion stage. In most cases, little radiation in 3.8 μm band is observed at this time, which suggests that there was no remarkable amount of soot formation then or the temperature in the plume was low.

The time delay between the first presence of strong radiation via 2.47 μm (emitted by the main combustion products, e.g. water vapor) and that from soot (seen via 3.8 μm band) suggests that the former is caused by basically the consumption of premixed mixtures and the latter event reflects rich fuel-air packages becoming exposed to high-temperature product. That is, the two processes are not concurrent in the very beginning.

(In some cases, however, as further discussed below the formation of soot was concurrent with not only the premixed combustion as seen via 2.74 μm but also the (supposedly preflame) reaction images captured via 3.42 μm , which undoubtedly needs an additional study to determine what causes this to happen unlike the typical cases explained above. Such a "confusing" observation is partially responsible for our repeated experiment accumulating a vast amount of results.) The remaining processes are further explained when the effects of individual variables are explained next.

(3) **Mutual Mismatch of Spectral Images.** Reviewing the sequential pictures shown in Fig. 7, generally, the radiation images in 3.8 μm and 3.42 μm bands match well with each other and those in 2.47 μm and 2.2 μm bands often do the same. However, these two groups did not necessarily compare each other in many cases.

Note that such mismatches were similarly found in a spark-ignition (SI) engine having a port fuel injection system [10]: The in-cylinder visualization exhibited some locally luminous burning volumes expected to stem from

liquid fuel layers formed around the intake valve and then revealed a similar mismatch as those of present diffusion flame images. In order to see if any mechanical reasons within the SIS might have caused the mismatch, various emitting objects were imaged to rule out such a possibility. (At present, a new apparatus is being prepared in order to identify separate spectra involved in each imaging band.)

Mentioning another confusing observation, there were some cases when the radiation in 2.47 μm (which was expected to reveal the formation of water vapor as resulting from the onset of premixed combustion) became evident prior to any detection of the same in 3.42 μm , which was interpreted to represent the formation of preflame species. Does it mean that the onset of the thermal flame kernel formation under such cases occurred without going through a low-temperature controlled (radicals-producing) self-ignition process? Furthermore, in other cases, the directions of reaction front propagation (combined effect of gas motions and chemical reactions) were different in the two groups of images, which was highly unexpected.

Possible reasons for the mis-match may be listed, including: multiple routes to the self-ignition; non-equilibrium of the mixtures; non-uniformity of temperature; preferential diffusion of species; a tumble motion of mixtures involving a swirl in the opposite direction of the other (as observed through a line-of-sight in the cylinder head); and more: The authors, however, do not attempt to offer any plausible explanation for this finding at present, but call for the attention of researchers in the field.

(4) **Fuel Injection Pressure Effects.** The onset of preflame reactions did not appear to be remarkably affected by the injection pressure. That is, they similarly occurred immediately after the fuel injection for the range of pressure investigated to date.

When the engine was operated by "medium" HIP of 130 MPa (19,000 psi) and the overall air to fuel ratio of 23-1 (Fig. 9), the reaction volume representing the premixed combustion zone was mostly confined within the piston bowl in the beginning, which propagated over near the cylinder wall thereafter.

With HIP, e.g. near 180 MPa (Fig. 7), it was observed that the region exhibiting the same reactions penetrated beyond the bowl to greatly spill over the zones closer to the piston periphery. (A greater size of reaction volume suggests a better utilization of intake air resulting in low soot emissions.) Even in the early stage of reaction, the size of radiation image reflecting the extent of preflame reactions was greater with HIP. It is reasonable to pronounce that the shape-geometry of spray development was hard to outline when the HIP was employed.

In discussing the reaction period affected by the injection pressure, with HIP the reaction developed more rapidly over a larger viewing area but completed sooner as seen as weak radiation in the later stage of combustion. On the other hand, with LIP, the radiation intensity remained strong during the later stage of the reaction period (3.8 μm), which indicates the presence of heavy soot at high temperature. Since the overall air-fuel ratio was maintained relatively the same for this comparison, an extended injection period with relatively LIP (Fig. 9) compared to that with HIP (Fig. 7) is also considered to partially contribute to

the late and extended burning.

For comparison purposes, results obtained with LIP of approximately 70MPa (10,000 psi), which represents the operating condition of some conventional engines, are also included (Fig. 10). When the engine was operated by using this low injection pressure, the overall air-fuel ratio was maintained at 50-1. Note that such a light load condition was often employed by others for in-cylinder imaging presumably in order to avoid soot layer formation over the optical window.

Among differences between images under this condition from those with HIP is that in spite of the overall lean mixture the radiation is very strong over a narrow volume of spray development. According to the spectral radiation image captured via 3.8 μ m band, there is no evidence that the soot formation occurs over the outer envelope near the spray tip, but in great amount along the axis of spray plume. This is quite in contrast with the case in HIP where the spray formation was widely dispersed with relative absence of rich pockets.

(5) **Start of Injection.** The fuel injection was varied to start at four different CA positions for analysis of most cases: 26 bTDC; 20 bTDC; 14 bTDC; and 8 bTDC. It is observed that the typical length of injection period varied from a few to several milliseconds, which represents angular periods ranging 10-20 CA depending upon engine air-fuel ratios investigated in the present study.

The preflame reaction period was longer with advance in the start of injection, and vice versa. Most notably, when the injection started early, the combustion completed early within a shorter period of time leaving very weak radiation images in all spectral bands, which indicates the combustion product temperature to be low at the later stage of reaction. At the same time, the soot emission was low (and also deposit formation over the window was smaller), while the engine knock was highly loud.

When the injection started late, the imaging view, which is barely big enough to observe a single spray plume (by installing the axis of a plume centered with respect to the optical window as shown in Fig. 2), starts to exhibit a separate new volume of radiation at the late stage of combustion.

Although such a secondary reaction zone is observed under other conditions, which is presumably from the adjacent spray coming into the viewing area caused by the overall swirl (or tumble) motion, such reaction volumes observed long after all spectral radiation images disappeared was in an obvious contrast to those cases with early or mediocre-late start of injections, which exhibited otherwise. Note that the late-burning packages observed after the first several firing cycles mentioned earlier are considered to be different from the apparent secondary spray plume mentioned above.

(6) **Overall Air-fuel Ratio.** In this analysis of HPD DI-CI engine combustion, the air-fuel ratio investigated ranged from 35-1 (50-1 when the LIP was employed) to 20-1. As expected, the richer the overall air-fuel ratio, the stronger the radiation images via all spectral bands. The spray development to be discussed later, however, does not indicate a proportionally growing plume volume with decrease of air-fuel ratio.

It is reminded that the engine operation at such rich overall mixtures was possible by the use of the HIP unit, which produced seemingly comparable soot emissions to those when a LIP was employed at the overall air to fuel ratio of 50-1. The period exhibiting the strong radiation, therefore, does not seem to necessarily represent the amount of soot emissions. That is, the relatively short radiating period with LIP (Fig. 10) is in contrast with the long radiating period with HIP (Figs. 7 and 9) while their emissions seem to be mutually indiscernible. It may be added again that the spray plumes had locally stronger radiation zones with LIP than those in HIP.

Since the period of fuel injection is related to the amount of fuel delivered per cycle, the radiating period is extended when the overall mixture was richer. When the HIP system was employed, again, the length of the radiating period did not necessarily result in increased amounts of soot emissions. The lasting strong radiation seems to suggest high temperatures in the products to help oxidize the soot.

Also as expected, the richer the overall mixture, the stronger the engine noise reflecting the increased heat release rate, which was somewhat alleviated when the intake air temperature was high as explained next.

(7) **Intake Air Temperature.** Recall that the reasons for investigating the effects of increased intake air temperature in the present HIP DI-CI engine include the analysis of a low-heat rejection HPD engine that employs ceramic components, which is expected to have high intake air temperature.

An increase of the intake air temperature clearly shortened the ignition delay, which in turn minimized the presence of the preflame images seen via 3.42 μ m, and resulted in an increased soot emission (also a greater deposit formation over the optical window). The decreased ignition delay by the temperature increase considerably alleviated the engine noise, which was unacceptably high in some cases such as when the injection pressure was high with early start of injection.

(8) **Spray Development.** According to the in-cylinder visualization conducted to date using the present four-spectral IR imaging system, the spray structure in a HPD HIP DI-CI engine may be different from those in conventional LIP DI-CI engines.

This consideration is stated based on the observation of spray development performed with the injection pressure ranging from 70MPa to 210 MPa (over 30,000psi) and air-fuel ratio varied from 50-1 to 20-1. When the injection pressure goes near 200 MPa (and air-fuel ratio of 20-1), as mentioned earlier it was even difficult to identify the shape of spray. That is, the fuel distribution appeared to be thinned over the combustion chamber, unlike relatively well defined shapes of spray (or reaction zones) when the engine was operated at fuel pressure lower than 140 MPa (20,000psi). Most notably, when the injection pressure was low, e.g. 70 MPa (around 10,000 psi) like in the conventional LIP engines, the spray development was locally defined exhibiting a limited extent of air-utilization.

At this time, it seems to be important to point out the following remarks. In spite of a vast amount of results analyzed in our present in-cylinder study, they seem to be yet insufficient to offer a generic nature of spray

development at present. Most of all, some of the present results offer more questions than answers: Some of unexpected and confusing observations, as briefly explained above, may partially explain the difficulties in characterizing the spray development and reaction in a HIP HPD CI-DI engine.

In addition, the injector unit, including the factory-delivered injector-tip employed in the present experiment, may not necessarily deliver behaviors representing many different injector systems being used in current Diesel systems.

Most of all, since the progressive change of spray development exhibited in the typical results obtained under varied conditions rather clearly indicate how they grew and differ from each other, it seems to be more reasonable to leave the readers to draw their own understanding of the processes, by presenting them as much details as the publication space permits.

HPD DI-CI Engine. During the course of conducting performance and in-cylinder visualization of high-power-density DI-CI combustion processes, it came to learn the development of such an engine to be highly promising. There is no doubt that the use of an HIP system is essential in such an engine, which permits a highly enhanced smoke-limited air utilization.

When the low heat rejection (LHR) engine strategy is employed in the design of HPD HIP DI-CI engine, the following may be an important concern: The high engine temperature resulting from the LHR would increase the temperature of both intake air and fuel. Since it would cause a deterioration of IMEP and increase of soot formation, it is highly desirable to minimize their temperature increases. Among the design methods for the goal are an extensive insulation of intake conduit (also for avoiding a deteriorated volumetric efficiency) and the injector from the high-temperature block, and even a positive cooling of fuel in order to prevent the fuel flow from producing premature cavitation (also for maintaining a proper lubricity), and alteration of fuel spray development and preflame reactions.

The increased intake air temperature may not necessarily be a negative aspect of the LHR engine strategy because the engine noise was reduced by shortening the ignition delay period. The increase of soot formation due to a short ignition delay was alleviated when the HIP was employed. It appeared to be necessary that the HPD engine would need a turbocharger (which was simulated in the present study by increasing the building air pressure) in order to achieve a high IMEP.

Since the operation of an HPD HIP CI-DI engine would include a wide variation of the intake air temperature and injection pressures, it will be desirable to shift the start of injection according to such a variation in order to obtain the best torque.

ACKNOWLEDGMENT

Authors wish to express their appreciation for support from the US Army Research Office (Contract No. DAAG55-98-0494 and DAAH04-96-1-0459) and Ford Motor Company.

REFERENCES

1. Themel, T., Jansons, M., Campbell, S. and Rhee, K.T., "Diesel Engine Response to High Fuel-Injection Pressures," SAE Paper 982683, 1998.
2. Han, Z., Hampson, G., Reiz, R., and Uludongan, A., "Mechanism of Soot and Nox Emission Reduction using Multiple-injection in a Diesel Engine," SAE Paper-960633, 1996.
3. Arcoumanis, C., Flora, H., Gavaise, M., Kampais, N., "Investigation of Hole Cavitation in a Vertical Multi-hole Diesel Injector," SAE Paper 2999-01-0524.
4. Clasen, E., Campbell, S., and Rhee, K.T., "Spectral IR Images of Direct Injection Diesel Engine Combustion with High Pressure Fuel Injection," SAE Paper-950605, 1995.
5. Clasen, E., Song, K., Campbell, S., and Rhee, K.T., "Fuel Effects on Diesel Combustion Processes," SAE Paper-962066, 1996.
6. Abata, D., Stroia, B.J., Beck, N.J., and Roach, A.R., "Diesel Engine Flame Photographs with High Pressure Injection," SAE Paper-880298, 1988.
7. McComiskey, T., Jiang, H., Qian, Y., Rhee, K.T., and Kent, J.C., "High-Speed Spectral Infrared Imaging of SI Engine Combustion," SAE Paper- 930865, 1993.
8. Jiang, H., Qian, Y. and Rhee, K.T., "High-Speed Dual-Spectra Infrared Imaging," *Optical Engineering*, 32 (6), pp. 1281-1289, 1993.
9. Chang, C., Clasen, E., Song, K., Campbell, S., Jiang, H., Rhee, K.T., "Quantitative Imaging of In-cylinder Processes by Multispectral Methods," SAE Paper-970872, 1997.
10. Campbell, S. Lin, S., Jansons, M. and KT Rhee, "In-cylinder Liquid Fuel Layers, Cause of Unburned Hydrocarbon and Deposit Formation in SI Engines?" SAE Fuels and Lube Meeting, October 1999.

DME-Blended Alternative Fuels in Direct-injection Diesel Engine

S. KAJITANI, C. L. CHEN
Ibaraki University, Hitachi, Japan

M. ALAM, K. ITO
Hokkaido University, Hokkaido, Japan

KT RHEE,
Rutgers, The State University of New Jersey, Piscataway, New Jersey

Summary

For investigating low-soot-producing alternative fuels in the Diesel engine, the following were studied: (1) neat Diesel fuel for reference purpose; (2) neat dimethyl ether (DME); (3) blends of Diesel fuel and DME; and (4) blends of DME and propane. Essentially soot-free emission was possible from a CI engine by using fuels (2) and (4). The role of DME in reducing the soot emission in fuel (3) is found to be highly significant, and was interpreted to have enhanced mixing of fuel spray. The use of DME blending well with most hydrocarbon fuels in any proportion offers a novel technique for utilizing widely available inexpensive gaseous fuels in the Diesel engine without significant engine modifications.

INTRODUCTION

As a result of increasing concern for global warming, the high efficiency of the Diesel or compression ignition (CI) engine has recently become a more significant advantage over the spark-ignition (SI) engine producing a smaller amount of CO_2 per travel distance.

This "environmentally friendly" engine, however, produces other emissions particularly soot, for which several new methods of soot reduction are being implemented. They include the use of very high-injection pressure and exhaust gas treatment devices. At the same time, the fuel modification or reformulating such as the use of low-soot producing dimethyl ether (DME) [1-4] are investigated, as an alternative avenue of helping achieve the same goal.

Although some similar measures for low soot emissions have been explored, e.g. the use of methanol in CI engine where special ignition aids are necessary, DME is considered to be more promising thanks to its low self-ignition temperature (235 °C) having a cetane number higher than even the typical Diesel fuel.

The low soot emission from the DME-operated CI engine has been explained by its simple molecular structure without any direct C-C bond and the low boiling point (25 °C) resulting in rapid mixing of the fuel spray. DME on the other hand has some disadvantages as an alternative fuel in the CI engine. They include: a high vapor pressure requiring a pressurized fuel tank; a low energy content (approximately 70% that of Diesel fuel); and a low lubricity causing severe leakage and wear in the injector.

These disadvantages, however, may not be worse than others encountered in various methods being employed in the modern transportation systems: A pressurized fuel tank is widely used in taxicabs operated by compressed (or liquefied) petroleum gases for low emissions particularly in many urban areas. Methanol having a comparable energy content as DME is used in some city buses. A fuel additive to DME was found to be effective in minimizing problems associated with the low lubricity (or viscosity) [1,2].

FUEL BLENDS. During the course of studying the use of DME in the CI engine, it was discovered that this fuel can be mixed with most hydrocarbon fuels in any ratio, including Diesel fuel and gaseous fuels, e.g. propane [1]. This was considered to be a great advantage of the fuel for several reasons, some of which are listed as follows. The CI engine operated by a DME-Diesel fuel blend would reduce soot emission [5]. When propane was added the blend was expected to enhance the mixing of the fuel spray [1]. DME mixed with either Diesel fuel or propane or both result in an increased energy content in the blend. Also, the hydrocarbons which blend easily with DME are inexpensive and readily available through the well established fuel delivery infrastructures.

In order to facilitate a discussion of the techniques and results of the study, Table I is presented first by listing some relevant characteristics of several fuels namely, DME, Diesel fuel, propane, and butane. The contents of the table is self-explanatory and they will be referred to when needed in the rest of the paper.

Table I. Selected Characteristics of Fuels for CI engines

	Unit	DME	Diesel Fuel	Propane	Butane
Chemical Structure		$(CH_3)_2O$	$C_{12}H_{1.87n}$	C_3H_8	C_4H_{10}
Liquid Density	kg/m ³	667	831	500.5	578.8
Rel. Gas Density (air = 1)		1.59	-	1.52	2.07
Molecular Weight	g/mol	46.069	170	44.09	58.12
Cetane Number		>55	40-55	-	-
Boiling Point	°C	-25	180/370	-42	-0.5
Stoichiometric A/F	kg/kg	9.0	14.6	15.88	15.46
C	%wt	52.5	86	82	83
H	%wt	13.0	14	18	17
O	%wt	34.8	0	0	0
LHV	MJ/kg	28.8	42.7	46.35	45.72
Vapor Pressure	KPa-293K	530	-	830	210
Heat of vaporization	kJ/kg	467.13	300	372	358
Gaseous specific Heat	kJ/kg-K	2.99	1.7	1.67	1.68
Ignition Limit	l	0.34/	0.48/	0.42/2.0	0.36/1.84
Min. Ignition Energy	mJ	0.29	-	0.305	0.38
Self Ignition Temperature	°C	235	250	470	365
Laminar Flame speed	m/s	0.54	-	0.46	0.41
Velocity of Sound	m/s	980	1330		
Kinematic viscosity (liquid)	cSt	<1	3	-	-
Modulus of elasticity	N/m ³ x10 ⁻⁸	6.37	14.9		

In utilizing the advantages of DME as a low-soot producing fuel, which mixes well with many common hydrocarbons, several fuels were studied in a CI engine, namely: (1) Diesel fuel alone for comparison purposes; (2) neat DME; (3) DME blend with Diesel fuel; and (4) DME blend with propane. Except for Diesel fuel, Hitec-580 (provided by Ethyl, Japan Corp.) was included in a proportion of approximately 500 ppm (in DME) for fuels (2)-(4) in order to achieve a proper lubricity, which was found to eliminate or minimize wear in the injector [1,2].

Discussing the energy content of those fuels, Fig. 1 is presented. Since the low caloric value (LCV) of propane is about 8% higher than that of Diesel fuel, its blending effect is relatively high in increasing the energy content. The DI-CI engine used in the present study, however, was not successfully operated by blends in all mixing proportions but had an operational region permitting acceptable combustion as discussed later.

Prior to presenting engine measurements, several observations with blends are briefly discussed next. When DME and Diesel fuel were blended, they mixed well with each other without producing any separation. The resulting volume was about the same as the sum of the separate components. Similarly, the volume change in DME-propane blending was found to be insignificant.

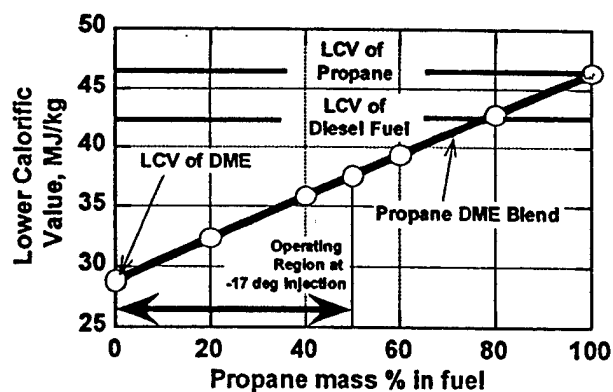


Fig. 1. Energy Content of DME-Propane Blend.

DME and propane were found to mix very well with each other resulting in a clear fluid, having the same appearance as DME. The DME-propane blend, however, produced bubbles when the container pressure was lower than the propane's vapor pressure (Table I).

In order to offer some insight into the spray formation, photos taken of fuel sprays under atmospheric pressure were examined as shown in Fig. 2 (a) Diesel fuel; (b)

Table-II Engine Specifications

Bore x Stroke	92 x 96mm
Displacement	638cm ³
Compression Ratio	17.7
Rated Output	15.6kW/cylinder @2600rpm
Injection Pump, Plunger	8mm dia. (Bosch type)
Injector, Four-hole Nozzle	0.26mm hole dia.

neat DME and (c) DME-propane blend. In spite of the limited fidelity of the photos and inability of duplicating a self-ignition environment, some obvious trends were exhibited. While the spray penetration with Diesel fuel is rather long and spray angle is narrow, those with neat DME and blend were short and wide, respectively. Note that in investigating sprays shown in Fig. 2, for the purpose of comparison, the same injection pressure of 8.82 MPa was used.

In addition to the wider spray angles of DME and DME-propane blends, since the propane or DME would be rapidly vaporized in the self-ignition environment, it is expected to have their blend sprays mixed in higher rates than a Diesel fuel spray in the combustion chamber, which is further discussed later.

ENGINE APPARATUS

The engine employed in the study was a typical direct injection (DI) CI engine manufactured by Yanmar Diesel Corporation and several pertinent specifications are listed in Table-II.

The engine apparatus was properly equipped in achieving the objectives, including: a pressure transducer to monitor injection pressure; a needle lift sensor to record the nozzle opening history; and an in-cylinder pressure transducer. The engine was also interfaced with a set of emission measurement devices [1]. Since they are widely used in the field, no further discussion is included here.

Mentioning the engine operating details, unless otherwise noted, all measurements were obtained under the engine conditions explained next. The engine was operated (on the engine manufacturer recommendation for the neat Diesel fuel) at an injection pressure of 20.1 MPa (2,915 psi) when the neat Diesel fuel or blends with a Diesel fuel content of over 50% was used. Note that the control of injection pressure was achieved by adjusting the spring preload in the injector. The neat DME or DME-propane blend was introduced into the engine with the injector needle opening pressure maintained at 8.82 MPa (1,279 psi), however. The engine operation was balanced with an external load equivalent to a mean effective pressure (P_{me}) of 0.4 MPa with the start of

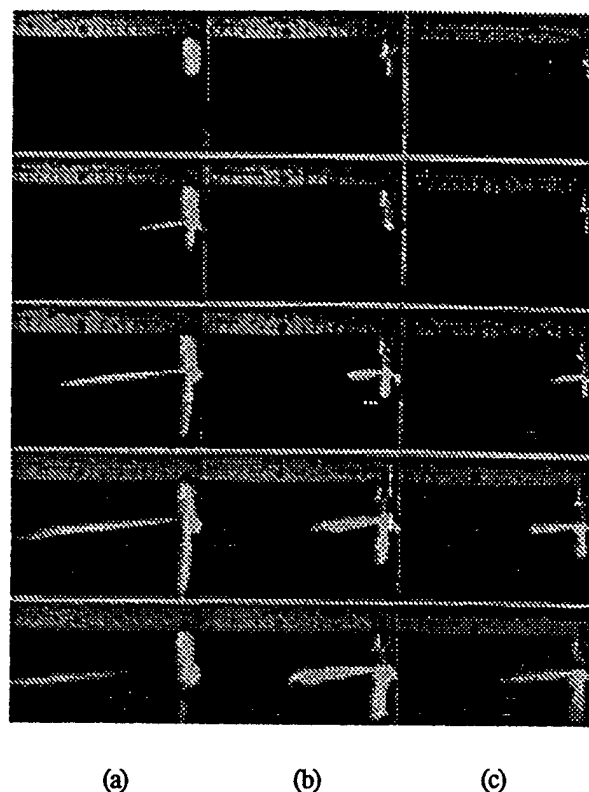


Fig. 2. Spray Characteristics of (a) Diesel Fuel; (b) neat DME; and (c) Blend.

fuel injection at 17 degrees of engine crank angle before top dead center (denoted by -17CA or 17bTDC) in most measurements.

In order to prevent premature vaporization in the fuel system, when neat DME or DME-blends were used, the fuel tank was pressurized by using nitrogen gas (from a bottle) by maintaining injector-pump-inlet pressures of 3.43 MPa (497.5 psi) [1]. When propane was included in the blend, however, it made sure to maintain the fuel tank at a pressure much higher than its vapor pressure (830 kPa, or 120.38 psi). The engine was operated at 960 rpm throughout the experiment. A schematic presentation of the apparatus is included in Fig. 3.

Because of the low viscosity of DME and its blends, the amount of return fuel in the injector was significant, often as much as over 30% of the total, which was due to leakage through the clearance in the injector. The higher the portion of DME, the greater the amount of leakage. In spite of a lubricity-enhancing additive as mentioned earlier (in order to minimize the wear of the plunger), when neat DME was used, the return amount was as high as seven times that with neat Diesel fuel (Fig. 4). When the DME content in the blend was lower than 20%, the difference in leakage between the two was insignificant, however.

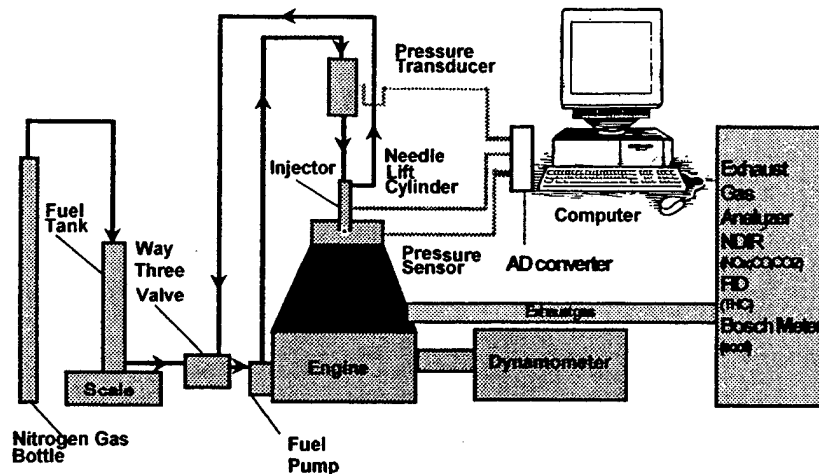


Fig. 3. Schematics of Experimental Apparatus.

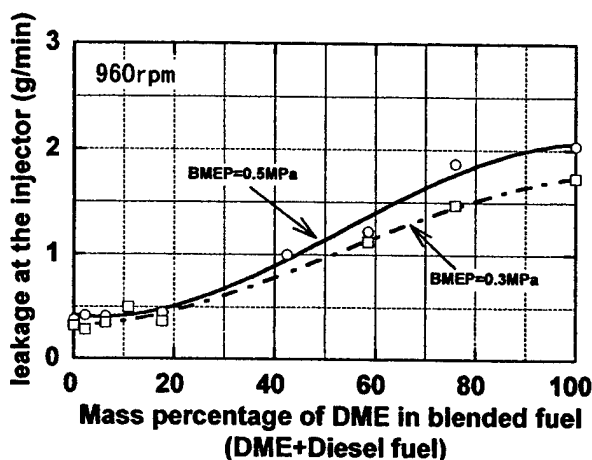


Fig. 4. Leakage in the injector for Varied Content of DME in DME-Diesel Fuel Blends.

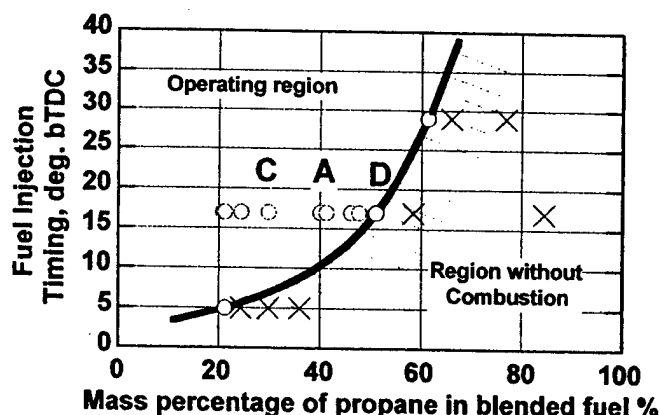


Fig. 5. Operating Region of a DI Diesel Engine Fueled by DME-blends.

OPERATIONAL REGION

Although DME can be mixed with most hydrocarbon fuels in any ratio (refer to Fig. 1), the engine produced combustion reactions only within an operational range (Fig. 5), which is conceivable in view that the self-ignition temperature of propane is too high to achieve a compression-ignition in the engine. Shown here is for DME-propane blends that the higher the propane content the more difficult the self-ignition. (Note that DME-blends with Diesel fuel had no limitation in achieving a successful combustion.)

In the figure, the left hand side marked by O, which has low proportions of propane, represents the blend ratios having a successful combustion, and the opposite side indicated by X is the region otherwise. It is also noted that the start of injection was a dictating parameter for the combustion, which is similarly found when Diesel fuels with varied cetane numbers are used in a typical CI engine.

RESULTS AND DISCUSSION

ENGINE PERFORMANCE. The responses of both the injector and the engine combustion to changes in fuels are discussed first by presenting: the injection pressure-time (p-t) history (Fig. 6); the needle lift (Fig. 7); the cylinder p-t diagram (Fig. 8); and the rate of heat release (ROHR) (Fig. 9).

In spite of the preset spring load as mentioned earlier, the injection p-t history varied to affect the opening of the needle for different fuels and blends (Fig. 6). The difference in bulk moduli appears to play an important role in the varied injection p-t histories. Under the same preload (20.1 MPa) for the neat Diesel fuel and its blends with DME, the higher the DME portion, the lower the pressure rise rate and the peak p-t. For the DME and its blend with propane, a similar trend was observed, that is,

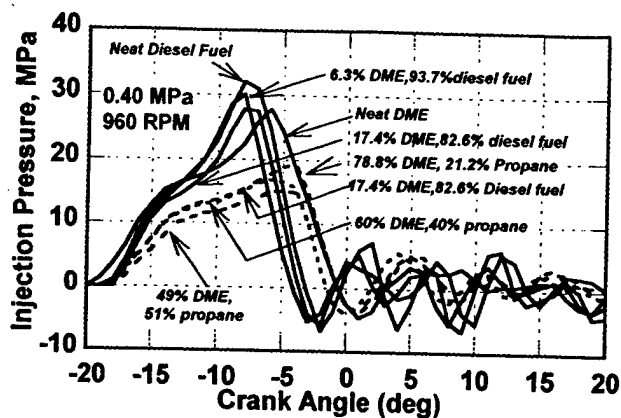


Fig. 6. Effect of Fuel Type on Injection Pressure History.

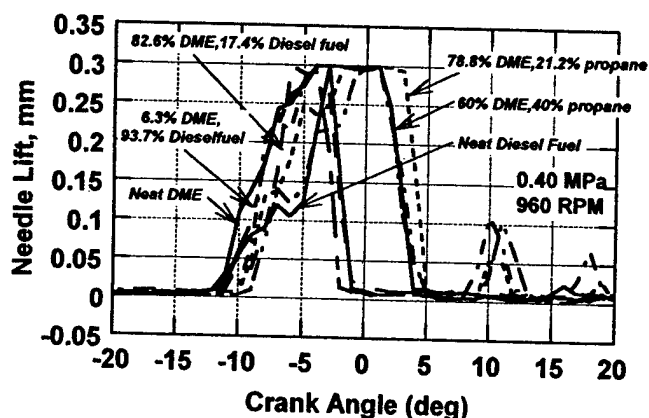


Fig. 7. Effect of Fuel Type on Needle Lift.

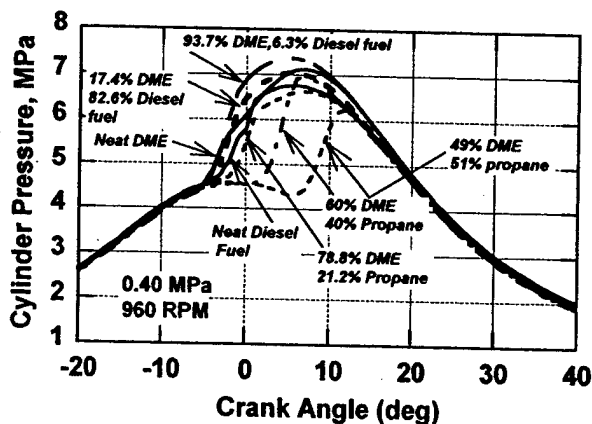


Fig. 8. Effect of Fuel Type on Cylinder Pressure-time (p-t) History.

the higher the propane content, the lower the pressure rise rate and the peak p-t.

The variations in the injection p-t history should have been reflected on the needle lift accordingly. That is, the

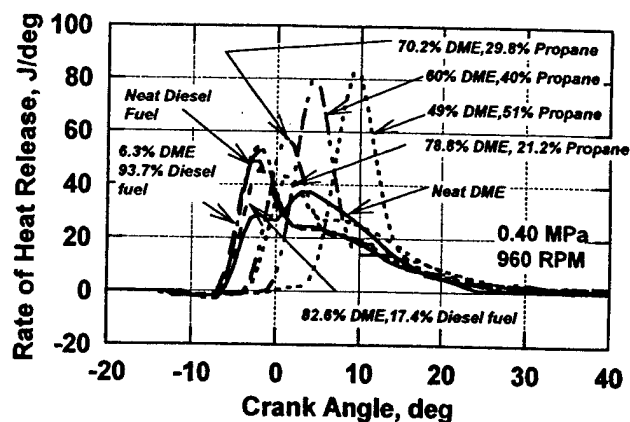


Fig. 9. Rate of Heat Release Affected by Fuel Type.

neat Diesel fuel having the lowest compressibility (highest modulus of elasticity) of all was expected to start the needle lift the earliest, and its blend with a higher content of DME had a more delayed opening. For the DME-propane blends, it should have been that the higher the propane content the more delayed the opening.

The needle lift histories, however, did not match with the injection p-t histories as shown in Fig. 6. Among the reasons for this is that the spring preloads on the needle for the opening pressure were different in two groups of fuels as mentioned earlier, i.e., 20.1 MPa (2,915 psi) and 8.82 MPa (1,279 psi) when the neat Diesel fuel or its blend with DME and the neat DME or DME-propane were used, respectively. It is also noted that since the engine operation was in balance with a fixed external load for all fuels tested in the engine, the throttle manipulation was necessary, which obviously changed the period of needle opening depending upon the energy content of fuel and the thermal efficiency.

Discussing the cylinder p-t diagrams (Fig. 8), they seem to be consistent with the needle lift. The earliest start of pressure rise and also the start of heat release (Fig. 9) for the neat and blends of DME with the Diesel fuel are explained by both their early starts of needle lift and the low self-ignition temperature of DME. Something unexpected in the figures was that the combustion started relatively early with the neat Diesel fuel while the start of injection was more delayed than that with DME or DME blends.

In addition, it is noted that CO_2 in the residual gas may have played a role in expediting the vaporizing-mixing process of a DME (and its blend) spray, however small it may be. According to the van der Waals' equation, when CO_2 is absorbed by DME, the process is exothermic. If this effect is not negligible when a DME is injected in a firing engine, the said exothermic reaction would further accelerate the vaporization and thus the mixing. As the fuel vaporizes, however, the latent heat of evaporation would lead the trend in opposite direction.

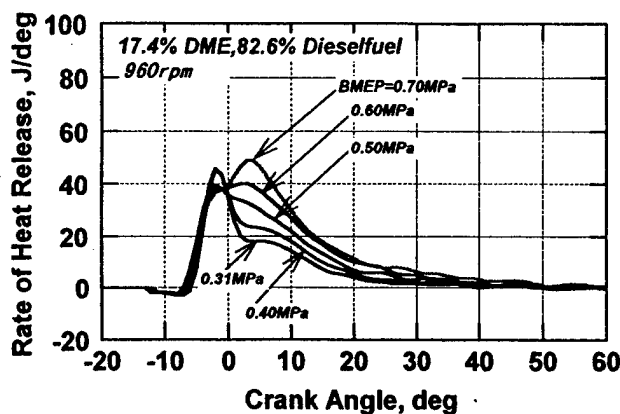


Fig. 10. Rate of Heat Release with Blend.
(DME 17.4%, and Diesel Fuel 82.6%)

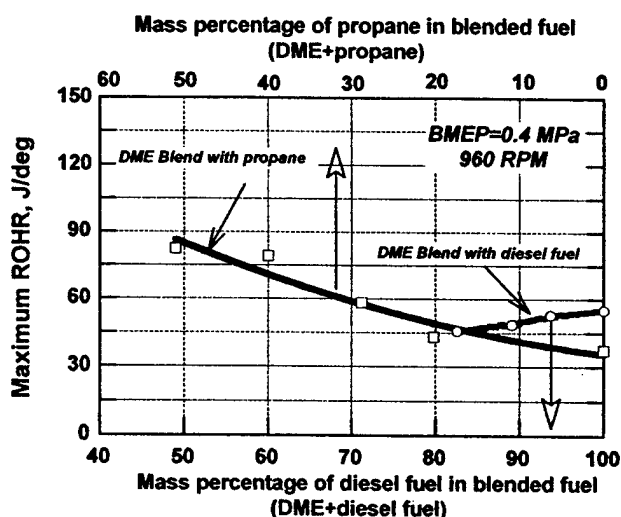


Fig. 11. Effect of Fuel Type on Maximum Rate of Heat Release Rate.

The trend in the start of heat release with DME-propane blends is also considered to be reasonable. Since propane has a self-ignition temperature much higher than DME, it was expected that the higher the propane content the later the start of heat release, which is well shown in Fig. 9. Note that in order to achieve the best cycle conversion efficiency for such fuels (with a low cetane rating), the start of injection should have been advanced accordingly, which was not evaluated in the present study.

The difference in fuel characteristics is reflected on the differentiation between the stages of the premixed combustion and the diffusion-controlled reaction, which was most obvious with the neat Diesel fuel, while DME had a minimum amount of heat release during the premixed combustion stage. Since the ignition delay with DME is very short, the amount of accumulated fuel vapor was small having less significant heat release in the premixed combustion stage.

The dominant premixed combustion stages with DME-propane blends are discussed next. When the propane content was high, the heat release curve looks like one expected in an entirely premixed combustion reaction. Explaining this, recall that propane has a very low boiling point and a high vapor pressure while it has a high self-ignition temperature (Table I). When a blend of DME and propane (having a relatively low boiling point) is injected into the cylinder, it is conceivable that the higher volatility component (here, propane) in the blend would be vaporized first to "perforate" the lower volatility fuel in the liquid phase, which would enhance the mixing of the entire spray. (Note this is expected to occur in other bifuel blends, i.e., Diesel fuel and DME.) Thus, any amount of propane in the blend would extend the ignition delay and in turn the vapor formation period. The latent heat of evaporation by propane off the spray would also cause an extended ignition delay by reducing the mixture temperature. These all are considered to help produce a dominant premixed combustion reaction with a minimum amount of heat release via the diffusion-controlled combustion (Fig. 9).

In order to assess the effect of the engine load on the combustion when the engine was operated by blends of Diesel fuel and DME, the rate of heat release was examined as shown in Fig. 10. For this, a Diesel fuel blend with 17.4% DME was used, which exhibited a p-t diagram quite comparable to that of the neat Diesel fuel. Unlike those in a Diesel fuel operated engine, the pattern of curves clearly changed with the engine load. Most of all, the higher the engine load, the smaller the differentiation between the premixed and diffusion-controlled combustion stages. At a high load, the heat release history looks like one expected in a single stage combustion, quite seemingly an entirely diffusion controlled combustion.

Going back to Fig. 9 and reviewing curves for the blends of DME, the amount of heat release in the premixed combustion stage is found to decrease with the content of DME. Since the peak ROHR relatively well represents the amount of heat release in the stage, Fig. 11 was plotted in order to assess the blend effects on the processes. Note that the amount (or the peak ROHR) also indicate the trend of the cycle efficiency, because the rapid consumption of fuel in the premixed combustion occurs at near constant-volume combustion. In brief, the content of propane (DME-propane blends) and that of DME (in DME and Diesel fuel blends) appears to help increase the cycle efficiency. However, it is noted that the combustion was not quite acceptable in the present engine when the propane content was higher than 50%, which limit may be raised if the engine is modified.

The amount of heat release via the premixed combustion process is quite dependent on the ignition lag period. That is, even for the neat Diesel fuel, the longer the period, the more time for fuel vaporization. Figure 12 was prepared in order to correlate the results in Fig. 11

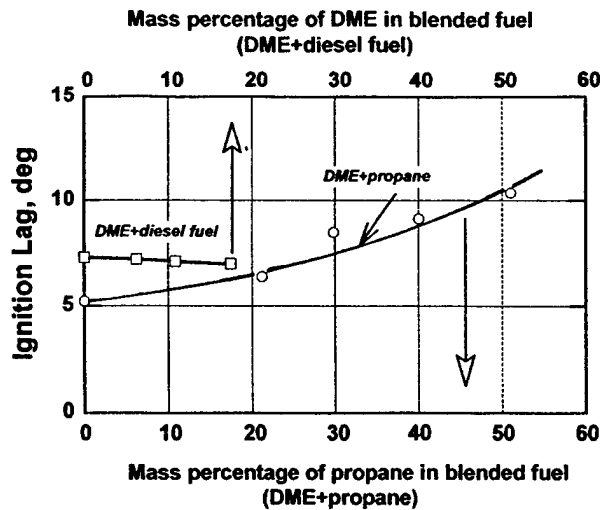


Fig. 12. Ignition Lag Affected by Fuel Type.

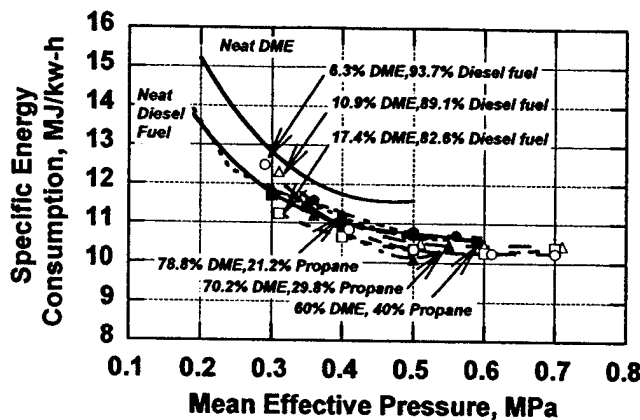


Fig. 13. Specific Fuel Consumption of Fuel Types for Varied Engine Load.

and the ignition lag: The correlation for both families of blends is very good.

Whenever the cycle efficiency is mentioned, other terms to be discussed are the specific fuel consumption (sfc) and the exhaust gas temperature (Figs. 13 and 14). Note that the notation in both figures are identical as shown in Fig. 14. The trend of sfc for blends is consistent with the cycle efficiency discussed above. For example, the higher the content of DME in blends of DME and Diesel fuel (to have a higher maximum ROHR and thus to achieve a higher cycle efficiency), the lower the sfc. (The variation of the exhaust gas temperature for the blends appears to be small.) It is noted that the high sfc at low engine loads are due to the somewhat constant amount of friction horse power, which becomes relatively small with the engine load increase.

The same trends were not prevailing in blends of propane and DME, however. The sfc was somewhat higher when the propane content increased to 40%, which, as mentioned earlier, should have been opposite if the start

symbol	DME + Diesel Fuel		symbol	DME + Propane Fuel	
	mass %			mass %	
	DME	Diesel Fuel		DME	Propane
○	6.3	93.7	●	78.8	21.2
△	10.9	89.1	▲	70.2	29.8
□	17.4	82.6	■	60	40
—			×	49	51

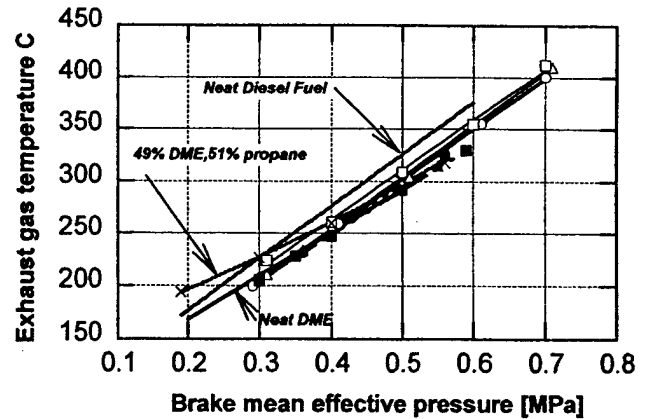


Fig. 14. Exhaust Gas Temperature Affected by Fuel Type.

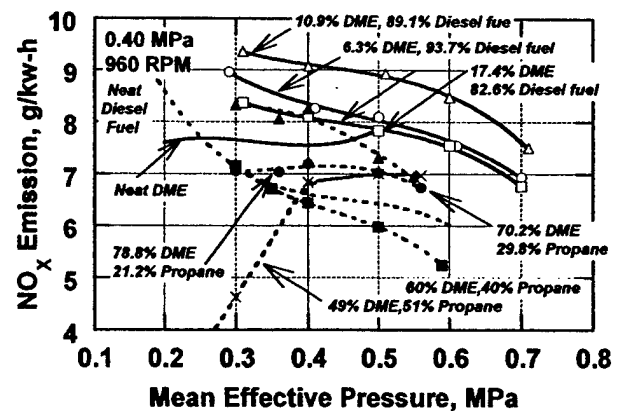


Fig. 15. Fuel Effect on NOx Emission under Varied Engine Load.

of injection was advanced by taking the increased ignition lag into consideration. When both Figs. 13 and 14 are compared to each other, they are consistent. That is, when the engine load was increased, the lower the sfc, the lower the exhaust gas temperature.

EMISSIONS. Measurements of oxides of nitrogen (NOx) made against the engine load are shown in Fig. 15. Briefly, the emission was highest with blends of DME with Diesel fuel, lowest with neat Diesel fuel and in between with blends of DME and propane. It is pointed out that the specific emissions (g/kw-h) decreased with the engine load for all fuels examined due to the (constant) amount of friction horse power becoming

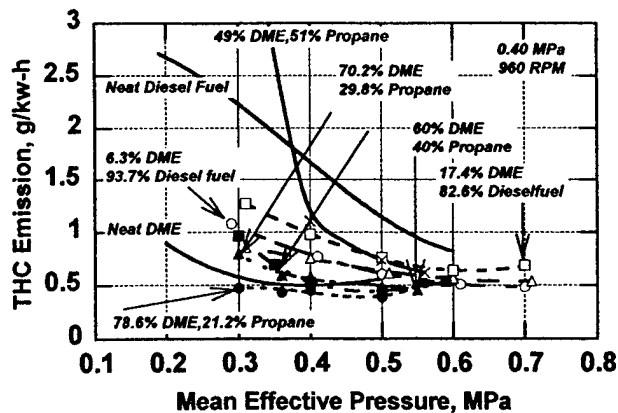


Fig. 16. Fuel Effect on Hydrocarbon (THC) Emissions under Varied Engine Load.

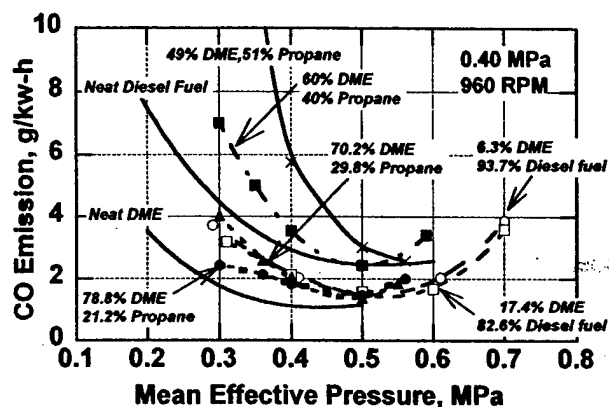


Fig. 17. Fuel Effect on Carbon Monoxide (CO) Emissions under Varied Engine Load.

relatively small with the engine load increase as discussed earlier.

NO_x. The highest NO_x emission with DME and Diesel fuel blends is explained by the fact that with these fuels the ignition started the earliest due to the high cetane number of DME. The same could have happened with DME-propane blends. In spite of a strong combustion (seen from ROHR), since the start of ignition lagged more than the former, the emission was accordingly lower.

THC. The general trend of total hydrocarbon (THC) emission for the fuels seems to be as expected (Fig. 16). When the engine load was high, the THC emission with DME-propane blends was low, which is explained by the improved mixing of spray to eliminate rich fuel pockets and thus to achieve better combustion. The high emission under light load is considered to occur due to an over mixing and low cylinder temperature. When a small amount of fuel is injected and the propane evaporates out of the spray, the vapor would be rapidly mixed with air and diffused over the chamber resulting in pockets too lean to have flame propagation. When the temperature in

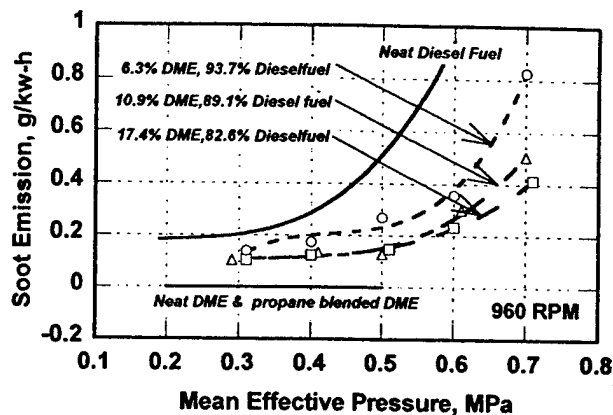


Fig. 18. Soot Emissions Affected by Fuel type under Varied Engine Load.

the cylinder is low (because of the low engine load), the consumption of the hydrocarbons in such pockets would be sluggish to be wasted in the exhaust. The high THC emission with a blend having a propane content of 51% is explained by an excessively long ignition delay to cause an over mixing, particularly when the engine load was low. The slightly high THC specific emission at high loads may be due to potentially improper mixing of the fuel (introduced at relatively low injection pressure).

CO. The emission of carbon monoxide (CO) appears to be consistent with the discussion made above on the THC emissions (Fig. 17). When the engine load was low, the complete oxidation of unburned hydrocarbon (including those from the over-mixed mixtures) would not be possible before the exhaust valve opened and at the same time to freeze oxidation of CO. The high emission at high engine loads is consistent with THC emissions which had an increasing trend, which would produce an incomplete oxidation.

Soot. The soot emission was negligible with the neat DME and DME-propane blends, which is pronounced to be one of the key advantages with those fuels (Fig. 18). When compared with the emission with the neat Diesel fuel, the effect of DME in its blend is found to be significant. For example, a considerable reduction of soot was achieved by a (small) content of 6.3% DME in the blend, which effect was most noteworthy at high engine loads where the emission with the neat Diesel fuel was too high to be reasonable. This effect is further discussed next.

In view that DME produce almost no soot in the CI engine, the reduction of soot in DME-Diesel fuel blends may be expected in diluting proportion of the DME content as represented by the solid line in Fig. 19. The reduction effect of DME, however, was far greater than the dilution effect as indicated by the dotted curve. Obviously, DME in the blend played an important role in other aspects. Among the probable reasons for this are that the low boiling point of DME and it completely

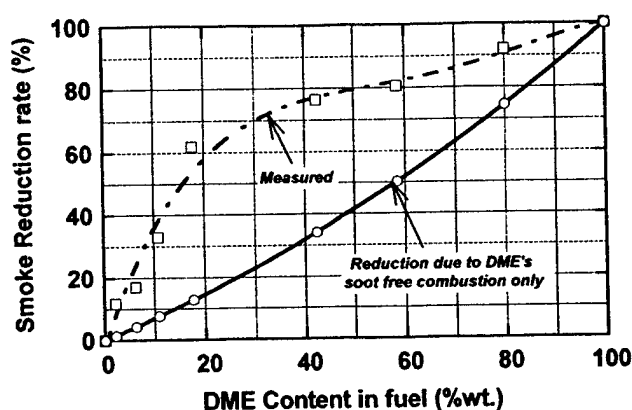


Fig. 19. Comparison of Soot Emission Measurement with Prediction Assuming a Dilution Effect.

mixes with Diesel fuel. When a blend spray is introduced in the cylinder, it is reasonable to expect that the high volatility DME would vaporize first by tearing up (perforating) the spray and droplets through out the liquid fuel blend to accelerate the mixing processes. The enhanced mixing will reduce the amount of rich fuel pockets exposed to high temperature combustion products, which is known to be the source of soot formation in the CI engine. According to the present measurement, the reduction effect is most significant when the DME content was around 20% of the blend. Note that this discussion limited to physical aspects of the spray formation and mixing does not include a possible chemical effects on soot reduction by DME.

Even Lower Emissions? The significant reduction of soot by DME-Diesel fuel blends may offer a new opportunity of achieving even lower exhaust (including soot) emissions. Since the blend would permit the engine be operated at a high overall fuel/air ratio, which will produce a high exhaust gas temperature. When it becomes possible, the exhaust gas treatment can be employed to further minimize the emissions in a similar way being employed in the gasoline-engine-operated vehicles.

CONCLUSIONS

For investigating low-soot producing alternative fuels, the following were tested in a typical direct-injection Diesel engine: (1) neat Diesel fuel; (2) neat dimethyl ether (DME); (3) Diesel fuel-DME blends; and (4) DME-propane blends. In order to minimize or eliminate wear in the injector, a lubricity-enhancing additive was included in a proportion of 500 ppm (in DME) for fuels (2)-(4).

Some of the findings from the present study are summarized in the following:

(1) DME is found to mixed well with most hydrocarbon fuels in any ratio, including Diesel fuel and propane.

(2) The spray formation varied for the respective fuels, namely in the spray penetration and the spray angle. The high volatility fuel in a blend is expected to vaporize sooner than other to perforate the host liquid fuels and to expedite the mixing of the fuel.

(3) The engine performance with these low-soot producing alternative fuels was quite comparable with that with the neat Diesel fuel.

(3) Essentially a soot-free CI engine operation is found to be possible when operated by neat DME or DME-propane blends.

(4) NO_x emissions were slightly higher with the neat DME and blends than with the neat Diesel fuel, which may be reversed by manipulation of the injection time.

(5) The emissions of total hydrocarbon and carbon monoxide were comparable to those with the neat Diesel fuel.

(6) A small amount of DME in Diesel fuel greatly reduced the soot emissions, which is considered to occur due to the DMA's role of enhancing the mixing to minimize rich pockets in the cylinder.

It might be added that these low soot producing DME blended alternative fuels is expected to pave the way of using exhaust treatment devices for further reduction of CI engine emissions.

ACKNOWLEDGMENT

Authors wish to express their appreciation to Mr. Sumitaka Minegishi who assisted the experiment. Ethyl Corp. (Japan) provided a fuel additive. One of the authors (KTR) received support from the US Army Research Office (Contract No. DAAH04-95-1-0430, and DAAH04-96-1-0459).

REFERENCES

1. S. Kajitani, C. L. Chen, M. Oguma, M. Alam, and KT Rhee, "Direct Injection Diesel Engine Operated with Propane-DME Blend Fuel," SAE Paper-982536, 1998.
2. S. Kajitani, C. L. Chen, M. Konno, and KT Rhee, "Engine Performance and Exhaust Characteristics of Direct-injection Diesel Engine Operated with DME," SAE Paper- 972973, 1997.

3. J. C. McCandless and S. Li, "Development of a Novel Fuel Injection System (NFIS) for Dimethyl Ether and Other Clean Alternative Fuels," SAE Paper-970220, 1997.
4. S. C. Sorenson. and S. E. Mikkelsen, "Performance and Emissions of a 0.273 Liter Direct Injection Diesel Engine Fueled with Neat Dimethyl Ether," SAE Paper-950064, 1995.
5. S. Kajitani, Z. L. Chen, H. Machida, and M. Oguma, "Engine Performance and Exhaust Gas Characteristics of a Compression Ignition Engine Operated with DME Glended Ga Oil Fuel," SAE Paper-982538, 1998.

Direct Injection Diesel Engine Operated with Propane-DME Blend Fuel

S. Kajitani, C. L. Chen, M. Oguma
Ibaraki University
Hitachi, Japan

M. Alam
Hokkaido University
Hokkaido, Japan

KT Rhee
Rutgers, The State University of New Jersey
Piscataway, New Jersey

ABSTRACT

A novel way of using low-cetane-number petroleum gases in a compression ignition (CI) engine is introduced, by directly injecting blends of such fuels with dimethyl ether (DME), a high-cetane-number alternative fuel for low soot emissions. This method both extends advantages of DME and complements its deficiency. Although DME mixes with most hydrocarbon fuels in any ratio, in order to demonstrate the feasibility of the new method and facilitate the analysis, DME-propane blends were investigated in a direct injection CI engine. Some findings of the study are listed.

In the engine operated by DME and propane blends, there was no need for significantly increasing the complexity of the fuel system than that employed in the use of neat DME. For the same reason, this method eliminates or minimizes cumbersome hardware necessary when the said gaseous fuels are separately introduced in CI engines.

When the content of propane was increased, which accordingly increased the heating value of the blend, the start of injection lagged, and self-ignition became sluggish itself, which resulted in a delayed start of heat release.

When the engine load was low, the more the propane content, the higher the specific fuel consumption and the greater the emissions of unburned hydrocarbon. This was interpreted in terms of an over-mixing due to rapid vaporization of propane out of the blend to diffuse and also low combustion chamber temperatures.

Mentioning other emissions with the DME-propane blends, soot emission was negligible, and the specific NO_x emission was in general lower than with neat DME, which decreased with an increase in both the propane content and engine load.

INTRODUCTION

Since the Diesel or compression ignition (CI) engine delivers a longer travel distance per amount of fuel (compared with spark-ignition, SI engines), it is considered to be a more environmentally friendly power-plant that emits smaller amounts of carbon dioxide (CO₂), a greenhouse gas associated with the global warming which appears to be an important issue at present. The CI engine, however, produces other emissions including soot, NO_x and odor, which severely limits its usefulness particularly in urban transportation systems.

While several advanced CI engine design strategies are seriously considered for reducing such emissions (and increasing the power output per displacement or weight), which include mating the engine with a very high injection pressure unit and exhaust treatment methods [1,2]*, the use of a new alternative fuel, dimethyl ether (DME) seems to be a promising method for helping achieve that goal [2-6]. Among the more important advantages of using DME are its high cetane number and low soot emission thanks to the absence of a direct C-C bond and oxygen contained in the fuel molecule. As a fuel in a CI engine, it is in contrast with methanol [7] which needs an additive such as a cetane improver or an ignition aid. As discussed later, DME can be mixed with most hydrocarbon fuels in any ratio, which offers several obvious advantages. It is also pointed out that DME can be directly derived from abundant resources such as natural gas, coal and vegetation (via methanol) [8-10].

On the other hand, in spite of the said desirable characteristics, DME as a candidate fuel in CI engines has some disadvantages: It has a high vapor pressure which

*Numbers in parentheses designate references at end of paper.

Table I. Selected Characteristics of Fuels for CI engines

	Unit	DME	Diesel Fuel	Propane	Butane
Chemical Structure		$(\text{CH}_3)_2\text{O}$	$\text{C}_{12}\text{H}_{24}$	C_3H_8	C_4H_{10}
Liquid Density	kg/m^3	667	831	500.5	578.8
Rel. Gas Density (air = 1)		1.59	-	1.52	2.07
Molecular Weight	g/mol	46.069	170	44.09	58.12
Cetane Number		>55	40-55	-	-
Boiling Point	$^{\circ}\text{C}$	-25	180/370	-42	-0.5
Stoichiometric A/F	kg/kg	9.0	14.6	15.88	15.46
C	%wt	52.5	86	82	83
H	%wt	13.0	14	18	17
O	%wt	34.8	0	0	0
LHV	MJ/kg	28.8	42.7	46.35	45.72
Vapor Pressure	KPa-293K	530	-	830	210
Heat of vaporization	kJ/kg	467.13	300	372	358
Gaseous specific Heat	kJ/kg-K	2.99	1.7	1.67	1.68
Ignition Limit	λ	0.34/	0.48/	0.42/2.0	0.36/1.84
Min. Ignition Energy	mJ	0.29	-	0.305	0.38
Self Ignition Temperature	$^{\circ}\text{C}$	235	250	470	365
Laminar Flame speed	m/s	0.54	-	0.46	0.41
Velocity of Sound	m/s	980	1330		
Kinematic viscosity (liquid)	cSt	<1	3	-	-
Modulus of elasticity	$\text{N/m}^2 \times 10^{-8}$	6.37	14.9		

requires a special handling such as a pressurized fuel container to avoid the fire hazard. This inconvenience, however, may be comparable to a similar measure being taken by taxicabs using liquefied or compressed petroleum gases for low-emissions in many urban areas. Also because of its low boiling temperature, DME is likely to be subjected to a supercritical point in the CI engine injector. If this is the case, when the fuel is suddenly issued out of the injector, cavitation is expected to accompany the fuel flow which would damage the nozzle hole.

DME has a low energy content, approximately 70% that of Diesel fuel (No. D-2) as further discussed later. In addition, since DME has a very low viscosity, it is likely to heavily leak as well as cause wear in the fuel plunger unless a lubricant is added [3]. These disadvantages, however, are considered to be surmountable by continuous research and development, e.g. a new injector design [11]. As explained in this paper, key advantages of using DME in a CI engine, e.g. a relatively high cetane number and low soot emissions are considered to offset such disadvantages.

Fuel Blend and Additional Effects. The present study is concerned with both extending DME's advantages and complementing the disadvantages. The core idea of the work undertaken is based on the fact that there are abundant amounts of inexpensive gaseous fuels in the world reserve, which are widely used in SI engines [12, 13] and that they may be nicely employed in CI engines by taking advantage of DME's ability of absorbing such gaseous fuels. Recall

that the use of gaseous fuel in the CI engine has been explored for a long time, mostly via fumigation [14], which involves knock-limited operations and an increased complexity of engine hardware.

The new method introduced in the present paper is to dissolve gaseous fuel(s) into DME (hereafter referred to as "blend") in order to directly inject it into the combustion chamber, which eliminates the need for on-board devices to meter-control-inject gaseous fuel into a CI engine. Although a multiple component gaseous fuel may be dissolved in DME, in order to demonstrate the feasibility of this new concept and for convenience of the analysis, a single component fuel, propane was chosen in the present study. Propane is also an inexpensive fuel available via a well-established delivery infrastructure.

This method of using DME-gaseous fuel blend serves several advantageous purposes or additional effects: (1) Since propane has a high low-heating-value (LHV), which is 8% higher than that of Diesel fuel, when propane is dissolved in DME (with a low LHV as mentioned earlier), the blending increases the energy content; (2) The low self ignition temperature of DME permits the use of gaseous fuel(s) in a CI engine without various cumbersome fuel system components and ignition aids, including: an additional (gaseous fuel) tank; gas regulator/injector; a pilot injection and glow-plug. (3) The high boiling point of gaseous fuel(s) in the blend is expected to expedite mixing of fuel spray in the cylinder, which may result in similar high atomization/mixing effects expected when a very high

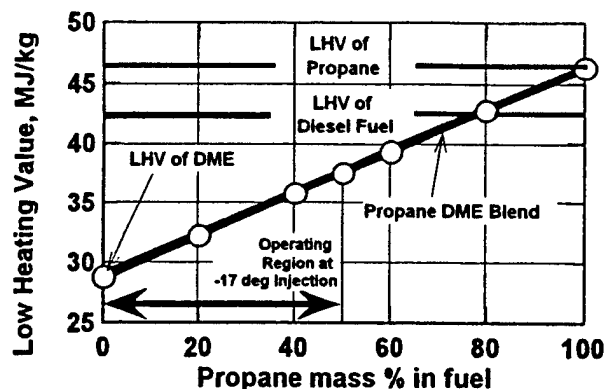


Fig. 1. Low Heating Value of Blended Fuels.

injection pressure fuel system is employed; (4) The simple C-H structure of gaseous fuel(s) would produce a low soot emission; and more.

In order to facilitate a discussion of the techniques and results of the study, Table I is presented by listing some relevant characteristics of several fuels namely, DME, Diesel fuel, propane, and butane.

Although the content of the table is self-explanatory and supplements the above discussion, a few additional remarks are in order. While DME has a self ignition temperature slightly lower than that of typical Diesel fuel (as reflected by its high cetane number), since theirs are high, propane and butane are difficult to be directly used in a CI engine. Recall that although such gaseous fuels are widely used in SI engines as mentioned earlier, the same has not been readily possible in the CI engine for application in transportation systems.

Reviewing the boiling points, consider the spray plume formation and vaporization when a DME-propane blend is injected into a CI engine combustion chamber, in comparison with a neat Diesel or DME spray. It is perceivable that the dissolved propane in the blend would be vaporized first to perforate the liquid flow and droplets by creating nuclei of vaporization, which will enhance the fuel mixing with air. (Note that when some premature nucleation occurs within the injector, it would damage the fuel passages.) If this happens, the processes would minimize rich fuel-pockets subject to high temperature combustion products reducing soot formation. In other words, while DME and propane are low soot producing fuels even when used individually, such an improved mixing in the blend fuel spray is expected to synergistically reduce the soot formation.

As briefly mentioned earlier, when propane is dissolved in DME, the blending will become a higher energy content fuel than the host liquid fuel. This will help eliminate the need for injecting an increased amount of fuel per cycle (i.e., the need for a high capacity injector) and reduce refueling frequency per a given travel distance, compared with when DME is used alone.

Figure 1 is included here in order to further elaborate the above discussion. As expected, the LHV of a blend proportionately increases with the propane content attaining almost the same LHV as Diesel fuel when the

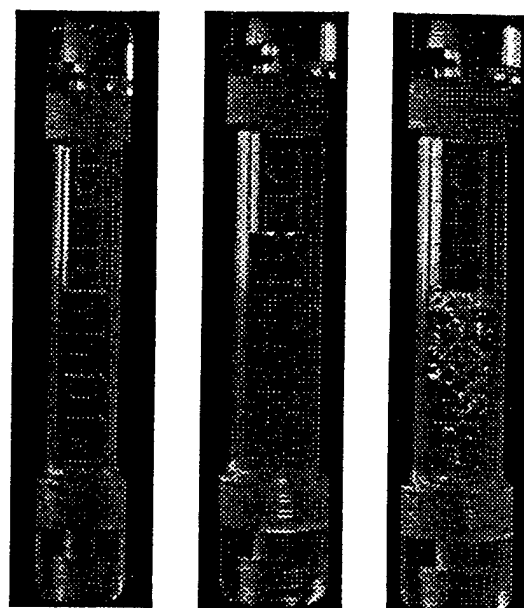


Fig. 2. Clarity of Fuels: (a) neat DME; (b) Blend; (c) Blend under a Low Pressure.

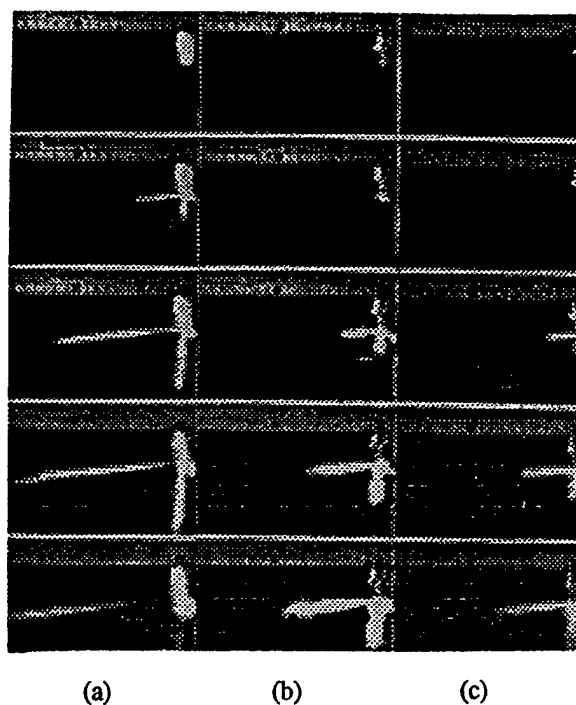


Fig. 3. Spray Characteristics of (a) Diesel Fuel; (b) neat DME; and (c) Blend.

blend nears 60% propane, which was near the upper limit of an operating range, as explained later. Note that, however, a more reasonable propane content in the blend for the CI

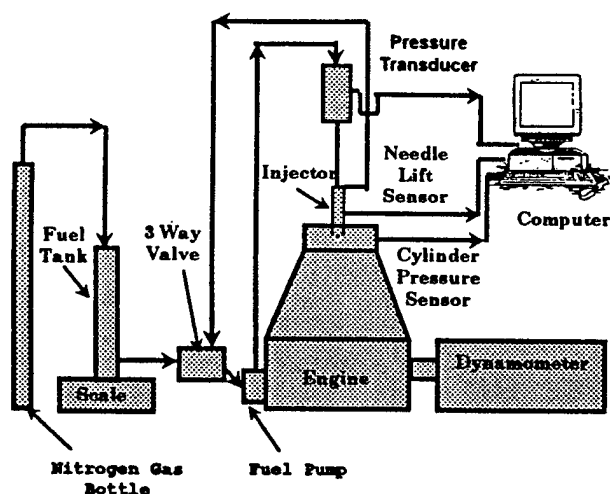


Fig. 4. Schematics of Experimental Apparatus.

engine employed in the present study was when it did not exceed 50%, which has a blend with an LHV almost 30% higher than neat DME. It is very possible to use a blend with higher propane content if the engine is somewhat modified, however.

In discussing the mixture characteristics, the preparation and handling of the blend are mentioned next. Recall that at a fixed temperature, when the pressure of a single-component fuel container is maintained at higher than its vapor pressure, there is no phase change in a container, e.g. DME in such an environment as shown in Fig. 2 (a). In exploring the possibility of directly mixing DME and propane together, two transparent containers of respective fuels were connected (in liquid phase) using a tube in between. It was discovered that they mixed soon each other to become a completely clear fluid without forming any meniscus (Fig. 2 (b)). At this time, the inclusion of a commercially available additive for increasing the lubricity [3] in DME did not appear to measurably affect the mixing of the two fuels, which was approximately 500 ppm of lubricant in DME. When the container pressure of the blend was below the propane vapor pressure (830 kPa, or 120.38 psi), the blend started to produce bubbles signaling the formation of propane vapor as shown in Fig. 2 (c). This supports the expectation of possible cavitation in the fuel flow and rapid perforation of fuel droplets in the fuel spray in a self-ignition environment, as mentioned earlier.

In order to obtain some insight into the spray formation in the cylinder, the fuels were injected under atmospheric pressure, which is shown in Fig. 3 (a) Diesel fuel; (2) neat DME and (3) DME-propane blend. In spite of the limited fidelity of the photos and inability of duplicating a self-ignition environment, they exhibit some obvious trends. While the spray penetration with Diesel fuel is rather long and spray angle is narrow, those with neat DME and blend were short and wide, respectively. Note that DME and blend were injected at a pressure much lower than Diesel

fuel in this experiment, as explained later. Without discussing the validity of employing the different injection pressures for those fuels, the present observation is considered to indicate relative and qualitative characteristics of spray formation in the cylinder.

EXPERIMENT

Engine and Apparatus. The engine apparatus used in the study was basically the same as that employed in an earlier study [3]. It was a typical direct injection (DI) CI engine, which was manufactured by Yanmar Diesel Corporation and several pertinent specifications are listed in Table-II.

Table-II Engine Specifications

Bore x Stroke	92 x 96mm
Displacement	638cm ³
Compression Ratio	17.7
Rated Output	15.6kW/cylinder-
2600rpm	
Injection Pump, Plunger	8mm dia. (Bosch type)
Injector, Four-hole Nozzle	0.26mm hole dia.

In implementing the objective of the study, the engine was sufficiently instrumented, including: a pressure transducer to monitor injection pressure; a needle lift sensor to record the nozzle opening history; and an in-cylinder pressure transducer. The engine was also interfaced with a set of emission measurement devices. Since they are widely used in the field, no further discussion is included here.

Realizing the need for a pressurized DME container, after reviewing various methods employed in previous studies [4,5,15,16], it was decided to use nitrogen gas (from a bottle) in order to maintain the injector-pump-inlet pressures at 3.43 MPa (497.5 psi), which is known to prevent vapor lock from occurring within the fuel system. The consumption of fuel was measured by using a scale on which the fuel tank was placed. A schematic presentation of the apparatus is given in Fig. 4.

Throughout the experiment, the engine was operated at a fixed speed of 960 rpm with the injector needle opening pressure maintained at 8.82 MPa (1,279 psi) when either neat DME or blend was used. Note that the injector opening pressure was recommended (by the manufacturer) to be 20.1 MPa (2,915 psi) when Diesel fuel is used in the engine. Unless stated otherwise, all of engine measurements included in this paper were made with an external load equivalent to a brake mean effective pressure (P_{me}) of 0.4 MPa.

Two separate experiments were conducted, namely measurements at a fixed injection time and a varied injection time. The former was to characterize the engine response to the new fuel and blends, and the latter was basically to investigate the injection timing effect on the engine performance and emissions.

RESULTS AND DISCUSSION

The experimental results are presented in graphical form as shown in Figs. 5-24, where unless noted otherwise the solid lines represent measurements using neat DME, respective dotted lines indicate blends or neat Diesel fuel. In spite of using the abovementioned fuel additive for increasing the lubricity of the blends, which did not result in any measurable deterioration throughout the previous study [3], the nozzle needle was frequently replaced in the present experiment in order to eliminate any possible interference by injector wear on the fuel metering and spray formation.

As indicated above, the results obtained under a fixed injection time, which was at 17 degree before the top dead center (denoted by 17 bTDC, or -17 CA), are presented first.

Operating Region. Prior to setting up an experimental plan, one of the most important steps taken in the study was to determine the operational region of the CI engine using blends with variation of the propane content in DME. For this, the start of injection in crank angle (CA) was varied for each blend. As shown in Fig. 5 which presents the operational region, the left-hand side of the curve marked by the circle is where the combustion reaction occurred in the engine, while the region in the opposite side of the curve indicated by X represents where firing was not possible at all for respective blends in the engine.

Regarding the effect of propane in DME, the higher the propane content in a blend, the earlier the injection timing, which is a similar trend observed when neat Diesel fuel with a lower cetane number is used in a typical DI-CI engine. In view of the poor self-ignition of propane (Table-I), it is conceivable that an increased propane content in the blend would decrease the compression ignition property, that is, resulting in a lower cetane number.

More specifically, when a blend with 50% propane content by mass (hereafter denoted by a "50P" blend, i.e., 0P corresponds to neat DME) was used, the engine operated with the start of fuel injection at 17 bTDC, and a 60P blend was about the upper limit for achieving any combustion reactions in the present engine.

Combustion Characteristics. Several measurements obtained from the engine are plotted in Figs. 6-8, including: the injection pressure; needle lift and cylinder pressure-time histories. The (solid and dotted) curves represent results from: (1) 0P (neat DME); (2) 21.2P; (3) 40P; and (4) 51P, as individually indicated in each figure. The engine was operated with injection starting at -17 CA (at a speed of 960 rpm with an external load of $P_{me} = 0.4$ MPa) with no other change in engine operation except for changing the fuel blend in this experiment.

Evidently, the higher the propane content, the lower the injection pressure (Fig. 6), which suggests the role of propane contributing to a low bulk modulus of elasticity (It was not found in the literature but inferred from its lower density than DME (Table-I)). Since the preload spring in the injector needle was set the same, it is reasonable to expect a shift of needle lift accordingly, which can be confirmed in

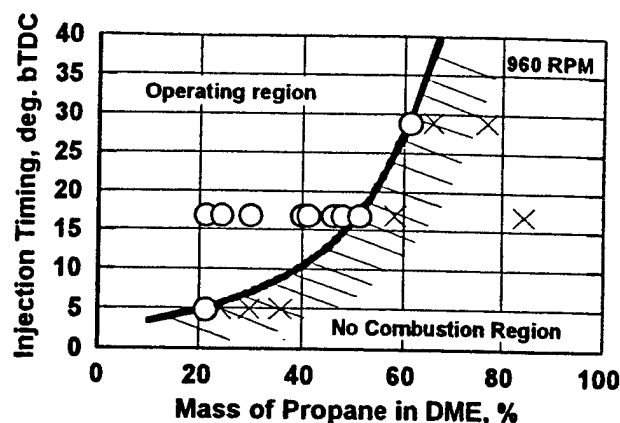


Fig. 5. Operating Region of a DI Diesel Engine Operated by DME-blends.

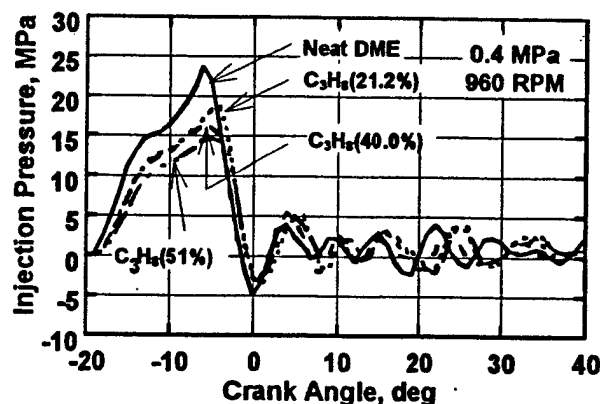


Fig. 6. Injection-Pressure Histories of DME-blends.

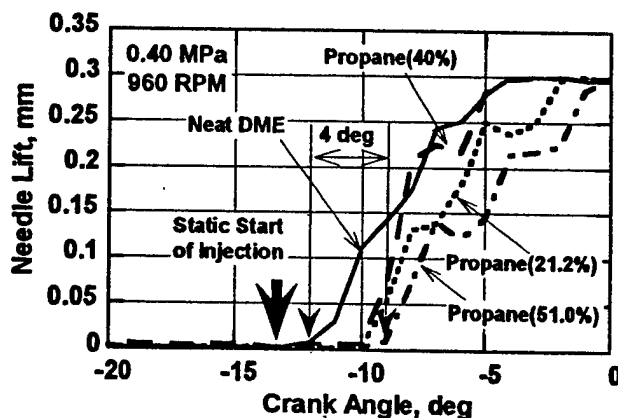


Fig. 7. Injector Needle Lift.

Fig. 7. That is, the higher the propane content in a blend, the more retarded the start of injection. Also, it is reasonable to expect that a delayed needle opening (under a fixed preload spring) would introduce a reduced amount of fuel into the combustion chamber, if no other measure was made. In order to balance the engine operation with the same external load, however, the injection period was adjusted (by throttle manipulation) for respective blends.

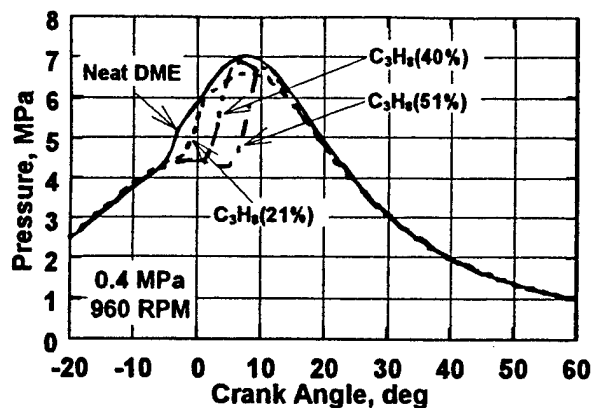


Fig. 8. Cylinder Pressure-time History with Neat DME and Blends.

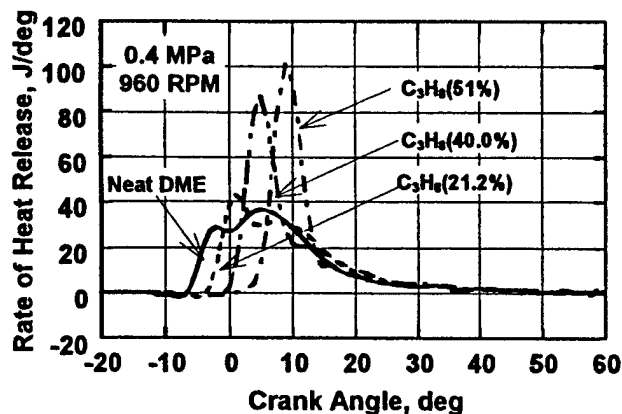


Fig. 9. Rate of Heat Release with Neat DME and Blends.

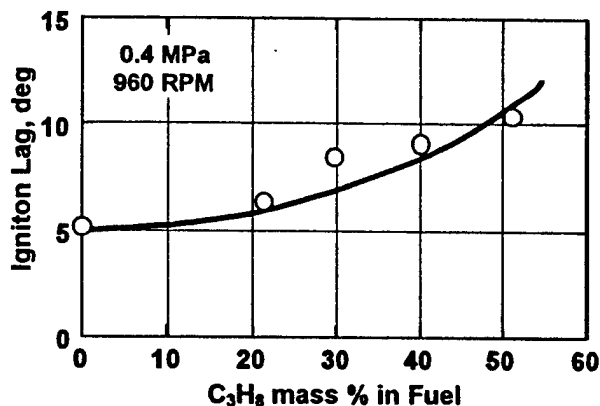


Fig. 10. Effect of Propane Content on Ignition Lag.

The fact that an increased content of propane in a blend delays both the start of injection (Fig. 7) and the start of self-ignition (refer to Fig. 5) will evidently affect the cylinder pressure-time (p-t) history. The effects of increased propane content on the p-t diagram and heat release history are shown on Figs. 8 and 9, respectively. In order to obtain better insight into the self-ignition tendency of blends, Fig. 10 was prepared by plotting the ignition delay (as defined as

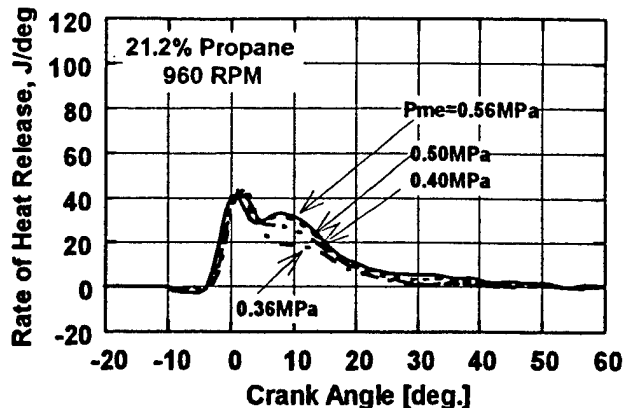


Fig. 11. Rate of Heat Release Curves with Blend with 21.2% Propane Content (21.2P).

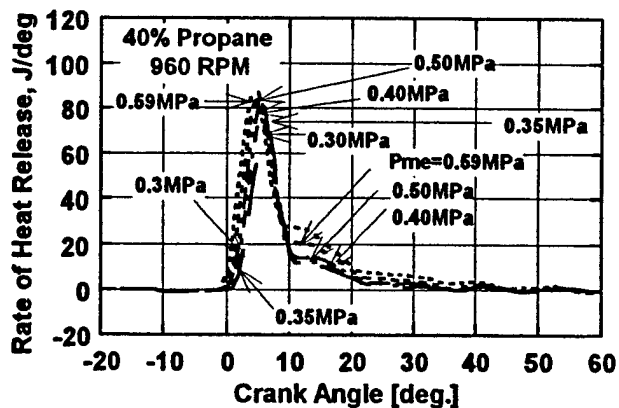


Fig. 12. Rate of Heat Release Curves with 40P Blend.

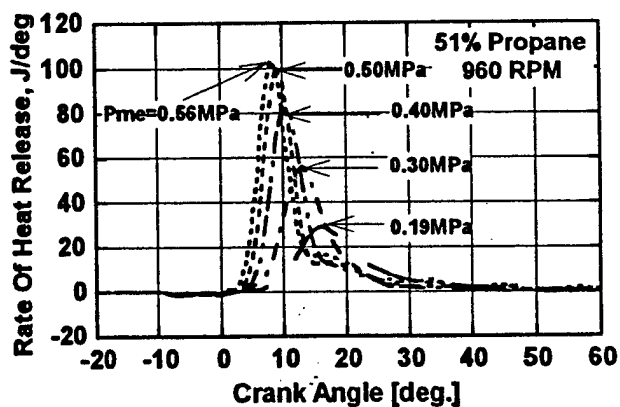


Fig. 13. Rate of Heat Release Curves with 51P Blend.

the period of time from the start of injection to the start of combustion) vs. the content of propane in the blend. The delay varied by as much as five CA when the content ranged up to 51%.

The curves in Fig. 8 are quite consistent with the above statement, that is, the higher the propane content, the later the start of combustion although the peak pressures were mutually comparable to each other. (It is noted that,

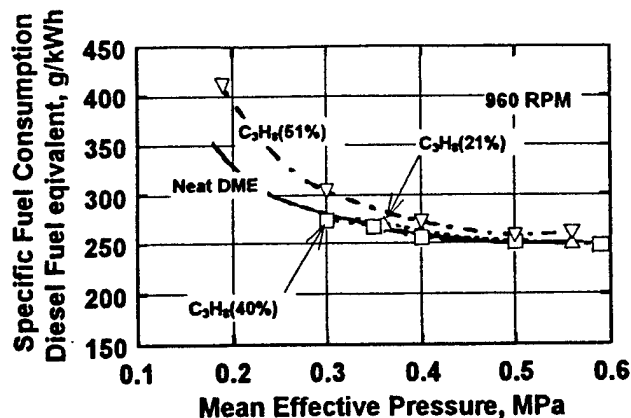


Fig. 14. Specific Fuel Consumption.
(Diesel Fuel Equivalent)

for blends with a high propane content, if the start of injection was advanced a more typical p-t diagram peaking around 5-10 aTDC would have been obtained. This effect will be evaluated later.) On the other hand, the higher the propane content, the greater the amount of heat release during the premixed combustion stage (Fig. 9). This is comparable to the same trend for Diesel fuel with lower cetane number, which often achieves a greater constant-volume combustion (to achieve a higher thermal efficiency).

In view of the probable variation in the amount of fuel injected into the cylinder for different blends, as briefly mentioned above, at this time the amount of fuel introduced into the engine was varied (via throttle manipulation) to have corresponding mean effective pressures as plotted by individual heat-release history curves in Figs 11-13. Looking at Fig. 11, when the propane content was low, there was no significant change in the start of combustion as well as the "pattern" differentiating between the premixed and the diffusion combustion stages. When the propane portion increased in the blend (e.g. 51P in Fig 13), however, the pattern considerably varied with the change in the load. This is interpreted to occur due to a varied amount of propane vapor accumulated prior to the onset of self-ignition. With a fixed timing of the start of injection at -17CA, according to the present measurement, a blend with 40P seemed most likely to be the upper limit for satisfactory engine combustion. It is reminded that when the engine operation and design parameters are modified (e.g. compression ratio, injector design and the start of injection), the upper propane content (and also the operational region shown in Fig. 5) for satisfactory engine operation would be raised.

Other Engine Measurements and Exhaust Emission. Figures 14 and 15 report measurements of the specific fuel consumption (sfc) and exhaust gas temperature respectively of the engine operated by blends under varied engine loads. For relatively high engine loads, the sfc was mutually comparable for three blends, namely 21P, 40P and 51P. Under a fixed engine load, the sfc is quite consistent with the corresponding exhaust gas temperature, that is, the higher the sfc, the higher the exhaust gas temperature. (Note

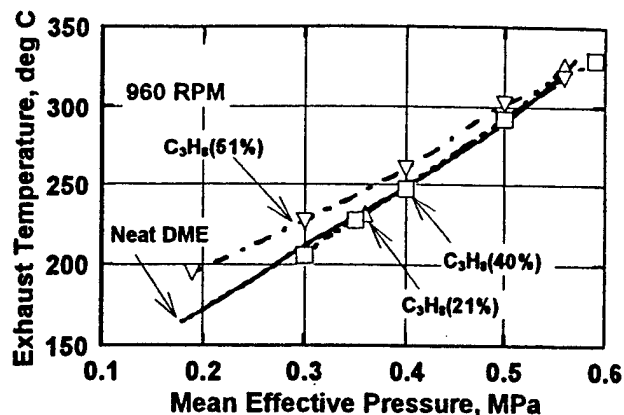


Fig. 15. Exhaust Gas Temperature.

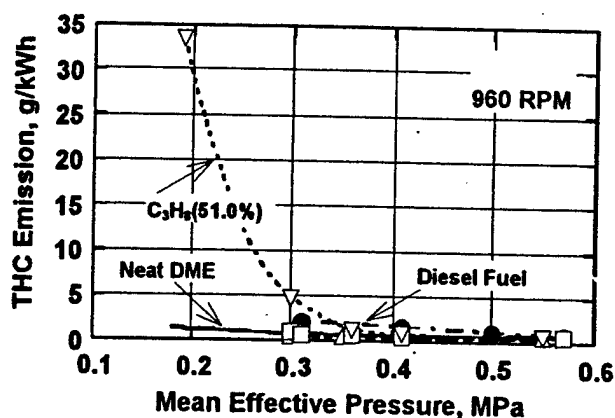


Fig. 16 (a). Total Hydrocarbon Emission.

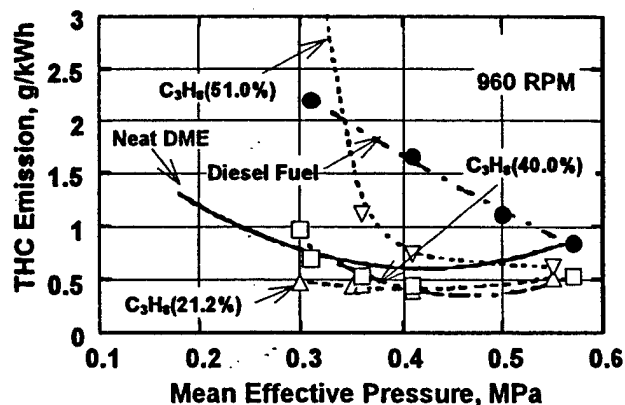


Fig. 16 (b). Total Hydrocarbon Emission.
(Enlarged View of Fig. 16 (a))

that an increased exhaust gas temperature with engine load was expected due to the richer overall fuel/air.)

Exhaust unburned hydrocarbon measurements (THC) are presented in Fig. 16. In general, THC emission is quite low when DME and blends were used in comparison

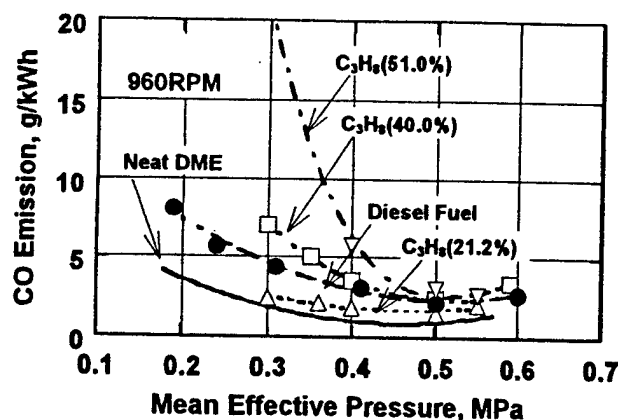


Fig. 17. Carbon Monoxide Emission.

with Diesel fuel. When the measurements with DME and blends were compared with each other, the results with blends produced lower by as much as one half the former.

An obvious deviation from this statement was the engine operation by a blend with 51P, which exhibited extremely high THC emissions when the load was low. Among the more probable reasons for this observation are an over mixing of a portion of propane and a low reaction temperature in the combustion chamber when the load was low. Mentioning the possibility of over mixing, when the propane content is high in a blend, the cetane number becomes relatively low resulting in a prolonged ignition delay. At the same time more propane vaporized leaving the host fuel would mix with air more readily to produce lean mixture pockets beyond flammability (Table-I). If this is the case, the self-ignition flame kernels produced in mixtures in the flammable range would not propagate reaction fronts to the over-mixed lean mixtures.

When the engine load is low, the average gas temperature in the combustion chamber will be so low that the consumption of propane, particularly in the excessively lean mixture pockets, will be sluggish before being wasted in the exhaust and yielding a high THC emission.

These discussions seem to be consistent with the exhaust CO measurement (Fig. 17). When there are pockets of excessively over-mixed propane as considered above, their full oxidation for a timely heat release (while the piston is near the TDC) is not likely to be achieved but instead will undergo incomplete reactions. If this happens, it is not difficult to expect large amounts of CO emission, particularly under light loads. Therefore, the relatively high CO emissions from blend fueled engine operations are considered to have originated from propane instead of DME, which has a relatively low self-ignition temperature and low minimum ignition energy compared with propane (Table-I).

In addition, recall that blend has a wider spray angle than DME (and far wider than Diesel fuel). While the propane expedites vaporization and mixing of the spray is considered to help reduce soot formation, which is advantageous, if its role of dispersion is too excessive, a large amount of THC and CO emission will be inevitable. This is obviously a disadvantage most likely to occur if the engine is operated under light loads. It is expected that this

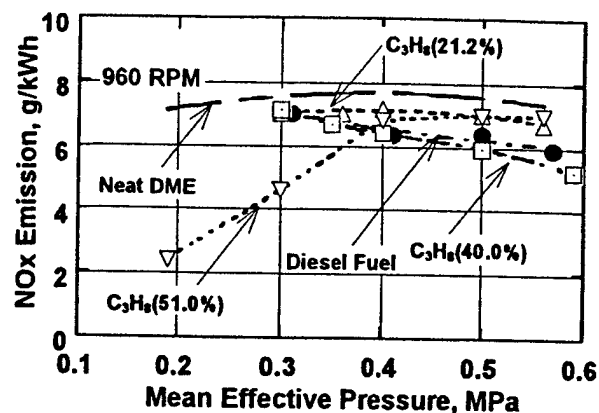


Fig. 18. NOx Emission.

disadvantage also can be eliminated/minimized by means of proper modifications of the engine and injection system.

The emission of NOx is explained next (Fig. 18). In general, DME and its blends produce higher NOx emissions, although they have the advantage of low soot emissions. When the emissions from neat Diesel and DME are compared with each other, the high occurrence of NOx with DME was explained by the early start of combustion resulting in an extended period of NOx formation and more after-compression of combustion products attaining a higher temperature [3]. Regarding the measurements with blends made in the present study, it was found that the higher the propane content the lower the NOx emission. This finding is also consistent with an expectation of increased mixing by propane in a blend when THC and CO emissions were explained. That is, when the mixing of spray is increased, the amount of fuel-rich mixture pockets are expected to be small resulting in low-temperature combustion products in the cylinder, which will reduce the NOx formation. Therefore the finding, which is the higher the propane content, the lower the NOx emission, seems to be reasonable. An equally important consideration for the low NOx with increase of propane content may be a delayed start of ignition with a high propane-content blend (Figs. 8 and 9).

Although the decreased NOx for the blends with an increase of the load may appear to be somewhat puzzling, the specific NOx presented here is considered to be consistent with the same expectation of the mixing effect of propane thinning the mixture pockets. Also, some unique characteristics of spray formation of blends, which had a shorter penetration and a wider spray angle (Fig. 3), might have contributed to the low (specific) NOx formation by blends with a high propane content under high engine loads, which need further study.

Retarded Injection. After completing measurements under a fixed start of fuel injection (at 17bTDC), as present above, a limited experiment was conducted for a delayed injection time, as explained next.

In a typical CI engine, the soot emission may be reduced by advancing the start of fuel injection, but with an increased NOx emission, and vice versa. In a DME (or blend) operated CI engine, this exclusivity does not seem to

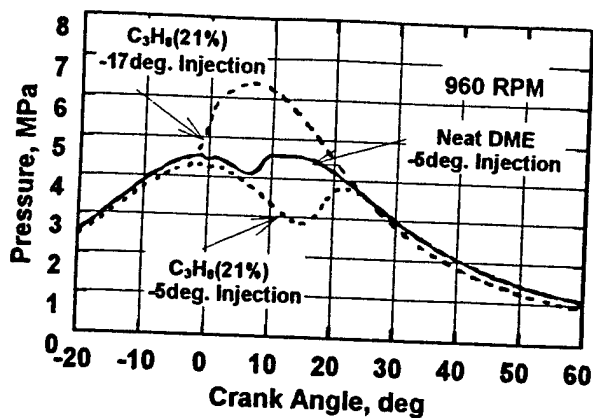


Fig. 19. Cylinder Pressure Histories with Delayed Start of Injection.

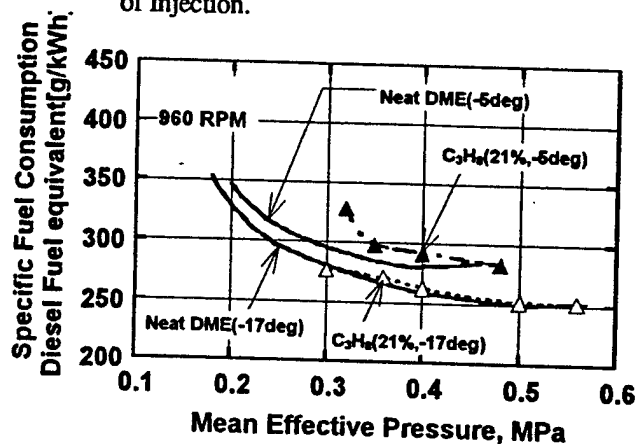


Fig. 20. Comparison of Specific Fuel Consumption with Delayed Start of Injection.

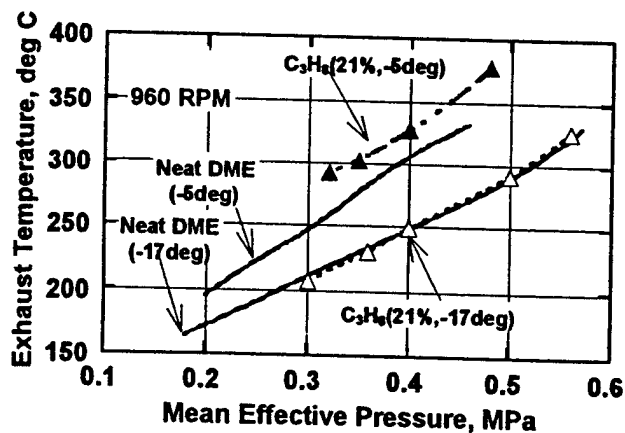


Fig. 21. Exhaust Gas Temperature with Delayed Start of Injection.

hold anymore [3]. This means that a delayed start of fuel injection may be a viable method of reducing NO_x emissions in a DI-CI engine without increasing soot emissions, which was among the reasons for obtaining the present measurements. It is noted that any measure of reducing emissions will acceptable only if the engine

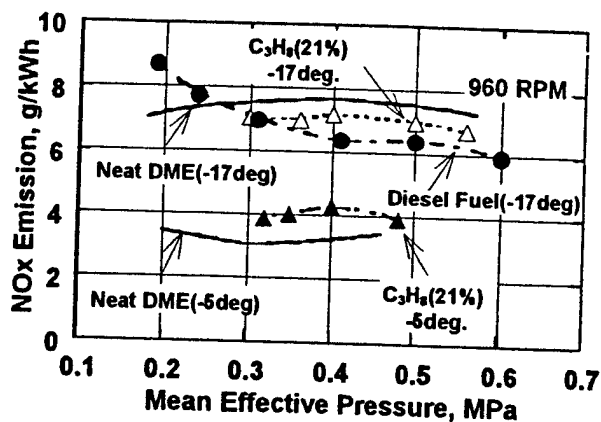


Fig. 22. NO_x Emission with Delayed Start of Injection.

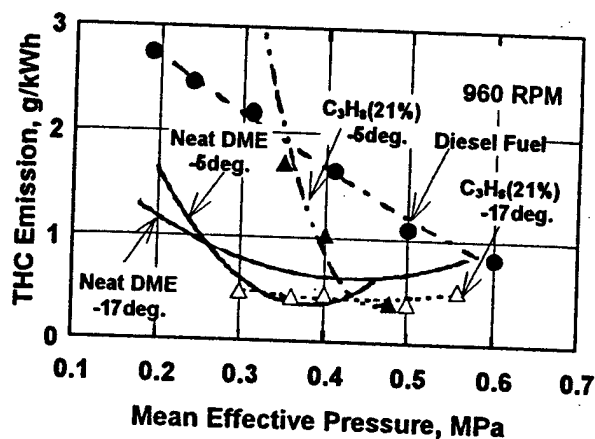


Fig. 23. Total Hydrocarbon Emission with Delayed Start of Injection.

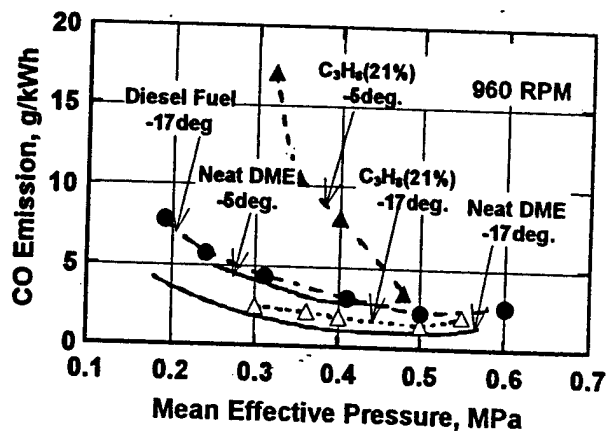


Fig. 24. Carbon Monoxide Emission with Delayed Start of Injection.

performance does not suffer a severe penalty.

In this experiment, a blend with 21P was used, which exhibited highly satisfactory engine operations. Note that because of the limited versatility of the engine employed in the present study, the adjustment of the injection time was in a rather crude scale, namely one notch (teeth) change

between connection gears in the engine and (Bosch) injection pump resulting in a shift from 17bTDC to 5dTDC. Consequently the present measurements were obtained at 5bTDC as shown by p-t diagram and specific fuel consumption (sfc) in Figs. 19 and 20, respectively.

As expected, the sfc was all higher with the retarded injection timing (Fig. 20), which is basically due to a very late start of combustion and results in a poor cycle conversion efficiency (Fig. 19). As expected, the exhaust gas temperature measurements were considerably higher when the injection was retarded (Fig. 21).

The NO_x emissions, on the other hand, achieved some significant reduction by retarding injection (Fig. 22). It is noteworthy that the specific emission did not decrease with the engine load unlike in the previous measurements with a 17bTDC injection. The unburned hydrocarbon emissions (THC) were much higher with 5 bTDC injection than the previous, which suggests that the timing adjustment was excessively retarded. The increase of CO emission with the late injection, however, did not seem to be as significant as in THC emissions.

In spite of the inability of fine adjustment of the injection time with the present apparatus, the results illustrate some meaningful insight as to reduction of NO_x emission from a CI engine operated by DME blends with propane. That is, the emission can be reduced without any penalty of soot emission in a similar way with neat DME. An excessive delay caused some significant increase of THC but some minor change in CO emissions.

As an additional advantage of using DME or blends, it may be noteworthy to point out that since a CI engine can be operated at a rich fuel/air ratio (perhaps even near stoichiometric) without generating excessive amounts of soot emission, a high exhaust gas temperature can be attained. When it is possible, the low-soot-emission fuels are expected to facilitate the use of exhaust gas treatment devices such as a catalytic converter.

CONCLUSION

A new method of operating compression ignition (CI) engines by blends of dimethyl ether (DME) and gaseous fuel(s) is reported. This approach both took advantage of low soot producing DME (also having a high cetane number and a property of easy-mixing with most hydrocarbon fuels) and complemented its disadvantages, particularly of having a low heating value.

In order to demonstrate the feasibility of this new method in a CI engine and to implement a simpler analysis, blends of DME-propane were investigated in the present study and compared with neat DME and Diesel fuel.

The significance of employing the present blending method of DME with a gaseous fuel and findings from the engine experiment are summarized below.

(1) It was necessary to add a lubricant to DME for directly using the existing injection system designed for Diesel fuel.

(2) Although DME can be mixed with most hydrocarbons in any ratio, the upper limit of propane content in the blend was realized when the blend was directly

injected in the same manner as Diesel fuel, which was also affected by the start of injection. Blends with a propane content lower than 40% (mass) exhibited satisfactory engine combustion. However, this limit may be raised by modifying the engine operation and design parameters.

(3) The blend method may be a viable strategy for using widely available inexpensive petroleum gases (with low cetane number) in CI engines without additional cumbersome fuel or ignition system components.

(4) The absorption of propane in DME increased the energy content, which, however, did not increase the complexity of the fuel system needed when DME was used alone.

(5) Some indirect evidence is observed that, when a blend is injected, propane with a higher boiling point than DME vaporized to help expedite mixing in the cylinder, and may even result in over mixing.

(6) Under a fixed injector condition, the higher the propane content in the blend, the later the start of injection and the lower the cetane number, which resulted in a delayed start of combustion.

(7) Within an acceptable operational region, the higher the propane content, the lower the emissions of unburned hydrocarbon and carbon monoxide (also compared with neat DME) under high engine load operations. The emissions were high when the load was low.

(8) The specific emissions of NO_x decreased with the propane content. This is explained by the role of propane in enhancing the mixing, which is considered to reduce rich mixture pockets producing lower-temperature combustion products.

(9) Soot emissions were negligible with blends.

The use of the present low-soot-emission fuels permitting a CI engine to operate at a fuel/air ratio even near the stoichiometric may pave the way for using exhaust gas treatment devices including a catalytic converter.

ACKNOWLEDGMENT

Authors wish to express their appreciation to Mr. Sumitaka Minegishi who assisted the experiment. Ethyl Corp. (Japan) provided a fuel additive. One of the authors (KTR) received support from the US Army Research Office (Contract No. DAAH04-95-1-0430, and DAAH04-96-1-0459).

REFERENCES

1. T. Themel, M. Jansons S. Campbell, and KT Rhee, "Diesel Engine Response to High Fuel-Injection Pressures," SAE Paper-982683, 1998.
2. Non-thermal Plasma, SAE SP-1395, 1998.
3. S. Kajitani, Z. Chen, M. Konno, and KT Rhee, "Engine Performance and Exhaust of Direct-injection Diesel Engine Operated with DME," SAE Paper- 972973, 1997.

4. S. C. Sorenson, and S. E. Mikkelsen, "Performance and Emissions of a 0.273 Liter Direct Injection Diesel Engine Fueled with Neat Dimethyl Ether," SAE Paper-950064, 1995.
5. T. Fleish, C. MacCarthy, A. Basu, C.C. Udovich, P. Charbonneau, W. Slodowske, S. Mikkelsen, and J. McCandless, "A New Clean Diesel Technology: Demonstration of ULEV Emissions on a 1994 Model Diesel Engine using Dimethyl Ether," SAE Paper-950061, 1995.
6. R. Verbeek, R. and J. V. Weide, "Global Assessment of Dimethyl-Ether: Comparison with Other Fuels," SAE Paper-971607, 1997.
7. T. Murayama, N. Miyamoto, T. Yamada, J. Kawashima, and K. Itow, "A Method to Improve the Solubility and Combustion Characteristics of Alcohol-Diesel Fuel Blends," SAE Paper-821113, 1982.
8. J.B. Hansen, B. Voss, F. Joensen, and I. D. Sigurdardottir, "A Large Scale Manufacturing of Dimethyl Ether - A New Alternative Diesel Fuel from Natural Gas," SAE Paper-950063, 1995.
9. M. E. Karpuk, and S. W. Rowley, "On-board Dimethyl Ether generation to Assist Methanol Engine Cold Starting," SAE Paper-88167, 1988.
10. T. Murayama, T. Chikahisha, J. Guo, and M. Miyano, "Study of a Compression Ignition Methanol Engine with Converted Dimethyl Ether as an Ignition Improver," SAE paper-922212, 1992.
11. J. C. McCandless and S. Li, "Development of a Novel Fuel Injection System (NFIS) for Dimethyl Ether-and Other Clean Alternative Fuels," SAE Paper-970220, 1997.
12. R. L. Hoekstra, P. V. Blarigan and N. Mulligan, "NO_x Emission and Efficiency of Hydrogen, Natural Gas, and Hydrogen/Natural Gas Blended Fuels," SAE Paper-961103, 1996.
13. M. S. Newkirk, and E. A. Bass, "Reactivity Comparison of Exhaust from Heavy-Duty Engines Operating on Gasoline, Diesel, and Alternative Fuels," SAE Paper-952442, 1995.
14. M. Alperstain, W. Swim and P. Schweitzer, "Fumigation Kills Smoke," SAE Transactions, vol. 66, 1955, pp 574-595.
15. B. L. Edgar, R. W. Dibble, and D. W. Naegeli, "Autoignition of Dimethyl Ether and Dimethoxy Methane Sprays at High Pressures," SAE Paper-971677, 1997.
16. R. Christense, S. C. Sorenson, M. G. Jensen and K. F. Hansen, "Engine Operation on Dimethyl Ether in a Naturally Aspirated DI Diesel Engine," SAE Paper-971665, 1997.

Diesel Engine Response to High Fuel-Injection Pressures

T. Themel, M. Jansons, S. Campbell, and KT Rhee
Rutgers, The State University of New Jersey
Piscataway, New Jersey

ABSTRACT

A single-cylinder direct-injection (DI) Diesel engine (Cummins 903) equipped with a new laboratory-built electronically controlled high injection pressure fuel unit (HIP) was studied in order to evaluate design strategies for achieving a high power density (HPD) compression ignition (CI) engine.

In performing the present parametric study of engine response to design changes, the HIP was designed to deliver injection pressures variable to over 210 MPa (30,625psi).

Among other parameters investigated for the analysis of the HPD DI-CI engine with an HIP were the air/fuel ratio ranging from 18 to 36, and intake air temperature as high as 205°C (400°F). The high temperatures in the latter were considered in order to evaluate combustion reactions expected in an uncooled (or low-heat-rejection) engine for a HPD, which operates without cooling the cylinder.

Engine measurements from the study include: indicated mean effective pressure, fuel consumption, and smoke emissions.

It was found that a Diesel engine incorporated with an HIP under varied operational conditions, including those encountered in uncooled engine design needs variation of injection parameters, namely the start of injection and the rate shape.

When the engine operating condition shifts, the rapid variation of those parameters are needed in order to optimize the engine power delivery and fuel consumption as well as to minimize smoke emissions.

Other engine responses to the varied parameters in the high-pressure Diesel engine are also reported in the paper.

INTRODUCTION

The Diesel engine, or compression ignition (CI) engine has several advantages over the spark-ignition (SI) engine. It is more efficient, reliable, fire-safe, and environmentally-friendly than the SI engine, and therefore is almost exclusively employed in long-haul heavy-duty trucks and buses, basically the entire US military fleet (safer fuel

and less vulnerable), and merchant marine (lower insurance premium). The engines being used in mining galleries are all CI systems.

A great portion of passenger cars in countries which are trading with the US (in particular Europe and Japan) are powered by CI engines. Since the CI engine is more efficient, it emits less greenhouse gas (CO₂) than a comparable SI engine, a contribution towards the world-wide efforts of minimizing global warming.

The CI engine will be more widely used if it achieves a higher power-density (HPD, horsepower per displacement or weight), cleaner emissions, and quieter operation, goals which have become more sought after and attainable in recent years. For example, consider the two former goals: Better air utilization for a HPD will increase the exhaust gas temperature, which facilitates development of an efficient catalytic converter. Also high air utilization, which has been limited by the smoke emission, has become more feasible through the use of modern electronically-controlled high injection pressure fuel systems (HIP). In addition, the HIP offers a potential for increasing the engine speed, another approach to an HPD.

In developing an HPD CI engine mated with an HIP, however, many design problems will have to be overcome, including a greatly increased engine block temperature (therefore temperatures of intake air, fuel and lubricating oil). The increase will undoubtedly affect processes of CI combustion, notably the preflame reactions and onset of self-ignition, as well as the subsequent heat release and pollutant formation. The impacts on the processes would be more unpredictable when operated at high speeds.

When the methodology of the uncooled CI engine is incorporated in a HPD, which eliminates parasitic components (e.g. the water pump and radiator) as well as the water jacket, the engine power density will further increase. However, the many problems including those mentioned above will undoubtedly become more difficult to solve. In spite of such difficulties, development of an uncooled HPD CI with an HIP operated at high speeds is a great challenge worthy to strive for because it offers a new dimension of opportunity for engine technology advancements and usefulness.

Realizing the need for analysis of the engine response to an HIP, which is expected to alter various in-cylinder reactions as mentioned above, a new study was initiated towards a goal of HPD by the uncooled direct injection (DI) CI engine methodology. Since no such HPD engine is widely used at present, a more reasonable approach was to employ an experimental apparatus representing a real-world DI-CI mated with an HIP operated under varied thermal conditions. This was because the existing DI-CI reciprocating engine is considered to be the system basis employed for the goal of the new HPD engine. Results from the study, thus, were expected to help construct a more useful road-map to the development of an HPD CI engine. The study was also directed to assessing the new engine concept and whether it would satisfy regulatory as well as user requirements.

EXPERIMENTAL

When a DI-CI engine with an HIP is operated at high speeds in order to achieve a HPD, the heat release per displacement will become closer to that in a typical SI engine. This will greatly increase the overall engine temperature, which will affect the in-cylinder reactions to become presumably very different from those in the conventional DI-CI engine. In order to closely investigate the processes, the engine apparatus was constructed to offer engine combustion environments representing as closely as possible those in an HPD DI-CI engine, which is discussed next.

Engine. A Cummins 903 engine (V-8) was utilized to make a unit of V-2 apparatus, a saw-off of a quarter of the original engine, which then was modified to operate only one cylinder and to have the remaining cylinder-piston reciprocate without compression in order to help achieve dynamic balancing. The engine has a bore-stroke of 140-121 mm (displacement of 1.85 liters) and compression ratio of 13.5 to 1. Since the same family of 903 engine has been widely used in the past, no additional discussion on the engine dimensions is made here.

This single-cylinder engine was installed with a new intake-air (electric) heating unit which can increase the air temperature as high as 205°C (400°F) at high speeds, because such a high intake air temperature was expected in an uncooled engine whose combustion reactions were to be also studied. The air was supplied from the building via a pressure controller (maintained at 30.9 KPa or 4.5 psi and higher depending upon the intake air temperature as explained later) and a flow metering unit. The engine cooling was done by using a closed-flow unit (with glycol as coolant) connected to a water-cooled heat exchanger for temperature control. The unit was designed to accommodate a coolant temperature as high as 149°C or 300°F.

The apparatus lined up with an electric dynamometer was sufficiently instrumented in order to implement the objective of the study, including an in-cylinder pressure transducer, temperature probes, and a smoke meter.

High Injection Pressure Fuel System (HIP). Since high utilization of the intake air is an important

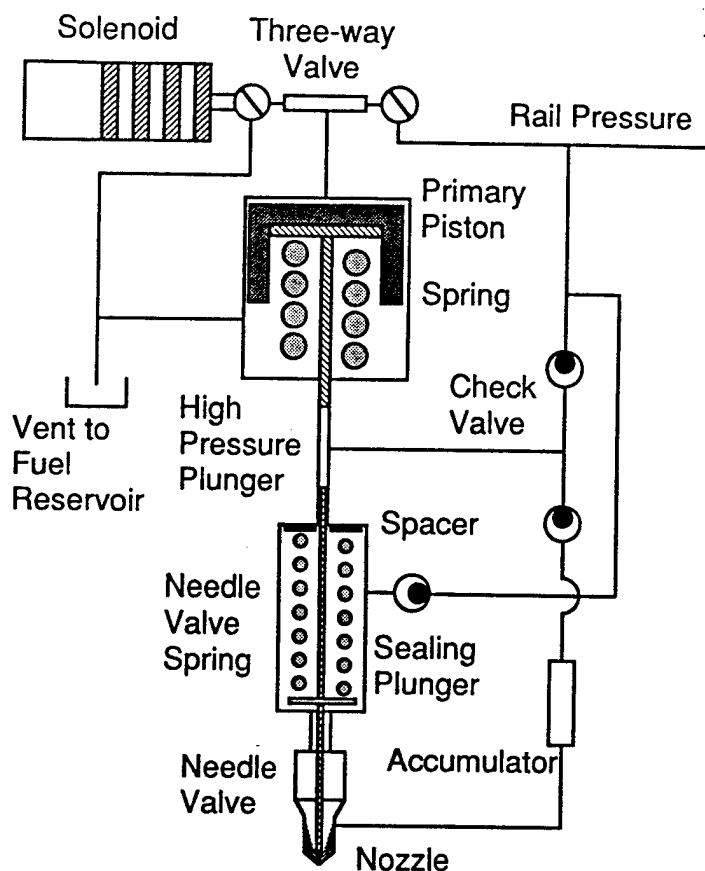


Fig. 1. Laboratory-built Electronically Controlled High Injection Pressure (HIP) Fuel Unit.

precondition for achieving an HPD DI-CI engine, which is facilitated by an HIP, a considerable amount of design and development work on a new HIP was a logical step taken in the present study. Note that for earlier studies, a laboratory-built HIP which delivered an injection pressure of up to 165 MPa (24,000psi) was employed [1-3]*, which offered the basic expertise toward the new design-construction of an improved HIP, which is explained in the following.

In developing and characterizing an HIP unit, one of the more uncertain issues associated with the system performance is the actual injection pressure that a unit can deliver. For example, in a common-rail type HIP, the pressure at the accumulator does not represent the injection pressure at the nozzle tip due to pressure drop expected to occur between the two locations. The pressure intensifier type HIP to be discussed next, however, is considered to be more apprehensive on the issue, that is it generates the injection pressure closer to the nominal value.

A schematic drawing of our new HIP is shown in Fig. 1, and was basically the same design as BKM's Servo-jet type [4]. It is a "pressure intensifier type" having a primary piston where a variable low pressure fuel (as high as 12 MPa or 1,750 psi in this) is connected via a three-way

*Numbers in parentheses designate references at end of paper.

valve at a position as shown in the drawing. The fuel trapped in the lower side of the primary piston and accumulator is compressed by the factor of the area ratio (17.5 for the present design) between the piston and plunger. Since the needle valve is under the same high pressure, no fuel escapes through the nozzle at this time. When the injection is to be made, the three-way valve is switched to a valve position 90 degrees clock-wise from that shown in the figure. This will abruptly relieve the pressure on the upper portion of the primary piston by draining the fluid to the vent reservoir. The subsequent pressure imbalance across the sealing plunger, then, lifts the needle to spill the fuel at a high pressure into the combustion chamber.

The present unit was designed/fabricated in such a way as to directly engage it with the low-pressure fuel supply port in the Cummins 908 engine cylinder head, which was not possible in the factory-delivered Servo-jet unit. That is, the original stock PT-type injector in the engine was simply replaced by the newly designed unit with no additional modification of the head. This resulted in a unit with the same external dimensions as the PT injector. This consideration suggested a direct use of, in the new unit, both a nozzle tip holder and the nozzle tip as well as the o-ring from the PT injector.

By taking the high pressure fuel injection into consideration, which will produce high injection rates, a stock nozzle tip having the smallest nozzle hole diameter (0.15mm) available to us was incorporated in the new unit. (This measure was also meaningful for flexibility and economic reasons.) In designing the new unit, however, a computational analysis indicated that the nozzle tip holder in the existing PT-nozzle was not made sufficiently strong to withstand the high-pressure generated by the present intensifier. Consequently, all of the components in the unit were newly fabricated in our laboratory except for the three-way solenoid valve and the abovementioned nozzle-tip.

Regarding the pressure at the nozzle tip before the injection, recall the dead-weight type calibration-device for testing pressure gages, which utilizes a similar concept as the present unit does. Except for the dynamic and transient nature of the performance in the present unit, the injection pressure at the opening of the nozzle, thus, is considered to closely represent the nominal pressure determined by the (low) rail pressure and the area ratio mentioned above. Although the physical concept of the dead-weight device employed in the unit is perceptive, it would be desirable if the pressure-time history at the tip would have been determined for backing up this expectation, however.

The control of the injection pressure, therefore, was made by adjusting the fuel rail pressure from a gear-pump. On the other hand, the amount of fuel injected by the new unit was controlled by the thickness of a spacer placed at the upper end of the needle valve spring. The purpose of using the spacer was to vary the cut-off pressure of fuel injection. That is, the thicker the spacer, the stronger the preload of the spring and the earlier closing of the needle valve. Note that the cut-off pressure without any spacer was adjusted at approximately 61 MPa (10,000 psi). For varied amounts of fuel injection, the unit opens the needle valve at the same time, but closes it sooner for a smaller amount of fuel injected but at a higher cut-off pressure.

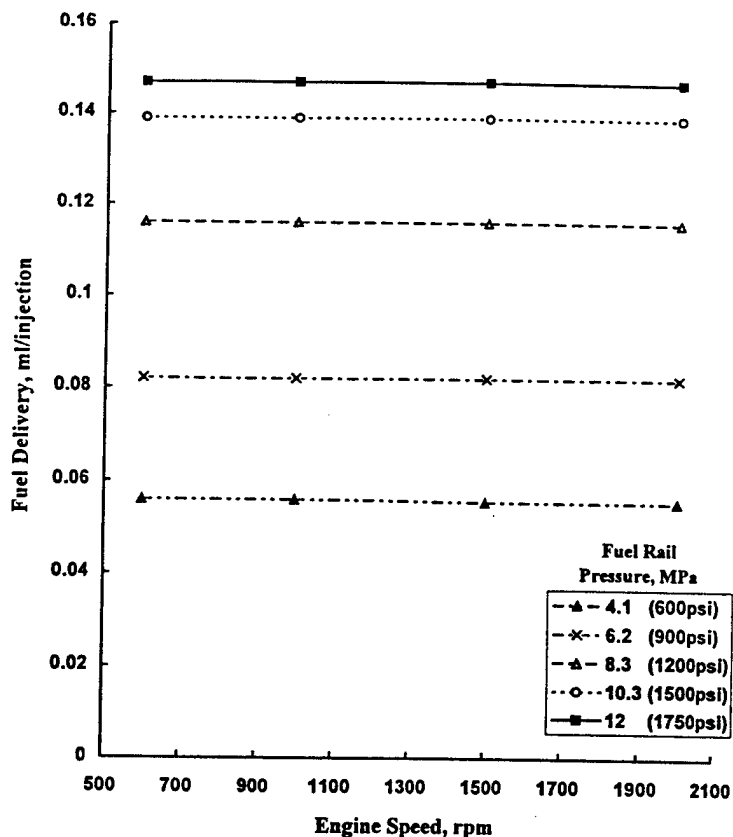


Fig. 2. Relationship of Fuel Delivery to Engine Speed and Fuel Rail Pressure (Spacer thickness, 0.76 mm).

Characterization of HIP. After completing construction of the new unit, an extensive system characterization was performed using a bench-top test device. The injection time was determined by placing a pressure transducer at a location approximately 10 mm away from the nozzle hole while the period of energizing the three-way valve was varied. This determines the period of connection between the rail pressure and the primary piston. The timing of the pressure transducer signal was compared with the end of the energizer period when the needle was expected to rapidly lift up.

Figure 2 shows the relationship of the amount of fuel delivery to the engine speed for varied rail pressure. The result exhibits a predictable performance of the new unit, a trend which was the same for all spacer thicknesses employed in the experiment. Note that the rail pressure represents the injection pressure determined by the intensifier (area) ratio, that is 17.5. For example, the rail pressure of 12 MPa corresponds to an injection pressure of 210 MPa (30,625 psi) at the nozzle opening.

Results obtained using all of the spacers were combined to plot Fig. 3, which facilitated determination of the amount of fuel delivery. As expected for a given spacer thickness, the higher the rail pressure the greater the amount of fuel delivered. The results shown in the figure for variation of spacer thickness and rail pressure were employed for the range of the present parametric study of the

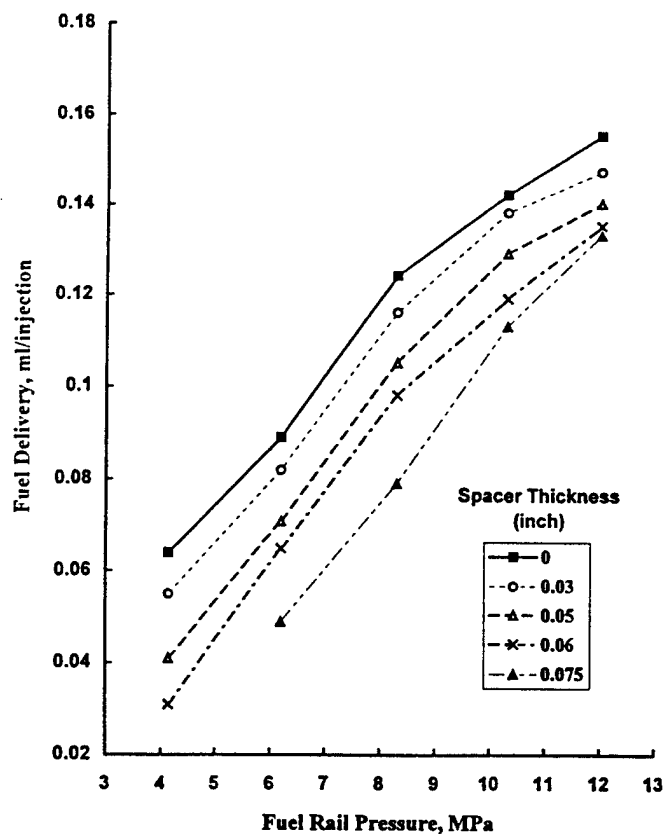


Fig. 3. Fuel Delivery Affected by Rail Pressure and Spacer Thickness.

HPD CI-DI engine with HPI. For example, the mass of air flow into the engine was compared with the fuel delivery from this plot in order to determine the overall air-fuel ratio for each engine running condition.

RESULTS AND DISCUSSION

The experiment was conducted in two steps. At first, the engine equipped with the new HIP was operated by varying injection time for different intake air temperatures as listed in Fig. 4. This was done at 1,000 rpm speed and 210 MPa injection pressure (by having rail pressure of 12 MPa). Measurements shown in Fig. 4 suggested that the start of injection at 10 degrees of crank angle (CA) before the top-dead-center (bTDC) was proper for the experiment. Therefore, the first part of the experiment was performed at this fixed injection time.

The analysis of the large amount of engine measurements accumulated in the above experiment, however, indicated that the fixed injection timing for a wide range of engine variation was improper as explained later. Consequently, the same engine experiment was performed at varied injection times producing the best-torque under the respective operating conditions, the second step of the experiment which was not planned in the beginning.

Explaining the results, the indicated mean effective pressure (IMEP) determined from the pressure-time data are

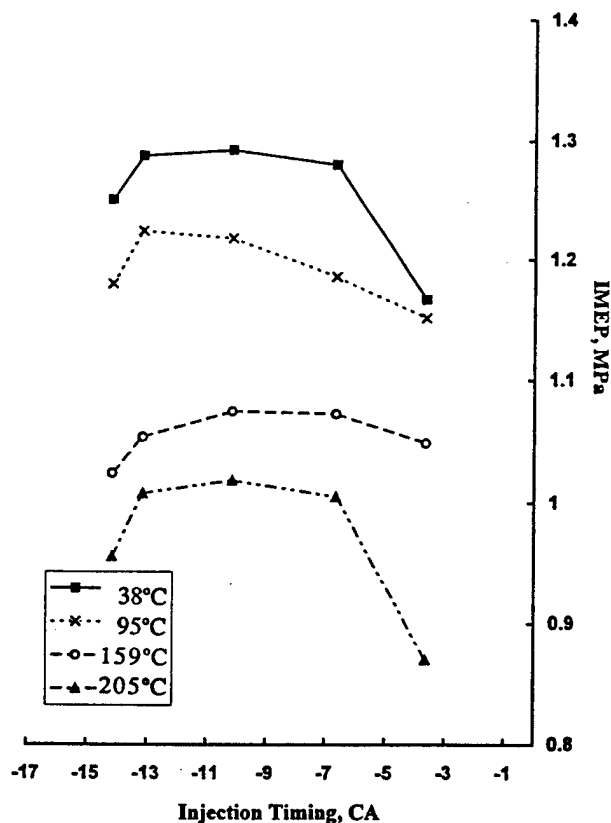


Fig. 4. IMEP for Varied Injection Timing and Intake Air Temperature (1000rpm, Rail Pressure 12Mpa).

shown in Fig. 5 for varied engine conditions as noted by individual symbols. The family of curves obtained for fuel injection pressures in MPa of 210 (30,625 psi), 180 (26,250 psi), and 144 (21,000 psi) is included, respectively. The overall results exhibit a trend as expected, which is the lower the air/fuel ratio, the higher the IMEP. The engine speed did not appear to significantly affect the results for the range of investigation in the study, which is further discussed below. Most notably, it was possible to run the engine as rich as 18 to 1 air/fuel ratio while the smoke emission was no worse than that observed with the conventional PT injector operated at leaner overall ratios of 35 to 1.

The increase of IMEP achieved in the present CI-HIP engine by better utilization of the trapped air, which increased by a factor of almost two compared with the conventional engine, is highly promising in paving the way to designing an HPD engine. It is pointed out that the generation of high injection pressures requires an increased consumption of the power from the host engine, which will deteriorate the specific fuel consumption, as further discussed later. Nevertheless, the present results by the use of an HIP seemed to shed some strong light into a possibility of operating a CI engine at richer air/fuel ratios, which are more closer to the stoichiometric.

Although no attempt was made to measure engine noise in the study, it is pointed out that noise became higher when the engine was operated overall rich, i.e., as it came closer to the stoichiometric. Expecting that the elimination

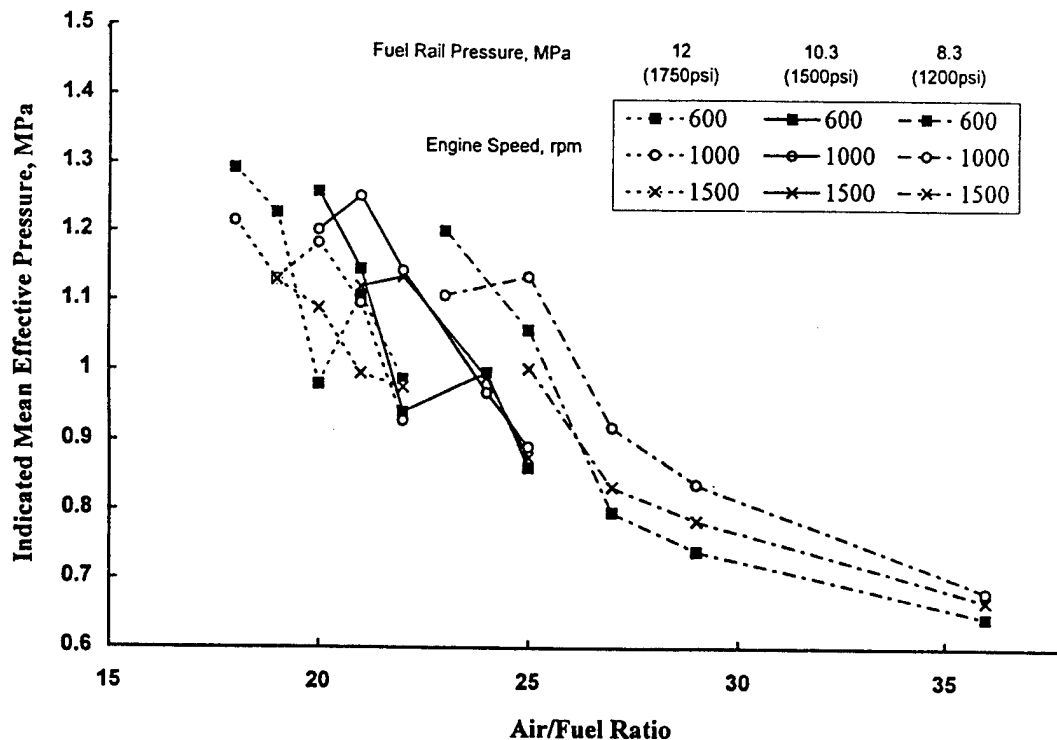


Fig. 5. Indicated Mean Effective Pressure (IMEP) as a Function of Air/fuel Ratio (all engine speeds at Intake Air Temperature 38°C and Injection Timing of 10 BTDC).

of exhaust NO_x emission by a catalytic converter would be facilitated when the exhaust gas temperature greatly increases via a high air utilization, no attempt was made to measure its emissions. To support this consideration, it is noted that the exhaust temperature ranged between 360-416° C (680-780° F) when the engine ran at air/fuel ratios of 30-20 to 1.

Recalling Fig. 3, since for a given thickness of the spacer, the higher the rail pressure (thus the injection pressure) the greater the amount of fuel flow through the nozzle, the IMEP increased with the rail pressure (Fig. 6). This trend was similarly found for other intake air temperatures. As briefly mentioned above, the speed effect on the measurement was small except that it appeared to peak at 1000 rpm, the same speed employed for determining the (optimum) injection time (Fig. 4). An additional discussion is made later on the need for varied injection time as related to this observation.

Intake Air Temperature. The measurements explained above were obtained for intake air temperatures (°C) at 38, 95, 150, and 205, respectively. Figures 7-10 were plotted for comparison purpose of intake temperature effects on IMEP for varied overall air/fuel ratios and injection pressures. Although the observation of a higher IMEP by a richer air/fuel ratio was expected, its great deterioration at higher intake air temperature was a surprise. Since the fuel system was adjusted to deliver a fixed amount of fuel according to the bench-top calibration (Fig. 3), the intake pressure was increased to compensate the deterioration of volumetric efficiency with increase of the air temperature. It is reminded that the measurements were obtained for high

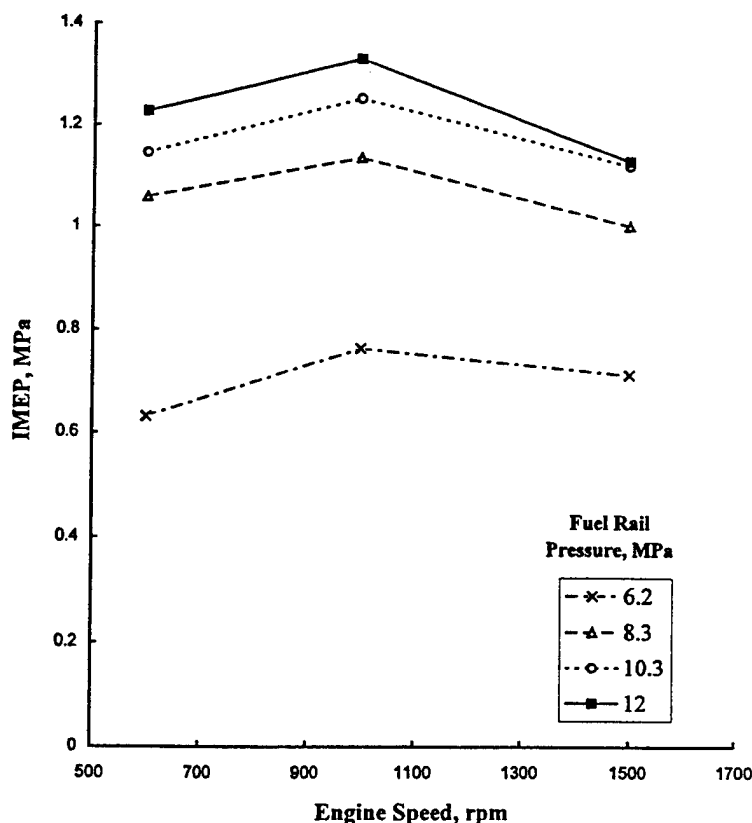


Fig. 6. IMEP as a Function of Injection Pressure (Spacer, 0.76mm). Intake Air Temperature, 38°C.

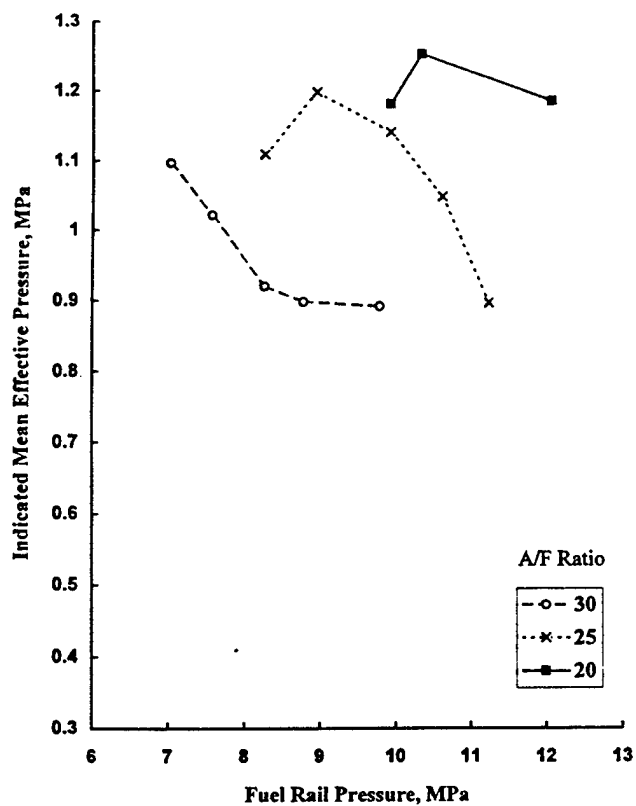


Fig. 7

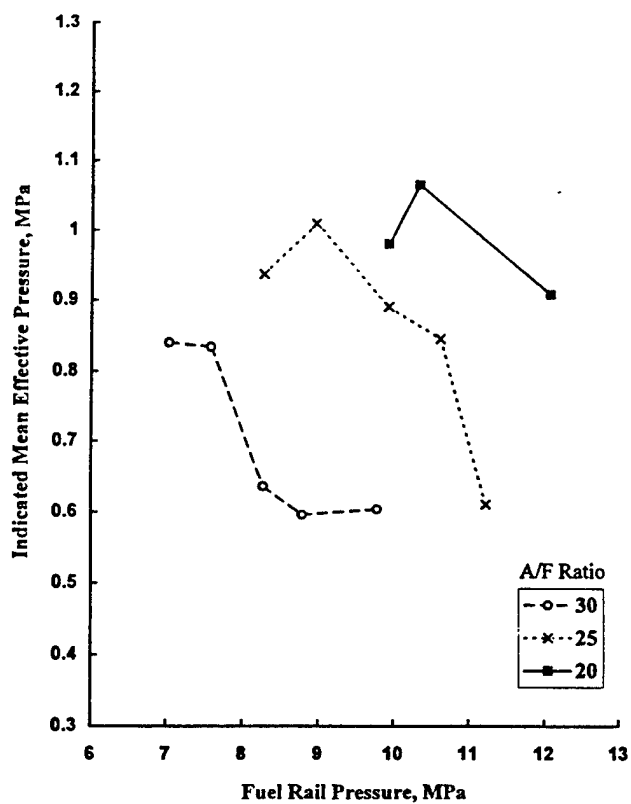


Fig. 9

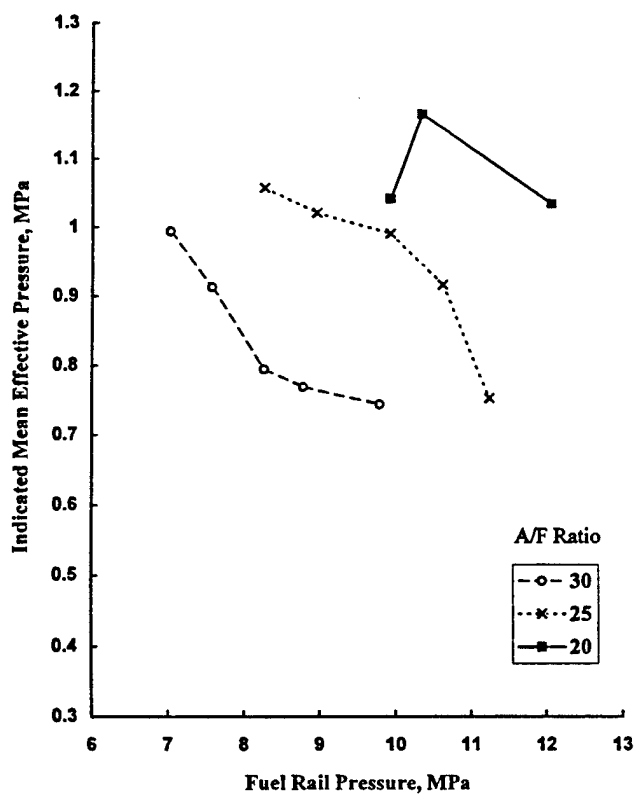


Fig. 8

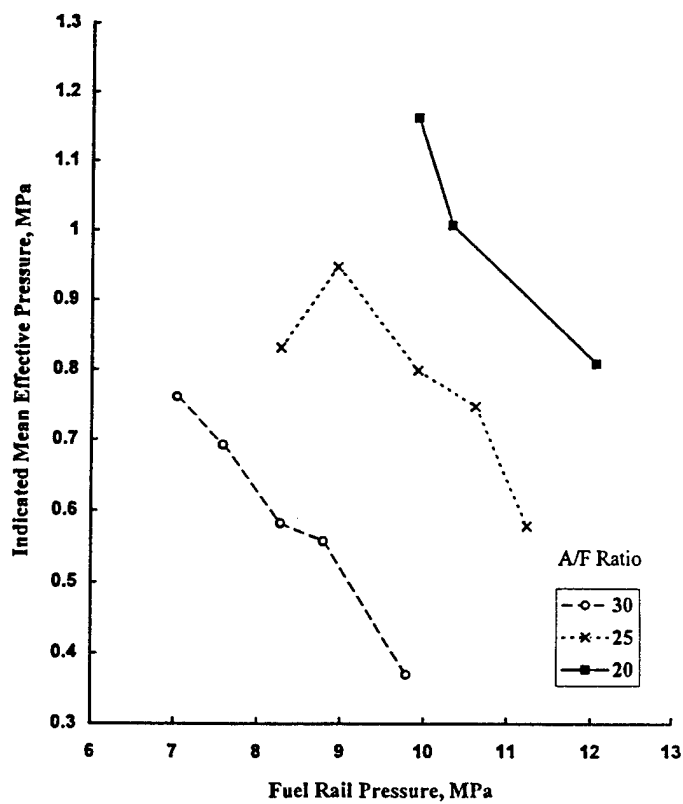


Fig. 10

Figs. 7-10. Indicated Mean Effective Pressure (IMEP) as a Function of Air/fuel Ratio and Rail Pressure for Varied Intake Air Temperatures (T_a): Fig. 7, $T_a = 38^\circ\text{C}$; Fig. 8, $T_a = 95^\circ\text{C}$; Fig. 9, $T_a = 150^\circ\text{C}$; Fig. 10, $T_a = 205^\circ\text{C}$.

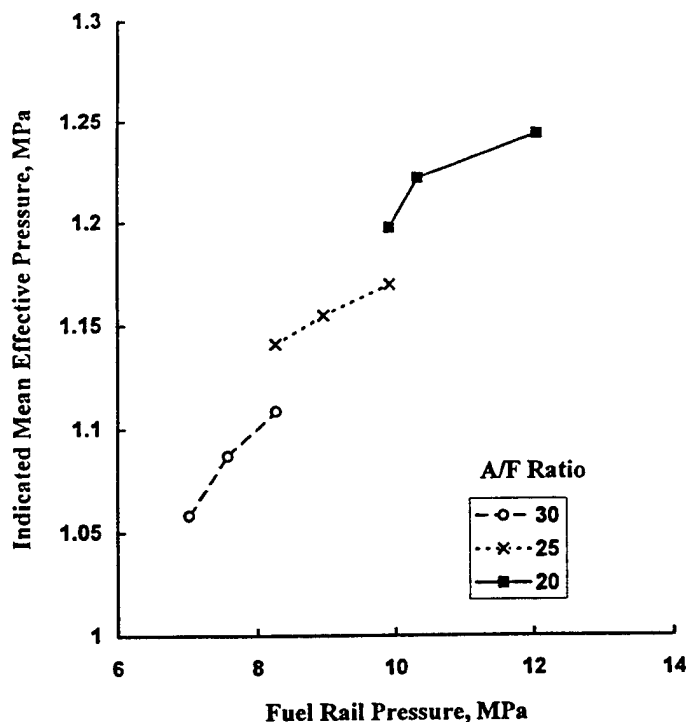


Fig. 11. Indicated Mean Effective Pressure as a Function of Fuel Rail Pressure (1000rpm, 38°C Intake Air Temperature) for Variable Injection Timing.

temperatures of the intake air in order to assess the engine response when the uncooled (low heat-rejection) design is incorporated, which would have a high engine-block temperature resulting in the intake air heating.

Several reasons for the significantly decreased IMEP with increased intake air temperature may be considered. First of all, since the ignition delay (ID) would decrease with the temperature, a fixed injection time (and even the rate shape) should have been shifted for an optimum power torque output. Next, a decreased ID will result in a smaller amount of heat release from the premixed combustion stage (and thus an increased amount of heat release via the diffusion-controlled combustion) to cause a deteriorated cycle efficiency. Note that when these happen, the formation of soot, in general, is expected to increase, which in fact was the exact observation in the experiment. While such a deterioration of combustion and energy conversion efficiency is considered, recall Fig. 3 showing the calibration results determining fuel flow rate obtained at room temperature using a bench-top apparatus. Those measurements, however, may not be repeated when the intake temperature was increased, because of a probable decrease in the flow rate with increase of the temperature. If this is the case, a decreased IMEP is expected to occur, which needs further investigation.

Also, what was most unexpected was the somewhat decreasing trend of IMEP with increase of the rail pressure (thus the injection pressure), which was contrary to an

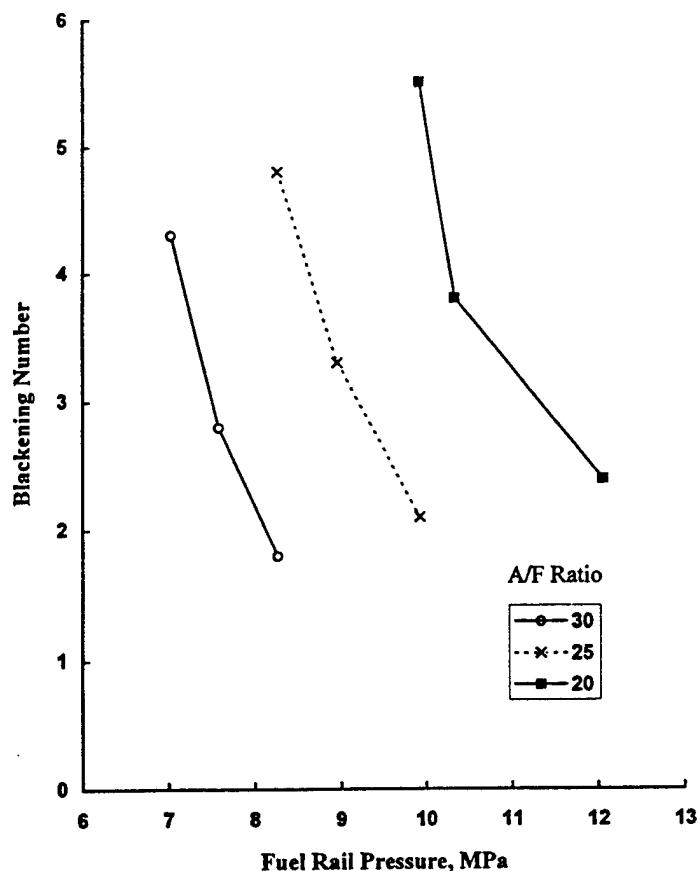


Fig. 12. Smoke Emission, Bosch Blackening Number as Function of Fuel Rail Pressure and Air/fuel Ratio.

expectation that combustion would improve when a "better" fuel spray is achieved by an HIP. The decreasing trend was found in *all* temperatures of intake air and air/fuel ratios. Reviewing the measurements, it came to examine the effect of the injection time, which was tested in the beginning and set at 10 bTDC for the experiment (Fig. 4). This was because when the injection pressure was varied, the change in ignition delay was considered to be altered enough to affect the energy conversion efficiency. Note that the need for shifting the injection time is unusual in the conventional CI-DI engines equipped with a mechanical injection unit, which mostly maintain the injection time at a fixed CA.

Figure 11 shows the results obtained in a similar measurement performed as above by varying the injection time that produces the best torque for each engine condition especially at respective injection pressures. The overall trend was quite the same at other intake air temperatures, which indicates an obvious need for adjusting the engine fuel system to deliver a new injection time in order to obtain the best IMEP. This observation led us to recall the adjustment of ignition time in the SI engine under different engine conditions.

Since an HPD from a CI engine is meaningful if the exhaust smoke emission is acceptably low, its measurement was conducted (using a Bosch smoke meter) and the results are plotted in Fig. 12. As expected the higher the injection

pressure, the lower the smoke emission. When the injection pressure was at 210 MPa, the measurement with air/fuel ratio of 20 was almost as low as that obtained for air/fuel ratio of 30 (injection pressure of 145 MPa, or 21,000 psi). The result suggests that an additional reduction is possible if the injection pressure is further increased in all air/fuel ratios investigated. It is reminded that these measurements were much lower than those observed in the same engine with the (low-pressure) conventional PT injector.

A HIGH-POWER-DENSITY CI ENGINE

The present study was directed towards investigation of some engine design strategies to achieve an HPD DI-CI engine, in particular when the engine is equipped with ceramic components for uncooled operations. Several issues may be discussed in consideration of achieving the goal.

An increased air utilization appears to be highly promising by the use of an HIP as demonstrated in the present study. It was possible to operate an engine having an injection pressure of 210 MPa by using an HIP at air-fuel ratio as high as 18-1 to produce smoke emissions comparable or lower than those from a DI-CI engine equipped with a conventional low pressure injection unit. The high air utilization, however, resulted in several consequences, including high engine block and exhaust temperatures, and increased noise. Note that the temperatures will become higher when an uncooled engine design approach is employed, whose impacts on the goal of developing an HIP are in need of discussion.

Most of all, the volumetric efficiency will greatly deteriorate, in an uncooled high air-utilization engine, to cause a low mean effective pressure as studied in the present work. The use of a high performance turbocharger or supercharge, therefore, may become a precondition for an HPD uncooled engine, which also may have to use inter-cooling. In addition, the high engine temperature will undoubtedly increase the injector as well as the fuel temperature. The results obtained in the present study suggest it is probable that the fuel flow rate out of the injector may be affected with the injector temperature. When there is no positive remedy for this, the fuel would attain super critical temperatures. This then will modify the spray formation, affect the lubrication of the injector itself and even damage the nozzle holes by cavitation in the fuel stream.

The high exhaust gas temperature, on the other hand, may be a useful ingredient for achieving an HDP engine by facilitating the incorporation of a turbocharger in the engine. Also, the high exhaust temperature may offer an opportunity for using an exhaust catalytic converter to produce a cleaner emission, which then may make it possible to further increase the air utilization.

The development strategies of an uncooled HDP DI-CI engine using ceramic components is certainly a great challenge involving various technical problems as briefly discussed above. There is no question that they would not be easy to surmount, but they offer an exciting opportunity for advancing the engine technology.

ACKNOWLEDGMENT

The present work has been performed under the sponsorship of the U.S. Army Research Office (Contract No. DAAH04-95-1-0430, and DAAH04-96-1-0459).

REFERENCES

1. Clasen, E., Campbell, S., and Rhee, K.T., "Spectral IR Images of Direct Injection Diesel Engine Combustion with High Pressure Fuel Injection," SAE Paper-950605, 1995.
2. Clasen, E., Song, K., Campbell, S., and Rhee, K.T., "Fuel Effects on Diesel Combustion Processes," SAE Paper-962066, 1996.
3. Chang, C., Clasen, E., Song, K., Campbell, S., Jiang, H., Rhee, K.T., "Quantitative Imaging of In-cylinder Processes by Multispectral Methods," SAE Paper-970872, 1997.
4. Abata, D., Stroia, B.J., Beck, N.J., and Roach, A.R., "Diesel Engine Flame Photographs with High Pressure Injection," SAE Paper-880298, 1988.

Engine Performance and Exhaust Characteristics of Direct-injection Diesel Engine Operated with DME

S. Kajitani, Z. L. Chen, M. Konno
Ibaraki University
Hitachi, Japan

KT Rhee
Rutgers, The State University of New Jersey
Piscataway, New Jersey

ABSTRACT

Neat dimethyl ether (DME), as an alternative fuel candidate for Diesel engines, was investigated by measuring primarily engine performance and exhaust gas characteristics. In addition, other responses of the engine to the new fuel were also determined at the same time, including the injector needle lift and heat release. The engine measurements with this fuel were compared with those obtained by using conventional Diesel fuel.

Findings from the present work include: (1) It was necessary to add a small amount of lubricating additives to DME, if a conventional fuel injection system is employed. This was to achieve satisfactory injector performance and to minimize some excessive wear. (2) Engine performance for both fuels was basically comparable to each other, except for a better energy conversion efficiency with DME. (3) In the DME-operated engine, emissions of soot and unburned hydrocarbon (THC) were almost negligible, but NO_x emission was about the same as in the Diesel oil operation. (4) The reduction of NO_x emission by delaying the injection time was highly significant with DME.

INTRODUCTION

Since it is a derivative of methanol and also can be made from natural gas, both of which are known to be low-emission fuels in Diesel engines [1,2]*, DME was expected to deliver some similar emission characteristics. Importantly, the fuel has an advantage of better self-ignition characteristics, which has motivated recent interest in evaluating its wide use for Diesel engines.

In addition to oxygen contained in the molecule, the absence of a direct C-C bond in DME ($\text{CH}_3\text{-O-CH}_3$) is responsible for better spray combustion resulting in low soot emissions, which has been a formidable task to achieve in

Diesel fuel operated compression-ignition engines. The emissions of other pollutants, however, are difficult to predict, but they were expected to be no worse than those with conventional Diesel fuel (or gas oil). Because of its low self-ignition temperature (235°C), DME was employed as an ignition improver when the use of methanol in Diesel engines was explored [3-5], which advantage lacks in such fuels that produce low soot emissions.

In spite of these seemingly favorable characteristics, other responses of direct-injection (DI) Diesel engines to this new fuel were examined for acceptability [6-9]. For example, in view of a high elastic modulus of DME compared with Diesel fuel, which is further discussed later, the needle lift of the conventional injector was expected to shift when it is operated by the new fuel. If it shifts even by a few crank angle degrees, the subsequent combustion processes will be remarkably altered, which will affect not only the engine performances but also the emissions. An in-depth understanding of such unpredictable engine behaviors is not only of academic interest but also a important precondition for a successful application of this new fuel in Diesel engines.

One of most serious problems faced in the use of DME in DI Diesel engines was that due to its low lubricity, when delivered via the conventional (Diesel oil) injection system, sever wears resulted to cause excessive leaks in the injection system [7]. Without a new injection system developed for using this alternative fuel, which is not a simple task to implement [10], it seemed to be more reasonable to modify the fuel by increasing the lubricity. This was taken into consideration in the present study.

Reviewing more the negative side of this fuel, it has a high vapor pressure under the normal operating

*Numbers in parentheses designate references at end of paper.

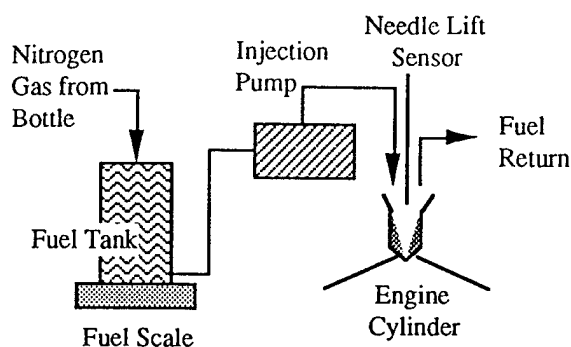


Fig. 1. Fuel System for Supplying DME to the Engine.

environment [11] so that it was necessary to take some special measures in the fuel handling and fuel delivery system of the engine. Even if this fuel in DI Diesel engines produces a satisfactory performance and low emissions, the problems associated with the high vapor pressure are expected to remain important to overcome when DME is used as an alternative fuel in Diesel engines. The relatively low fire hazard with the use of gas oil in Diesel engines, which is an important advantage in military and marine applications, is not likely to be expected when DME is widely used.

The low energy content of the fuel compared with gas oil may be a problem also, which would require about twice as frequent fuel fillings as compared with Diesel fuel for a comparable vehicle. Such problems, however, would not be more severe than those encountered in the use of methanol or natural gas, which have seriously been considered as an alternative fuel in Diesel engines, a measure investigated in order to achieve vehicles with ultra low emissions.

EXPERIMENT

Engine and Apparatus. Because it is important to investigate the responses of real-world engines when a new fuel is used in place of the conventional Diesel fuel, a commercial engine was directly used in the present study with a minimum modification. The engine employed in the study, therefore, was a DI Diesel engine manufactured by Yammer Diesel Corporation having dimensions as shown in Table-I. Since the engine is a typical DI unit with a Bosch-type fuel injector, for which specifications are also listed in Table-I, no additional elaboration of the engine is made here.

Table-I Engine Specifications

Bore x Stroke	92 x 96mm
Displacement	638cm ³
Compression Ratio	17.7
Rated Output	15.6kW/cylinder-2600rpm
Injection Pump, Plunger	8mm dia. (Bosch type)
Injector, Four-hole Nozzle	0.26mm hole dia.

As pointed out earlier, however, since the fuel has a high vapor pressure in the laboratory environment, the fuel system was pressurized by nitrogen gas (from a bottle) in order to prevent leaks and vapor-lock from occurring in the fuel system. Figure 1 shows a schematic presentation of this arrangement having a scale for determining fuel consumption during the engine operation.

The engine apparatus was instrumented sufficiently for implementing the objective of the study, including installation of a needle lift sensor (in the injector), a pressure transducer and interfacing the engine with emission measurement devices. Since these equipment are widely used in the field, no further discussion is added here.

The experiment was conducted for DME by obtaining engine performance and emission characteristics as well as monitoring other engine responses by comparing the same obtained by using (pump-grade) conventional Diesel fuel.

Upon reviewing various methods employed in previous studies [7-11], in most of the experiments in the present work, the fuel tank was pressurized at 3.43MPa (35kgf/cm²) when DME was used, which was therefore the inlet fuel pressure to the injection pump. In DME operations, the injection nozzle opening pressure was set at 8.82MPa (90kg/cm²) when the engine ran at 960rpm, which was chosen about the same as a previous study [7], for a mutual comparison purpose. Note that the recommended opening pressure of the engine for Diesel fuel, on the other hand, was 20.1MPa (205kg/cm²).

Fuel Additive. In the very beginning of the study, in order to investigate how serious negative impacts would occur to the engine, particularly in the injection system by the use of straight DME, the engine apparatus was operated without any change to the new fuel. The engine ran quite smoothly for a period of about 30 minutes from the start, but thereafter some unstable changes in speed and load were observed. This was soon followed by a severe stall leading to stop, and then it was no longer possible to start the engine. A careful inspection of the engine revealed serious wear on the needle of the injector nozzle, and a rather remarkable amount of scoring on the injector plunger as shown in Fig. 2.

From this initial engine testing with the new fuel, it became obvious that no meaningful study could be performed for straight DME in a Diesel engine unless some modification is made on the fuel. After some trial-and-error fuel-engine operation, it was found that an addition of Hitec560 (provided by Ethyl Japan Corp.) in portion of 100ppm to DME did not exhibit any detectable wear in the fuel system, at least for a period in completing the present experiment. Although this additive might have altered both the combustion and emission characteristics somewhat, it was a very minimum measure required to achieve an acceptable engine performance.

RESULTS AND DISCUSSION

The results from the work are presented in graphical form in Figs. 3-22, where the solid lines, in most

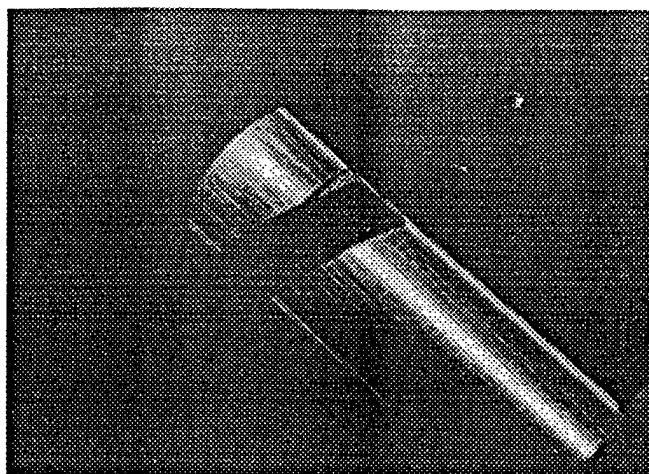


Fig. 2. Photograph of Injector Exhibiting Severe Wear after Used with DME.

cases, represent measurements with DME, and dotted lines indicate those with the conventional pump-grade Diesel oil. In spite of the increased lubricity of DME by the additive, in order to eliminate any possible artifact of injector wear on the spray formation, the nozzle needle was frequently replaced throughout the experiment.

Effect of Feed Pressure on Nozzle Opening. One of the key issues studied in the present work was to delineate some conflicting results of engine performance and emission as reported by others, which is further elaborated later. The key consideration taken for explaining the confusion was the fact that the DME application in Diesel engines involved differences not only in the fuels' physical properties, e.g. the elastic modulus of the two fuels (DME, $6.37 \times 10^8 \text{ N/m}^2$; Diesel oil, $1.49 \times 10^9 \text{ N/m}^2$) but also in the operating conditions including the fuel feed pressure, which ranged from 1.96 to 2.94 MPa (20 to 30 kgf/cm²) in other studies. These variations were expected to alter the nozzle opening time, which information lacks in previous studies.

In the first experiment, however, simply by following the engine manufacturer's recommendation, the nozzle opening pressure was adjusted for Diesel fuel at 20.1 MPa, with feed pressure at zero because there is no need for pressurizing the tank for this fuel. After obtaining measurements including the needle lift-tracing with this fuel, in a separate experiment, the fuel system was fed with DME at 3.43 MPa, because it needs pressurization in the tank, as explained earlier. The nozzle opening pressure was set 8.82 MPa at this time, which was the same as some of the other earlier studies. Note that the nozzle (static) opening pressure was controlled by adjusting the spring preload in the injector.

It is noted that this set of experiments varying both the feed pressure and nozzle opening pressure for the fuels may appear to be confusing in sorting out the individual effects on the needle lift. These initial experimental conditions were investigated, right after setting up the new

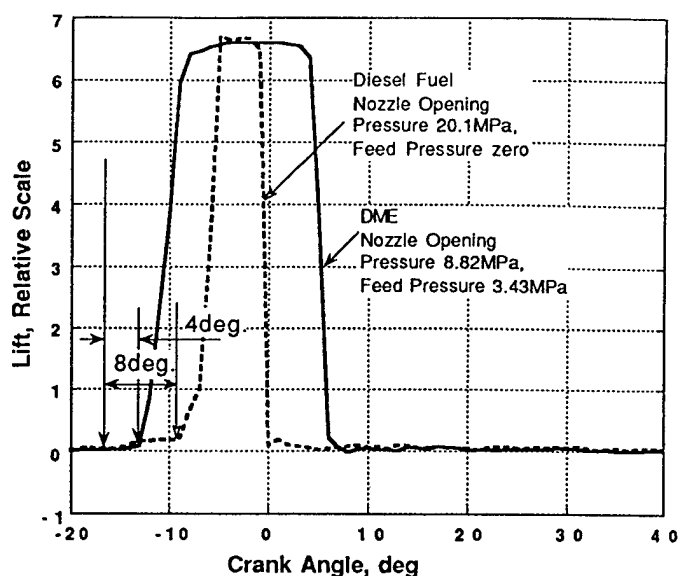


Fig. 3. Injector Needle Lift for DME and Gas Oil Operation.

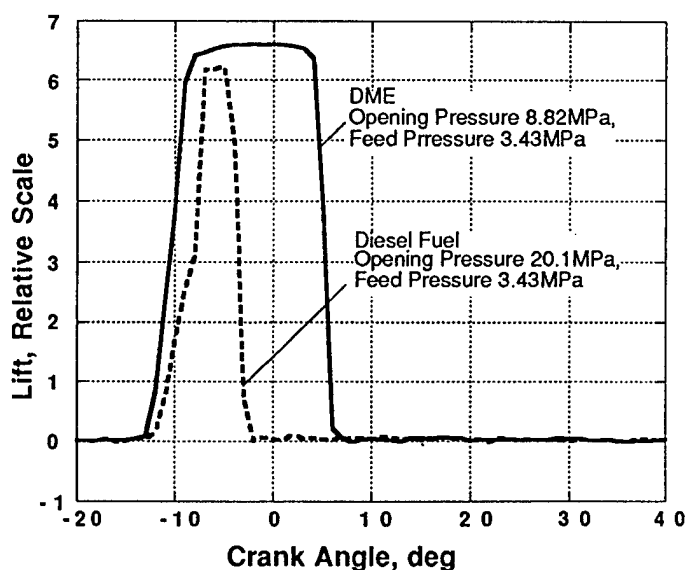


Fig. 4. Effect of Feed Pressure on Needle Lift.

apparatus, in order to duplicate a part of the previous studies in an attempt to explain some questions brought up by earlier studies as mentioned above.

Explaining the presetting of injection time and the engine's response, it was adjusted to occur at 17bTDC according to the recommendation by the engine manufacturer. As shown in Fig. 3, the actual start of injection indicated by the needle lift, however, was different from this (manual) preset timing: Under the setting, which was supposed to have the opening start at 17bTDC, the actual (dynamic) opening occurred at 13bTDC for DME and

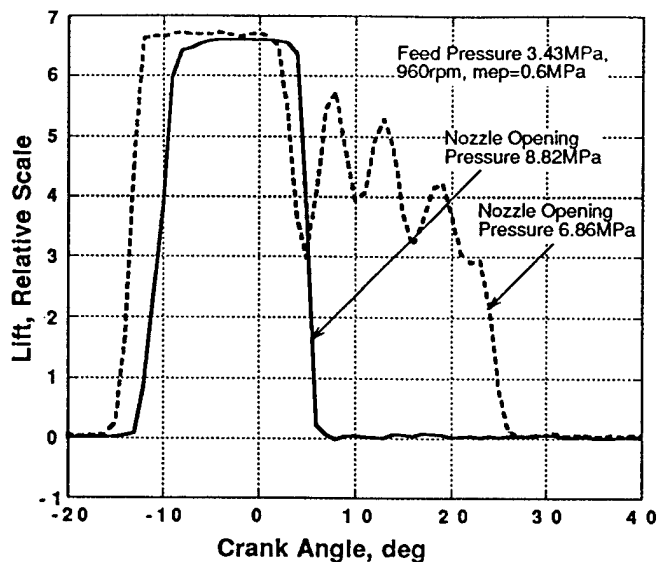


Fig. 5. Effect of Nozzle Opening Pressure on Needle Lift.

9bTDC for Diesel fuel, respectively. This exhibited that the opening with DME occurred earlier than gas oil by as much as by four crank angle degrees (CA). The results from these initial experiments seemed to offer some insight into the reasons for a significant difference in the start of pressure rise in a nearly matching experimental condition [7], which was not explained basically due to absence of the needle lift tracing.

This difference in the start of opening observed in the experiment was considered to occur by a combined effect of several variables, namely the feed pressure, the preset nozzle opening pressure, and the elastic modulus of the fuel. In order to sort out the multiple effects in this experiment, at this time the feed pressure was set the same, and new results (Fig. 4) were obtained to compare them with those shown in Fig. 3. Looking at the needle lift for Diesel fuel, the feed pressure was observed to be a strong factor affecting the nozzle opening time. That is, when the feed pressure was set the same, the opening pressure occurred at the about the identical time. The effect of the nozzle opening pressure on the start of injection, however, was not known from these experiments.

Effect of Opening Pressure on the Time of Nozzle Opening. An additional experiment with DME (Fig. 5), therefore, was performed by varying the opening pressure, i.e., 8.82MPa vs. 6.86MPa. With the low opening pressure, although it was about the same pressure as others employed, some considerable residual needle bouncing was observed, opposed to a relatively well-defined injection behavior with the higher opening pressure. The increased period of nozzle opening due to the bouncing, with the low nozzle opening pressure, was pronounced to be unusual and improper, as discussed more next. Note that there was a small amount of shift in the nozzle opening time when the opening pressure was varied. This effect seemed to be

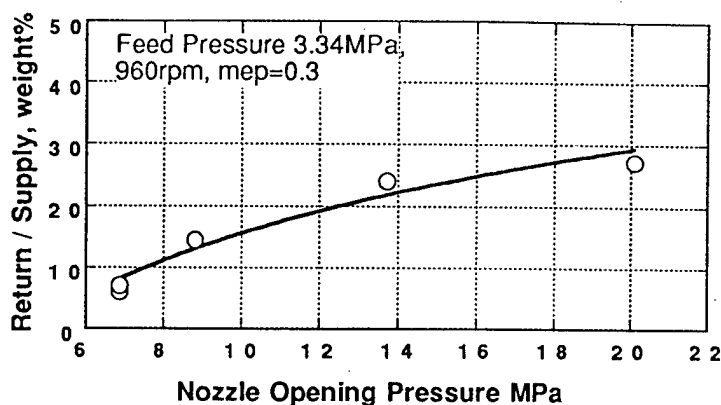


Fig. 6. Effect of Nozzle Opening Pressure on Fuel Return for DME.

measurable only when the opening pressures were low (refer to Fig. 4).

Regarding the suppressed residual bouncing by a high nozzle opening pressure, although there is no doubt that the increased spring preload on the nozzle needle would have played an important role, an additional factor may be considered, that is, the cooling of the injector. This consideration stemmed from the observation that when the opening pressure was set low (Fig. 5) the needle seemingly stayed almost afloat during the residual bouncing period, which is not a typical mode of needle bouncing in the Bosch type injector. This led to a new consideration that because of the elevated vapor pressure at high temperature with DME, the fuel at the nozzle tip might have been under a supercritical condition. If it is the case, it would have affected not only the plume formation characteristics but also the nozzle opening behavior. An indirect evidence for this consideration may be also seen from Fig. 6, which illustrates increased amounts of the fuel return for higher opening pressures. The high return was considered to increase the cooling of the injector nozzle to suppress the vapor pressure.

Effect of Injection Time. After evaluating the needle response to variation of several main parameters including those discussed above, the experiment was continued at this time by changing the start of injection time. (The change was not made in fine increments, since it required a considerable amount of engine modification, a conflicting measure to the original intent of performing the study with minimum engine change.) Two different injection times were studied, with settings of 17bTDC and 5bTDC (indicated by the manufacturer's manual), which had one tooth difference between the gears in the engine and injection pump. Note that the needle lift did not occur at the manual-indicated time, as explained earlier. In this experiment, the engine dynamometer was set at the speed of 960rpm and the load to deliver (brake) mean effective pressure (mep) of 0.3MPa (Fig. 7), and mep = 0.6MPa (Fig. 8), respectively.

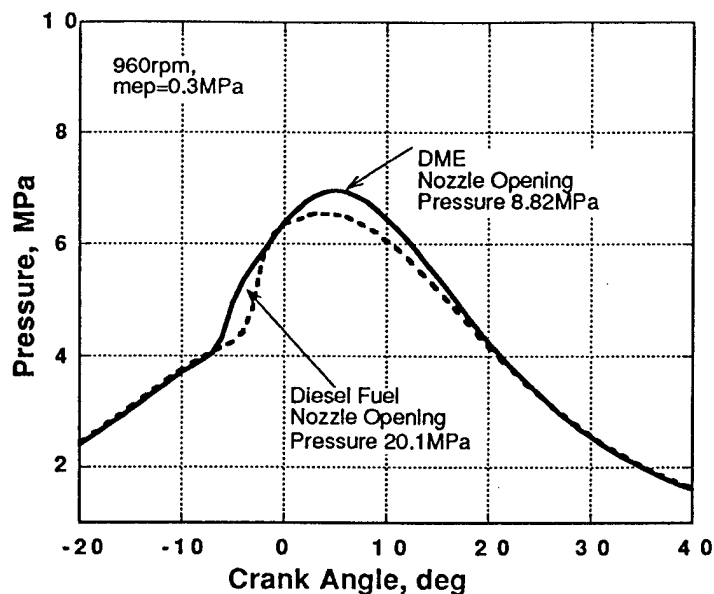


Fig. 7. Pressure-Time History for $P_{me} = 0.3$ MPa and 17bTDC Injection.

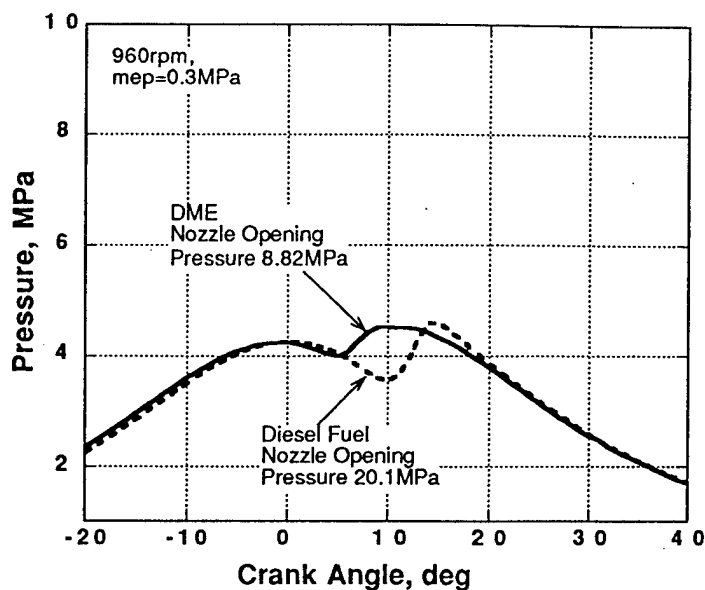


Fig. 9. Pressure-Time History for $P_{me} = 0.3$ MPa and 5bTDC Injection.

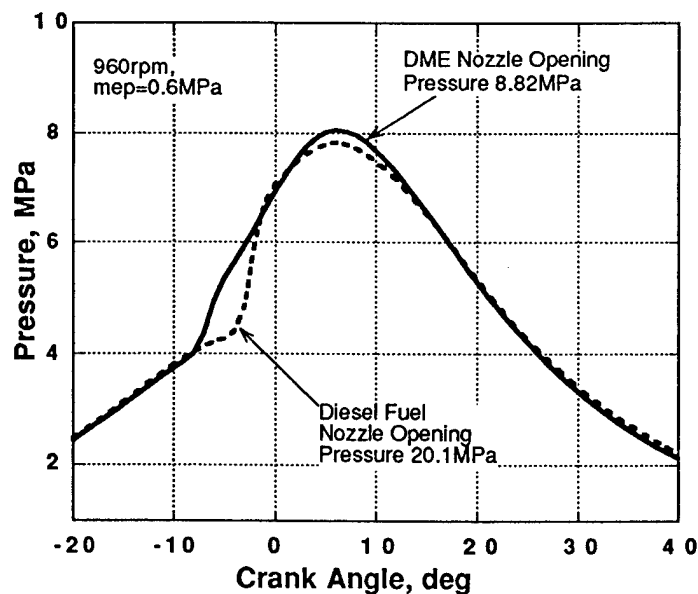


Fig. 8. Pressure-Time History for $mep = 0.6$ MPa and 17bTDC Injection.

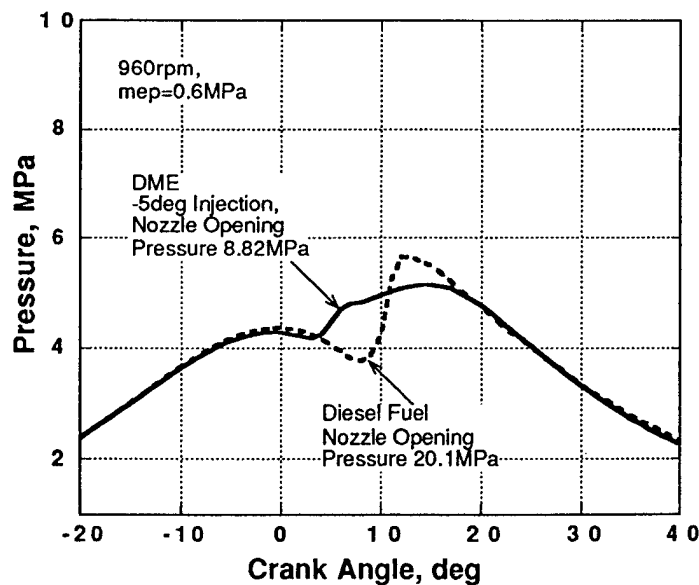


Fig. 10. Pressure-Time History for $mep = 0.6$ MPa and 5bTDC Injection.

Looking at the difference in the needle lift tracing as shown in Fig. 3, when the load was low (Fig. 7), the rapid pressure rise occurred earlier with DME than with gas oil by about the corresponding amount, although the peak pressure occurred almost at the same CA for both fuels. When the load was high (Fig. 8), the difference in start of pressure rise was even more obvious with DME compared with Diesel

fuel. The earlier start of pressure rise in both experiments did not appear to occur due to an easy (chemical) ignition tendency of DME but more the differences in the start of nozzle lift. Recall that the early nozzle opening occurred due to the difference caused by the feed pressure and to a small extent by the nozzle opening pressure.

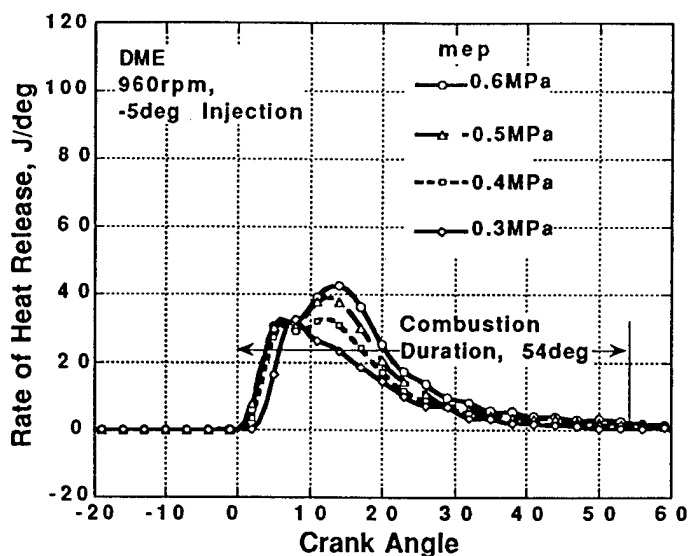


Fig. 19 Rate of Heat Release of DME Operation for 5bTDC Injection.

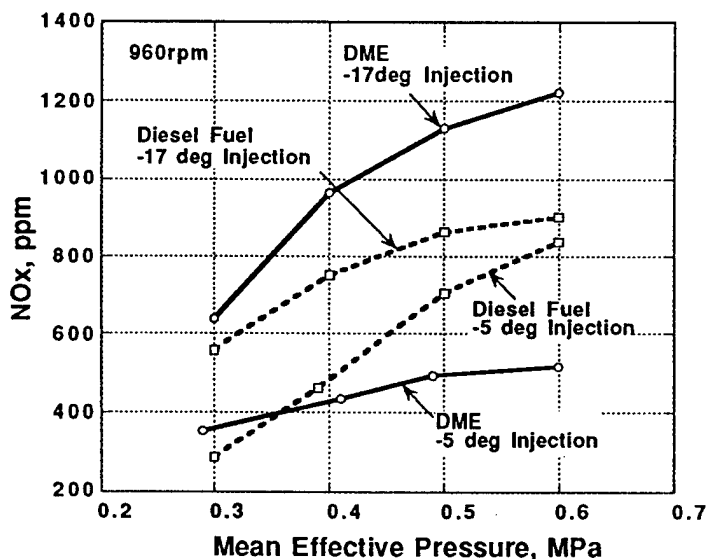


Fig. 20. NOx Emission.

Mentioning the mild premixed combustion with DME and its impacts, it is realized that the low soot emission with DME (as shown later in Fig. 22) is not due to a great amount of fuel consumption in its premixed combustion stage, which is the case in the typical gas oil operated Diesel engine producing a low soot emission. Recall also that in such engines, the shorter the ignition delay (Fig. 17), the milder the intensity of premixed combustion causing a quiet engine operation, which is consistent with the present DME fueled engine operations. However, a common observation of a short ignition delay in

a Diesel engine to produce high soot emissions is no longer true in the DME operated engine.

It is worthy to discuss reasons for the mild premixed combustion in a DME fueled engine (Figs. 18 and 19). Since the energy content of DME is only about one half that of gas oil, under a similar injector operation and the same external load condition, DME has about twice as long a period of fuel injection than gas oil. While, as shown in Fig. 18, the injection of gas oil completed within a short period of time, particularly when the engine load is low, it continued even far after the onset of the premixed combustion stage for DME operation (Fig. 19). The continuing combustion for DME at a high load, therefore, is caused by the prolonged injection period. Under such a condition the DME spray plume is penetrated into the cloud of burned gas, which would have been a factor to produce a large amount of soot in typical gas oil operated Diesel engines, but it did not happen with DME. According to the present results, it seemed that the chemical aspect of fuel to produce low soot formation played a dictating role in producing low soot emissions. There are other physical aspects of the spray formation to produce low soot as discussed next. In spite of the longer injection periods with DME, its combustion completed sooner than with Diesel fuel (Figs. 18 and 19), which was considered to help achieve low SEC, as mentioned earlier.

In view of the long injection period and difference in other physical properties, including stoichiometric fuel/air, viscosity, surface tension and volatility, the spray formation of DME is expected to be quite different from that of Diesel fuel even under the same external load. As mentioned earlier, particularly if DME was under a supercritical condition in the nozzle, the fuel leaving the injection nozzle will be in or near a gaseous phase, which will result in formation of a wide (and short) spray plume. Note that Glensvig and Sorenson [12] suggested that a DME spray completes the evaporation within a very short period of time after injection. In addition, the high stoichiometric fuel/air ratio will have a greatly diluting effect in a DME spray. Also, the extended injection period means a greater momentum imparted on the DME spray, making it more dispersed. These all are expected help produce a lean local fuel/air ratio, that is, to have lean combustion compared with a Diesel fuel spray.

Exhaust Emissions. Three main emissions were measured for both fuels operated under mutually comparable conditions, namely NOx, unburned hydrocarbon (THC) and smoke. Considerably high NOx emission was observed when the engine was operated by DME under the engine-manufacturer recommended injection time for gas oil, i.e., injection at 17bTDC injection time (Fig. 20). It is noted that this observation is in contrast with low NOx emission reported by others [7]. One of the most probable reasons for the high emission is considered to be the unusually early start of combustion with DME (Figs. 8 and 15), as much as four CA. Recall that it was explained to occur due to the increased fuel feed pressure. The difference would have been somewhat smaller if the actual injector opening was the same for both fuel. Note that the dispersed fuel spray

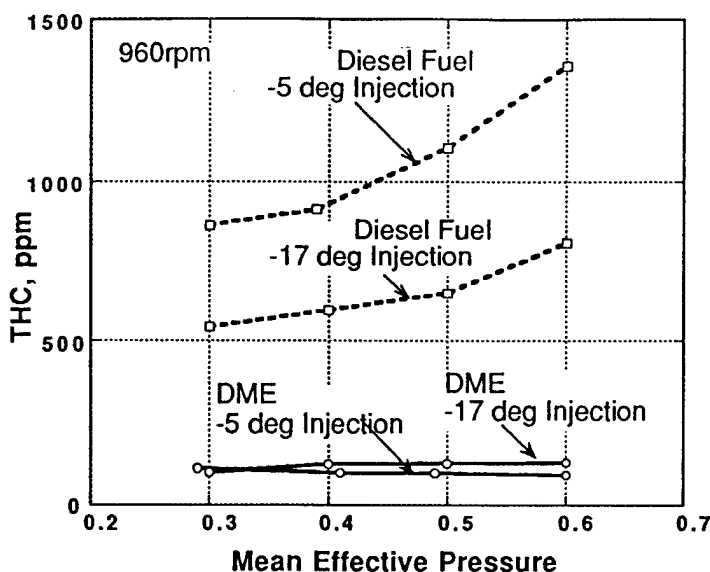


Fig. 21. Unreacted Hydrocarbon Emission.

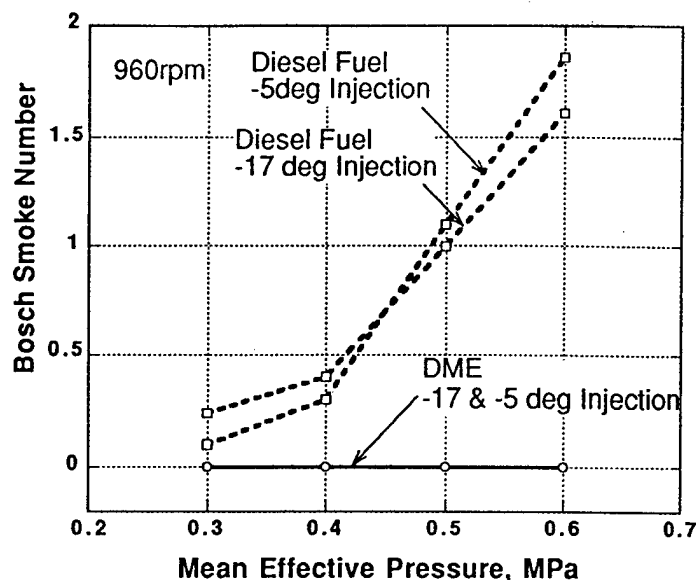


Fig. 22. Exhaust Smoke in Bosch Scale.

formation with DME would help produce low NO_x emission.

When the injection time was delayed by changing from 17bTDC to 5bTDC, however, the NO_x emission was much lower with DME. This finding is explained by the high rate fuel injection (mass of fuel/deg) with gas oil operation compared with its counter part (Fig. 15) producing high-temperature combustion products with the piston located still near the TDC. This is not expected to occur with DME due to a prolonged injection resulting in a continued combustion with the piston moving away from the TDC.

The emission of THC from the DME-operated engine was very low (Fig. 21), while THC was about the amount expected from a typical gas oil operated Diesel engine, regardless of injection time for a wide range of engine loads. This finding may be explained in terms of several parameters, including the average cylinder temperature (ACT), fuel-air ratio in the spray and chemical characteristics of the fuel. The low ACT (Figs. 14 and 16) and exhaust gas temperature (Fig. 12) with DME certainly do not seem to explain the finding. The dispersed locally lean fuel spray formation expected with DME, as explained earlier, may be a factor consuming the maximum amount of fuel before being wasted in the exhaust. This consideration, however, does not seem to be consistent with an expectation of having high-temperature pockets to explain the high NO_x emission with DME. It leads to expect the chemical aspects of the fuel to rapidly consume the unreacted fuel before emission, that is the low self-ignition temperature of DME.

The emission of soot with DME operation was virtually zero (Fig. 22) under the entire experimental conditions investigated in the present study. The reasons for the low emission may be considered by listing various factors, including: the local fuel/air ratio, start of ignition, ACT, and fuel characteristics.

The absence of rich fuel pockets or any exposure of such mixtures to high-temperature combustion products is a precondition for low soot emission from conventional gas oil operated Diesel engines. The formation of a fuel-rich mixture may not be likely in DME spray plumes since the fuel is highly volatile, becoming a gaseous jet or attaining a high specific volume as soon as leaving the injector, which transfers a greater amount of momentum during a longer period of injection compared to the gas-oil injection (Figs. 13 and 15). Consider, however, this mode of fuel injection has a potential to produce large amount of soot: Since DME is self-ignited no later than gas-oil is, and since DME continues to flow into the cylinder even far after the onset of ignition, the direct exposure of fuel leaving the nozzle would be inevitable. This will cause dehydrogenation of the fuel molecules, which is a process known to increase the soot formation. The low soot formation observed with DME in a Diesel engine may then suggest that the DME spray formation may be sufficiently fuel lean as considered above, or even if it is not the case, the fuel itself has characteristics of resisting soot formation. As briefly mentioned earlier, since DME is an oxygenate like a methanol, which is known to produce low soot in Diesel engines, it may not be difficult to expect a low soot emission by the fuel. Therefore, it seems be reasonable to consider that the low soot with DME in Diesel engines is either or both the lean fuel/air spray structure and the fuel's intrinsic tendency of low soot formation in Diesel engines.

It may be added that the commonly known mutual exclusivity between the NO_x formation and soot emission in Diesel combustion is no longer applicable in DME operated Diesel engines. Therefore, the control of NO_x emission by retarding the injection time appears to be a plausible method without increasing soot emission. Furthermore, since the fuel does not produce soot, and it reveals high thermal efficiency, when new regenerative NO_x absorbing devices being developed in the field are incorporated in DME

operated Diesel engines, some ultra-lean emission high-efficiency vehicle may be achieved.

SUMMARY

The use of neat dimethyl ether (DME) in a conventional direct injection (DI) Diesel engine was studied as an alternative fuel that produces a high-efficiency and low emissions. In order to obtain a better understanding of the engine's response to this new fuel, the present study was performed by using some additional engine measurement devices compared to others reported earlier. Particularly, the study was directed to closely monitoring the behaviors of the fuel injector, which was considered to help understand reasons for some conflicting results by others.

Some findings from the study may be listed as follows. DME can not be directly used in the conventional DI Diesel engine, so that either the fuel or the engine will have to be modified. This is mainly due to the fuel's incompatibility with the fuel delivery system resulting in excessive wear in the injector within a short period of the engine operation. A viable remedy proposed for this problem as employed in the study was to add a small amount of lubricant to DME, which did not appear to produce any noticeable negative engine performance and emissions. Note that the study was performed by obtaining measurements using both DME and conventional Diesel fuel under the comparable operating conditions for the purpose of mutual comparison.

The engine operated by DME exhibited remarkably high energy conversion efficiency, which was consistent with low exhaust gas temperatures. In addition to the high vapor pressure of the fuel, due to a low energy of DME causing the injection period to be much longer than its counter part, the spray formation was expected to be over all fuel lean and dispersed, which would affect the exhaust emissions.

The engine with DME produced very high NO_x emissions when operated at the injection time recommended for the conventional Diesel fuel. The high NO_x with DME (compared with gas oil) is considered to be caused by the remarkably early injector (needle lift) opening, which is attributed to the increased feed pressure, a necessary measure due to the high vapor pressure under the normal operational environment. This high NO_x emission was considerably reversed when the injection time was delayed.

The emissions of unburned hydrocarbon and soot were negligible with DME. This was explained in terms of physical aspects of spray formation and chemical characteristics of fuel including the fuel's low self-ignition temperature and tendency of producing low soot. There is no doubt that some in-cylinder visualization of the reaction processes would have helped understand some of unanswered questions.

ACKNOWLEDGMENT

Messrs. Hideyuki Machida, Sumitaka Minegishi and Osamu Sukagawa assisted the experiment. Ethyl Japan

Corporation provided Hitec560. The US Army Research Office supported one of the authors (KTR) under Contract No. DAAH04-95-1-0430.

REFERENCES

1. Hansen, J.B., "A Large Scale Manufacturing of Dimethyl Ether- A New Alternative Diesel Fuel from Natural Gas," SAE Paper 950063, 1995.
2. Karpuk, M.E. and Rowley, S.W., "On-board Dimethyl Ether Generation to Assist Methanol Engine Cold Starting," SAE Paper 881678, 1988.
3. Galvin, M.P., "Aspirated Ether Ignition System for Methanol Fueled Diesel Engines", 8th ISAF, p.601,1988.
4. Karpuk, M.E., Wright, J.D., Dipbo, J.L., and Jantzen, D.E., "Dimethyl Ether as an Ignition Enhancer for Methanol Fueled Diesel Engines," SAE Paper 912420, 1991.
5. Murayama, T., Chikahisa, T., Guo, J. and Miyano, M., "A Study of a Compression Ignition Methanol Engine with converted Dimethyl Ether as Ignition Improver," SAE Paper 922212, 1992.
6. Cipolat, D. "Methanol/ Dimethyl Ether Fueling of a Compression Ignition Engine," 11th ISAF, p.411, 1991.
7. Sorenson, S.C., Mikkelsen, S.E., "Performance and Emissions of a 0.273 Litter Direct Injection Diesel Engine Fueled with Neat Dimethyl Ether," SAE Paper 950064, 1995.
8. Fleish.T., MacCarthy, C., Basu, A., Udovich, C.C., Charbonneau, P., Slodowske, W., Mikkelsen, S. and McCandless, J., "A New Clean Diesel Technology: Demonstration of UL-EV Emissions on a 1994 Model Diesel Engine Using Dimethyl Ether," SAE Paper 950061,1995.
9. Kapus, M.E., Cartellieri, W.P., "ULEV potential of DI/TCI Diesel Passenger car engine operated on Dimethyl Ether," SAE Paper 952754, 1995.
10. Kapus, P., Ofner, H., "Development of Injection Equipment and Combustion System for DI Diesels Operated on Dimethyl Ether," SAE Paper 950062, 1995.
11. Holidorff, H. and Knapp, H., "Vapor Pressure of N-Butane, Dimethyl Ether, Methyl Chloride, Methanol and Vapor-Liquid Equilibrium of Dimethyl Ether-Methanol," Fluid Phase Equilibria, 40, p. 113, 1988.
12. Glansvig, M. and Sorenson, S.C., High Pressure Injection of Dimethyl Ether, ASME ICE Fall Technical Conference, vol 3, p. 57, 1996.

Quantitative Imaging of In-Cylinder Processes by Multispectral Methods

C. Chang, E. Clasen, K. Song, S. Campbell, and K. T. Rhee
Rutgers University

H. Jiang
Detroit Diesel Corporation

Copyright 1997 Society of Automotive Engineers, Inc.

ABSTRACT

With the objective of achieving better investigation of engines-fuels by obtaining instantaneous quantitative imaging of in-cylinder processes, several steps have been taken for some years at Rutgers University. They are: (1) Construction of a new multispectral high-speed infrared (IR) digital imaging system; (2) Development of spectrometric analysis methods; (3) Application of the above to real-world in-cylinder engine environments and simple flames. This paper reports some of results from these studies.

The one-of-a-kind Rutgers IR imaging system was developed in order to simultaneously capture four geometrically (pixel-to-pixel) identical images in respective spectral bands of IR radiation issued from a combustion chamber at successive instants of time and high frame rates.

In order to process the raw data gathered by this Rutgers system, three new spectrometric methods have been developed to date: (1) dual-band mapping method; (2) new band-ratio method; and (3) three-band iteration method. The former two methods were developed to obtain instantaneous distributions of temperature and water vapor concentrations, and the latter method is to simultaneously find those of temperature, water vapor and soot in gaseous mixtures, i.e., to achieve quantitative imaging.

Applications of these techniques were made to both SI and CI engine combustion processes as well as bench-top burner flames. Discussion is made on the methods and new results.

INTRODUCTION

BACKGROUND. Investigating how design-operation and fuel variables affect in-cylinder events, a question may arise: What in-cylinder information would be most desirable when experimentally studying the reaction processes?

A plausible answer to this question, which is perhaps as old as the advent of the internal combustion engines (ICE), is considered here. That is, in order to improve our understanding of the reactions, it would be desirable to obtain instantaneous distributions of temperature and species within the combustion chamber at successive instants of time. Such pieces of information may be referred to as "quantitative images." When they are made available, there is no doubt that a better understanding about the engine can be achieved, including the thermal budget, knock and even emissions. This goal, in fact, has been sought after by many auto-engineers using various methods such as different probes and electro-optical diagnostic methods in the past. While their measurement were made mostly at a limited number of points at a time, (visible-ray) photos obtained of combustion processes at high rates have helped in gaining a global understanding of the in-cylinder phenomena.

Realizing powerful advances in modern sensors and data processing technologies, a new approach of ICE-research was initiated at Rutgers University some years ago in order to achieve the goal of quantitative imaging as extensive as possible. This approach is, in a sense, an attempt of gaining multiple effects expected when both methodologies of point measurements and cinematography are combined together. This paper reports the new research methods and some of recent results obtained from the work.

PREVIOUS STUDIES. Several earlier studies relevant to the present work are discussed at first. They are summarized in Fig. 1 along with new methods to be discussed here. It was 1947 when Uyehara and Myers [1]* first reported a laboratory-built two-color (emission spectrometry) measurement system applied to determination of the instantaneous flame temperature in a Diesel engine

*Numbers in parentheses designate references at end of paper.

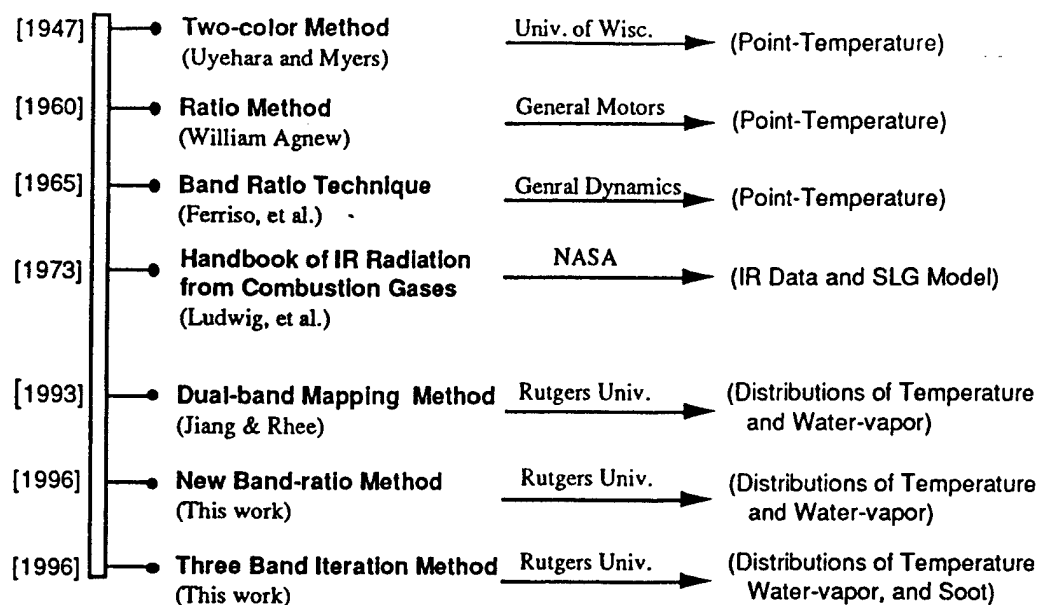


Figure 1. Multiple-band Spectrometric Methods for Temperature and Species Measurement in Flames.

combustion chamber. The basic concept of this new technique was the ratio of spectral radiation intensities of soot was directly related to the flame temperature, which assumed that soot was a gray-body and that radiation from gaseous species was negligible via two bands they employed. Note that a similar methodology was employed by others in later years [2]. They continued to develop new two-color (absorption spectrometry) methods for in-cylinder temperature measurement by employing sodium vapor [3] and water vapor [4] as radiatively participating species.

The concept of the ratio method was also introduced in 1960 by William Agnew [5] to determine temperatures of the end gas in an SI engine (near the peak). In this emission spectrometry method, he indicated that two readings from detectors receiving respective spectral radiations by water vapor in a laboratory flame was related to the mixture temperature. The ratio method was explained by using the Plank's equation,

$$E = C_1 / \lambda^5 [\exp (C_2/\lambda T) - 1] \quad (1)$$

where, C_1 and C_2 are constants. The concept of the method, again, was that the ratio of the emissive powers at two wavelengths, E_1/E_2 was a function of temperature only, which in his method was experimentally determined for a working relationship,

$$E_1/E_2 = [D_1/D_2] (K_2/K_1) [E_2/E_1] \quad (2)$$

where, D is the output of the detector and K is the relative sensitivity of the detector system via each wave band of λ .

In the above equations, K_2/K_1 and E_2/E_1 were determined by calibration using a bench-top burner apparatus, and D_1/D_2 was the experimental measurement relating to

temperature of the mixture. Two wavelengths employed in his method were those for receiving radiation from water vapor, 1.89 μ m and 2.55 μ m. Note that his calibration was done to relate the ratio of detector readings to temperature closer to the peak value along the line of sight in the flame.

In 1965, Ferriso, et al. [6] introduced a so-called band-ratio technique (BRT), which was similar to the ratio method by Uyehara and Myers, and Agnew. They, however, employed measurements of radiation via rather wide band filters, namely: (A) 2.63-3.3 μ m; (B) 2.3-2.63 μ m; (C) 1.7-2.3 μ m; and (D) 1.3-1.7 μ m. They experimentally demonstrated that ratios of detector signal output (i.e., $\theta_{C/B}$, $\theta_{D/C}$, and $\theta_{D/B}$) were related to the exhaust gas temperature from a rocket motor. What is to be mentioned here is that since the band widths were so wide, their measurements involved radiation from more than one species in the combustion products. This may be one of the reasons why the relationships of θ vs. T were relatively crude [6], which is further discussed later.

Thanks to NASA Handbook (SP-3080) of infrared (IR) radiation (of gaseous mixtures) provided by Ludwig, et al. [7] in 1973, which contains the spectral absorption coefficients of individual gaseous species at varied temperatures and pressures, more meaningful work became possible. Agnew in 1960 probably did not have access to such data when he conceived his ratio method so that he resorted to experimental means in order to obtain the working calibration curve for his system.

After developing a new high-speed two-color IR imaging system at Rutgers [8, 9], which was to simultaneously capture two geometrically identical images in respective spectral bands, results from the NASA IR data and single-line-group (SLG) model [7] were employed in order to develop a new dual-band mapping method (DBMM). In an earlier paper [10], without giving a detailed

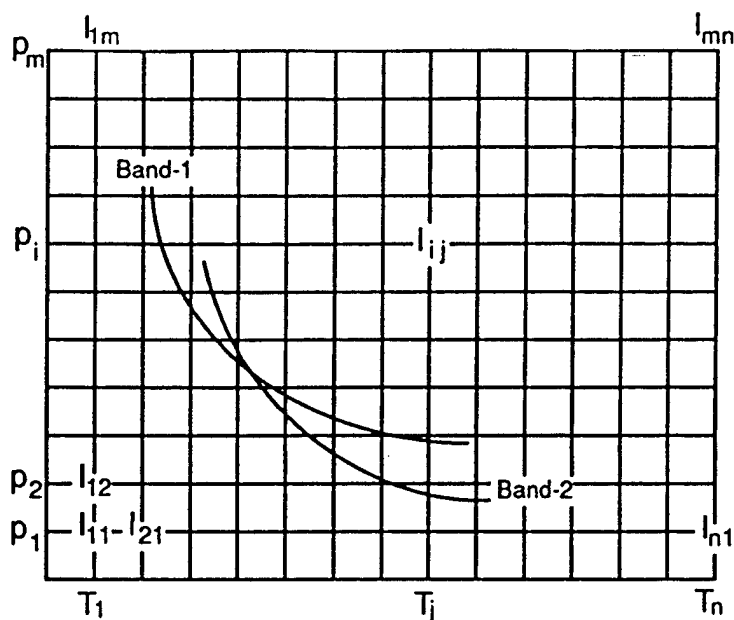


Figure 2. Algorithm for Dual-band Mapping Method (DBMM).

elaboration of the method, distributions of temperature and water vapor concentration obtained by this method were reported. In the following, the DBMM is discussed in comparison with other methods developed during the course of the present work.

RUTGERS SPECTROMETRIC METHODS AND RESULTS

DUAL-BAND MAPPING METHOD (DBMM). When a volume of uniform gaseous mixture in a known concentration of source (target) species having a given physical thickness is at a specified temperature and pressure, it is possible to calculate the spectral radiation intensities of the mixture. The core of the DBMM is to find temperature and species concentration in such a mixture when two spectral intensities are given, a reverse process of the former.

In order to achieve this goal, a new algorithm was developed as discussed by using a spectral intensity matrix (I_{ij}) of the mixture (Fig. 2), which covers, for a given wave band (Band-1), in a range of varied partial pressure of water vapor (p_i) and temperature (T_j). Then, an iso-intensity line is traced over this matrix according to the spectral intensity measured from the experiment. Then the same is made for the intensity matrix for another band (Band-2), and overlap these two matrixes with each other in order to find the crossing point of both iso-intensity lines. This is like finding two unknowns from two simultaneous equations.

In spite of the straight-forward concept of this method, error in the final result is likely to be high due to the two somewhat mutually paralleling lines as seen from Fig. 2. Even a small uncertainty in measurement would lead to a rather large error in the results. Furthermore, since the physical length of individual optical paths through a real-world flame is difficult to determine, the error could increase more. It is noted again, in spite of such limitations stemming

from probable imperfect measurements, the results obtained by this method are unique. A sample result is shown when a new band-ratio method is explained later.

RUTGERS FOUR-COLOR IMAGING SYSTEM.

Prior to discussing other spectrometric methods, the Rutgers high-speed four-band IR digital imaging system (referred to as the Rutgers System or Super Imaging System, SIS) is explained. While the abovementioned two-color system continued to be used for flame and engine studies [8-11], and also for implementation of the DBMM [10], an entirely new system was developed as schematically shown in Fig. 3. Since this SIS was described earlier [12-14], it is only briefly explained here.

Referring to Fig. 3, the radiation from an object is collected by the cassegrain assembly (152mm diameter), which is spectrally split to place four spectral images over respective high-speed digital imaging units. The SIS, therefore, can be used to simultaneously obtain four separate sets of 64x64 digital image in corresponding spectral bands. Ideally, images of four different pieces of information can be obtained at successive crank angles (CA).

While the spectrometric techniques were being developed for achieving quantitative imaging by processing the digital data captured using the SIS, the main topic of the present paper, the raw results alone have been useful in finding some new observations. They include: preflame reactions [11-14]; liquid-fuel layers over the cylinder head surface; and postflame oxidation [12,13], which were not reported earlier by others.

NEW BAND RATIO METHOD. The computer program developed for the abovementioned DBMM, which contained spectral absorption coefficient data under varied temperatures and total pressures, and incorporated with the SLG model, was further improved. The SLG model from

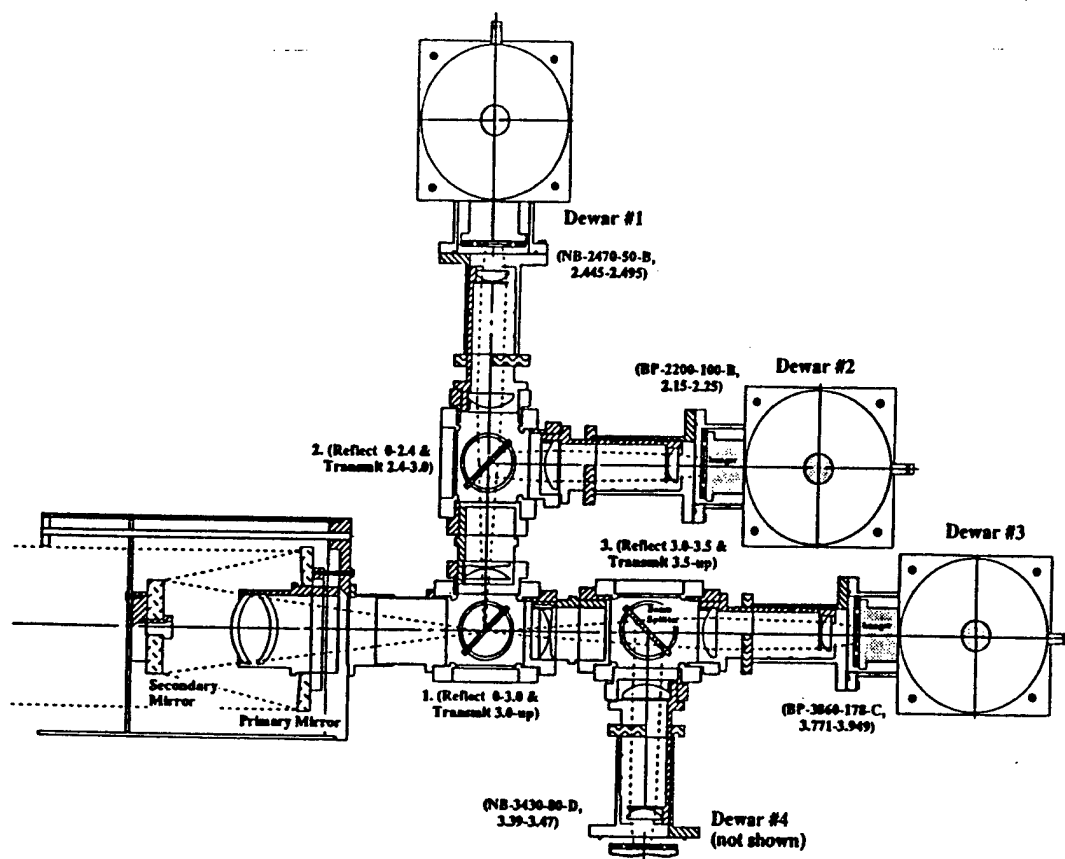


Figure 3. Schematic Presentation of Optical Portion of Rutgers SIS.

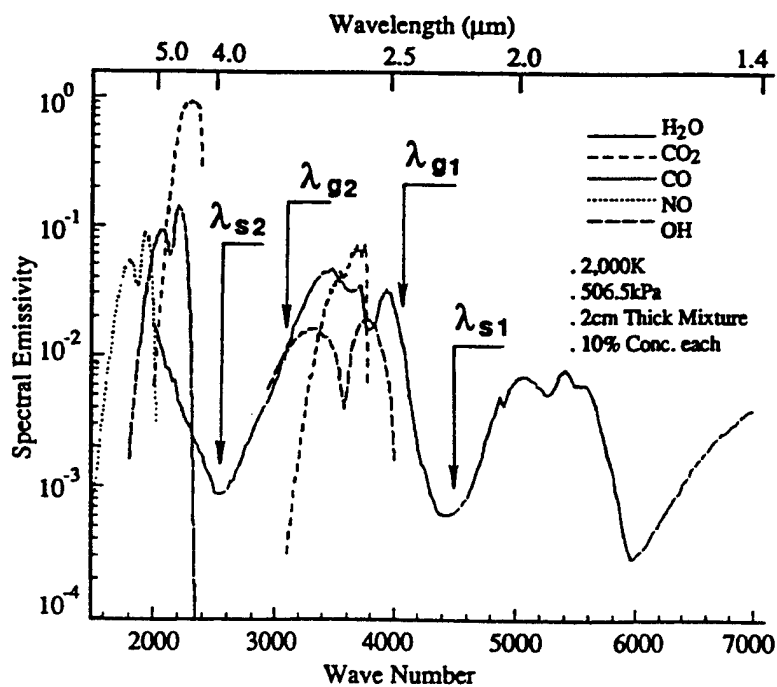


Figure 4. Spectrogram Constructed by using Rutgers DBCP for a Gaseous Mixture.

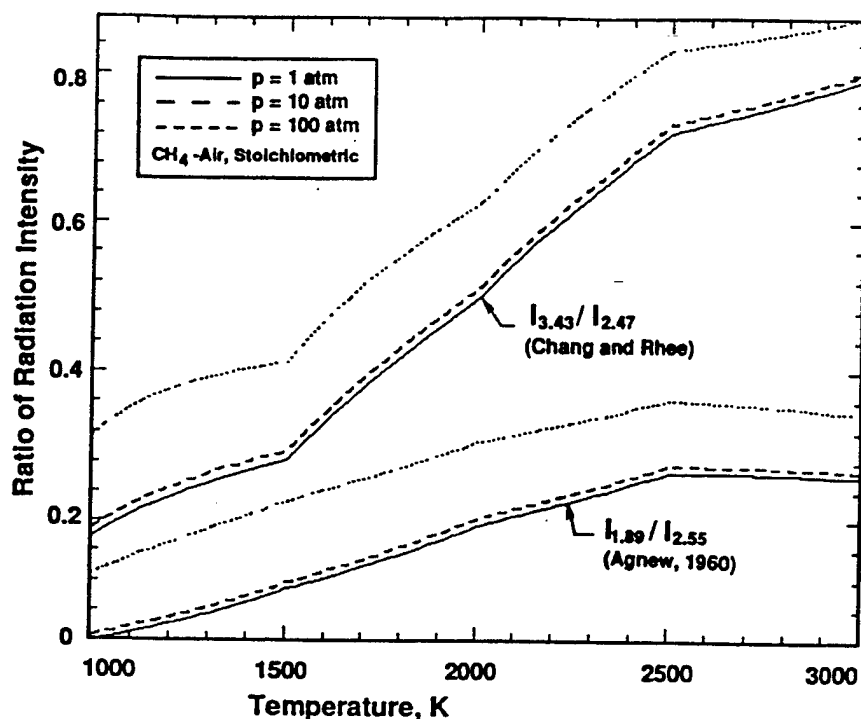


Figure 5. New Band Ratio Method (NBRM) to Determine Temperature in Gaseous Mixtures.

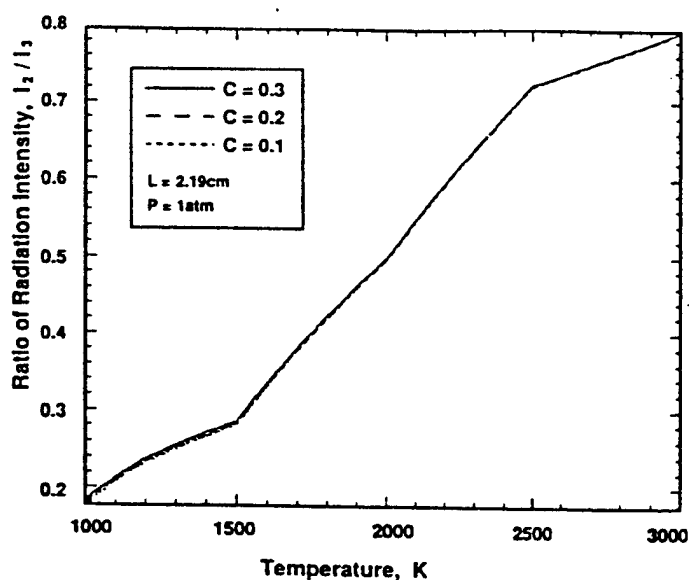
NASA's IR handbook [7] was to facilitate utilization of those absorption coefficients given for each wavenumber, such as for calculation of the spectral radiation intensity and emissivity of a specified gaseous mixture. For example, Fig. 4 was prepared by using this data-based computer program (DBCP). This was done for a sample gaseous mixture (thickness 2cm) composed of H_2O , CO_2 , CO , NO , and OH with concentration $C=0.1$ in mole fraction each under pressure, $P=10\text{atm}$. The figure suggests that bands at $2.47\mu\text{m}$ and $3.43\mu\text{m}$ have strong radiation by water vapor, which are employed in the following spectrometric method. Development of this DBCP paved the way to the analysis of spectral characteristics of radiating species in the present IR domain to come up with the new band-ratio method (NBRM), as shown in Fig. 5.

The figure is self-explanatory and it indeed supports Agnew's earlier experimental work and Ferriso's BRT measurement method. It is noted that this result was constructed by the abovementioned DBCP to relate the ratio of spectral intensities from mixture containing a target species to temperature of the mixture under a specified total pressure. No experimental factor is involved in the result.

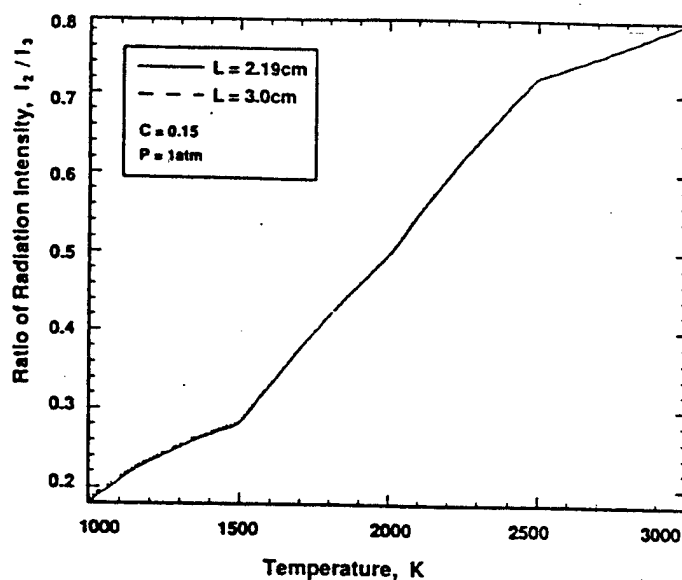
There are several new features in the NBRM: (1) It includes the pressure effects on the relationship, which neither Agnew nor Ferriso, et al. considered in their methods; (2) The method employs a single radiatively participating species; (3) Its band widths are narrow to improve the accuracy; (4) The analysis permits identification of a pair of desirable bands for achieving more accurate temperature determination; and (5) The relationship is universally applicable unlike the detection system-dependent curves generated via experiment [5,6].

Regarding the pressure effect on the NBRM, Fig. 5 indicates how significant it may be when reactions under varying pressure are considered such as in an engine cylinder. The NBRM was applied to two wave bands employed by Agnew [5] as shown by the solid-line, which is compared with dotted curves for high pressures in the same figure. This illustrates the NBRM's need for incorporating the effect of reaction pressure in order to obtain accurate temperature results. In selecting bands (i.e., filters in experiment) for the NBRM, it is desirable for them to pass radiation from only a single source species. For example, when this method is applied to a hydrogen-air flame, not only the selection of bands will be simple but also the measurement accuracy will be high because there is only water vapor emitting IR radiation in the product. When bands which permit some strong radiation by additional species (e.g. carbon dioxide an/or soot) to pass together with radiation from the target species (here, water vapor) were employed by the NBRM, the relationship in Fig. 5 was not unique indicating errors to be made in measurements. Recall that, since wide bands tend to include radiations from more species, those employed for the Ferriso's BRT were considered to be inappropriate.

In typical hydrocarbon-air flames, many species including intermediate species are formed and also consumed, which radiate more or less in the IR band domain. They can not be considered all in a simple spectrodiagram shown in Fig. 4. Even a narrow band rarely passes radiation by only a single species without interference by others. If such interference is not negligible, the accuracy will suffer. Note that the accuracy will be enhanced, however, when additional bands (for corresponding species, otherwise



(A)



(B)

Figure 6. Characteristics of New Band Ratio Method Indicating Minimum Dependency of:
(A) Species Concentration and (B) Path Length.

causing interference) are employed, which is demonstrated by the new method as discussed later.

When two solid lines in Fig. 5 are compared with each other, the measurement accuracy is expected to be higher for a steeper curve, which suggests the selection of a proper pair of bands to be important in the NBRM. The last statement is reiterated because unlike the voltage measurements out of the sensors employed by others in the past, the present method is to find temperature from intensities of the mixture, which is independent of the system response, e.g. values of K in Eq. (2).

Additional analyses revealed that the relationship (Fig. 5) was found to be quite independent of the species concentration and physical length of the optical depth, as shown in Fig. 6. These characteristics are very important in applying the NBRM in the typical combustion environment where concentration and flame thickness vary greatly along the line of sight. These results illustrate that ϵ_2/ϵ_1 in EQ (2) is not affected by the variation of concentration and optical length, L . It becomes reasonable if the optical thickness is relatively small as seen from the Beer's law, $\epsilon = 1 - \exp(-\kappa L)$. That is, when κL is very small, $\epsilon \sim \kappa L$. Note that κL is indeed small in many combustion environments, which is optically thin, except for soot-laden flames whose solution is considered by another method later.

CALIBRATION. At this time, the method of the system calibration for determining spectral intensities from the digital images is explained. The purpose of this calibration is to accurately measure, for individual pixels, the radiation intensity of a (target) mixture (either in a bench-top flame or engine cylinder). Note that the ratio relationship

to temperature (Fig. 5) needs no calibration. For this, the imaging system is placed at exactly the same geometric orientation with respect to the target as in the actual (engine) experiment. Then, the digital output from pixels are compared with those obtained when the target is replaced by a blackbody at a known temperature. The conversion matrixes of the system-response permit the construction of spectral intensity distribution at the target using the raw data, i.e.,

$$I_{ij} = a_{ij} v_{ij} + b_{ij}, \quad (3)$$

where, v is digital output in voltage. Note that the system response in Eq. (3) includes the combined effects of: (1) optical window in the engine; (2) optical elements in Fig. 3; (3) individual pixels; (4) the location of pixel with respect to the axis of the path; and (5) electronic components. Since the need for such characterization is well known, no further elaboration is made here.

In addition, effects of deposit formation over the optical window on the measurement is discussed. While in visible range imaging, even a small amount of window deposit degrades the image quality, which occurs within a short period of engine operation, imaging in the present IR domain is found to be lightly affected by the deposit. For example, the quality of in-cylinder image obtained of a gasoline-operated SI engine, after more than 20 minutes of continuous operation (without cleaning the IR window) from the (cold) start, still appeared to be reasonably good [13]. Similar insensitivity was also found in imaging of a reacting spray plume of a direct injection CI engine [11,14]. Such a high transmission of IR radiation through the deposit-layered window, however, does not necessarily guarantee accurate quantitative imaging. On the other hand, the ratio method of

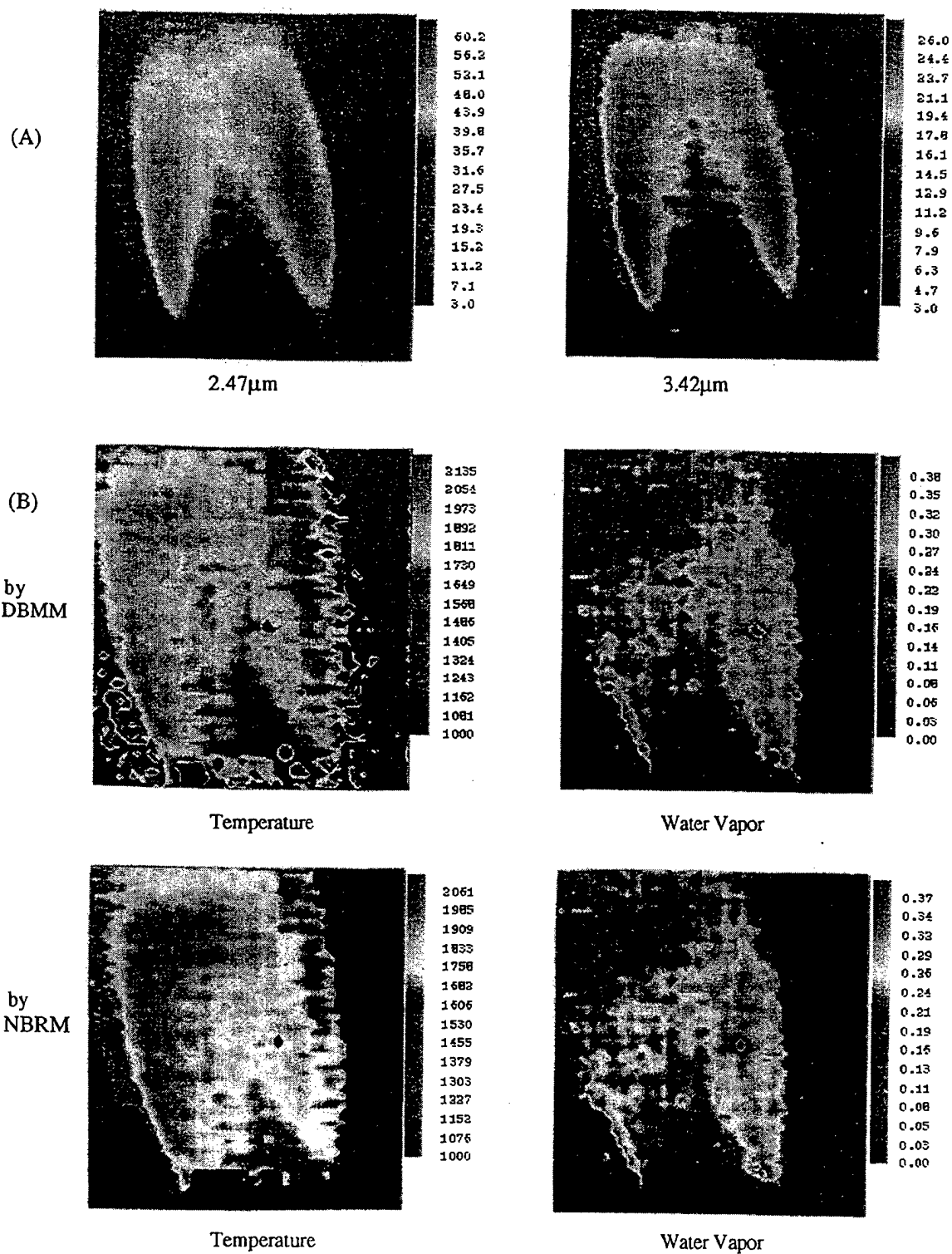


Fig. 7. (A) Spectrometric Intensity Images of a Hydrogen-air Flame in 2.47 μ m and 3.42 μ m, and (B) Distributions of Temperature (K) and Water Vapor (atm-cm) by DBMM and NBRM.

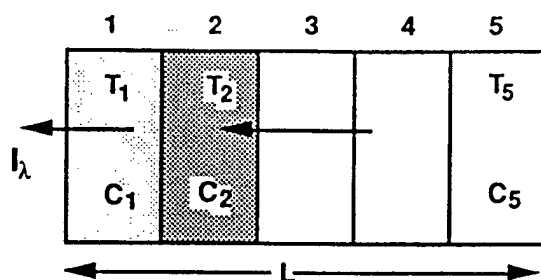


Figure 8. A Case Analyses of a Flame with Designated Temperature and Water Vapor Concentration.

processing spectral IR data has advantages over others such as single-band imaging, because effects due to either absorption or emission (by the deposit) on both band measurements would tend to cancel each other minimizing the error.

SAMPLE RESULTS BY NEW SPECTROMETRIC METHODS. A set of results obtained by using the DBMM and NBRM is shown in Fig. 7. The spectral IR radiation images of a hydrogen-air diffusion flame in bands of $2.47 \mu\text{m}$ and $3.43 \mu\text{m}$ were obtained (Fig. 7-(A)) from a setup, which is a duplicate of a laminar-flow burner employed by Lewis and von Elbe [10,15]. The raw data was processed to construct intensity images by using system response matrix (Eq. 3) in order to achieve quantitative imaging by the methods. Shown in Fig. 7-(B) are the temperature distribution (TD) in K, and water vapor distribution (WVD) in atm-cm determined by using the DBMM and the NBRM, respectively. Once the TD is determined, since the emissivity is calculated using the Plank's equation, the WVD is found using the Rutgers DBCP mentioned earlier. The presentation is made in pseudo-color in order to display more local variations.

It is pointed out that the distributions are two-dimensional as seen by the imaging system, and that each point measurement, within the matrix, represents that of the corresponding line of sight in the direction perpendicular to the image plane. The two methods produce mutually comparable results except for the border zones where the DBMM overestimates the temperature. This is found to occur due to an assumption of the identical flame thickness throughout the flame in DBMM, which is not realistic because it is small around the border.

In spite of differences between flames by the present DBMM / NBRM experiment and Lewis and von Elbe [15], (For example, one was an instantaneous measurement and the other was a time-averaged local measurement using the sodium-line reversal method, and also fuel) the results are mutually comparable each other. The absence of a similar result in literature, however, did not facilitate any further evaluation of the WVD.

WHAT TEMPERATURE? When the target mixture is uniformly mixed, the temperature determined by using the present ratio method would be the same at any point over the mixture. The temperature along the line of sight, however,

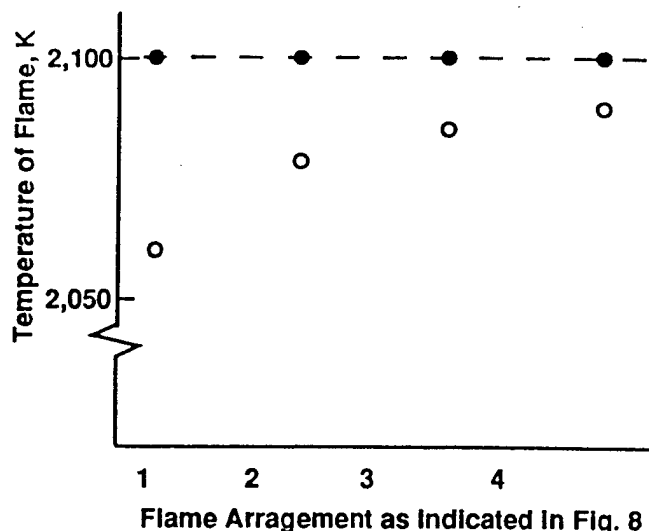


Figure 9. Temperature Determination by NBRM for various Flame Configurations.

varies in most combustion products so that the nature of measurements obtained by the method needs a discussion. A question comes to mind as to whether it is either close to the average temperature, or the highest temperature of the mixture somewhere along the line of sight, or other values. The same issue was also addressed in earlier studies [3,4].

In order to resolve the above question, the temperature determined by the NBRM was evaluated by using a simplified flame configurations as described in Fig. 8. The flame is assumed to consist five equal-thickness segments within the total thickness L having respective uniform temperatures (T_i) and water-vapor concentrations (C_i). Spectral radiation intensity at one side of the flame, I_λ will be a result of emission-transmission of individual segments as determined by

$$I_\lambda = I_{\lambda_1} + \tau_{\lambda_1} I_{\lambda_2} + \tau_{\lambda_1} \tau_{\lambda_2} I_{\lambda_3} + \dots$$

$$= \sum_i^n \left(\prod_m^{i-1} \tau_{\lambda_m} I_{\lambda_i} \right) \quad (4)$$

Note that, in the radiative participation by these mixtures, the absorption of radiation by a segment, as issued from others, is included to affect its thermal budget, as specified at each segment. In this analysis, for the sake of simplicity the temperature considered in each segment is assumed to be the result of various processes including such absorption.

In this evaluation, two spectral intensities (via wave bands of $2.47 \mu\text{m}$ and $3.43 \mu\text{m}$) are determined by using Eq. (4) and the Rutgers DBCP. The ratio of these two, then, are used for finding temperature by the NBRM for several cases as considered next. Note that the flame thickness $L = 2\text{cm}$ and the total pressure $p = 1\text{atm}$.

Results are shown in Fig. 9 for the following flame configurations: "1" in flame arrangement indicates a mixture of combustion product when segment-2 is occupied by a mixture at $2,100\text{K}$ with water vapor concentration $C = 0.12$ and other segments are with radiatively transparent species;

"2" means when segments-2 and-3 are filled with the same mixture; and so forth. For these cases, the NBRM determines exactly the same temperature, as indicated by the filled-in dots, which proves that the method is valid at least for such a uniform mixture.

On the other hand, since the flame is not uniform in general, other cases were considered, including those as same as the above but having segment-1 filled with a mixture at 1,100K and $C=0.06$. Results for these cases are indicated by open-dots in the figure. Important characteristics of temperature by the NBRM deduced from this analysis may be listed: (1) The temperature determined by the method is quite close to the peak temperature; (2) When the water vapor concentration is high in the segment with the peak temperature, the determination is closer to the peak value; and (3) The effect of low-temperature mixtures in a flame (e.g. segment-1) on the measured temperature may be significant in some cases.

THREE-BAND ITERATION METHOD (TBIM).

The NBRM can be applied to relatively "clean" flames with minimum soot formation. There are many flames, however, containing significant amounts of soot emitting strong radiation, which defeats the application of the NBRM. A new three-band iteration method (TBIM) was developed for such cases. This method permits simultaneous determination of distributions of temperature, water-vapor and soot in combustion products as explained next.

Figure 10 is introduced in order to discuss the basic concept of the TBIM, which is similar to Fig. 5 and assumes to have only water vapor and carbon dioxide in the mixture. The lowest curve in the figure indicates the spectral intensity of combustion products from a hydrocarbon ($H/C=2$)-air mixture to produce a water vapor concentration, $C=0.10$ (for 2,000K and 1 atm), which was constructed by using the DBCP. Other upper curves represent the radiation from the same mixture containing soot as specified by given volume fractions, f_v . In this method, in addition to two unknowns as considered earlier by the NBRM, one more affecting the emissivity of a mixture is determined, which is to find the absorption coefficient of the soot using the Rayleigh-limit expression [16,17],

$$\kappa_{s\lambda} = \frac{36n^2k(\pi/\lambda)f_v}{[n^2(1-k^2)+2]^2+4n^4k^2} \quad (5)$$

where, n , nk are complex refractive indices of soot determined by the dispersion equation [18].

The governing equations for the problems, therefore, are established Beer's Law for three spectral bands, namely 3.8 μ m, 2.47 μ m, and 3.42 μ m as:

$$\begin{aligned} E_{380T} &= 1 - \exp(-\chi_{380S} - \chi_{380H}) \\ E_{247T} &= 1 - \exp(-\chi_{247S} - \chi_{247H}) \\ E_{342T} &= 1 - \exp(-\chi_{342S} - \chi_{342H}) \end{aligned} \quad (6)$$

where,

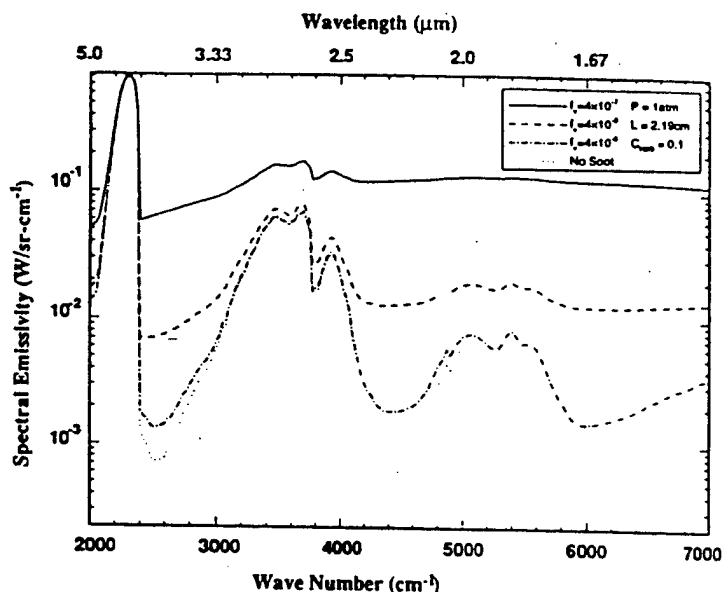


Figure 10. Spectrodiagram of Combustion Products of a Hydrocarbon-air Flame with Soot.

$$\chi_{380S} = \kappa_{\lambda} L / 3.80^{\alpha}$$

$$\chi_{247S} = \kappa_{\lambda} L / 2.47^{\alpha}$$

$$\chi_{342S} = \kappa_{\lambda} L / 3.42^{\alpha}$$

and $\alpha=0.95-1.0$ [19]. Note that the final results are found to be insensitive to the value of semiempirical constant, α . Here, χ for water vapor (at different temperatures and pressures) is determined from the DBCP. In the equation, the roles by soot and water vapor are denoted by subcharacters, S and H, respectively.

Mentioning the iteration method for finding the solution, Fig. 11 is offered here. Although the radiation from water vapor is small in 3.8 μ m band in low pressure reactions, the effect is, nevertheless, included in the present TBIM in order to minimize the error particularly in high pressures. In the calculation, at first, measurements via 3.42 μ m and 2.47 μ m are assumed to be free of soot radiation to use the NBRM for determining the initial value of flame temperature. Next, the extinction coefficient, χ by water vapor is calculated, which is reflected on determination of κL on 3.8 μ m band. The κL effect is then subtracted from χ for the two bands used for the initial estimation of temperature. The new temperature calculation by the NBRM for the two band, then, becomes more accurate than the initial estimate. The next steps are for improving the accuracy by going back to calculation of the extinction coefficient of water vapor for 3.8 μ m band. The iteration process is continued until a converging temperature value is found.

RESULTS OBTAINED BY TBIM. This new method was applied to the measurement of a bench-top burner and in-cylinder mixtures of a (cold) gasoline SI engine and a Diesel oil (D-2) operated direct injection (DI) CI engine.

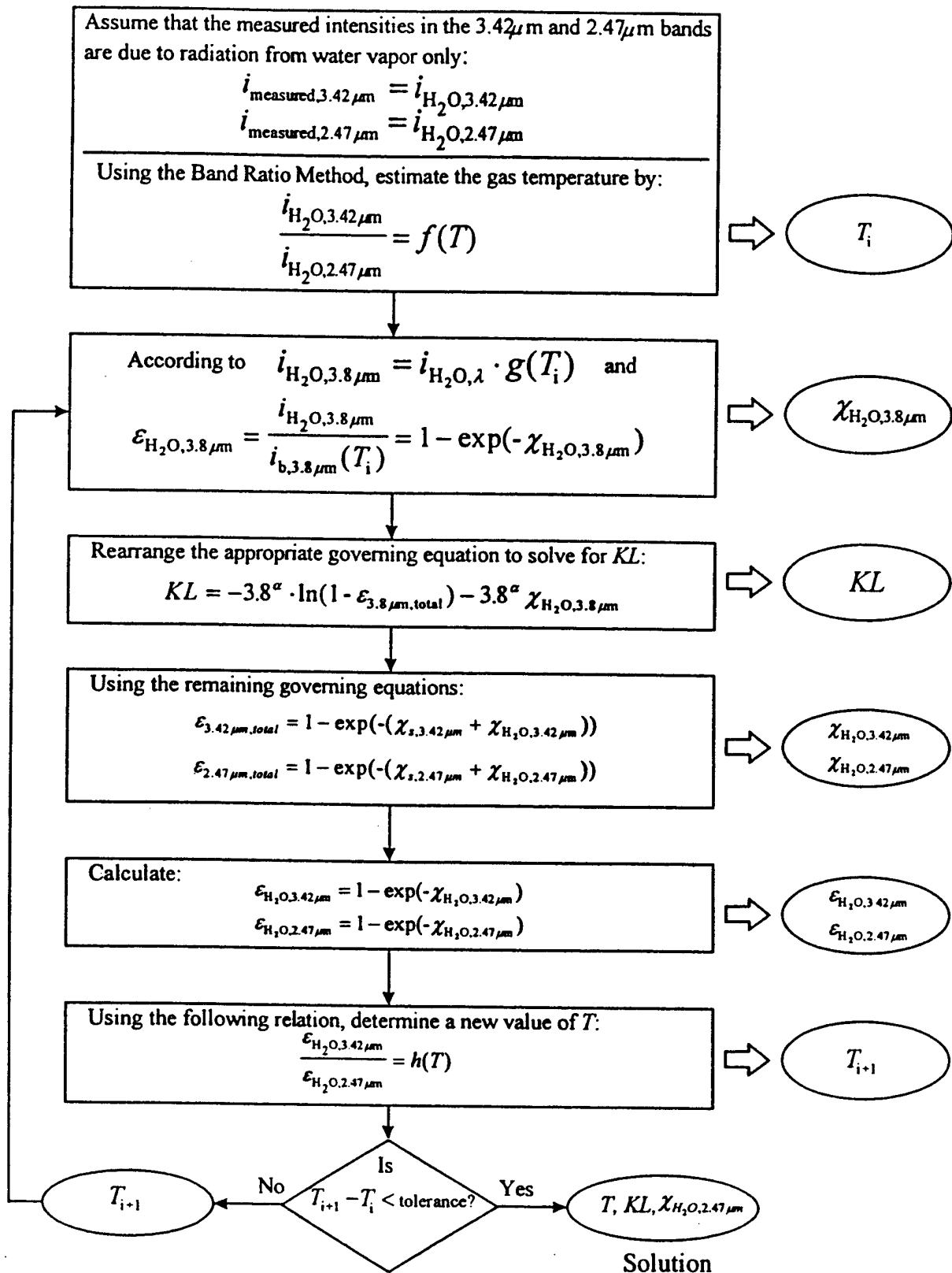


Figure 11. Flow-chart for the TBIM applied to Soot-laden Hydrocarbon-air flame.

Prior to presenting some results from the CI study, a short description of the experimental apparatus is made here. More details may be found elsewhere [11,14]. A single-cylinder DI-CI engine was mated with a section of Cummins 903 four-valve cylinder head where a high-pressure electronically-controlled injection system was installed. For imaging, one of the intake valves was replaced by an optical access (37mm diameter), which is barely big enough to observe one of eight sprays made through nozzle holes with 0.15mm diameter. The high-pressure injection system used in this experiment is basically a BKM's Servo-jet type [20]. In order to achieve versatility of the system, however, almost the entire unit was newly fabricated at Rutgers [11,14] to operate at pressures over 165MPa. The imaging, therefore, was made through the cylinder head to look down the spray from the top. In addition to gathering of raw spectral digital images by the SIS, other engine data were also collected, including the matching pressure-time data as required by the NBRM, which is a part of the TBIM.

The raw data matrixes were converted to corresponding spectral intensity distributions by using the calibration method as explained earlier. Figure 12-(A) shows these intensity images of a spray plume at successive CA with injection starting at 9CA before the top-dead-center (bTDC) as indicated by a look-up-table (LUT) shown in Fig. 13. The spray is directed diagonally as indicated by the arrow mark shown in box for 5.5CA bTDC. They are in bands of $2.47\mu\text{m}$, $3.42\mu\text{m}$ and $3.80\mu\text{m}$, which were to capture radiation from water vapor and soot assuming interference from other species is negligible (refer to spectrodiagrams shown in Figs. 4 and 5).

Discussing the spectral intensity images, the first image of spray was captured *immediately* after the fuel injection via $3.42\mu\text{m}$ band, which was reported earlier [11,14]. This new observation was explained by chemiluminescent radiation issued by some unknown species, which may include OH, CH, C_2 , aldehydes, and others expected in preflame reactions during the ignition delay period. The new finding seems to be reasonable because the fuel-air mixture undergoes many elementary reactions prior to exhibiting explosive (visible) premixed flame reactions, and because the early mixture formation occurs at injection. The first images obtained via other bands, i.e., at $2.2\mu\text{m}$, $2.47\mu\text{m}$ and $3.80\mu\text{m}$ were all found at the same CA, which was captured in this case at 5.5CA bTDC. (This is far after finding the first preflame image in $3.42\mu\text{m}$ band around 9CA bTDC.) They represent the onset of the premixed combustion stage. In a great amount of results, where the first preflame zones were observed in the spray, there also the first premixed reaction center appeared. In some cases, however, the two zones do not necessarily match each other, which warrants further investigation.

In general, the spectral intensity distributions are somewhat different from each other particularly in the early stage of combustion, which is until around 1.5 after TDC. Thereafter the images in $2.47\mu\text{m}$ and $3.42\mu\text{m}$ are similar each other, which differs from that in $3.8\mu\text{m}$. The similarity of images representing radiation by water vapor in the later stage of combustion is explained by the negligible amount of radiation by other species expected then, which is opposite in


 -5.5	-2.0	1.5	5.0	8.5
12.0	15.5	19.0	22.5	26.0

Fig. 13. Look-up-Table for Fig 12.

the early stage of combustion indicating many different species presenting to issue individual radiations.

The TBIM was employed to obtain distributions of temperature (K), water vapor (atm-cm) and soot (κL) by processing the abovementioned spectral intensity data, as shown in Fig. 12-(B). In order to construct the quantitative images, digital results were plotted according to corresponding color strips, for which several observations may be listed: (1) The numbers quantifying the characteristics of Diesel spray-plume combustion by high-pressure injection seem to be reasonable; (2) The local variation is continuous without abrupt changes except for those in the early stage of combustion; (3) The progress of reactions with time are smooth and gradual; and (4) No solution was obtainable for those in the early stage of combustion.

In addition to the absence of complexity in calibration, well-established governing equations and spectral absorption data from the handbook, as employed in the TBIM, the above observations seem to help trust the validity of the results. The quantitative images (e.g. distributions of temperature, κL and water vapor) are within values reported by others, except for low κL in the present measurement compared with those by mechanical injectors, which may be explained by the low-soot formation characteristics by the high-pressure injection system. The absence of abrupt local variation over the same quantitative image is expected in the continuum flow in the later stage of combustion. Similarly, the smooth changes in the distributions with time are expected in a progressively reacting spray. The inability of finding solutions in the early stage of combustion by the TBIM is also reasonable and compatible with the other observations. This is because the many intermediate species produced in the stage (recall the preflame images via $3.42\mu\text{m}$ band, for example) are expected to emit radiations added to those by water vapor and soot. Misrepresentation of spectral intensity measurements due to such interferences drove the iteration process of solution out of convergence, as indicated by the black zones in the results. (It is reminded that measurements of combined radiation from multiple species will cause erroneous results unless they are all included via additional governing equations, and corresponding spectral image data). These observations are not sufficient conditions for confirming the full validity of results, but certainly required conditions.

Reviewing the direction of spray (Fig. 13), the results in Fig. 12 indicate the region along the axis of spray is at low temperature, which was similarly found in combustion of spray by a mechanical injector [21]. The low-temperature

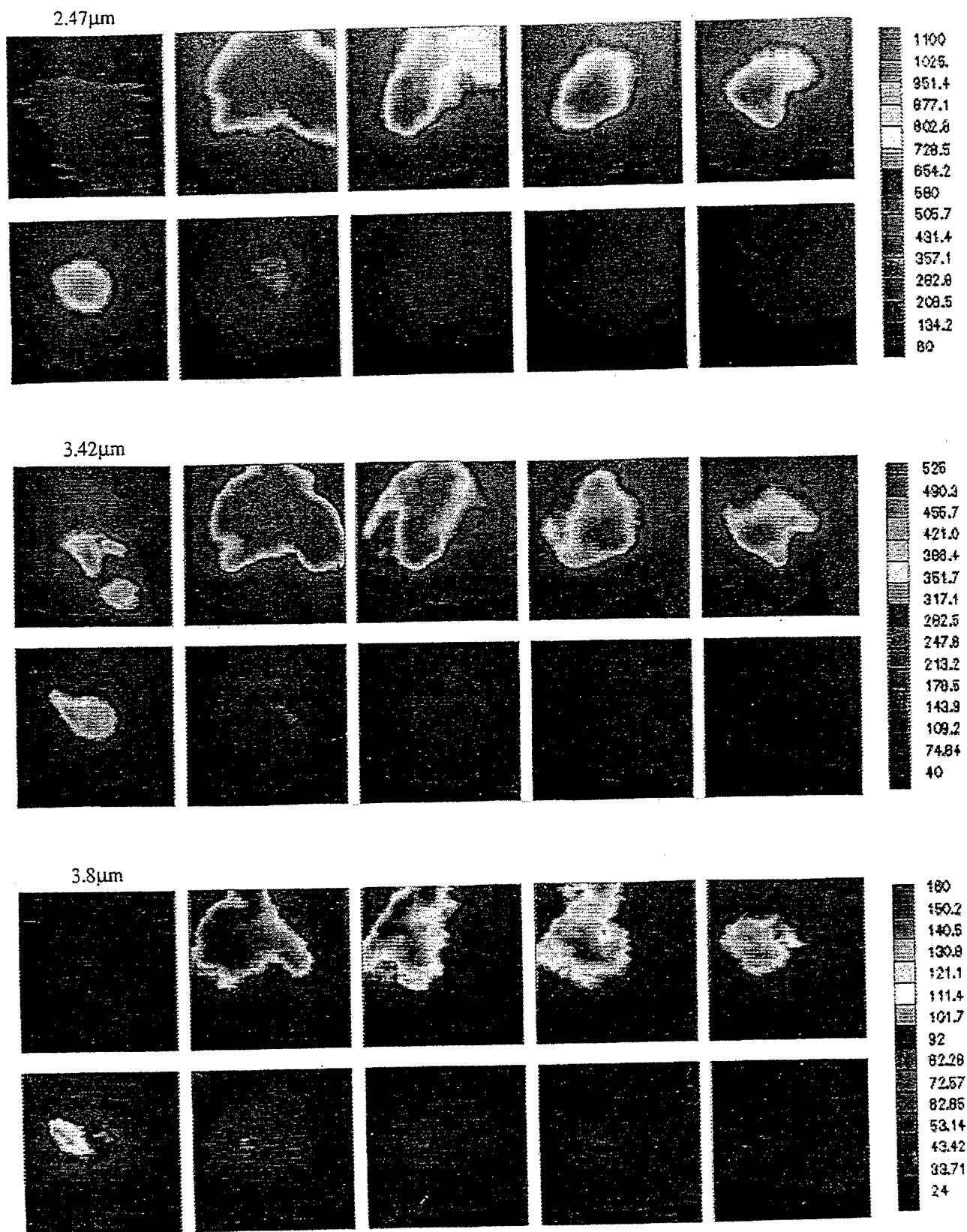


Figure 12. (A) Spectrometric Intensity Image of a Spray-plume in a DI-CI Engine at Successive Crank Angles.

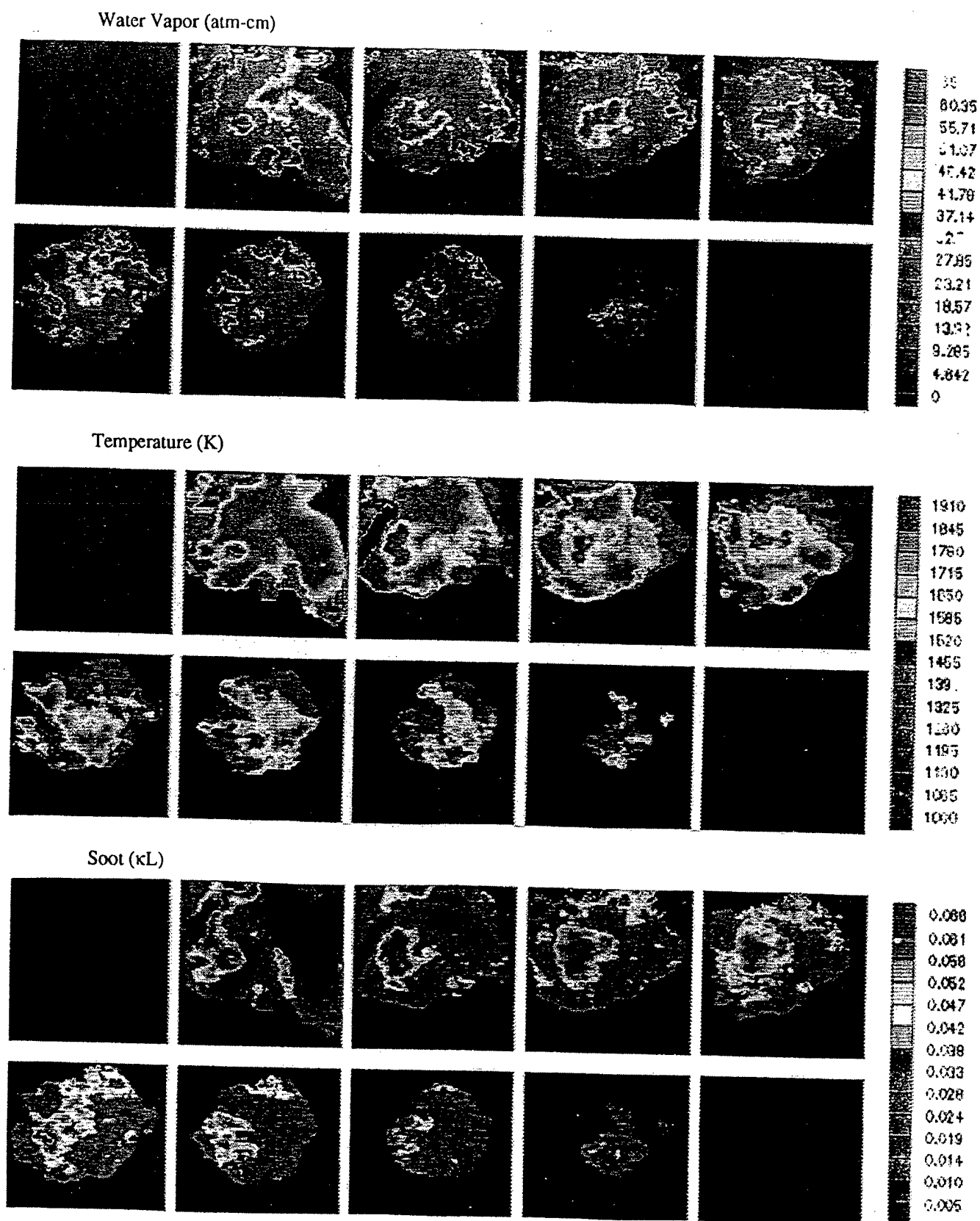


Figure. 12. (B) Distributions of Water Vapor (atm-cm), Temperature (K) and Soot (κL).

regions were interpreted to occur due to the continuous air entrainment expected along the spray axis [21]. Regarding the distributions of water vapor and κL , notably the concentrations are found to be high in the low-temperature zones.

The low κL in those zones may indicate more rapid consumption of soot there, which, however, does not seem to be consistent with the following observation. Since the high temperature zones most probably represent combustion products formed from mixtures with near stoichiometric fuel-air ratios, the water vapor concentration in the corresponding zones should have been also high, which is not the case in the present measurements. The most plausible interpretation of the distributions appears to be a physical factor, which is the high temperature effect on the specific volume of products. Inspecting the data again, when the temperature varies by a factor of two, the concentration inversely changes by about the same value. This finding is most obvious in the later stage of combustion to suggest insignificant impacts by the chemical reactions on the species distributions then.

SUMMARY

Instantaneous distributions of temperature, water vapor and soot were determined in flames by using the Rutgers Super Imaging System (SIS) and new spectrometric methods. Such information may be viewed as "quantitative images."

The SIS permits simultaneous measurement of IR digital images (matrixes) in the same geometrical configuration but in separate spectral bands at successive crank angles at high rates. The spectrometric methods are for processing this raw data to obtain the distributions. These techniques were applied to the investigation of bench-top flames and in-cylinder reactions of both SI and CI engines.

Three new spectrometric methods were presented in this paper: Dual-band mapping method (DBMM); New band-ratio method (NBRM) and Three-band iteration method (TBIM). These methods all employ a new data-based computer program (DBCP) constructed by employing experimental IR data for gaseous species and single-line-group (SLG) model from NASA Handbook (SP-3080).

The concept of DBMM is to find distributions of water vapor and temperature from a mixture when two spectral IR intensity matrices of the mixture are given, which is a reverse process of a common problem of finding the latter when the former are given. Solutions by the method are unique, but errors can be high.

The NBRM is consistent with a few earlier experimental methods employed for temperature measurement in gaseous mixtures. Its concept was conceived during the process of analyzing IR data in the NASA Handbook using the DBCP that the ratio of two spectral intensity of a radiating species in a gaseous mixture is uniquely related to the mixture temperature. Other important characteristics of the method (e.g. pressure effect) were also discovered.

The governing equations of TBIM are basically the Beer's law expressions for three separate species. The three simultaneous equations included absorption coefficients of gaseous species (from DBCP) and those for soot calculated

by the Rayleigh-limit expression plus dispersion equation. Because of the implicit nature of the problem, determination of the final results for each pixel was performed by an iteration method.

Instantaneous spectral intensities of a hydrogen-air flame were processed by both DBMM and NBRM. The results are mutually comparable with each other except for some expected errors by the DBMM. They are also consistent with time-averaged measurements obtained from the similar flame using the sodium-line reversal method as found in literature.

The simultaneous determination of distributions of temperature, water vapor and soot formation was achieved by the TBIM. This was made by processing high-speed spectral IR digital images of a reacting spray plume in a direct-injection CI engine equipped with a high-pressure injection system as operated by Diesel oil (D-2). The results appear to be reasonable in view that any indirect evidence does not challenge the validity and that they are comparable with results by others. The new quantitative images as well as the raw data offer some new insight into the reactions in the cylinder.

ACKNOWLEDGEMENT

The present work has been performed under the sponsorship of the U.S. Army Research Office (Contract No. DAAH04-95-1-0430) and AASERT (DAAH04-94-G-0201), Ethyl Corporation and Ford Motor Company.

REFERENCES

1. Uyehara, O.A. and Myers, P.S., "Flame Temperature Measurements-Electronic Solution of the Temperature Equations," SAE Quarterly Transactions, vol. 1, No. 4, 1947.
2. Matsui, Y., Kamimoto, T., Matusuoka, S., "A Study on the Application of the To-color Method to the Measurement of Flame Temperature and Soot Concentration in Diesel Engines," SAE Paper-800970, 1980.
3. El Wakil, M.M., Myers, P.S., and Uyehara, O.A., "An Instantaneous and Continuous Sodium-line Reversal Pyrometer," ASME Transactions, Paper No. 50-A-94, 1950.
4. Myers, P.S. and Uyehara, O.A., "Accuracy of and Representative Results Obtained with an Infrared Pyrometer Measuring Compression Temperatures," Inst. of Mechanical Engineers, pp. 64-75, 1965.
5. Agnew, W.G., "Two-wavelength Infrared Radiation Method Measures end gas Temperatures near their Peaks," SAE Journal, October 1960.
6. Ferriso, C.C., Ludwig, C.B., and Boynton, F.P., "A Band-ratio Technique for Determining Temperatures and Concentrations of Hot Combustion Gases from Infrared-emission Spectra," 10th Symp. (Int'l) on Combustion, 161, The Combustion Institute, 1965.

7. Ludwig, C.B., Malkmus, W., Reardon, J.E., Thomson, J.A.L., Handbook of Infrared Radiation from Combustion Gases," NASA SP-3080, 1973.
8. Jiang, H., McComiskey, T., Qian, Y., Jeong, Y.I., Rhee, K.T., and J.C. Kent, "A New High-Speed Spectral Infrared Imaging Device Applied for Imaging Gaseous Mixtures from Combustion Devices," Combustion Science and Technology, 90, 5-6, p. 341, 1993.
9. McComiskey, T., Jiang, H., Qian, Y., Rhee, K.T., and Kent, J.C., "High-Speed Spectral Infrared Imaging of Spark Ignition Engine Combustion," SAE Paper-930865, 1993.
10. Jiang, H., Qian, Y. and Rhee, K.T., "High-Speed Dual-Spectra Infrared Imaging," Optical Engineering, 32 (6), pp. 1281-1289, 1993.
11. Clasen, E., Campbell, S., and Rhee, K.T., "Spectral IR Images of Direct Injection Diesel Engine Combustion with High Pressure Fuel Injection," SAE Paper-950605, 1995.
12. Song, K., Clasen, E., Chang, C., Campbell, S., Rhee, K.T., "Post-flame Oxidation and Unburned Hydrocarbon in a Spark-ignition Engine," SAE Paper-952543, 1995.
13. Campbell, S., Clasen, E., Chang, C., and Rhee, K.T., "Flames and Liquid Fuel in an SI Engine during Cold Start," SAE Paper-961153, 1996.
14. Clasen, E., Song, K., Campbell, S., and Rhee, K.T., "Fuel Effects on Diesel Combustion Processes," SAE Paper-962066, 1996.
15. Lewis, B. and von Elbe, G., *Combustion, Flames and Explosions of Gases*, p. 281, Academic Press Inc, 1961.
16. Chang, S.L. and Rhee, K.T., "Computation of Radiation Heat Transfer in Diesel Combustion," SAE Paper-831332, 1983.
17. Bard, S. and Pagni, P.J., Carbon Particles in Small Pool Fire Flame," J. of Heat Transfer, vol 103, pp 357-362, 1981.
18. Dalzel, W.H. and Sarofim, A.F., "Optical Constants of Soot and their Application to Heat Flux Calculation," ASME Trans. vol. 9, p. 100, 1969.
19. Hottel, H.G., Broughton, F.P., "Determination of True Temperature and Total Radiation from Luminous Flames," Industry and Energy Chemistry, 4-2, p. 166, 1932.
20. Abata, D., Stroia, B.J., Beck, N.J., and Roach, A.R., "Diesel Engine Flame Photographs with High Pressure Injection," SAE Paper-880298, 1988.
21. Jeong, Y.I., Qian, Y., Campbell, S. and Rhee, K.T., "Investigation of a Direct Injection Diesel Engine by High-Speed Spectral IR Imaging and KIVA-II," SAE Paper-941732, 1994.